Efficient Adoption of Residential Energy Technologies Through Improved Electric Retail Rate Design

Noah Rauschkolb

Submitted in partial fulfillment of the
requirements for the degree of
Doctor of Philosophy
under the Executive Committee
of the Graduate School of Arts and Sciences

COLUMBIA UNIVERSITY

2023

Abstract

Efficient Adoption of Residential Energy Technologies

Through Improved Electric Retail Rate Design

Noah Rauschkolb

This dissertation combines methods from engineering, operations research, and economics to analyze how emerging residential energy technologies can be effectively used to reduce both energy costs and carbon emissions. Our most important finding is that air-source heat pumps can be used to reduce both energy costs and carbon emissions in four out of the five major climate regions studied, but that electric retail rate reform is needed to provide customers with appropriate incentives. In cold climates, it may be advantageous to use heat pumps in tandem with fossil fuel-powered furnaces; in warmer regions, furnaces can be cost-effectively abandoned altogether. We do not find that distributed rooftop solar panels or distributed battery storage are effective tools for reducing the cost of energy services. Rather, in our simulations, customers adopt these technologies in response to poor price signaling by electric utilities. By reforming electric retail rates so that the prices paid by consumers better reflect the cost of energy services, utilities can promote the adoption of technologies that reduce both aggregate costs and carbon emissions.

Contents

List of Figures

List of Tables

Acknowledgements

I thank my friends, family, teachers, and students.

Executive Summary

The energy system is experiencing the confluence of a number of important changes. Utility-scale electricity production from renewable energy resources has nearly doubled in the past decade, with projections that renewables will be the largest source of electricity generation by 2050 (Energy Information Administration, 2020). Simultaneously, customers are exploring opportunities to further reduce their emissions at home by adopting rooftop solar photovoltaic panels and distributed storage, and by electrifying end use technologies traditionally powered directly with fossil fuels (including vehicles and heating).

A significant barrier to the efficient adoption of customer-side technologies is the design of electric retail tariffs. Most residential customers pay their utility bills through volumetric tariffs that are based on the average cost of energy services, rather than the marginal cost of an additional unit of energy. This deprives them of the appropriate price signals required to incentivize efficient adoption and use of emerging technologies.

This thesis draws on methods from engineering and economics to make several important contributions. These include: providing the first data-driven model of distribution system costs that explicitly disentangles the cost of sustaining distribution capacity with the cost of growth; using optimization to identify the least-cost portfolio of technologies for satisfying a collection of customers' energy needs and using it to compare optimal portfolios across multiple climate regions; and analyzing how to adapt electricity tariffs to incentivize customers to make more efficient decisions about technology adoption and use.

The thesis proceeds as follows. In Chapter 1, we analyze electric utility distribution costs

and build an econometric model that describes the main determinants of electric distribution costs using data reported by 101 major U.S. investor-owned utilities. We find that the fraction of a utility's capital expenses that is attributable to load growth is relatively small, representing less than 10% of distribution capital expenses for a typical utility. This is visualized in Figure 1.3, which plots per-kW capital expenses vs. the compounding annual growth rate (CAGR) of distribution capacity. While it is evident that utilities that are quickly expanding their capacity spend more on distribution than utilities with constant (or declining) peaks, distribution costs are better-explained by other factors, such as the density of customers within the service territory, the fraction of energy sales to residential customers, and the fraction of distribution assets installed underground.

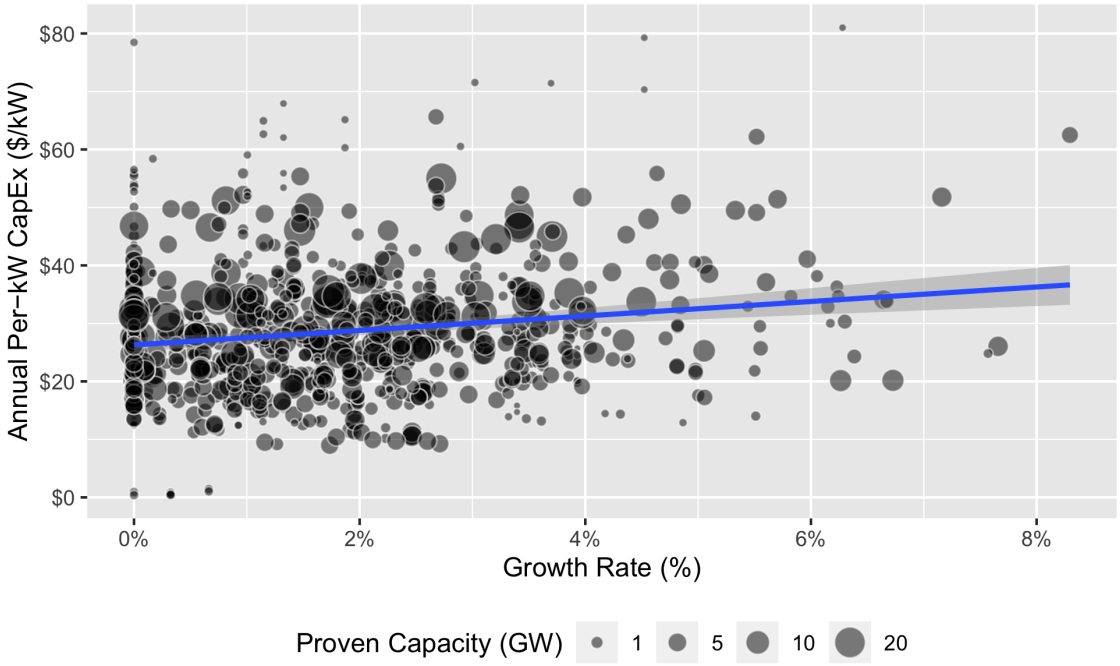

Figure 1: Relationship between per-kW-capacity distribution capital costs and growth rate for major U.S. utilities. 808 points representing 101 utilities over eight years. The best-fit line represents the univariate regression of capital expenses (in $ per-kW) on the compounding annual growth rate of distribution capacity, weighted by the utility's proven capacity. The shaded region covers a level 0.95 confidence interval.

Insofar as past trends are predictive of the future, this indicates that a well-planned capacity expansion strategy – as would be required to accommodate heating and transportation electrifi-

cation – could be incorporated into existing capital projects while only raising the average cost of electricity by a fraction of a cent.

In Chapter 2, we discuss the drivers of residential energy demands and use an open source building energy simulation tool to simulate hourly energy demands for 75 residences in five climate regions throughout the continental United States. We observe that there is significant variation in annual demands for space heating and cooling energy both between regions and among residences within a region. The annual profiles of heating and cooling loads (aggregated across 15 residences) for the five regions are represented in Figure 2. The variation in annual heating and cooling demands has important implications on energy consumption, the sizing of heating and cooling equipment, and the requirements for utility infrastructure.

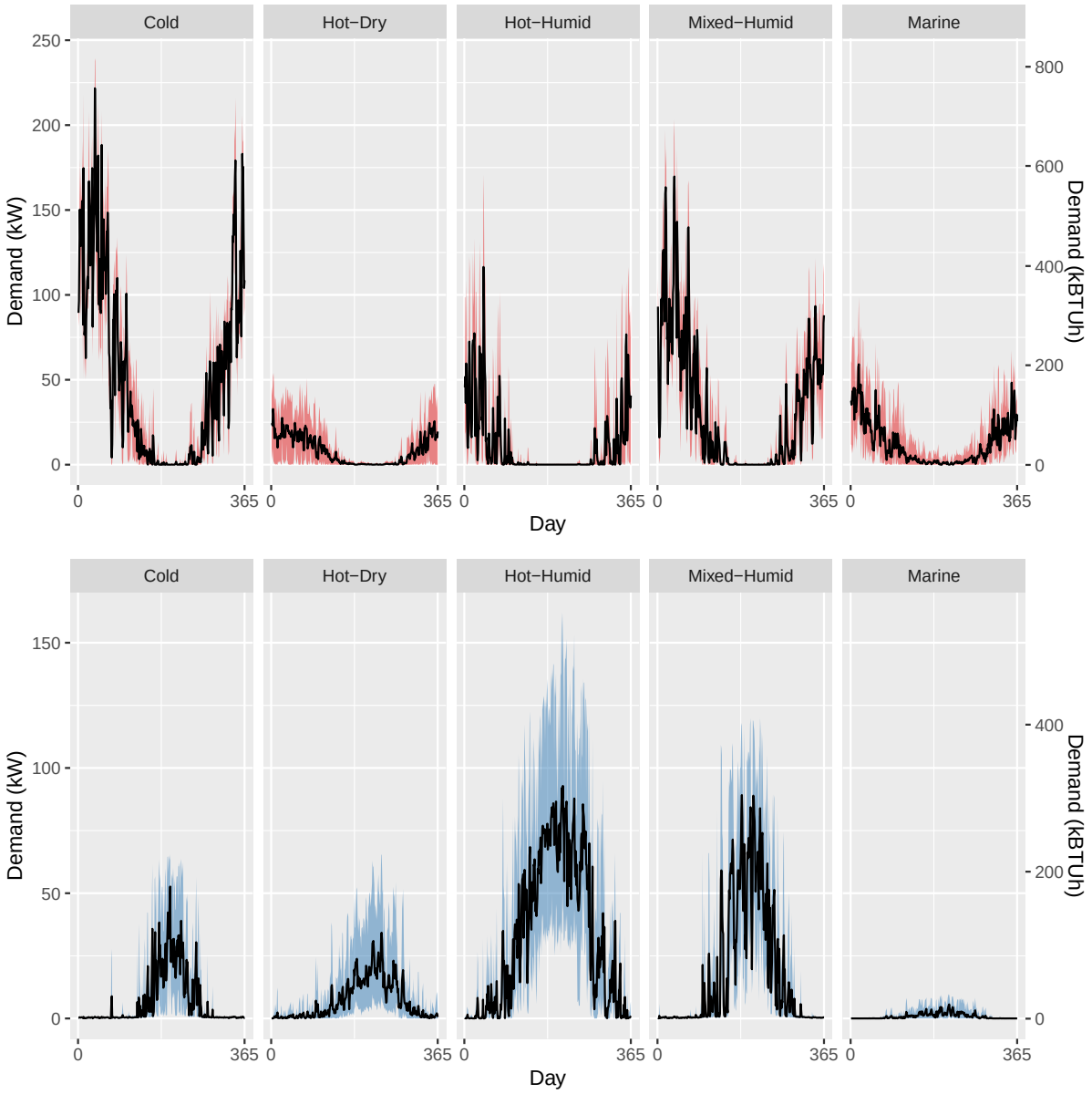

Figure 2: Annual profile of daily heating and cooling demands in each of the five climates, aggregated across the 15 residences. The solid black line represents the average demand for each day of the year. The ribbon shows the range between the minimum and maximum hourly demands on each day. The y-axis is in units of kW on the left and kBTUh on the right. This is computed through a direct conversion of 3.412 kBTUh = 1 kW.

In Chapter 3, we provide background on several emerging customer-side technologies and discuss how their adoption could impact electric loads. These include heating electrification, rooftop solar photovoltaic panels, distributed battery storage, energy efficiency investments, and

electric vehicles. We observe that the impact that a given technology has on electric load can vary tremendously depending on the local climate and system conditions. In particular, when the temperature falls, the efficiency of air-source heat pumps declines as the heating load increases. This creates a non-linear relationship between the outdoor temperature and electricity demand for heating, which makes an "electrify everything" strategy very energy-intensive in cold climates.

In Chapter 4, we develop a mixed-integer linear programming model capable of identifying the least-cost portfolio of technologies for satisfying a collection of residential customers' energy needs. This model is used to test how the optimal configuration of customer-side technologies varies with the local climate region, distribution system conditions, and varying assumptions about technology cost and performance.

The number of residences adopting each technology in each region is summarized in Figure 4.2. We find that distributed rooftop solar panels are generally not part of a least-cost portfolio of technologies because (1) their high capital cost outweighs the value of the electricity they produce and (2) they are generally ineffective at deferring infrastructure upgrades. While rooftop solar is not found to reduce costs, electric heat pumps can be adopted as a cost-savings measure in four out of the five climates studied due to their high efficiencies and ability to serve both heating and cooling needs. This result holds even when the social cost of carbon is neglected.

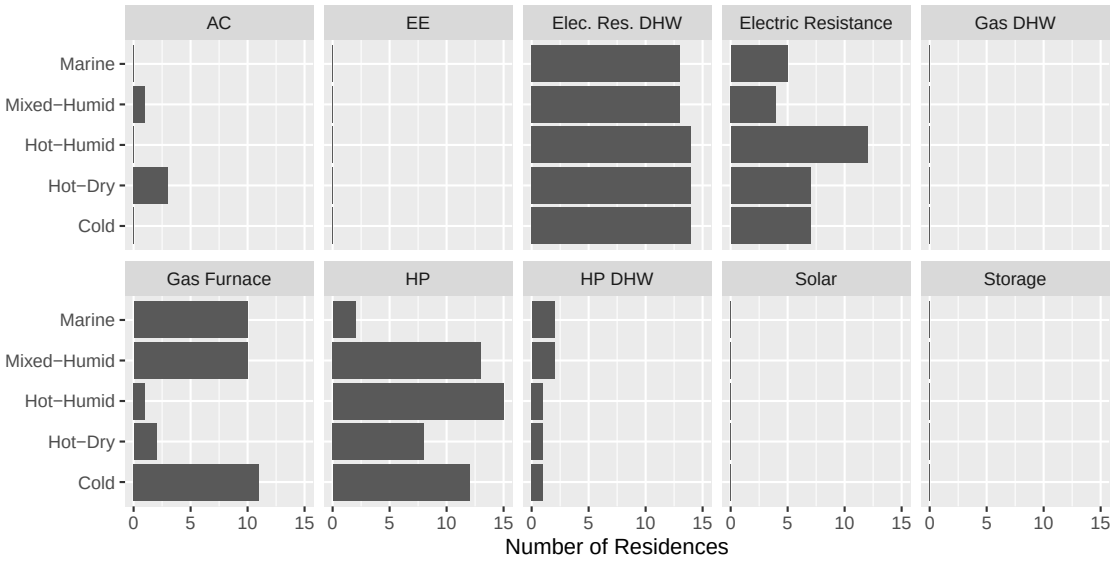

Figure 3: Number of residences adopting a given technology in each climate in the optimized models. "AC" and "HP" denote space cooling and heating energy. "EE" denotes energy efficiency.

In Chapter 5, we adapt the model from Chapter 4 to simulate how different designs for residential retail tariffs influence customers' decisions about adoption and use of various technologies, including electric heat pumps, distributed solar, and battery storage. This allows us to understand the conditions under which inaccurate pricing can increase costs.

We find that the design of the residential rate tariff can have a significant influence on customers' decisions about technology adoption and use. In particular, electric tariffs that are set significantly above the cost of energy tend to over-incentivize the installation of technologies that reduce demand (such as rooftop solar panels) while discouraging the adoption of some beneficial technologies that increase demand (such as heat pumps). This leads to significant increases in the total cost of energy services and, in some cases, carbon emissions. We note that the thresholds at which non-cost-reflective tariffs become problematic vary with both the climate region and assumptions about the cost of technologies. This suggests that a pragmatic strategy for tariff reform should encompass considerations about the specific climate characteristics and the technologies in play.

Chapter 1

A Data-Driven Model of Electric Distribution Costs

Households in the United States consume over 1.4 trillion kilowatt-hours of electricity each year, costing them nearly $200 billion (U.S. Energy Information Administration, 2021a). Residential customers also consume between four and five trillion cubic feet of natural gas each year, costing another $45 to $55 billion (U.S. Energy Information Administration, 2022b). Over one-quarter of U.S. households experience some form of energy insecurity, such as forgoing basic necessities in order to pay their energy bills, receiving a disconnection notice from their utility, or keeping their homes at unsafe temperatures to reduce their energy burden (U.S. Energy Information Administration, 2022a).

This chapter breaks down the various expenses that contribute to residential customer energy costs in the United States, focusing on the electricity sector. Additionally, we contribute to the literature by developing a novel data-driven model of electric distribution costs, which is used understand how large-scale electrification of heating and transportation could impact infrastructure costs. To do this, we separately examine annual capital investments and operations and maintenance (O&M) expenses for 101 major investor-owned utilities (IOUs) in the United States over eight years. We employ econometric methods to study how utility costs vary with

the growth rate of the distribution system's peak capacity, the proportion of distribution assets installed underground, the geographic density of customers within the utility's service territory, and the share of sales to residential customers.

We find that all of the attributes described above are significant in explaining a utility's per-kW capital costs ($p<0.05$). Notably, while the growth rate of a distribution system's proven capacity[1] is significant in explaining capital investments, it only accounts for a small fraction of recent investment (less than 10% for a utility with median characteristics). However, if the annual growth in peak loads increases significantly in response to electrification of heating and transportation, growth-related costs could come to represent a larger share of utility costs and ratepayers' bills.

None of the variables described above are significant in explaining O&M costs. The best indicator of a utility's per-kW O&M expenses is the region in which it is located, but this likely serves as a proxy for unobserved variables such as labor and regulatory compliance costs.

Section 5.1 discusses distribution system costs and reviews the relevant literature. Section 1.2 describes the sources of public data used in this analysis and the development of explanatory variables. Section 4.2 discusses empirical methods, including univariate, multivariate, and fixed effects regression. Section 4.5 summarizes the estimated coefficients and addresses their significance. Section 1.5 discusses the results and uncertainties. Section 1.6 outlines potential policy implications and highlights opportunities for future work.

1.1 Background and Literature Review

The U.S. Energy Information Administration breaks down the cost electricity into three components, plotted in Figure 1.1. The blue region describes the cost of generation, the brown region the cost of transmission, and the green region the cost of distribution.

Most studies focused on decarbonizing the energy system limit their focus to the generation

[1] "Distribution system capacity" refers to the aggregate peak load that can be accommodated by a distribution utility across its entire system. Because this is difficult to measure (it is not simply equal to the sum of transformer capacities), we use the term "proven capacity" to refer to the maximum peak load ever observed on a utility's distribution system.

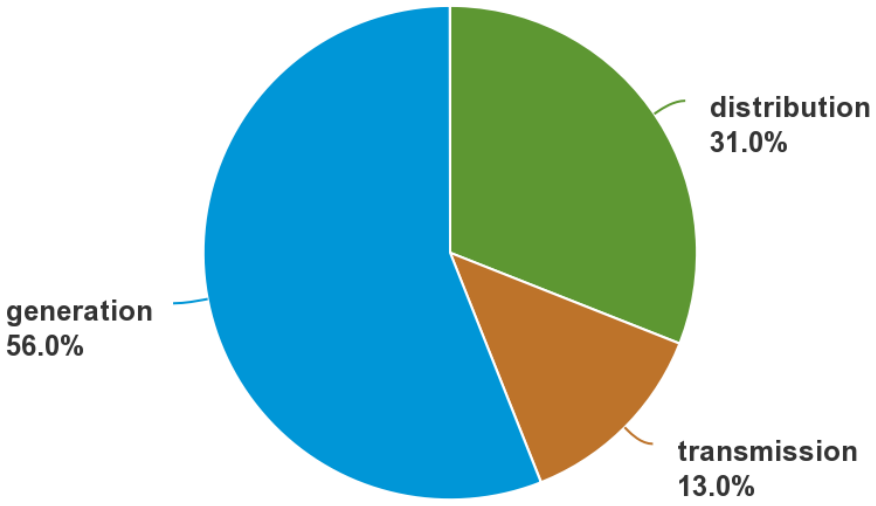

Figure 1.1: Major components of the average price of electricity, as categorized by the Energy Information Administration.

and transmission systems. EPRI's U.S. National Electrification Assessment (Electric Power Research Institute, 2018a) predicts that efficient electrification could cause load to increase by 24–52% by 2050. However, this work is based on EPRI's US-REGEN model, which does not impose any "constraints or expenditures related to transmission or distribution within a region" (Electric Power Research Institute, 2018b, p. 2-15). NREL's 2017 Electrification and Decarbonization report concludes that electrification of end-use services across transportation, buildings, and industrial sectors could lead to a doubling of electricity consumption by 2050 (Steinberg et al., 2017, p. vi). This analysis utilizes NREL's Regional Energy Deployment System, which only models the electricity system at the resolution of 134 balancing areas across the contiguous United States (S. Cohen et al., 2019). Intra-balancing area transmission and distribution are not modeled (S. Cohen et al., 2019, p. 57). Likewise, the EPA's Integrated Planning Model splits the contiguous United States into 67 model regions but does not model power flows within them (US EPA, 2019). MacDonald et al. (2016a) represent the transmission system with more detail but do not model local distribution systems explicitly. Instead, the authors assume that distribution costs scale proportionally with generation and transmission costs, composing 32% of the total levelized cost of energy (MacDonald et al., 2016b).

A handful of papers have used empirical approaches to estimate the drivers of utilities' distribution costs, mainly for benchmarking utilities against one another. Roberts (1986) studies financial reporting data from 65 IOUs in 1978. Notably, the author does not find evidence that increased customer density decreases costs, even when controlling for the percentage of the firm's distribution equipment installed underground. Conversely Filippini and Wild (2001), who analyze aggregate utility expenditures (minus purchased power) for 59 Swiss utilities, find that increased customer density significantly reduces distribution costs per unit of energy sold. Filippini, Hrovatin, and Zorič (2004) study annual reports from five Slovenian utilities from 1991 to 2000, concluding that a 1% increase in customer density reduces costs by approximately 0.60%. Yatchew (2001) studies data from 81 municipal distribution utilities in Ontario, concluding that a 10% increase in length of wire per customer increases the per-customer cost by 3.8%. Fenrick and Getachew (2012) analyze financial and technical data submitted to the Rural Utilities Service by 163 Midwestern power cooperatives located in nine states. They find that increased customer density and larger proportions of distribution lines buried underground decrease O&M costs, while a larger proportion of deliveries to residential customers increases O&M costs.

While some of these empirical studies recognize the distribution system's peak demand or capacity as a driver of costs either explicitly (using system capacity as an explanatory variable) or implicitly (normalizing costs by capacity before performing a regression against other variables), none in our review identify *increases* to peak capacity as an independent driver of costs. In contrast, utility analysts have historically characterized a large share of capital investments as causally related to growth in peak capacity. Baughman and Bottaro (1976) assume that all capital expenditures in the transmission and distribution systems are directly related to growth in capacity (measured in "miles energized" for cables and new transformer capacity for transformers), concluding that a mile of new distribution lines in some parts of the country costs three times as much as it does in others. In their 1992 guide for electric utility cost allocation, the National Association of Regulatory Utility Commissions (NARUC) recommends classifying all transmission system investments as related to load growth, except those specifically related to siting generation, interconnecting with power pools, serving specific large customers, or

replacing existing equipment in kind (NARUC, 1992).[2] ICF Consulting (2005), which develops the methodology formerly used by many New England utilities for their avoided cost studies, recommends assuming as a default heuristic that 50% of transmission and distribution investments are related to load growth.[3]

When analysts model distribution costs as only a function of peak load, they are tacitly assuming that new distribution capacity can be built at a cost comparable to maintaining existing capacity. Such is the case in The Energy Information Administration's National Energy Modeling System, which assumes that capital expenses in the distribution system scale directly with the sum of the non-coincident peak loads of each customer class (Energy Information Administration, 2019c). In this model, capital expenditures range from approximately \$20/kW to more than \$100/kW annually, depending on the utility's region. O&M costs are modeled similarly, but with separate coefficients for capacity (\$/kW) and volumetric sales (\$/kWh) (Energy Information Administration, 2019b). If electrification causes peaks to double, the computed distribution costs would exactly double as well. Similarly, Vibrant Clean Energy, LLC et al. (2020) draw on the results produced by R. L. Fares and King (2017)[4] to assess the value that distributed energy resources (DERs) could offer to the electricity system, concluding that DERs can effectively be used to defer some distribution system reinforcements. By assuming that building new distribution system capacity bears the same annual expense as sustaining existing capacity, the authors risk underestimating the cost of significantly expanding capacity to accommodate new load.

The most rigorous treatment of distribution costs in a large-scale energy systems analysis appears to come from Larson et al. (2020), who model capital expenditures in the distribution

[2]NARUC's discussion of marginal distribution costs revolves around distinguishing between customer-related and capacity-related costs, paying relatively little attention to determining whether the costs identified as capacity-related are incurred because of growing peaks.

[3]Synapse Energy Economics (2018) developed a subsequent version of the methodology described in ICF Consulting (2005), this time recommending top-down accounting analyses to identify expense accounts that are primarily growth-related and discounting expenses registered in these accounts by an allowance for the cost of replacing retired equipment in kind.

[4]R. L. Fares and King (2017) use ordinary least squares (OLS) regressions to relate annual distribution costs to three predictors: total number of customers, peak load, and volumetric sales. The models that regress costs against peak loads estimate coefficients of \$34/kW for capital expenditures and \$18/kW for O&M.

system as the sum of the capital invested in new capacity and the cost of replacing depreciated assets. While this general approach to modeling distribution system costs is sound, the coefficient used to model the cost of new capacity ($1,351/kW) is based on an estimate of the per-kW gross capital investment already made in the distribution system, not on the marginal cost of increasing capacity.[5] This approach to estimating marginal distribution capacity costs presents several problems that are discussed in Section 1.5.

A more common approach to estimating the cost of additional distribution system capacity – often employed by utilities and their consultants – is the marginal cost of service (MCOS) study. Since the late 1970s, electric utilities throughout the United States have been regularly asked to conduct MCOS studies as part of their rate case proceedings (Parmesano & Martin, 1983). These studies are intended to establish, among other figures, the cost in dollars of increasing distribution system capacity by one kilowatt. While MCOS studies may appear to be a promising tool for estimating the cost of increasing distribution system capacity to accommodate electric vehicles and heat pumps, they are not well-suited to this purpose. Contemporary MCOS methodologies base their cost calculation on the value of deferring a local system expansion plan by one year (Hanser et al., 2018; Woo et al., 1994).

Because this methodology is typically based only on historical and forecast expenses (rather than counterfactual expenses), a utility will develop very different estimates of their marginal distribution capacity cost ($/kW) depending on whether or not there are planned growth-related investments within the study period's time horizon (Pérez-Arriaga & Knittel, 2016). For example, as part of New York State's "Value of Distributed Resources (VDER)" order, the major utilities were directed to perform enhanced marginal cost of service studies that computed marginal capacity costs with a high level of spatial granularity (State of New York Public Service Commission, 2017). The responding utilities produced figures ranging from $0/kW for load areas with no growth-related investments (Demand Side Analytics, 2018) to those exceeding $500/kW for load areas with growth triggering costly system reinforcements (Hanser et al., 2018). While the results produced by MCOS studies may be useful for designing time-varying electricity rates

[5] See (Fowlie & Callaway, 2021) for a discussion of embedded and marginal distribution costs.

and utility-administered demand response programs, they offer little insight into what to expect from sustained peak load growth due to electrification. Consequently, those analyses that use the numbers produced by these MCOS studies to forecast the cost associated with sustained load growth, such as Elmallah, Brockway, and Callaway (2022), are most likely producing biased results.

This chapter employs a similar empirical approach to Yatchew (2001) and Fenrick and Getachew (2012) but draws on a significantly bigger data set and includes the growth rate of system capacity as an explanatory variable to assess the impact of load growth on distribution costs. By drawing on data from 101 major U.S. utilities representing over 50% of domestic retail sales, this chapter aims to establish a set of heuristics that could be used to estimate the costs associated with a prolonged expansion of distribution system capacity, as would be required to meet long-term decarbonization goals through end-use electrification.

1.2 Data

In this section, we discuss data sources and the development of model variables. Electric utility data were collected from multiple public sources. Financial and operational data were collected from FERC Form 1 (Federal Energy Regulatory Commission, 2009) for the years 2000 to 2007. These years were chosen because they are representative of a period of relatively high sales growth in the electricity sector. For this period, sales of electric energy grew at an average rate of 1.4% annually (Energy Information Administration, 2019d). This finding is consistent with the estimated sales growth rate in the high electrification scenario in NREL's Electrification Futures Study (Mai et al., 2018). By contrast, from 2008 until 2018, electric energy sales grew at a rate of just 0.2% annually (Davis, 2017; Energy Information Administration, 2019d).

FERC Form 1 provides financial and operating data for all major U.S. IOUs.[6] Among these, 107 distribution utilities provided complete financial and system peak data for the selected years. Four utilities were removed from the dataset because of outlier values for either growth rate

[6]Major utilities are defined as having: (1) one million megawatt-hours or more of sales; (2) 100 megawatt-hours of annual sales for resale; (3) 500 megawatt-hours of annual power exchange delivered; or (4) 500 megawatt-hours of annual wheeling for others (deliveries plus losses) (Federal Energy Regulatory Commission, 2009)

or costs. Two more were removed because a significant change in service territory (due to a merger or acquisition) made it impossible to track year-to-year growth in system capacity. The remaining 101 utilities accounted for just under 2 million gigawatt-hours (GWh) of sales in 2003, which represented 55% of that year's domestic retail electric volume (Energy Information Administration, 2019d). Because we are using eight years of data, there are 808 data points used in each regression.

In Figure 1.2, we reproduce Figure 1.1 using data from Federal Energy Regulatory Commission (2009). We note that the green region, labeled "distribution" in Figure 1.2 is actually composed of three separate cost categories. Distribution capital costs include investments in buildings, poles, wires, transformers, and conduit. Distribution O&M includes labor, purchased maintenance, and other recurring costs, as well as some sporadic costs such as repairs to storm damage (Lazar, 2016). Admin/General expenses include office space, customer service, and sales expenses. When we separately categorize admin/general expenses, we observe that just 17% of the average utility's expenses are directly related to building and maintaining the distribution system. The central goal of this chapter is to identify how this may change if electrification of space and water heating precipitates the need for large reinforcements of the distribution system.

There is no known public resource that records the total distribution system capacity of electric utilities. While FERC Form 1 includes reporting of individual substation capacities, inconsistencies in reporting between utilities (and between consecutive years for a given utility) make it impractical to use these data directly for our analysis. Instead, we compute the "proven capacity," $C_{i,t}$, for utility i in year t as the maximum of observed system peaks up to and including that year.[7] For example, if a utility achieved an all-time peak of 3 GW in 2001, but only 2.9 GW in 2002 (perhaps due to a cooler summer), we assume the system capacity for that year remains at 3 GW. This generates a monotonically increasing variable, $C_{i,t}$.

We separately examine capital costs and operations and maintenance (O&M) expenses for the distribution system. All financial figures used herein represent actual outlays made in a given

[7]The monthly system peaks for each utility are recorded in Federal Energy Regulatory Commission (2009) on page 401b, column e. The maximum of these monthly peaks is taken as the annual peak for each utility–year combination.

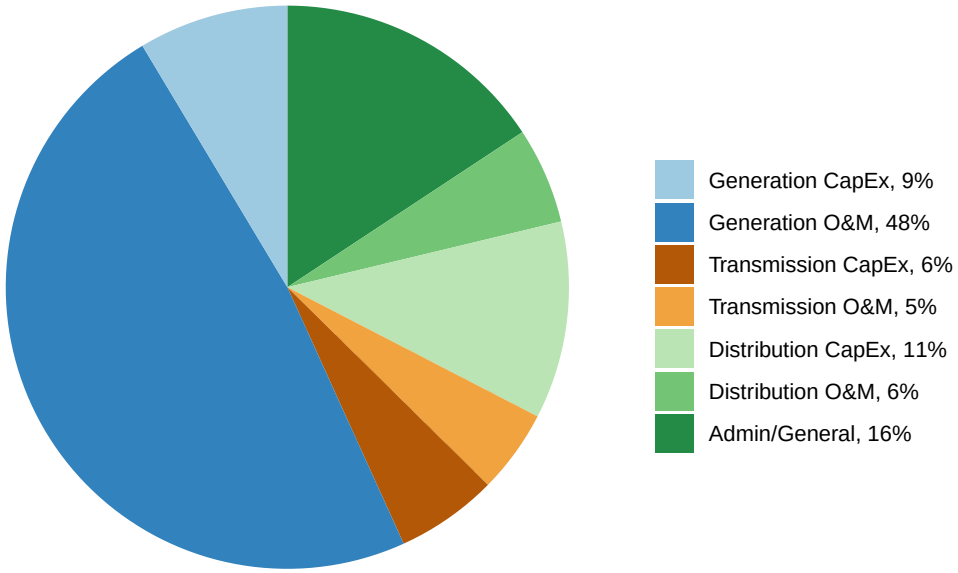

Figure 1.2: Reproduction of Figure 1.1 using data on utilities with regulated generation from Federal Energy Regulatory Commission (2009).

year, not depreciation. If a utility's capital expenses increase in a given year, this implies a real increase in annual spending on capital assets.[8]

The summary statistics for proven capacity and costs are provided in Table 1.1. $CapEx_{i,t}$ and $OpEx_{i,t}$ describe, respectively, the capital and O&M expenses incurred by utility i in year t. To make comparisons between utilities of different sizes meaningful, our analysis centers on per-kW distribution costs, defined as distribution expenses divided by proven system capacity.[9] The total per-kW distribution capital expense is denoted $CapEx_{i,t}^{kW}$ and the total per-kW distribution O&M is denoted $OpEx_{i,t}^{kW}$. All financial figures are adjusted to 2018 dollars. Though overall costs vary by several orders of magnitude between utilities of different sizes, the per-kW capital and O&M costs exhibit considerably less variability.

[8]Total Distribution Plant Additions are recorded on page 206, line 75(c) of Federal Energy Regulatory Commission (2009). Total Distribution Expenses (O&M) are recorded on page 322, line 156(b). The copy of Form 1 data used in this analysis was accessed through S&P Global (2021).

[9]A similar approach is used in Kopsakangas-Savolainen and Svento (2008), except instead of normalizing by the proven capacity, they normalize by the volume of sales (producing a figure in \$/kWh).

Table 1.1: Summary statistics of capital and O&M expenses, computed over 808 data points (101 utilities over eight years). $C_{i,t}$ is the proven capacity in MW. $CapEx_{i,t}$ and $OpEx_{i,t}$ are the overall distribution capital and O&M expenses for each utility. $CapEx^{kW}_{i,t}$ and $OpEx^{kW}_{i,t}$ are the per-kW (proven capacity) capital and O&M expenses.

	$C_{i,t}$ (MW)	$CapEx_{i,t}$ ($)	$OpEx_{i,t}$ ($)	$CapEx^{kW}_{i,t}$ ($/kW)	$OpEx^{kW}_{i,t}$ ($/kW)
Minimum	7	83,242	85,816	0.4	0.4
5%	86	1,403,947	1,567,595	13.2	9.2
25%	1,439	35,928,049	25,050,648	20.9	13.6
Median	3,053	69,090,853	47,744,916	27.2	17.0
Mean	4,587	131,942,503	80,364,501	28.6	20.0
75%	6,261	166,369,825	93,462,371	34.5	23.4
95%	16,789	496,617,661	271,851,419	51.0	42.8
Maximum	23,613	1,114,231,772	593,461,903	81.0	92.5
Standard Deviation	4,853	172,216,133	96,372,471	11.6	11.2

The growth rate of proven capacity, $Growth_{i,t}$, is computed using a 5–year rolling window.[10] This is described in Equation 1.1, which is an inversion of the classic "compounding interest" formula. This approach is similar to how Mai et al. (2018) compute the compounding annual growth rate of electricity sales.

$$r_{i,t} = \left[\frac{C_{i,t+2}}{C_{i,t-2}}\right]^{1/4} - 1 \tag{1.1}$$

To compute customer density, $Density_{i,t}$, the total number of customers for utility i in year t is divided by the utility's service territory area in square miles. This area is computed using the Department of Homeland Security's Electric Retail Service Territories database (Department of Homeland Security, 2019).[11] We expect a negative correlation between density and distribution

[10]Measuring growth only between consecutive years would produce a computed growth rate of zero for years in which the observed system peak does not increase, even if utilities are investing in anticipation of future load increases. Furthermore, electric utilities plan their investments over several years, and large capital expenditures tend to either respond to anticipate significant increases in system peak. Consequently, investments associated with load growth and a related increase in proven capacity do not necessarily occur in the same year. 1.4.4 presents results for the regressions performed using different estimates of the growth rate. In order to compute the growth rates for the entire 8-year window from 2000-2007 (inclusive), we include observed system peaks from 1998-2009.

[11]The DHS database only reports current service territory data. If a utility's service territory changed significantly between the study years and the most recent update of the DHS database, this would not be captured in our

costs because higher density means more load can be served by a single length of feeder (Filippini, Hrovatin, & Zorič, 2004; Filippini & Wild, 2001; Yatchew, 2001).

The percentage of underground assets, $Underground_{i,t}$, is computed as the ratio of the gross value of underground conduit and conductors divided by the gross value of all distribution assets. Larger shares of underground assets would be expected to increase capital costs (more labor is required to bury a line), though this may be offset in part by a reduction in O&M costs (fewer lines are likely to be damaged in a storm) (Fenrick & Getachew, 2012).

$Residential_{i,t}$ is defined as the proportion of volumetric sales (kWh) to residential customers.[12] Higher proportions of sales to residential customers are expected to increase distribution costs (Fenrick & Getachew, 2012).

Summary statistics for the explanatory variables are provided in Table 1.2. These statistics describe a highly heterogeneous set of observations. While the mean and median observed growth rates of system capacity are broadly consistent with the growth rate of aggregate energy sales projected in Mai et al. (2018), at least 5% of utility-year combinations have no observable growth in proven capacity. Likewise, 5% of observations have annual growth rates exceeding 4.8%.

Customer density, like population density in general, is found to be exponentially distributed in the dataset. The maximum observed value for customer density is twenty times larger than the median. In all regressions that include customer density, a natural log transformation is used. This method prevents a few utilities with very high densities from distorting the results.

We also note the sizable range in investments in underground assets and sales to residential customers. There are examples of utilities with no underground conductors or conduit, as well utilities with nearly half of their distribution assets underground. Similarly, for some utilities, nearly three-quarters of sales are to residential customers. Others exclusively serve commercial

estimate of customer density.

[12]The total number of retail customers is recorded in Federal Energy Regulatory Commission (2009) on page 301, line 12f. The gross values of underground conductors and underground conduit are recorded on page 207, lines 66g and 67g, and the gross value of all distribution assets is recorded on line 75g. The volumetric sales to residential customers are recorded on page 301, line 2d. The total volumetric sales to all customers are recorded on page 301, line 12d.

	$Growth$	$\ln(Density)$	$Underground$	$Residential$
Minimum	0%	-1.1	0%	0%
5%	0%	1.2	5%	21%
25%	0.7%	2.9	11%	30%
Median	1.6%	3.7	18%	35%
Mean	1.9%	3.6	19%	34%
75%	2.7%	4.6	23%	39%
95%	4.8%	5.8	38%	47%
Maximum	8.3%	6.7	46%	73%
Standard Deviation	1.5%	1.4	10%	9%

Table 1.2: Summary statistics of the explanatory variables. *Growth* is the annual growth rate of system peak, computed over a 5-year rolling window. *Density* is the density of customers in the utility's service territory (customers/square-mile). *Underground* is the proportion of total distribution assets categorized as either underground conductors or underground conduit. *Residential* is the proportion of volumetric energy sales to residential customers (compared to commercial or industrial).

and industrial loads ($Residential = 0\%$);

1.3 Methodology

In order to develop an empirical model of electric distribution system costs, we perform a series of regressions relating per-kW capital and O&M expenses to various factors, including the growth rate of proven system capacity, the proportion of distribution assets installed underground, the natural logarithm of customer density within the utility's service territory, and the share of sales to residential customers.

In the first model, we run a simple regression of the per-kW capital costs on the estimated growth rate of proven capacity. Observations are weighted by the utility's proven capacity so that the resulting model parameters can be understood to represent the costs associated with an average unit of capacity across all utilities. The formulation for this model is described in Equation 1.2, where $Growth_{i,t}$ is the growth rate of system capacity in percentage points, the β terms are the estimated intercept and coefficient, $Year_t$ is a fixed effect for the year, and $\epsilon_{i,t}$ is an error term.

$$CapEx_{i,t}^{kW} = \beta_0 + \beta_{Growth} Growth_{i,t} + Year_t + \epsilon_{i,t} \tag{1.2}$$

The regression's fit is visualized in Figure 1.3. Each point on the scatter plot of per-kW capital cost vs. growth rate represents one utility for one year, where the size of the point is proportional to the utility's proven capacity. Points on the left side of the plot represent utilities in years with low load growth, while points further to the right represent utilities that are rapidly expanding their system capacity. The best-fit line delineates the weighted regression described above. The intercept on the y-axis (which includes the intercept term as well as the mean of the fixed effects) is the average per-kW distribution cost for the case of no growth. This statistic describes the per-kW distribution capital cost associated with sustaining a given capacity level through routine replacement of equipment. The slope of the best-fit line describes the growth rate-coefficient, β_{Growth}, which is interpreted as the change in per-kW costs in response to a one percentage point increase in the growth rate. The y-intercept, which describes the average annual cost of maintaining an existing capacity level without growth, is estimated as $\beta_0 + \overline{Year_t}$. The alternative specifications described below include additional explanatory variables but follow the same basic architecture.

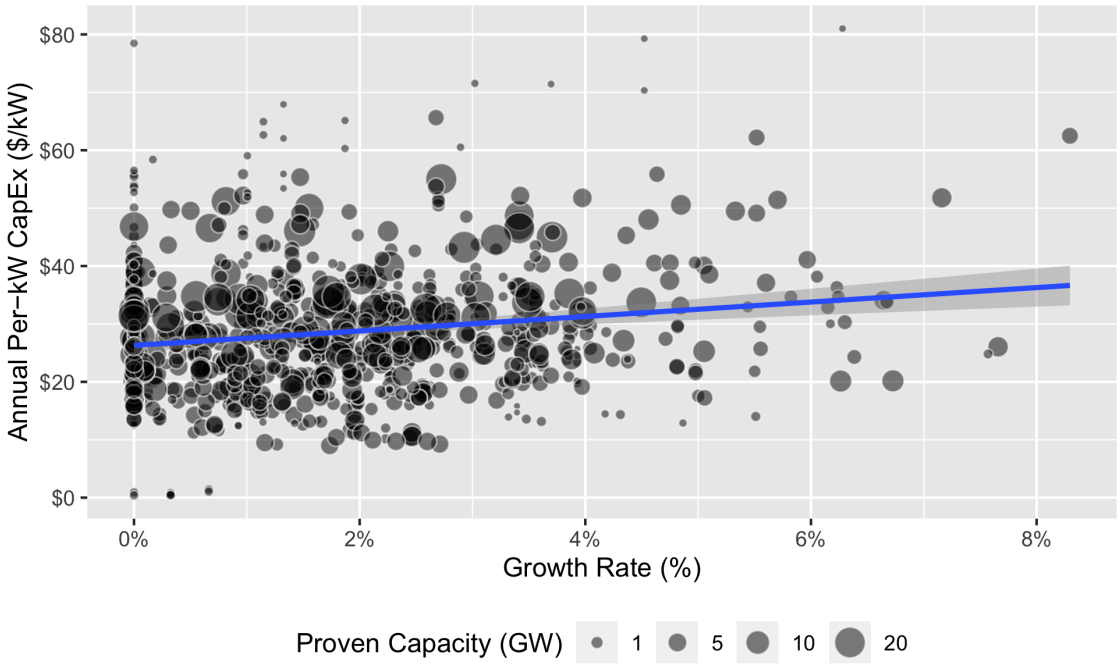

Figure 1.3: Relationship between per-kW-capacity distribution capital costs and growth rate for major U.S. utilities. 808 points representing 101 utilities over eight years. The best-fit line represents the univariate regression of capital expenses (in $ per-kW) on the compounding annual growth rate of distribution capacity, weighted by the utility's proven capacity. The shaded region covers a level 0.95 confidence interval.

In the second empirical model, we add controls for the previously discussed utility attributes: the percentage of underground assets, the natural logarithm of customer density, and the share of sales to residential customers. If any of these variables independently affect distribution costs and are correlated with growth (e.g., if load is growing more rapidly in cities due to urbanization), then omitting them would produce a biased estimate of β_{Growth}. The formulation for this model is described in Equation 1.3, which modifies Equation 1.2 by adding $\boldsymbol{X}$, a matrix of the attribute variables, and $\boldsymbol{\beta}$, a vector of associated coefficients to be estimated. The average cost of maintaining an existing capacity level without growth is estimated as $\beta_0 + \boldsymbol{X}\boldsymbol{\beta} + \overline{Year_t}$.

$$CapEx_{i,t}^{kW} = \beta_0 + \boldsymbol{X}\boldsymbol{\beta} + \beta_{Growth} Growth_{i,t} + Year_t + \epsilon_{i,t} \tag{1.3}$$

In addition to these characteristics, we expect distribution costs to vary with other factors,

including the regulatory environment, the price of inputs (including labor and materials), weather, and the geographic terrain. As some of these factors are difficult to quantify accurately, we use indicator (dummy) variables for the utility's region, R_i,[13] as a proxy. This method is expected to capture some of this unobserved heterogeneity without overfitting the model (as a state-level indicator would likely do). The region variable is commonly used as an indicator of electric system costs in energy modeling exercises (Baughman & Bottaro, 1976; Energy Information Administration, 2019c).[14] It is included in the third and fourth models.

It seems reasonable to expect that the factors that affect the cost of maintaining an existing level of distribution capacity could also affect the cost of increasing that capacity. We address this by including interaction terms between each of the attribute variables and the growth rate in the fourth regression. For example, if having a large proportion of underground assets means that it is more costly to upgrade distribution infrastructure to accommodate a higher peak, this would be captured in the fourth regression as an interaction between *Growth* and *Underground*.

Finally, a fifth model includes fixed effects for each utility, denoted $Utility_i$. This approach, described in Equation 1.3, removes the unobserved time-invariant characteristics particular to each utility. These include the utility attributes used in the multivariate regression (which are not perfectly constant from year to year, but exhibit little variation for a given utility) as well any constant features that vary between utilities but do not significantly change during the study period (such as labor and policy costs). This approach does not remove the effects caused by time-varying heterogeneity specific to each utility, such as state-specific regulatory changes that occur within the study period. However, because a separate fixed effect is included for the year in all models, country-wide trends that affect costs for all utilities are captured. Of the models discussed, this formulation provides the highest degree of confidence that the estimated growth rate coefficient is unbiased.

[13]The utilities are divided into six regions: Mid–Atlantic, New England, Southeast, Southwest, Midwest, and West. Mid-Atlantic is treated as the reference group in the regressions that include a fixed effect for the region. Summary statistics for each individual utility, including its region, are included in Appendix A.

[14]Baughman and Bottaro (1976) divide the continental United States into nine regions, finding significant differences in costs. Energy Information Administration (2019c) groups U.S. utilities into 22 different regions and finds that the highest–cost region (New York City and Westchester, NY) has unit costs that are more than five times those in the lowest–cost regions (Texas, Michigan, and Wisconsin).

$$CapEx_{i,t}^{kW} = \beta_0 + \beta_{Growth} Growth_{i,t} + Year_t + Utility_i + \epsilon_{i,t} \tag{1.4}$$

The above formulations are also used to estimate models for O&M expenses, $OpEx_{i,t}^{kW}$. The results of these regressions are presented in Section 1.4.2.

1.4 Results

1.4.1 Capital Expenses

Table 1.3 summarizes the results of the regressions of per-kW capital costs. The rows are the explanatory variables described in Section 1.2, the columns represent the different specifications described in Section 4.2, and the value in each cell is the β-coefficient associated with a variable for a given model with the standard errors in parentheses.

Column (1) presents the results from running capital costs on growth without controls. The intercept term (which includes the average of the fixed effects) is interpreted as the per-kW recurring cost for sustaining a given capacity level. According to this model, a utility with no load growth will spend $26.47 per kW each year on distribution-related capital projects. These may be incurred to improve reliability and resilience or comply with new standards. A hypothetical utility with a 1 GW peak and zero growth would be expected to spend $\$26.47 * (1e6kW) = \$26,470,000$ each year on sustaining distribution capacity.

The growth rate coefficient, β_{Growth}, is the change in a utility's per-kW capital expenses

[15]The mean of the fixed effects is included in the intercept term. For the formulation in column 5, the intercept is computed by separately calculating the means of the fixed effects for year and utility and adding these together. To compute the standard error for the intercept, we compute separate clustered standard errors for each year and utility by bootstrapping, compute the mean standard error for each group, then combine these using a root-mean-square calculation. For columns 3 and 4, the reference region described by the intercept term is the Mid-Atlantic.

[16]The mean of the fixed effects is included in the intercept term. For the formulation in column 5, the intercept is computed by separately calculating the means of the fixed effects for year and utility and adding these together. To compute the standard error for the intercept, we compute separate clustered standard errors for each year and utility by bootstrapping, compute the mean standard error for each group, then combine these using a root-mean-square calculation. For columns 3 and 4, the reference region described by the intercept term is the Mid-Atlantic.

Table 1.3: Results from regression models of distribution capital expenses. The coefficient in the *Growth* row describes the dollar-per-kW increase in distribution capital costs when the growth rate increases by one percentage point. Values in parentheses are the standard errors clustered by utility. [16]

	Annual Per-kW Distribution Capital Costs				
	(1)	(2)	(3)	(4)	(5)
Intercept	26.47***	14.30***	15.37***	12.79***	27.20***
	(1.41)	(1.07)	(0.75)	(0.74)	(0.54)
Growth	1.70***	0.74**	0.67**	2.04	0.76***
	(0.53)	(0.35)	(0.27)	(1.52)	(0.20)
Underground		0.57***	0.34***	0.34***	
		(0.11)	(0.10)	(0.12)	
ln(*Density*)		−1.69***	−0.27	0.02	
		(0.65)	(0.78)	(0.91)	
Residential		0.23**	0.12*	0.17	
		(0.11)	(0.07)	(0.10)	
Midwest			−0.85	−0.87	
			(1.81)	(1.83)	
New England			17.40***	17.30***	
			(2.93)	(2.98)	
Southeast			1.43	1.45	
			(2.06)	(2.05)	
Southwest			−2.05	−2.13	
			(2.70)	(2.70)	
West			10.85***	10.84***	
			(3.34)	(3.35)	
*Growth*Underground*				0.003	
				(0.03)	
*Growth**ln(*Density*)				−0.17	
				(0.25)	
*Growth*Residential*				−0.02	
				(0.03)	
R^2	0.065	0.373	0.602	0.603	0.072
Adjusted R^2	0.055	0.365	0.594	0.594	−0.071
Observations	808	808	808	808	808
Year Fixed Effects	*X*	*X*	*X*	*X*	*X*
Utility Fixed Effects					*X*

*p<0.1; **p<0.05; ***p<0.01

when its growth rate increases by one percentage point. In the first specification, this cost is estimated as \$1.70 per-kW-percentage-point. If the hypothetical utility described above increases its capacity by 1% (10 MW) in a given year, it would be expected to spend an additional $\$1.70 * (1e6kW) * (1 \text{ percentage point}) = \$1,700,000$ on growth-related costs, which amounts to \$170 per new kilowatt of capacity. If the utility's proven capacity stays constant in subsequent years, then it would be expected to spend $\$26.47 * (1.01e6kW) = \$26,734,700$ each year in capital expenses to sustain that capacity. In this way, an increase in capacity to accommodate new load results in both an upfront cost as well as recurring annual costs.

It should be stressed again that because the first model does not account for some important factors that are correlated with growth, it is likely that the estimated coefficients are biased. Column (2) presents results for the multivariate regression that controls for the proportion of underground assets (percentage points), the natural log of customer density per square mile, and the share of sales to residential customers (percentage points). The regression in column (3) includes these variables and the region dummy. Notably, the estimated coefficient for growth rate in these formulations is only \$0.67–\$0.74 per-kW-percentage-point, less than half of the value estimated in the model run without controls. This finding suggests that some part of the correlation between high per-kW costs and the high growth rate observed in the first regression is better explained by other features of the utility.[17]

The coefficient for the proportion of underground assets describes the increase in annual per-kW capital costs for a utility when the share of underground assets increases by one percentage point. According to column (2), utilities with a one percentage point higher proportion of their assets underground spend \$0.57 more per-kW of capacity each year on capital expenses. For column (3), this number is estimated at \$0.34 per kW.

Our results also suggest that utilities with higher customer densities have lower distribution costs. If the natural log of customer density increases by one, distribution capital costs decrease by \$1.69 per kW according to the specification in column (2). This finding is likely because a

[17]The intercept coefficients are also nominally smaller because the newly-added explanatory variables capture part of the sustaining cost. A detailed comparison of the growth vs. sustaining costs is addressed in the Section 1.5.

given length of conduit or conductor in a dense region can serve more customers (and more load) than the same asset in a less dense region. This effect is not significant when we add regional dummies, perhaps in part because the region variable captures some of the same variation in the underlying data. Per-kW capital costs also increase with a higher share of residential customers.

Results in column (3) indicate that the utility's region is also significant in explaining distribution capital costs. For a utility located in New England, the annual cost of maintaining a given level of peak capacity is $17.40 per kW more than the reference utility located in the Mid-Atlantic region. While not all regions demonstrate statistically different costs than the Mid-Atlantic, the set of indicator variables as a whole are highly significant (a partial F-test yields a statistic of 91). Inclusion of the region variable increases the adjusted R-squared from 0.365 to 0.594.

The multivariate regression with interaction terms (column 4) tests whether some of the variables that impact the cost of maintaining a given capacity level also impact the cost of growth. We find that none of the interaction coefficients computed are statistically significant and that the inclusion of the interaction terms does not improve the adjusted R-squared over the formulation summarized in column (3), nor does it provide a statistically different fit ($F = 0.808$). Statistical interactions are challenging to prove with regression and often require a significantly larger dataset than primary effects (Gelman, 2018). With only 808 data points, the failure of this exercise to prove that attributes like customer density affect a utility's growth cost does not rule out the possibility of an underlying relationship.

Column (5) presents results from the regression that includes utility fixed effects. This specification estimates a growth rate-coefficient of $0.76 per-kW-percentage-point, consistent with the estimated coefficients computed in columns (2) and (3). These findings indicate that the estimates obtained from the multivariate analyses are not likely biased by omitted time-invariant heterogeneity between utilities. Other potential sources of bias in the estimated coefficient for growth rate are discussed in Section 1.5.

1.4.2 Operations and Maintenance Costs

We repeat the regression models used to explain per-kW capital expenses, this time with per-kW O&M as the dependent variable. Regression results are summarized in Table 1.4.

Notably, we do not find any statistically significant relationships in the specifications in columns (1) or (2). Adding the regional dummies in column (3) improves the fit, raising the adjusted R-squared to 0.353. New England utilities have the highest O&M costs, incurring $11.60 per kW more each year than Mid-Atlantic utilities. For O&M costs, the region variable likely serves as a proxy for labor, insurance, and other input costs that vary throughout the country.

1.4.3 Disaggregated Capital Costs

In recent years, per-capita electricity consumption has remained relatively constant (Energy Information Administration, 2017), so most measured load growth has come from an increase in the number of customers rather than an increase in per-customer consumption. Because load growth and customer growth are so tightly coupled, it is difficult to distinguish between those expenditures that are causally related to an increase in load (such as upgraded transformers) and those that are customer-related but correlated with an increased system peak (such as the installation of new meters). Because electrification of heating and transportation is poised to increase per-customer load, it is valuable to separate load-related expenses from customer-related expenses.

One approach to separating load effects and customer effects would be to include measurements of both in the model formulation. However, because these two variables are highly collinear

[18]The mean of the fixed effects is included in the intercept term. For the formulation in column 5, the intercept is computed by separately calculating the means of the fixed effects for year and utility and adding these together. To compute the standard error for the intercept, we compute separate clustered standard errors for each year and utility by bootstrapping, compute the mean standard error for each group, then combine these using a root-mean-square calculation. For columns 3 and 4, the reference region described by the intercept term is the Mid-Atlantic.

[19]The mean of the fixed effects is included in the intercept term. For the formulation in column 5, the intercept is computed by separately calculating the means of the fixed effects for year and utility and adding these together. To compute the standard error for the intercept, we compute separate clustered standard errors for each year and utility by bootstrapping, compute the mean standard error for each group, then combine these using a root-mean-square calculation. For columns 3 and 4, the reference region described by the intercept term is the Mid-Atlantic.

Table 1.4: Results from regression models of distribution O&M expenses. Notably, there is no statistically significant relationship observed between O&M costs and the growth rate of system capacity. Values in parentheses are the standard errors clustered by utility.[19]

	Annual Per-kW Distribution O&M Costs				
	(1)	(2)	(3)	(4)	(5)
Intercept	17.61***	17.69***	24.12***	19.75***	19.71***
	(0.8)	(0.8)	(0.6)	(0.7)	(0.3)
Growth	0.25	0.31	0.09	2.44	0.12
	(0.36)	(0.33)	(0.28)	(1.56)	(0.14)
Underground		−0.03	−0.08	0.06	
		(0.09)	(0.07)	(0.08)	
ln(*Density*)		0.35	−0.51	−0.99	
		(0.61)	(0.74)	(0.66)	
Residential		−0.02	0.04	0.12	
		(0.08)	(0.08)	(0.09)	
Midwest			−4.19*	−3.87	
			(2.45)	(2.41)	
New England			11.56***	12.01***	
			(3.51)	(3.58)	
Southeast			−7.69***	−7.36***	
			(2.75)	(2.70)	
Southwest			−9.94***	−9.67***	
			(3.08)	(3.05)	
West			−0.61	−0.23	
			(4.17)	(4.11)	
*Growth*Underground*				−0.06**	
				(0.03)	
*Growth**ln(*Density*)				0.22	
				(0.28)	
*Growth*Residential*				−0.04	
				(0.03)	
R^2	0.003	0.006	0.366	0.392	0.006
Adjusted R^2	−0.007	−0.007	0.353	0.377	−0.147
Observations	808	808	808	808	808
Year Fixed Effects	*X*	*X*	*X*	*X*	*X*
Utility Fixed Effects					*X*

*p<0.1; **p<0.05; ***p<0.01

(more customers produce a higher peak), coefficient estimates derived from this regression would be unreliable. This was observed by R. L. Fares and King (2017), who chose to perform separate regressions for each explanatory variable: system peak, number of customers, and volumetric sales.

Sidestepping this problem, we use the disaggregated "account-level" capital expense data from FERC Form 1, categorizing each expense into one of four categories: Load, Conductors, Access, and Customers.[20] Summary statistics for these categorized expenses are provided in Table 1.5.

	Load ($/kW)	Conductors ($/kW)	Access ($/kW)	Customer ($/kW)
Minimum	0.09	0.16	0.00	-0.60
5%	2.80	3.62	2.13	1.13
25%	5.54	6.02	3.90	2.61
Median	7.82	8.10	5.25	3.89
Mean	8.13	9.46	5.91	4.35
75%	10.29	11.03	7.41	5.42
95%	14.20	19.88	12.38	9.32
Maximum	36.02	36.92	18.89	21.46
Standard Deviation	3.88	5.37	3.09	2.76

Table 1.5: Summary statistics of distribution capital expenses by category. For a typical utility, investments in transformers and conductors represent over 60% of per-unit capital costs. The aggregate per-kW costs are reported in Table 1.1.

To identify how these demand-related costs are affected by various explanatory variables, we adapt the univariate regression that includes a fixed effect for the utility (column 5 in Table 1.3) so that the dependent variable is computed using figures from each of the four categories, instead of the aggregate distribution capital cost data.

By disaggregating the capital expenditures data, we can see how spending patterns on different

[20]The "Load" category includes substation equipment (including batteries) and line transformers. The "Conductors" category includes capital investments for overhead and underground wires. The "Access" category includes physical infrastructure required to reach a customer, including structures, poles, towers, fixtures, conduit, and land rights. "Customer" expenses include meters, services, customer installations, and leased property on customer premises. Lighting, which represents less than 3% of a typical utility's annual capital expenditures, is omitted.

asset types relate to peak growth. Table 1.6 describes the results of the disaggregated-cost fixed effects regression.

	Annual Per-kW Distribution Capital Costs			
	Load	Conductors	Access	Customers
Intercept	6.8***	7.8***	5.0***	3.7***
	(0.3)	(0.2)	(0.2)	(0.1)
Growth	0.13**	0.29**	0.14	0.15***
	(0.07)	(0.12)	(0.08)	(0.05)
R^2	0.014	0.048	0.018	0.029
Adjusted R^2	-0.139	-0.100	-0.132	-0.121
Observations	808	808	808	808
Year Fixed Effects	X	X	X	X
Utility Fixed Effects	X	X	X	X
Note:				*p<0.1; **p<0.05; ***p<0.01

Table 1.6: Results from the regression that includes a fixed effect for the utility (column 5 in Table 1.3), applied to disaggregated distribution capital expenses. The results indicate that capital spending on conductors is significantly more sensitive to the growth rate of peak capacity than other categories. The intercept is computed by separately calculating the means of the fixed effects for year and utility and adding these together. Values in parentheses are the standard errors clustered by utility.

The regression estimates that per-kW spending on conductors increases by \$0.29 when the growth rate of system capacity increases by one percentage point. By comparison, spending on load- and customer-related equipment each increase by only \$0.13–0.15/kW in response to a one percentage point increase in growth rate. In a scenario where load increases but the number of customers and their locations stay the same, one should anticipate that the balance between these costs may shift.

1.4.4 Alternative Estimates of the Growth Rate

In the previous sections, the growth rate of system capacity, *Growth*, is estimated empirically as the compounding growth rate of a utility's proven distribution system capacity, computed using a 5-year rolling window. Because a utility's proven capacity only increases in years that set

new record peaks, it is systematically biased to underestimate the distribution system's actual peak capacity in years with milder weather. Consequently, using a very narrow time window to estimate the growth rate will produce estimates of zero in the years when the distribution system is not stressed to its capacity, even if the utility is actively expanding capacity. Conversely, using a wider window is inherently less precise: an excessively wide window may cause the (non-zero) growth rate in a given year to be biased down by including several years of low load-growth in the rolling window. The aggregate effect is that there will be less observed variation in the growth rate for a given utility. The choice of a 5-year rolling window is intended to serve as a compromise, dampening the effects of inter-annual variation in observed peaks without flattening out any observable variance in the growth rate for a given utility.

This section presents the results of regressions applied using two alternative estimates of *Growth*, computed using a 3-year rolling window and a 7-year rolling window. These results are then compared to the original estimates that use a 5-year rolling window. All three estimates of the growth rate are described by Equation 1.5, where n is the width of the rolling window in years.

$$r_{i,t} = \left[\frac{C_{i,t+\frac{n-1}{2}}}{C_{i,t-\frac{n-1}{2}}}\right]^{\frac{1}{n-1}} - 1, \quad C_{i,t} \geq C_{i,t-1} \tag{1.5}$$

Table 1.7 provides summary statistics of the estimated growth rates. The growth rate computed over a 3-year rolling window, $Growth^3$, has more than 25% of estimated observations equaling 0%. $Growth^3$ also has a significantly higher maximum observation than $Growth^5$ or $Growth^7$, likely because the effects of multiple years of capacity growth are observed in one or two years when the proven capacity jumps, which happens whenever the distribution system reaches its design conditions.

Table 1.8 summarizes the regression results. In columns (1)-(3), we use the multivariate regression that controls for the three utility attributes discussed in Section 1.2. In columns (4)-(6), we use the regression that includes a fixed effect for the utility. Columns (1) and (4) compute *Growth* using a 3-year rolling window, columns (2) and (5) compute *Growth* using

Table 1.7: Summary statistics of the compounding annual growth rate, estimated using a 3-year, 5-year, and 7-year rolling window. The growth rate estimated over a 3-year window has a significantly higher standard deviation than the 5-year and 7-year estimates.

	$Growth^3$	$Growth^5$	$Growth^7$
Minimum	0.00%	0.00%	0.00%
5%	0.00%	0.00%	0.00%
25%	0.00%	0.67%	0.92%
Median	1.05%	1.64%	1.65%
Mean	1.82%	1.86%	1.83%
75%	3.09%	2.69%	2.53%
95%	6.15%	4.82%	4.39%
Maximum	13.91%	8.30%	6.21%
Standard Deviation	2.20%	1.53%	1.29%
Observations	808	808	606

a 5-year rolling window (the estimate used throughout the chapter), and columns (3) and (6) compute *Growth* using a 7-year rolling window.

The estimated growth rate coefficients in columns (1) and (4) are significantly smaller than the estimates in columns (2),(3),(5), and (6), indicating that the regressions that use a 3-year window to compute *Growth* attribute a smaller proportion of capital investments in the distribution system to capacity growth than regressions that use a wider window. One explanation is that because the growth rate is computed over a narrower window than the other estimates, growth in proven capacity (which is a function of both the actual system capacity and the weather) is not always observed in the same years that growth-related investments occur. In other words, even if the utility is actively expanding capacity to accommodate load growth, that growth may not be observed immediately if the network is not regularly stressed to its design conditions.

The estimated growth rate coefficient in columns (3) and (6), which use a 7-year rolling window, are similar to those estimated using a 5-year rolling window. The estimate in column (3) has a higher standard error, which renders the estimated coefficient insignificant. The estimated growth rate coefficient for the regression that uses a 7-year rolling window and includes a fixed

Table 1.8: Regression results using three different specifications for the growth rate. Columns (1)-(3) use the multivariate regression with controls. Columns (4)-(6) use the regression with fixed effects for the utility. Columns (1) and (4) summarize the regression results where *Growth* is computed using a 3-year rolling window, columns (2) and (5) summarize the results where *Growth* is computed using a 5-year rolling window (the specification used in the previous sections), and columns (3) and (6) summarize the results where *Growth* is computed using a 7-year rolling window.

	Annual Per-kW Distribution Capital Costs					
	(1)	(2)	(3)	(4)	(5)	(6)
Intercept	14.39***	14.30***	14.24***	25.13***	23.86***	24.69***
	(0.99)	(1.02)	(0.87)	(0.57)	(0.49)	(0.36)
$Growth^3$	0.32			0.23*		
	(0.21)			(0.12)		
$Growth^5$		0.74**			0.76***	
		(0.35)			(0.20)	
$Growth^7$			0.70			0.78***
			(0.55)			(0.28)
Underground	0.59***	0.57***	0.59***			
	(10.97)	(10.83)	(10.92)			
log(*Density*)	−1.72***	−1.69***	−1.82***			
	(0.66)	(0.65)	(0.65)			
Residential	0.24**	0.23**	0.24**			
	(10.52)	(10.75)	(11.30)			
R^2	0.366	0.373	0.386	0.019	0.019	0.044
Adjusted R^2	0.358	0.365	0.376	−0.133	−0.133	−0.159
Observations	808	808	606	808	808	606
Year Fixed Effects	*X*	*X*	*X*	*X*	*X*	*X*
Utility Fixed Effects				*X*	*X*	*X*
Note:	*p<0.1; **p<0.05; ***p<0.01					

effect for the utility is similar to the coefficients produced using a 5-year rolling window.

As discussed earlier, proven capacity is an imperfect approximation of the actual distribution system capacity, especially if one is interested in measuring changes in capacity between years. Much of the uncertainty discussed herein would be removed if comprehensive infrastructure data were made available for a broad sample of utilities. Until such a time, these estimates provide a heuristic for those interested in modeling electric distribution system expansion.

1.5 Discussion

The results suggest that while increases in system capacity are significant in explaining electric distribution capital costs, they represent a relatively small share of those costs. The majority of a typical utility's annual capital expenses are associated with sustaining a given capacity level, as described by the intercept term and attribute coefficients. Figure 1.4 depicts the proportion of capital costs related to growth for a single year for an electric utility with median characteristics[21]. At a typical annual growth rate between 1–2%, less than 10% of capital costs are explained directly by load growth. Even at an annual growth rate of 5%, less than 20% of a generic utility's annual distribution capital expenses are directly related to load growth.

The estimates of the increase in distribution costs from load growth are lower than many previous estimates, such as ICF Consulting (2005), which assumes that 50% of transmission and distribution investments are causally related to load growth. A review of infrastructure filings from state public service commissions indicates that it is not uncommon for utilities to report that load growth is only responsible for a small portion of their capital expenses. As part of its 2017 rate case, Central Hudson Gas & Electric Company in New York State reported a detailed schedule of its forecasted capital expenses from 2018–2022. Only 3% of capital investments in the distribution system were labeled as related to load growth (Central Hudson Gas & Electric Corporation, 2017, p. 120-122).[22] In California, Pacific Gas & Electric spent an average of $99

[21]Per table 1.2, a utility with median characteristics has a proven capacity of 3 GW, 40 customers per square mile ($ln(Density) = 3.7$), 18% of distribution assets invested as either underground conductors or underground conduit, and 35% of sales to residential customers.

[22]The rate case filings corresponding to the time period of this study did not include granular project data that

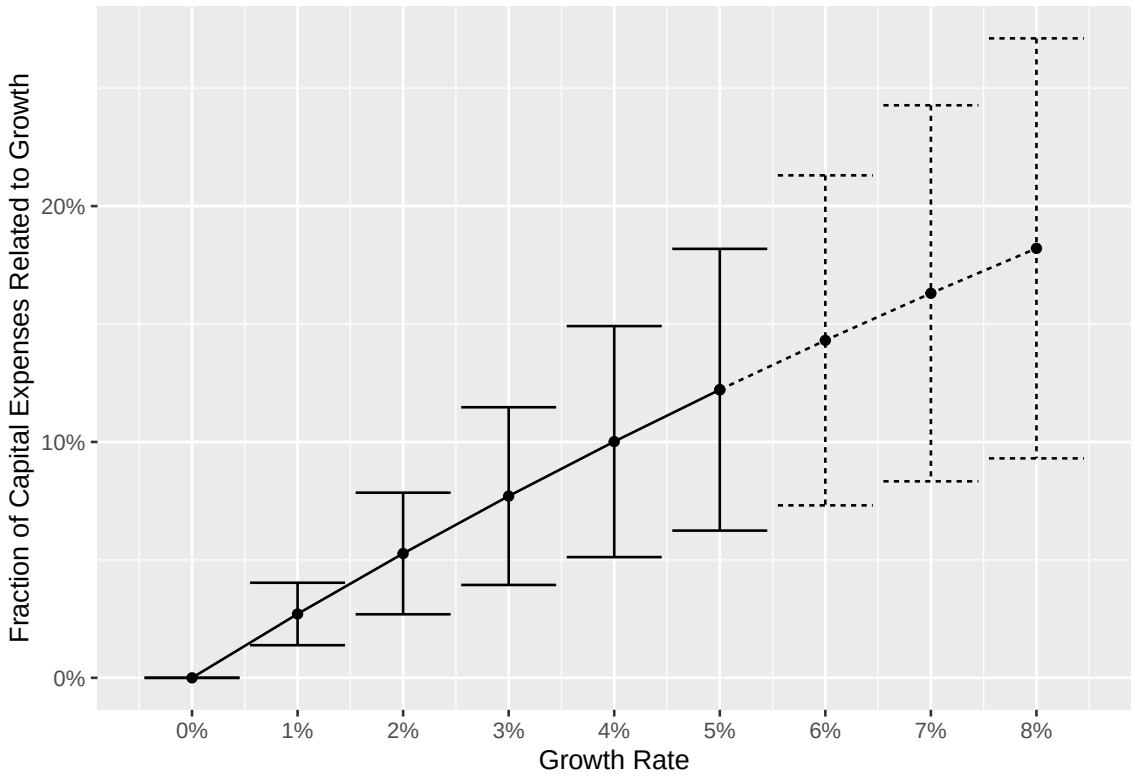

Figure 1.4: Upfront growth costs as a proportion of total distribution capital expenses vs. growth rate of system peak. For each percentage point on the x-axis, separate "growth" and "sustaining" costs are computed for a typical utility using the specification in Table 1.3, column (2), and the ratio of growth costs to overall distribution capital costs is plotted. Error bars are computed using the clustered standard errors of the growth rate coefficient. There is limited data for growth rates over 5%, so those estimates (represented with dashed lines) should be regarded as extrapolations.

million annually on projects related to expanding electric distribution capacity in 2000 and 2001 (Pacific Gas & Electric, 2018). This amounts to just 16% of their average distribution capital expenses for those years (Federal Energy Regulatory Commission, 2009).[23]

Multiplying the growth rate coefficient by a factor of 100 gives an estimate of the cost of an incremental unit of distribution capacity.[24] Our results indicate that this figure is around \$75/kW. This finding is at least an order of magnitude smaller than the estimates used in Larson

could be used to distinguish between growth-related and maintenance costs.

[23]We do not know of any public dataset that separately reports growth and maintenance costs incurred by a large sample of utilities. Such a dataset would help validate the empirical conclusions of this study.

[24]An example of this arithmetic, applied to the univariate regression, is provided in Section 4.5

et al. (2020), which assumes that new capacity costs $1,351/kW on average. There are several explanations for this discrepancy. For one, the authors draw on estimated distribution costs from Energy Information Administration (2019a), which includes administrative expenses (such as salaries and office space) as part of the distribution charge (Energy Information Administration, 2019b, p. 17). While some of these expenses may grow over time, it is not reasonable to assume that a doubling of per-capita electricity consumption would result in a doubling of administrative expenses. Additionally, a large proportion of distribution expenses – including land rights, structures, poles, towers, service drops, and meters – are not directly related to the level of consumption. If customers were to increase their loads by electrifying their heating and transportation needs, a utility may need to upgrade some of its transformers but would not necessarily need to replace its poles or on-site meters. Administrative and distribution expenses that are unlikely to increase in response to an increase in load should be excluded from an estimate of the marginal distribution capacity cost based on accounting methods.[25] Furthermore, the accounting-based approach is very sensitive to changes in assumptions about the cost of capital and the economic life of utility assets. Increasing the assumed discount rate used in Zhang, Jenkins, and Larson (2020) from 4.4% to 8% and decreasing the equipment life from 40 years to 30 nearly halves the estimated per-kW cost of distribution assets. Likewise, the median estimates used in Elmallah, Brockway, and Callaway (2022), which range from $368 per-kW to $1,875 per-kW for circuit upgrades and from $888 to $18,863 for substation upgrades appear to over-estimate the cost of sustained load growth.

Another important observation is that the share of underground distribution assets significantly increases recurring capital costs. Some of the fastest-growing utilities (measured by the growth rate of proven capacity) are also engaging in the most aggressive undergrounding campaigns. For example, Nevada Power Company, which more than doubled its proven system capacity from 1994 to 2007, also increased the proportion of its assets invested as either underground conductors or conduit from 33% to 44% over the same period. While burying power lines offers myriad advantages to a utility's customers (such as improved reliability and

[25]See Lazar (2016, Chapter 9.2) for a discussion of how investments in the distribution system are classified as customer vs. load-related.

aesthetics), those benefits should be weighed against costs and alternatives should be considered where appropriate.

Because a utility's peak load and the number of customers it serves are highly correlated,[26] we did not attempt to distinguish between costs incurred to facilitate an increase in capacity and those incurred to accommodate an increase in the number of customers. Thus, some of the costs attributed to load growth in this analysis may be causally related to an increase in the number of customers (such as expenditures on new meters and service drops). In a future where significant load growth is caused by electrification, one would expect an increase in peak-related infrastructure costs but not necessarily customer-related costs. The results from four separate regressions of different categories of distribution capital costs are provided in 1.4.3.

1.5.1 Long-Term Growth Costs

When considering persistent load growth over an extended period, as would be expected from increased electrification of heating and transportation, both the upfront cost of new distribution capacity as well as recurring capital and O&M costs associated with that infrastructure should be taken into account. This section presents an extrapolation exercise in which we use the estimated parameters from Section 4.5 to compute the distribution costs for a utility from 2022 to 2035 under different growth scenarios.

This exercise uses the estimated parameters from column (2) of Tables 1.3 and 1.4 to forecast capital and O&M expenses.[27] We take the attributes of a typical 3 GW utility with 40 customers per square mile, 18% underground assets, and 35% of volumetric sales to residential customers, then assume five different capacity growth rates: 0%, 0.5%, 1.5%, 3%, and 5%. The resulting distribution expenses over time are plotted in Figure 1.5.

In the zero-growth scenario, the utility spends $132m annually between capital and O&M costs to maintain 3 GW of capacity. In the 0.5% growth rate scenario, the utility spends an

[26]The data used in this study indicate no statistically significant increase in proven capacity–per–customer from 2000–2007. Proven capacity and total customer count have a correlation coefficient of 0.95, making them functionally collinear (the logs of these variables have a correlation coefficient of 0.96).

[27]While the column (2) specification was used for simplicity, one would expect similar results from columns (3-5). All of the formulations except (1) have similar growth coefficients after accounting for interactions.

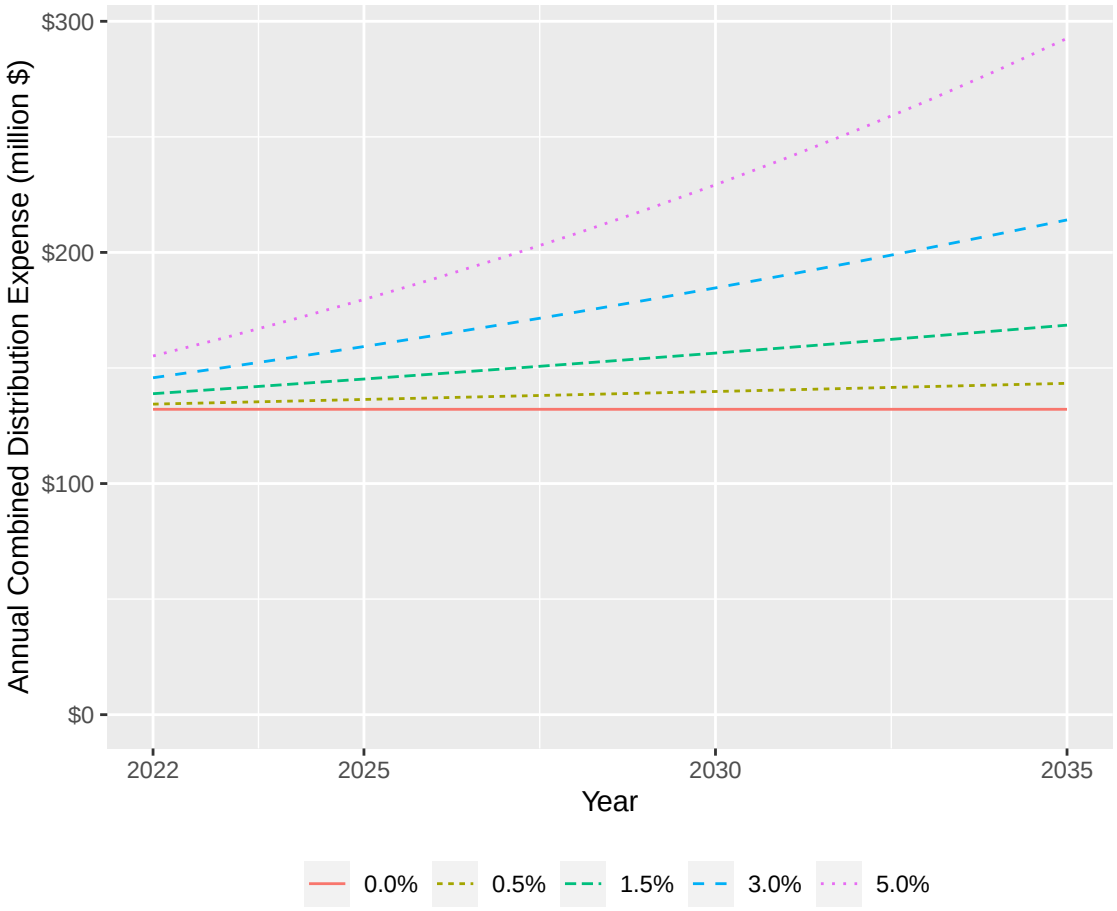

Figure 1.5: Annual distribution expenses (capital + O&M) for a typical 3 GW utility at five different growth rates from 2022-2035 (inclusive). The higher growth rates represent scenarios with aggressive electrification of heating and transportation. In the 5% growth rate case, annual expenses nearly double between 2022 and 2035.

additional $93m over the 14-year horizon to build and maintain an additional 217 MW of capacity by 2035. In the extreme case of 5% annual growth, the utility nearly doubles capacity while incurring $1.19b in additional expenses over the time horizon. A comprehensive summary of these results is provided in Table 1.9.

Since both capital and O&M costs are dominated by recurring annual expenses (rather than the one-time cost of increasing capacity, as described by the growth rate coefficient), we find that the growth rate has a relatively modest impact on average distribution costs. Assuming

Table 1.9: Growth rates and associated expenses for a typical 3 GW utility over the 14-year interval from 2022-2035 (inclusive). "Total Expenses" and "Additional Expenses" are aggregated (undiscounted) over the entire 14-year interval. "Capacity Increase" and "Additional Expenses" are measured in reference to the 0% growth case. "Average Electricity Cost" estimates the average distribution cost in $/MWh, assuming a constant load factor of 60% and that all expenses are recovered in the same year that they are incurred. If volumetric sales scale linearly with peak, then a 5% growth rate is only expected to increase delivery expenses by about $1/MWh ($0.001/kWh) over the zero-growth scenario. If expenses are discounted at an annual rate of 8%, the present value of distribution expenses (capital plus O&M) over the 14-year interval range from $1,089m for 0% growth to $1,686m for 5% growth.

Growth	Capacity		Total Expenses		Additional		Average
Rate	Increase (2035)		Capital	O&M	Expenses		Distribution Cost
(%)	(MW)	(%)	(millions)	(millions)	(millions)	(%)	($/MWh)
0.0%	-	-	$1,113	$737	-	-	$8.38
0.5%	217	7%	$1,172	$772	$93	5%	$8.48
1.5%	695	23%	$1,299	$847	$296	16%	$8.68
3.0%	1538	51%	$1,516	$975	$641	35%	$8.98
5.0%	2940	98%	$1,863	$1,178	$1,191	64%	$9.37

that load factors remain constant at approximately 60%[28] and that new capital costs are borne by ratepayers in the year they are incurred, a 5% growth rate would only increase the average distribution cost by about $1/MWh (0.1 cents/kWh) over the zero-growth scenario.

To provide a point of comparison, if one applies the methodology from ICF Consulting (2005) (assuming that distribution capital expenses are evenly split between growth and maintenance costs and that all O&M costs are unrelated to growth) to the complete data from 101 utilities, the median cost of growth across all utilities is $578/kW and the median recurring cost for sustaining capacity is $30/kW-year (capital plus O&M). If these coefficients are applied to the typical 3 GW utility above, the forecast expenditure over the 14-year interval is $1,260m in the zero-growth case and $3,551m in the 5% growth case, a 182% increase. This difference would amount to an increase of over $5/MWh (0.5 cents/kWh) in distribution costs, from $5.06/MWh in the zero-growth case to $10.30/MWh in the 5% annual growth case. Relative to the empirical

[28]The load factor describes the ratio of the average consumption of electricity to the observed peak. Electric vehicles are likely to increase load factors because they can be charged off-peak, leading to flatter daily consumption curves. Electric heating is poised to decrease load factors in areas where significant buildout is required to accommodate winter peaks.

model, the 50% heuristic appears to underestimate sustaining costs and overestimate the cost of increasing capacity for new load.

Conversely, if one assumes that distribution costs are correlated only with the distribution system's peak capacity (as is assumed in Vibrant Clean Energy, LLC et al. (2020) and Energy Information Administration (2019c)), then the average cost of distribution ($/MWh) would be entirely independent of the growth rate of the system peak. This assumption could lead analysts to underestimate how rapid growth due to electrification might impact ratepayers.

1.6 Conclusion and Policy Implications

We described the main determinants of electric distribution costs using annually-reported financial and operating data from 101 investor-owned utilities over eight years. We found through regression analysis that the growth rate of proven capacity, the proportion of assets installed underground, the density of customers within the utility's service territory, and the share of sales to residential customers are all significant in explaining per-kW distribution capital costs. None of the above variables were found to be useful in explaining O&M costs. The only reliable explanatory variable we found of per-kW O&M costs is the utility's region. Regional dummies, which explain part of the variation in capital and O&M costs, likely serve as proxies for other unobserved variables that change locally (such as labor or policy costs). Future work should identify these factors and quantify their effects directly.

Based on historical system peaks, we estimate that load growth represents less than 10% of distribution capital costs for a typical utility with an annual capacity growth rate of 1–3%. A 5% growth rate from 2021–2035 would nearly double distribution capacity while only increasing the average distribution cost by about $1/MWh (0.1 cents/kWh) relative to the zero-growth case. These results indicate that many of the distribution system reinforcements needed to accommodate widespread electrification of heating and transportation are achievable without significantly increasing costs to consumers.

Another notable result of our analysis is that distribution system costs vary widely throughout

the country and between utilities with different attributes. This finding suggests that widespread electrification of heating and transportation may become economical for some utilities before others. The Southwest has the lowest distribution costs (both capital and O&M), making Southwestern customers prime candidates for early adoption of end-use electrification as the grid becomes cleaner.

In conducting this analysis, we found that limited centralized data on distribution infrastructure posed a significant challenge to comparing capacity and growth between utilities. While utilities report transmission line additions to FERC, no such data are reported for distribution infrastructure. Moreover, while substation capacity data is reported, inconsistencies in reporting make it impractical to use these data for empirical analysis. If loads are growing in one part of a utility's service territory and shrinking in another, the approach used in this analysis (based only on observed peaks) would be unable to detect changes to aggregate system capacity. Standardized reporting of distribution line miles and aggregate transformer capacities would enable more accurate modeling in future work.

Load growth from electrification may be faster than recent trends and will likely come from higher per-customer consumption rather than growth in the number of customers. Because of the speed at which heating and transportation would need to be electrified in order to meet decarbonization goals, utilities should begin incorporating electrification into their infrastructure planning as soon as possible. Our estimates may serve as a helpful reference for practitioners and policymakers engaged with this effort.

Chapter 2

Simulation of Residential Energy Demands

In this chapter, we use the open-source building energy modeling (BEM) software packages EnergyPlus and ResStock to simulate hourly demands for buildings in five different climate regions across the United States. These data are then used in subsequent chapters as constraints to the optimization algorithms.

We observe that residential energy demands vary tremendously throughout the United States. In particular, space heating and cooling demands vary widely among regions, and between buildings within a region due to differences in construction properties. Domestic hot water demands and electric plug loads show considerably less variation.

2.1 Background and Literature Review

A number of factors influence residential energy demands. These include the climate in which the residence is located, the size of the residence, various features of the building's construction (including the envelope properties), as well as the number of residents and their habits.

Using BEM software to model residential energy demands offers two key advantages over a simpler model of electrical and thermal loads, such as a linear heating/cooling-degree model,

which assumes that the thermal demand for conditioning a space is a simple linear function of the outdoor temperature (Waite & Modi, 2020). First, it accounts for the effects of solar radiation and latent heat gains. Radiation can offset heating loads during the heating season and amplify cooling loads in the summer, while latent heat gains from infiltration can increase cooling loads related to dehumidification.

Second, building energy simulations allow for heating and cooling loads to vary based on differences specific to each building, including the underlying building physics and massing,[1] variable heating and cooling preferences, and different occupancy patterns. Consequently, the simulated heating and cooling loads better reflect the underlying building physics and diversity found in the real building stock.

2.1.1 Space Heating and Cooling

Space heating and cooling loads in buildings are driven by differences between ambient weather and the desired indoor conditions. According to Fourier's Law, the instantaneous conductive heat loss (or gain) through a building's envelope is directly proportional to the difference between the inside and outside temperatures. We may define the hourly "heating degrees" as the difference between the inside and outside temperatures when the outside temperature is below the inside temperature (e.g. if the inside temperature is 65°F and the outside temperature is 35 F, there are 30 heating degrees). Conversely, cooling degrees are the difference between the inside and outside temperatures when the outside temperature is above the inside temperature.

Since at least the 1930s, engineers have been using annual "heating-degree-days" and "cooling-degree-days" as metrics to describe the climatic drivers of heating and cooling energy demands (Marston, 1935). The heating degree days (HDDs) for a given location are an approximate integral of the hourly heating degrees throughout a typical year. HDDs are calculated by taking a year of temperature data, computing the average of each day's observed highs and lows, subtracting this number from 65, and summing all of the positive results. Cooling degree days (CDDs) are

[1] Building massing shifts heating and cooling loads to later hours, which is one of the reasons why peak air conditioning loads in the summer tend to occur in the late afternoon or evening, rather than at mid-day when the sun is the strongest.

computed the same way, but by summing only the negative results (reported as an absolute value). All else being equal, a building in a region with 10,000 HDDs should lose about twice as much heat through conduction as a building in a region with 5,000 HDDs.

Figure 2.1 plots the annual heating-degree-days and cooling-degree-days for the continental United States. We observe that HDDs and CDDs vary widely. In southern Texas and Florida, there are less than 1,000 annual HDDs; in the Upper Midwest, the annual HDDs can exceed 10,000. Likewise, CDDs range from near-zero in the Mountain states to over 1,800 in the South (National Oceanic and Atmospheric Administration, 2018).

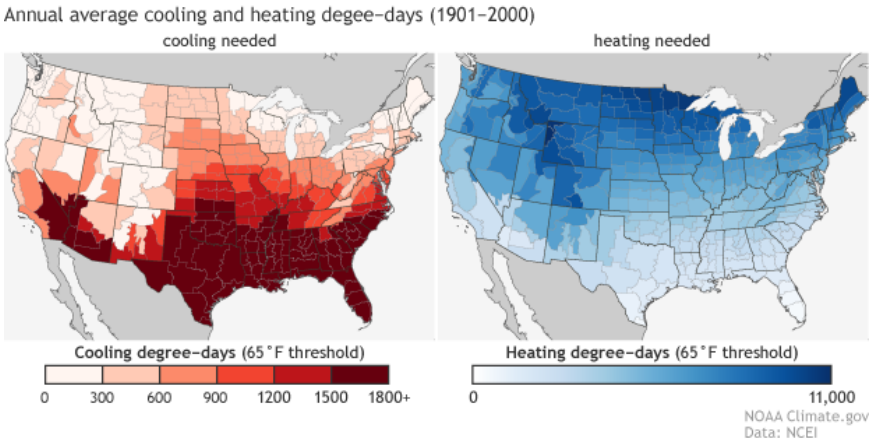

Figure 2.1: Maps of heating degree days and cooling degree days for the continental United States. Homes in southern states have the greatest number of cooling degree days, driving up air conditioning loads. Homes in the northern states have the greatest number of heating degree days, driving up space heating loads (National Oceanic and Atmospheric Administration, 2018).

In addition to conductive losses through a building's envelope, space heating and cooling loads include the energy associated with conditioning outdoor air that enters the building, either through controlled ventilation or unmanaged infiltration. When cold air enters a building, it must be heated up to room temperature. Because air has a relatively constant specific heat, the amount of energy required to bring outdoor air up to room temperature is proportional to the difference between the indoor and outdoor temperature. For a building with a constant rate of infiltration, the energy required to heat ambient air over the course of a year is approximately proportional to the heating degree days.

When warm air enters a building, it is typically necessary to both cool and dehumidify it.

Removing moisture from the air to bring the humidity down to an acceptable level is referred to as latent cooling. To account for the effect of latent cooling needs, engineers at the Pacific Northwest National Laboratory developed the International Energy Conservation Code (IECC) map (Pacific Northwest National Laboratory, 2015). The IECC map, shown in Figure 2.2, uses 15 regions, each described with a number (designating the temperature regime) and a letter (designating the humidity regime).

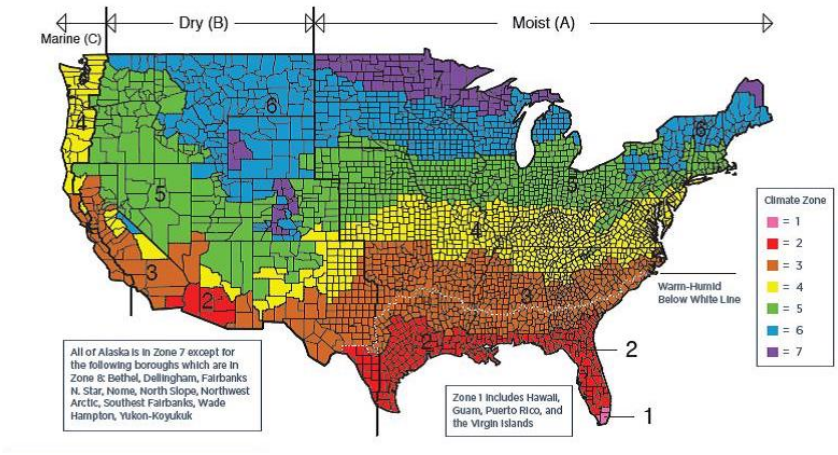

Figure 2.2: International Energy Conservation Code (IECC) Climate Regions. The numbers describe the temperature regime and the letters describe the humidity regime (U.S. Department of Energy & Pacific Northwest National Laboratory, 2015).

In 2003, the National Renewable Energy Lab simplified the IECC map into 8 climate zones, combined into five major climate categories/regions found in the continental United States. These are: hot-humid, hot-dry/mixed dry, mixed humid, marine, and cold/very cold. The Building America climate regions are illustrated in Figure 2.3.

Summary statistics from homes in the five climate regions are provided in Table 2.1. We observe that the average home in the Very Cold/Cold region uses 50% more energy for space heating than the average home in the Hot-Humid region, and nearly twice as much space heating energy as the average home in the Mixed-Dry/Hot-Dry region. This is due to a combination of their colder climate and larger-than-average floor area. Conversely, the average home in the hot-humid region uses about five times more energy for air conditioning than the average home in the Very Cold/Cold region and twice as much cooling energy as the average home in any other

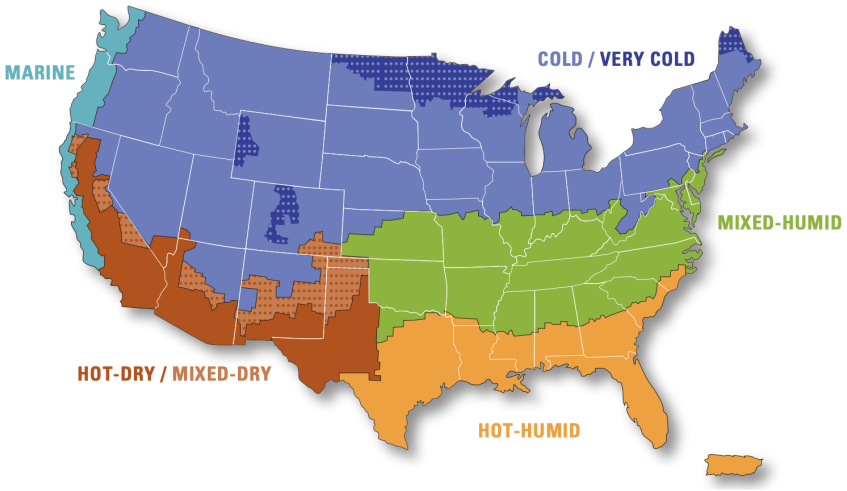

Figure 2.3: Building America Climate Regions. In this analysis, we select representative counties for the Cold, Hot-Dry, Hot-Humid, Mixed-Humid, and Marine regions (U.S. Department of Energy & Pacific Northwest National Laboratory, 2015).

region.

Table 2.1: Summary statistics of energy use in homes in each climate, as reported through U.S. Energy Information Administration (EIA) (2015). There is considerable variation in heating and air conditioning demands between regions. Of note, the average home in the Very Cold/Cold region uses 50% more energy for space heating than the average home in the Hot-Humid region, and nearly twice as much space heating energy as the average home in the Mixed-Dry/Hot-Dry region.

	Very Cold/Cold	Mixed-Dry/Hot-Dry	Hot-Humid	Mixed-Humid	Marine
Number of housing units (million)	42.5	12.7	22.8	33.5	6.7
Average area per housing unit (sf)	2,228	1,668	1,742	2,073	1,842
Heated area per housing unit (sf)	2,007	1,416	1,495	1,771	1,598
Cooled area per housing unit(sf)	1,334	1,256	1,483	1,530	713
Average site energy consumption (MMBTU)	94.2	51.8	59.7	80.7	57.3
Space heating consumption (MMBTU)	53.1	12.9	13.7	35.7	20.7
Water heating consumption (MMBTU)	16.5	14.5	10.9	15.1	16.2
Air conditioning consumption (MMBTU)	3.0	7.4	15.1	6.9	1.5
Refrigerator consumption (MMBTU)	2.5	2.6	2.7	2.6	2.7
Other consumption (MMBTU)	20.3	18.1	20.1	21.3	18.6

In addition to the climate region in which a residence is located, other factors can influence space heating and cooling demands, including the home's vintage, size, and construction (Administration, 2022). In the Midwest, homes built from 2010 to 2015 use on average about 40% less energy for space heating than homes built before 1960 (U.S. Energy Information Administration (EIA), 2015, CE3.3). In the South, energy use for air conditioning peaks in homes built between 2000–2009 (U.S. Energy Information Administration (EIA), 2015, CE3.4); newer homes use about 15% less energy, most likely due to the availability of higher-efficiency air conditioners.

2.1.2 Water Heating (DHW)

Domestic hot water (DHW) in homes is used by residents for showering, hand-washing, and cleaning dishes. Among the major end-uses in homes, water heating demand scales most closely with the number of household members. Table 2.2 shows the relationship between the number of household members and the amount of energy used for space heating, air conditioning, water heating (DHW), refrigeration, and all other end-uses. In 2015, the average two-person household consumed 12.5 million BTUs of energy for DHW heating; the average four-person household consumed 22.7 million BTUs. By comparison, the number of household members has only a very modest effect on the amount of space heating energy and refrigeration energy used for households with two or more members.

Table 2.2: Average energy demands for households of different sizes, in MMBTU (U.S. Energy Information Administration (EIA), 2015, CE3.1). Water heating and other (plug loads) scale most strongly with the number of households members.

Number of household members	1	2	3	4	5	6+
Space heating	29.9	36.2	37.7	37.4	38.1	39.1
Air conditioning	5.3	7.3	7.5	8.4	8.8	7.7
Water heating	7.4	12.5	17.7	22.7	24.1	28.7
Refrigerators	2.1	2.7	2.7	2.8	2.8	2.8
Other	13.1	19.9	22.1	26.4	26.6	29.4
Total	55.3	75.6	84.6	94.9	97.1	103.8

2.1.3 Plug Loads

Plug loads include refrigeration, lighting, electronics, laundry, and all other energy uses inside a home. Refrigeration energy tends to be relatively independent of the size of the household. Other plug loads tend to scale with the number of household members, though not as closely as domestic hot water. In Table 2.2, we observe that a household with 4 members uses approximately 30% more energy for lighting, electronics, etc. than a household with 2 members.

In our analysis, we simulate space heating, space cooling, water heating (DHW), and electric plug loads for homes from all five major climate regions found in the continental United States, as well as homes that range in size and vintage. This allows us to capture a representative range of characteristics affecting space heating, air conditioning, hot water heating, and plug loads.

2.2 Methodology

In each of the five major Building America climate regions, we select one example county meant to typify that particular climate. The five counties are: Erie, New York (cold); San Diego, California (hot-dry); Houston, Texas (hot-humid); Alexandria, Virginia (mixed-humid); and Marin, California (marine) (U.S. Department of Energy & Pacific Northwest National Laboratory, 2015). Summary statistics for these five example counties (along with modeling results) are provided in Table 2.6.

We use The National Renewable Energy Laboratory's ResStock Analysis Tool to sample construction and operational parameters that are representative of homes in each of the five counties (National Renewable Energy Lab (NREL), 2021).[2] These parameters are then used to construct individual EnergyPlus models for 75 residences (15 in each region), which contain detailed descriptions of all the major elements of a building that determine its energy use (wall construction, foundation type, occupancy patterns, etc.) and a model of the heating and cooling

[2]ResStock contains estimated probability functions describing the distribution of building properties for every county in the United States. By using ResStock to sample building properties, the modeled buildings can be said to be representative of the actual building stock in each example county. We note that this does not guarantee that the individual buildings are representative of the whole climate region

equipment installed within a building.[3]. The 15 residences in each region are presumed to reside on a single electric feeder and represent the full load on that feeder.[4]

Using the EnergyPlus models, we run year-long simulations using weather based on data from a typical meteorological year (TMY3).[5] From the results, we extract hourly demands for space heating, space cooling, water heating (DHW), and electric plug loads for the fifteen representative single-family homes in each county.

For simplicity, we exclusively model single-family detached homes with existing central warm-air furnaces. This is the most common heating topology for single-family homes in the U.S., found in about two-thirds of detached single-family homes that use space heating equipment (U.S. Energy Information Administration (EIA), 2015, Table HC6.1).

Summary statistics for the modeled buildings are provided in Tables 2.3 and 2.4. Table 2.3 provides descriptive statistics for several important variables, including the year built, the number of occupants, infiltration rates, and the areas of walls, floors, windows, and roofs. While the sizes of modeled residences vary significantly in all five climate regions (the largest homes have more than twice the floor area of the smallest), the mean floor area does not show a huge amount of variation between regions. Residences in the marine climate, which are the smallest, are only about 19% smaller on average than those in the mixed-humid climate, which are the largest. Consequently, the total floor area modeled in each region is similar.

We note that residences in the example hot-dry and hot-humid climates are significantly newer on average than those in the cold and mixed-humid climates, with residences in the marine climate falling somewhere in the middle. The vintages of the sampled buildings are based on the

[3]EnergyPlus is a building energy simulation tool that simultaneously models thermal zone conditions and heating/cooling system response. See (National Renewable Energy Laboratory (NREL), 2022)

[4]Most real feeders have many more customers than 15. Due to computational constraints, simultaneously optimizing decisions across hundreds of homes (see Chapter 4) would have been impossible. In a separate analysis, we found that the load factors achieved from aggregating energy demands across 15 residences were within 10% of those observed on feeders with aggregations of many more residences.

[5]TMY files hold "hourly meteorological values that typify conditions at a specific location" for one year, including ambient temperature, wind speed, and solar conditions. These files are constructed by concatenating 12 typical meteorological months from different years (Wilcox & Marion, 2008). They are commonly used by engineers and architects to forecast the consumption of a building during the design phase.

underlying distributions catalogued in ResStock.

The variation in building vintage also has a significant effect on the construction methods employed in each residence. Table 2.4 summarizes the number of modeled buildings in each climate with a specific wall construction. Despite being exposed to the coldest weather, homes in the cold and mixed-humid climates overwhelmingly use uninsulated wood stud construction. This construction approach, common in older buildings, allows for a large amount of heat loss in the winter. By contrast, the newer buildings in the hot-dry and hot-humid climates are more likely to have insulated walls, despite having much milder winters.

From the simulations, we extract one year of hourly time series for electric plug loads ($E_{r,t}^{PlugLoads}$), heating energy ($E_{r,t}^{Heat}$), cooling energy ($E_{r,t}^{Cool}$), and domestic hot water energy ($E_{r,t}^{DHW}$). r is an index for the residence, ranging from 1 to 15, and t is an index for the hour of the year, ranging from 1 to 8760.

2.3 Results

Table 2.5 shows the distribution of annual energy demands for the modeled residences in each climate region. In the cold, mixed-humid, and marine climates, space heating is the single largest energy end-use. In the hot-dry climates, plug loads are dominant. In the hot-humid climate, air conditioning/cooling is the largest end-use.

Table 2.3: Summary statistics for buildings modeled in EnergyPlus. Residences in the example hot-dry and hot-humid climates are significantly newer on average than those in the cold and mixed-humid climates, with residences in the marine climate falling somewhere in the middle. ResStock reports the building vintage based on binned decades, rather than individual years. We assume for simplicity that all buildings built in the 1940s are built in 1945, 1950s buildings are built in 1955, etc. All residences built before 1940 (the first category) are assumed to have been built in 1925.

		n	Min	25%	Median	Mean	75%	Max
Year Built	Cold	15	1925	1925	1955	1950	1960	1995
	Hot-Dry	15	1925	1955	1975	1968	1985	2005
	Hot-Humid	15	1925	1965	1965	1976	1995	2005
	Mixed-Humid	15	1925	1925	1955	1952	1965	1995
	Marine	15	1925	1955	1955	1960	1965	2005
InfiltrationRate (ACH50)	Cold	15	15	15	15	18	20	25
	Hot-Dry	15	10	15	15	15	15	20
	Hot-Humid	15	10	15	15	18	20	40
	Mixed-Humid	15	15	15	15	19	20	40
	Marine	15	10	15	15	16	18	25
Exterior Wall Area (sf)	Cold	15	909	1,472	1,833	1,784	2,059	2,622
	Hot-Dry	15	1,336	1,336	1,860	1,933	2,144	3,078
	Hot-Humid	15	1,336	1,689	2,294	2,291	2,857	3,398
	Mixed-Humid	15	1,336	1,576	1,860	2,006	2,300	3,398
	Marine	15	1,116	1,607	1,860	1,889	2,309	2,756
Floor Area (sf)	Cold	15	885	1,455	1,690	1,802	2,176	2,663
	Hot-Dry	15	1,220	1,220	1,690	1,910	2,176	3,301
	Hot-Humid	15	1,220	1,690	1,690	2,005	2,420	3,301
	Mixed-Humid	15	1,220	1,690	1,690	2,113	2,663	3,301
	Marine	15	885	1,455	1,690	1,704	2,176	2,176
Window Area (sf)	Cold	15	69	92	146	169	224	434
	Hot-Dry	15	103	123	138	178	222	343
	Hot-Humid	15	81	121	147	190	240	389
	Mixed-Humid	15	69	108	171	187	233	403
	Marine	15	81	131	184	184	224	327
Roof Area (sf)	Cold	15	330	813	1,364	1,356	1,875	2,433
	Hot-Dry	15	1,364	1,364	1,889	2,128	2,483	4,335
	Hot-Humid	15	1,216	1,451	1,889	2,073	2,088	4,657
	Mixed-Humid	15	630	1,364	1,660	1,746	2,028	3,621
	Marine	15	989	1,311	1,686	1,767	2,161	3,077

Table 2.4: Modeled residences in each region using a specific kind of wall construction. Homes in the example cold and mixed-humid climates overwhelmingly use uninsulated wood stud construction.

	Cold	Hot-Dry	Hot-Humid	Mixed-Humid	Marine
Brick, 12-in, 3-wythe, Uninsulated	1	2	1	2	1
CMU, 6-in Hollow, Uninsulated	2	4	2	2	9
Wood Stud, R-11	1	1	2	1	1
Wood Stud, R-19	1	1	1	0	0
Wood Stud, R-7	0	1	0	0	0
Wood Stud, Uninsulated	10	1	5	10	3
CMU, 6-in Hollow, R-11	0	4	4	0	0
CMU, 6-in Hollow, R-7	0	1	0	0	0
CMU, 6-in Hollow, R-19	0	0	0	0	1

Table 2.5: Distribution of annual energy demands for the modeled residences in each climate region. In the cold, mixed-humid, and marine climates, space heating is the single largest energy end-use. In the hot-dry climates, plug loads are dominant. In the hot-humid climate, air conditioning/cooling is the largest end-use.

		n	Min	25%	Median	Mean	75%	Max
Space Heating Energy, MMBTU	Cold	15	37.57	53.92	99.91	99.93	131.15	172.23
	Hot-Dry	15	0.02	5.48	13.29	16.08	22.61	50.43
	Hot-Humid	15	6.24	13.50	21.80	21.51	27.66	45.37
	Mixed-Humid	15	0.00	47.58	54.71	63.04	72.96	151.05
	Marine	15	0.00	8.43	18.84	23.91	28.09	110.18
Cooling Energy, MMBTU	Cold	15	0.00	7.47	13.43	13.17	19.18	26.80
	Hot-Dry	15	0.00	2.91	9.04	14.11	19.02	58.13
	Hot-Humid	15	23.73	46.96	57.14	64.56	78.95	128.84
	Mixed-Humid	15	0.00	28.01	38.29	35.26	44.55	55.56
	Marine	15	0.00	0.00	0.00	1.72	0.00	14.99
Water Heating Energy, MMBTU	Cold	15	2.93	8.00	12.16	11.74	15.14	21.65
	Hot-Dry	15	4.30	6.74	7.83	8.68	10.35	18.32
	Hot-Humid	15	5.64	6.48	6.99	7.81	8.58	14.26
	Mixed-Humid	15	3.76	6.59	10.96	10.01	12.63	18.43
	Marine	15	4.55	6.70	9.19	9.71	11.44	18.96
Electric Plug Loads, MWh (MMBTU)	Cold	15	3.49 (11.92)	4.25 (14.52)	5.48 (18.7)	6.55 (22.35)	9.13 (31.16)	11.93 (40.69)
	Hot-Dry	15	3.27 (11.16)	3.84 (13.11)	4.79 (16.36)	5.43 (18.52)	7.32 (24.97)	7.9 (26.95)
	Hot-Humid	15	3.94 (13.45)	5.59 (19.07)	7.6 (25.94)	7.17 (24.46)	8.3 (28.32)	11.21 (38.27)
	Mixed-Humid	15	0.97 (3.32)	4.83 (16.46)	7.02 (23.94)	6.63 (22.63)	8.7 (29.68)	10.55 (35.99)
	Marine	15	1.64 (5.58)	3.87 (13.21)	4.55 (15.52)	4.68 (15.98)	5.81 (19.82)	7.24 (24.71)

While these modeling results are broadly consistent with the survey-reported averages found in Table 2.1, there are some notable differences. The average modeled annual demand for space heating energy in all five climates is greater than the survey-reported values. This can be explained because we have chosen to only model detached single-family residences, which use about twice as much energy on average for space heating as apartments in buildings with two to four units and more than four times as much space heating energy as apartments in buildings with five or more units (U.S. Energy Information Administration (EIA), 2015, CE3.1).

We generally see consistency between the modeled air conditioning demands and the survey-reported demands in Table (U.S. Energy Information Administration (EIA), 2015, CE3.1). For example, the Residential Consumption Survey reports that the average home in the hot-humid climate consumes 15.1 MMBTU of electricity each year for air conditioning. At an average coefficient of performance of 4, this translates to 60.4 MMBTU of thermal energy for a single residence. The modeled air conditioning demand for this climate region averages to 64.6 MMBTU per-residence. Two exceptions are the marine climate and hot-dry climate, where the example counties (Marin, CA and San Diego, CA) have significantly less air conditioning demand than the region-wide averages.[6]

We see similar consistency between the modeled demands and the survey-reported demands for water heating and other/plug loads. Note that Table 2.1 reports "other" consumption in MMBTU but we report plug loads in Table 2.6 in MWh. To convert between them, we use a conversion factor of 3.412 MMBTU/MWh.

Heating and cooling demands do not only vary between regions; they also vary significantly among residences in a single region. In the cold climate, for example, the residence with the most space heating demand uses 358% more energy than the residence with the least. In all regions except the hot-humid climate, at least one residence has no space cooling demand at all, despite the average space cooling demand being significantly higher. By modeling residential energy demands using a distribution of input parameters, our modeled data better reflect the

[6]In this analysis, we were constrained to using counties where there were deregulated electricity markets that could be used to estimate hourly electricity costs. In filter analysis, it would be beneficial to also model demands in marine and hot-dry climates with more representative cooling seasons.

range of conditions seen in the actual building stock than a simpler model.

Per Table 2.6, the inter-region variation in heating and cooling demands can be explained in large part by the differences in heating degree and cooling degrees. Heating degrees range from 1,061 for the hot-dry climate to 6,579 for the cold climate. This approximately 6-to-1 ratio is comparable to the ratio in modeled heating demands between these two regions.

The annual demand for space heating in each of the five example neighborhoods are plotted in Figure 2.4. The black line represents the average load for each day (from January 1st to December 31st) and the colored shading shows the daily range. As one would expect, heating demand peaks in the winter in all five regions, on the first and last days of the year. The cold and mixed-humid climate have greatest heating peaks, with the cold climate's heating demand exceeding 800 kBTUh on the coldest days of the year (also seen in Table 2.6). The heating peak in the hot-dry climate is about one-fourth as large.

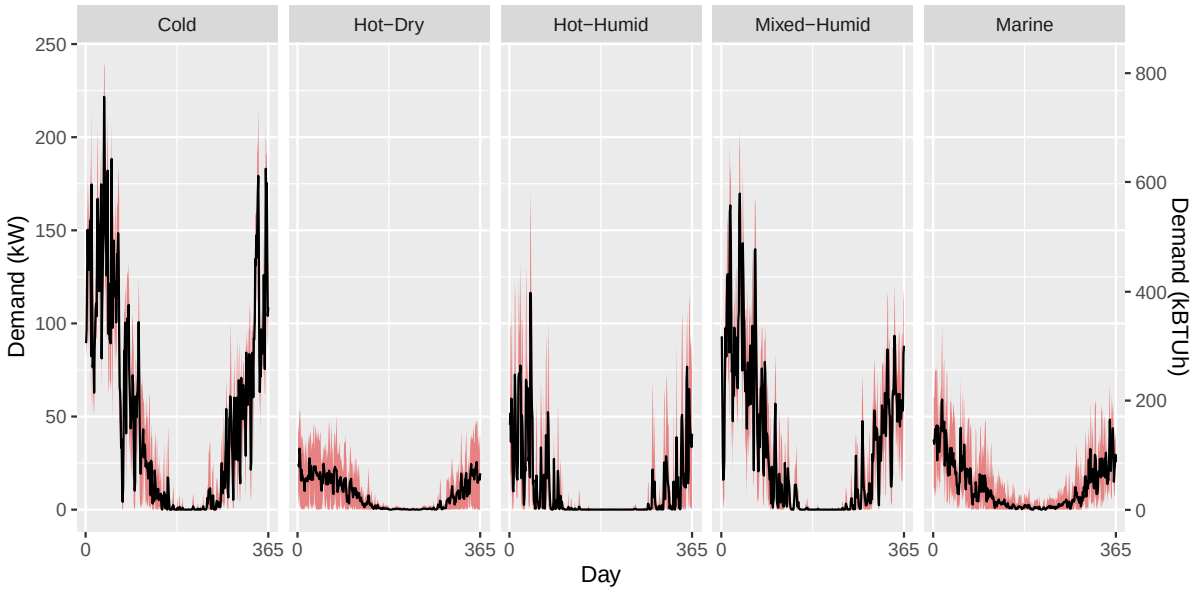

Figure 2.4: Annual profile of daily heating demands in each of the five climates, aggregated across the 15 residences. The solid black line represents the average heating demand for each day of the year. The ribbon shows the range between the minimum and maximum hourly heating demands on each day. The y-axis is in units of kW on the left and kBTUh on the right. This is computed through a direct conversion of 3.412 kBTUh = 1 kW.

Figure 2.5 plots the annual profile of daily cooling demands, following the same format as

Table 2.6: Heating and cooling information for the five climates studied. Heating, cooling, and DHW demands are measured in thermal units, whereas plug loads and the feeder peak are reported in electrical units. Consequently, the 66 kW cooling peak in the cold climate only draws 15-20 kW of electricity from the feeder because air conditioners have a COP of approximately 4. COPs for heating and cooling in each climate are computed as averages, using heating/cooling degrees (measured from 65°F for heating and 72°F for cooling) as weighting factors.

	Erie County, NY	San Diego, CA	Harris County, TX	Alexandria, VA	Marin County, CA
Building America Climate Region	Cold	Hot-Dry	Hot-Humid	Mixed-Humid	Marine
IECC Climate Region	5A	3B	2A	4A	3C
Conditioned Floor Area, sq.-ft.	27,026	28,653	30,080	31,691	25,565
Heating Degree Days	6,579	1,061	1,471	4,806	3,012
Cooling Degree Days	479	649	2,802	1,086	30
	Annual Demands, Aggregate (per-residence)				
Heating, MMBTU	1,499 (100)	241 (16.1)	323 (21.5)	946 (63.1)	359 (23.9)
Cooling, MMBTU	197 (13.1)	212 (14.1)	968 (64.5)	529 (35.3)	26 (1.7)
Water (DHW), MMBTU	176 (11.7)	130 (8.7)	117 (7.8)	150 (10)	146 (9.7)
Plug Load, MWh	98.2 (6.5)	81.4 (5.4)	107.5 (7.2)	99.4 (6.6)	70.2 (4.7)
	Peak Hourly Demands				
Heating Peak, kBTUh (kW)	816 (239)	184 (54)	583 (171)	693 (203)	337 (99)
Cooling Peak, kBTUh (kW)	224 (66)	223 (65)	553 (162)	409 (120)	33 (10)
Water (DHW) Peak, kBTUh (kW)	79 (23)	54 (16)	49 (14)	67 (20)	58 (17)
Plug Load Peak, kW	36	25	34	37	22
Feeder Peak (incl. thermal loads), kW	41	33	74	69	24
# Res. with Heating	15	15	15	14	14
# Res. with Cooling	12	11	15	14	2
Average Heating COP (HSPF), Low-Eff.	3.0 (10.1)	4.2 (14.2)	3.6 (12.4)	3.1 (10.7)	4.0 (13.7)
Average Heating COP (HSPF), High-Eff.	3.3 (11.2)	4.9 (16.8)	4.1 (14.2)	3.5 (12.0)	4.7 (15.9)
Average Cooling COP (SEER), Low-Eff.	4.3 (14.5)	4.4 (15.0)	4.0 (13.5)	4.0 (13.8)	4.3 (14.5)
Average Cooling COP (SEER), High-Eff.	6.8 (23.2)	7.1 (24.1)	6.3 (21.5)	6.4 (21.9)	6.8 (23.2)

Figure 2.5. As one would expect, cooling demands are largest in the summer months. Particularly in the hot-humid and mixed-humid environments, which have the greatest latent cooling loads.

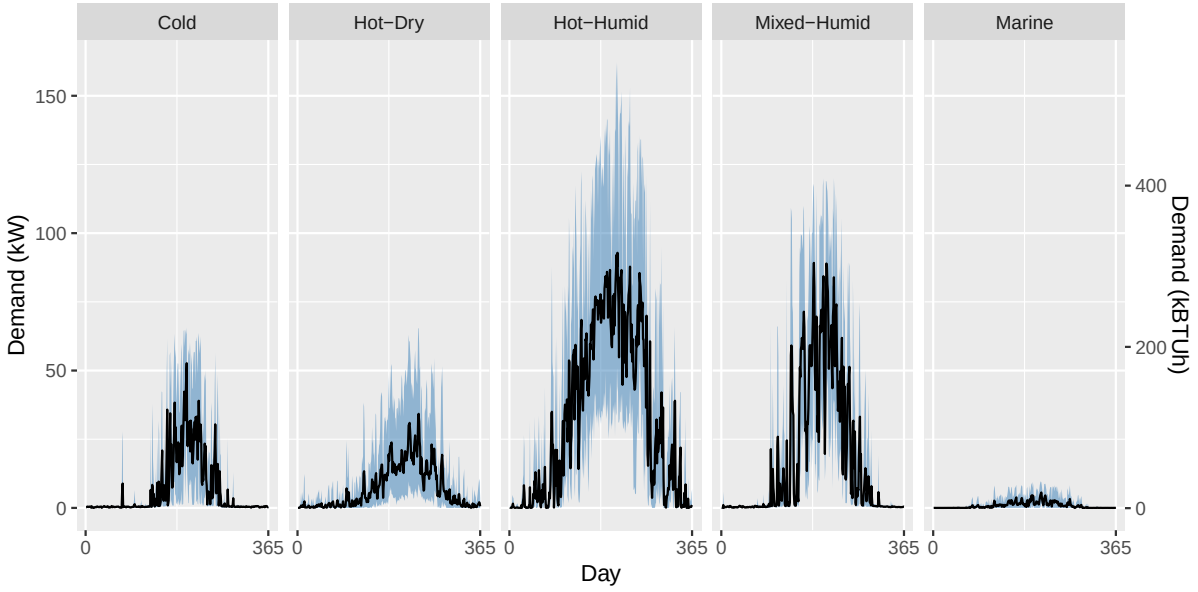

Figure 2.5: Annual profile of daily cooling demands in each of the five climates, aggregated across the 15 residences. The solid black line represents the average cooling demand for each day of the year. The ribbon shows the range between the minimum and maximum hourly cooling demands on each day. The y-axis is in units of kW on the left and kBTUh on the right.

Figures 2.6 and 2.7 show the domestic hot water and electric plug loads for each of the five example neighborhoods. While both demands have sizable diurnal variation (described by the width of the band), they exhibit little annual and inter-regional variation.

Representative feeder-wide daily profiles of energy demands are plotted in Figure 2.8. These are computed by taking all of the demand data from a given month, then computing the average demand of each type of energy at each hour of the day (30 or 31 observations for each hour). In the cold and mixed-humid climates, heating demands in January are relatively consistent throughout the day. In the other climates, heating demands show a stronger diurnal variation, peaking overnight and in the early morning. In July, the cold, hot-dry, hot-humid and mixed-humid climates all have sizable cooling demands that peak in the afternoon. Thermal demands are significantly milder in the shoulder seasons (April and October).

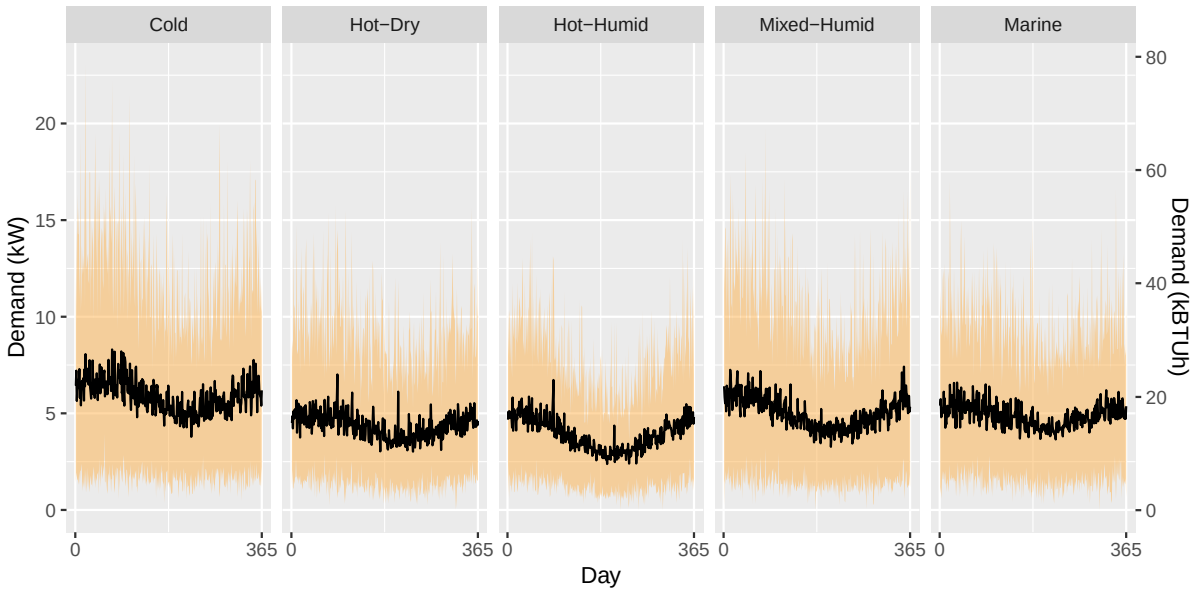

Figure 2.6: Annual profile of daily domestic hot water (DHW) demands in each of the five climates, aggregated across the 15 residences. The solid black line represents the average demand for each day of the year. The ribbon shows the range between the minimum and maximum hourly values on each day. The y-axis is in units of kW on the left and kBTUh on the right.

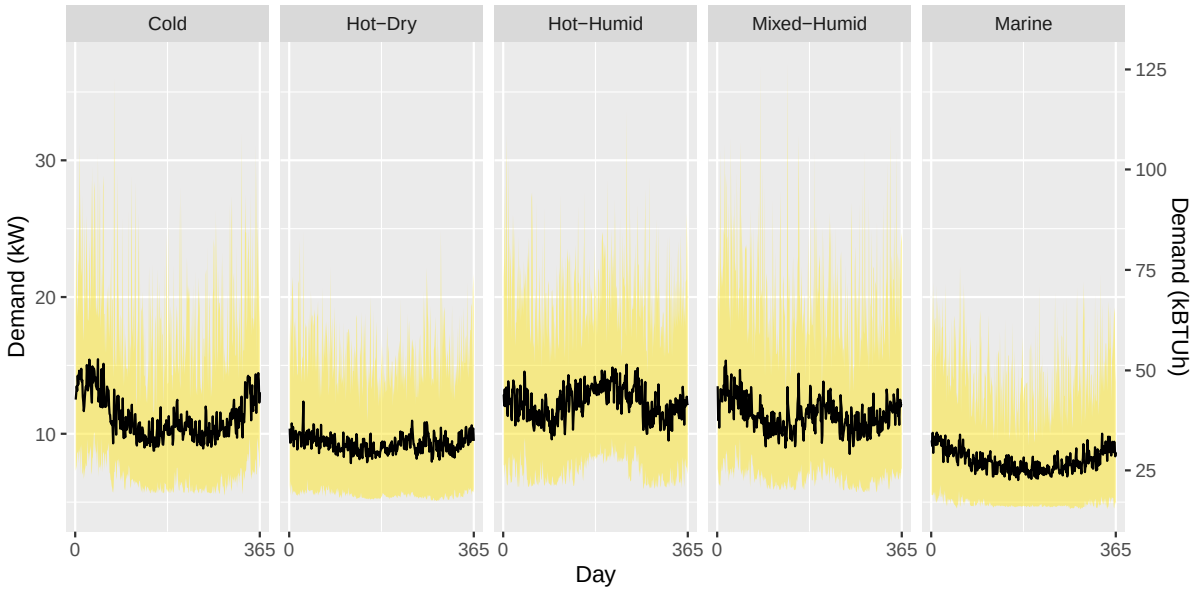

Figure 2.7: Annual profile of daily plug load demands in each of the five climates, aggregated across the 15 residences. The solid black line represents the average demand for each day of the year. The ribbon shows the range between the minimum and maximum hourly values on each day. The y-axis is in units of kW on the left and kBTUh on the right.

The cold, hot-humid, and mixed-humid climates all have large heating and cooling demands, observed in January and July, respectively. These heating and cooling loads exceed plug load demand by an order of magnitude. Conversely, the hot-dry and marine climates are much milder, rarely seeing feeder-wide demands exceed 50 kW. We note that these representative daily profiles do not show the most extreme conditions observed in the typical meteorological year. For example, the peak heating demand in the cold climate is 239 kW (see 4.2), well above the typical heating peak observed in January.[7] Figure 2.9 shows the same data, but each feeder's demand is represented in kBTU-per-1000sf for thermal loads and kWh-per-1000sf for electrical loads.

While heat transfer in buildings is driven by heating degrees and cooling degrees, not all residences respond the same way to a given temperature difference. Figure 2.10 plots the hourly heating and cooling demands (aggregated across all 15 residences) in each climate region against the outdoor dry bulb temperature. For each of the five climates, the heating demands increase roughly linearly as temperatures decrease below 65°F, and cooling demands increase roughly linearly as temperatures rise above 65°F. Note that the temperature dependencies of heating and cooling are not identical across climates: in the cold climate, heating demands increase more sharply with falling temperatures than in the mixed-humid or marine climates; in the hot-humid climate, cooling demands increase more sharply with rising temperatures than in other climates. These differences reflect variations in other climate variables (including solar radiation, wind speeds, and humidity) as well as differences in the housing stock and variations in heating and cooling preferences between regions.

These temperature-dependency graphs, along with the variation in heating- and cooling-degree days between climates, explain the variation in annual heating and cooling demands. For example, in the hot-humid climate the total cooling load (aggregated across 15 residences) increases at a rate of 13.3 kBTUh/cooling-degree[8] This climate region has 2,802 cooling degree days ($2,802 * 24 = 67,248$ cooling-degree-hours), per Table 4.2, indicating that the total annual demand

[7]These data do not include "design day" conditions, which lay outside the data found in a typical meteorological year.

[8]Cooling degrees are defined for temperatures over 65°F as the difference between the outdoor temperature and 65°F.

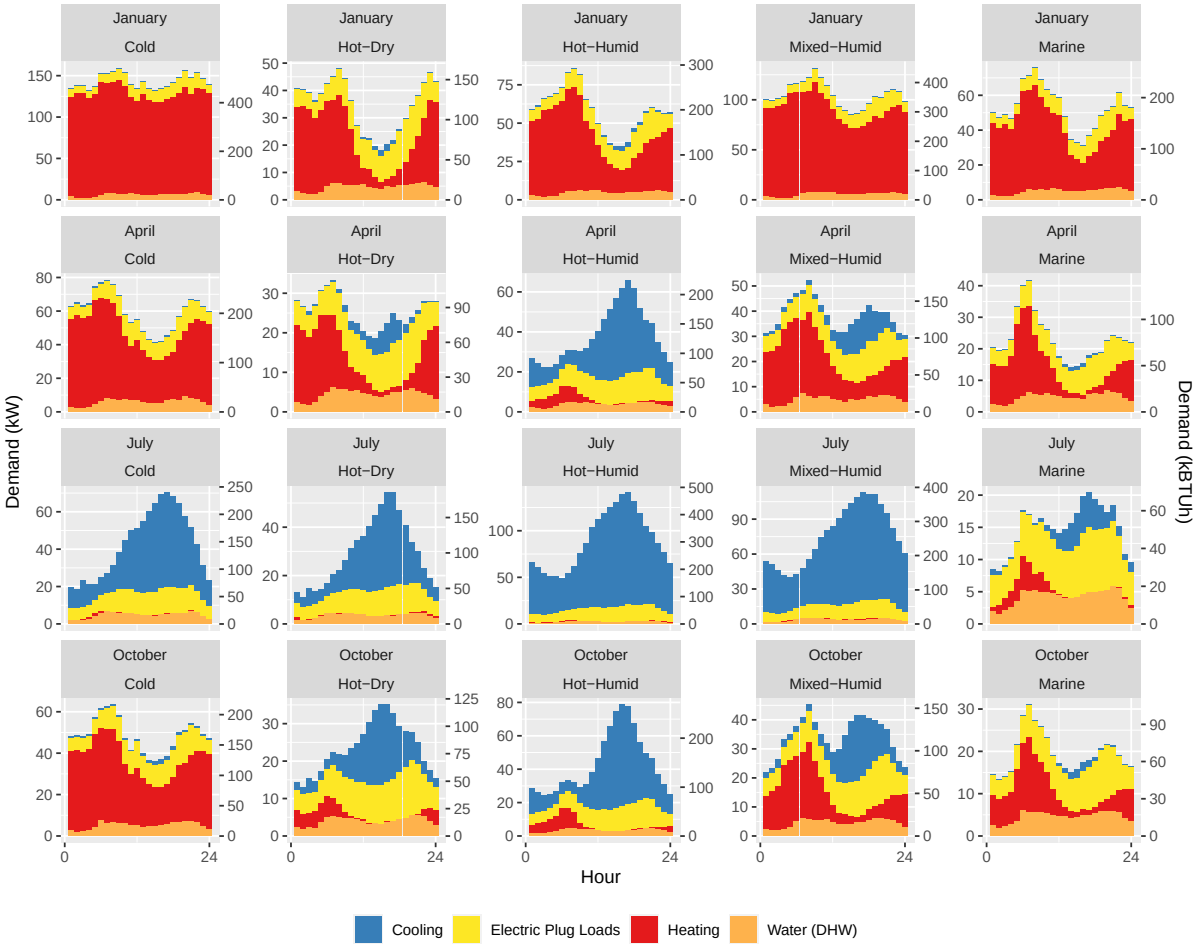

Figure 2.8: Typical daily profiles for heating, cooling, DHW, and electric plug loads. The cold, hot-humid, and mixed-humid climates all have large heating and cooling demands, observed in January and July, respectively. These heating and cooling loads exceed plug load demand by an order of magnitude. Heating demands are relatively stable during January in the cold and mixed-humid climates, but follow a stable diurnal trend in the hot-dry, hot-humid, and marine climates. Cooling demands show a consistent diurnal trend in the cold, hot-dry, hot-humid, and mixed-humid climates.

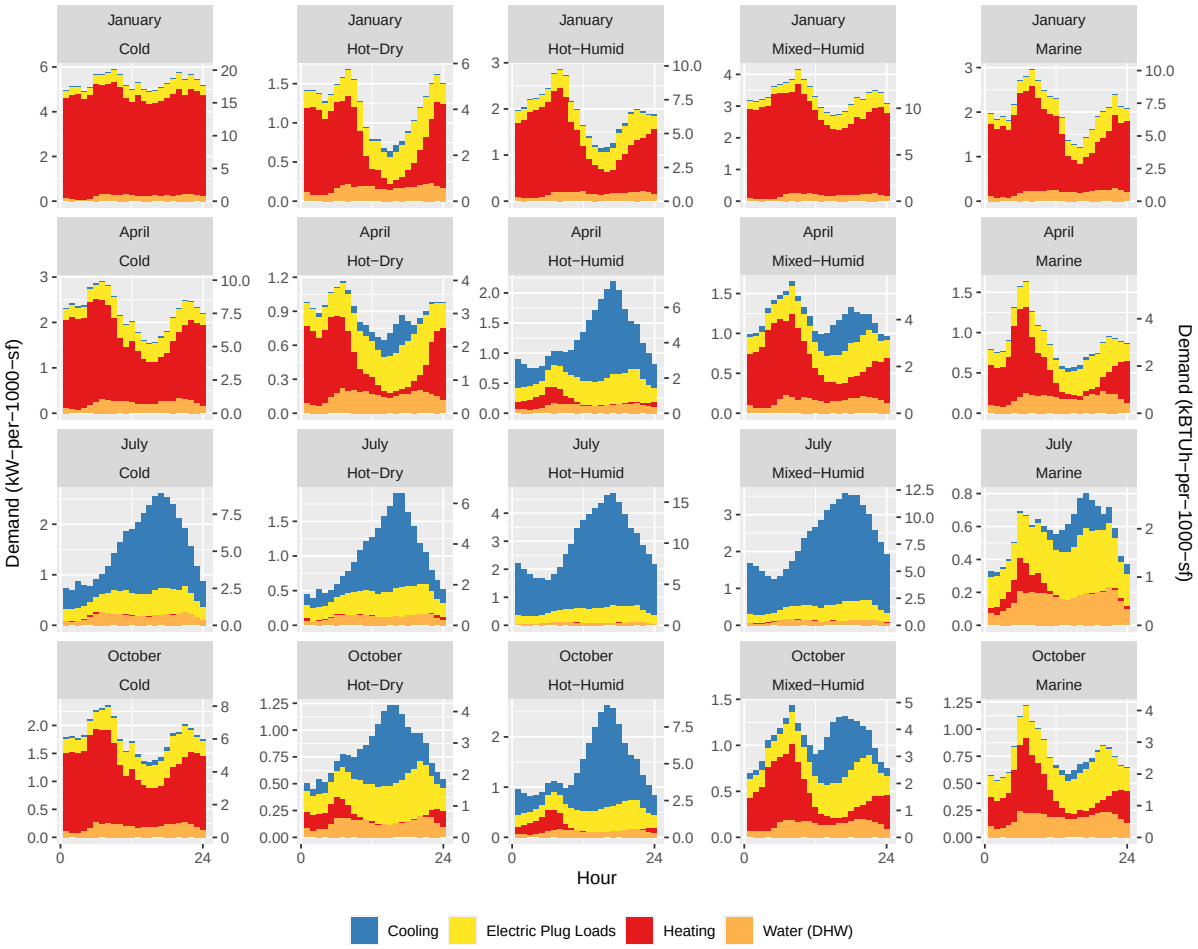

Figure 2.9: Typical daily profiles for heating, cooling, DHW, and electric plug loads, per 1000-sf. The cold, hot-humid, and mixed-humid climates all have large heating and cooling demands, observed in January and July, respectively. These heating and cooling loads exceed plug load demand by an order of magnitude.

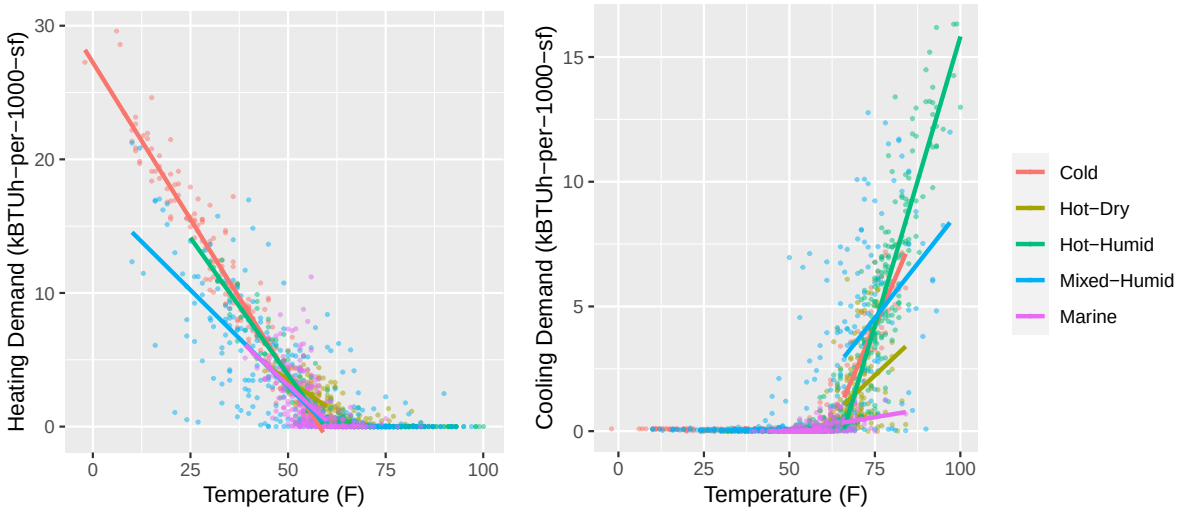

Figure 2.10: Temperature dependencies for heating and cooling in the five climate regions. Plots and line fits are based on 1,500 hourly data points sampled from the five regions. In the cold climate, heating demands increase more sharply with falling temperatures than in the mixed-humid or marine climates. In the hot-humid climate, cooling demands increase more sharply with rising temperatures than in other climates. These differences reflect variations in other climate variables (including solar radiation, wind speeds, and humidity) as well as differences in the housing stock and variations in heating and cooling preferences between regions.

for space cooling should be approximately $13.3kBTUh/F * 67,248 = 894,400kBTU/year \approx 894MMBTU/year$. This is within 10% of the computed cooling demand of 968 MMBTU in Table 4.2.

Likewise, in the cold climate, the total heating load (again aggregated across 15 residences) increases at a rate of 10.0 kBTUh/heating-degree. For the 6,579 heating degree days in this climate ($6,579 * 24 = 157,896$ heating-degree-hours), we would expect a total annual heating demand of $10.0kBTUh/F * 157,896 = 1,578,960kBTU/year \approx 1,579MMBTU/year$. Once again, this estimate is within 10% of the 1,499 MMBTU reported in Table 4.2.

The temperature-dependency graphs can also be used to extrapolate the maximum heating and cooling loads in each climate. For example, the maximum temperature observed in the typical meteorological year in the hot-humid climate is 103F, so we would expect a maximum cooling load of $13.3kBTU/F * (103F - 65F) = 505$ kBTUh. At 103F, a 14-SEER air conditioner can achieve a COP of approximately 3 $kW_{thermal}/kW_{electric}$ (10.2 kBTUh/kW), so the electric

load from cooling would be approximately $\frac{505kBTUh}{10.2kBTU/kW} = 49.5kW$. This would be observed in addition to any other plug loads on the feeder.

2.4 Conclusion

In this chapter, we described four categories of residential energy use, discussed their drivers, then used open-source building energy modeling software to construct year-long hourly simulations of these demands for 75 single-family homes across five U.S. climate regions.

Space heating and cooling loads vary significantly between regions, while domestic hot water loads and plug loads tend to be more closely related to the number of occupants in a residence. In three out of the five climate regions analyzed, space heating is the single largest residential energy end-use. In the other two climates, cooling/air conditioning and plugs loads are the largest end-uses.

Additionally, our modeling shows significant variation between residences within a region, due to differences in size and vintage.

In the next chapter, we describe several emerging customer-side energy technologies. In the subsequent chapters, we combine the analyses from these two chapters to produce a series of optimization formulations that explore how to reduce energy expenses and carbon emissions by employing emerging technologies to satisfy residential energy demands.

Chapter 3

Overview of Customer-Side Technologies

In this chapter, we provide background on five customer-side energy technologies: heating electrification, rooftop solar photovoltaic panels, distributed battery storage, energy efficiency, and electric vehicles. We observe that different technologies interact with the electric system in different ways. Energy efficiency (EE) decreases heating and cooling loads year-round. Rooftop solar photovoltaic (PV) panels decrease a customer's net load in the middle of the day when the sun is strongest, often generating excess electricity that can be injected to the grid. Distributed battery storage allows customers to store excess solar generation for later use or buy excess electricity from the grid at off-peak hours and use it when needed. Electrification technologies like electric vehicles (EVs) and heat pumps (HPs) increase a customer's electricity consumption while reducing their direct consumption of fossil fuels.

Because of the range of ways that different emerging technologies interact with the energy system, and the variability in demands for energy services between regions, we have good reason to believe that different technologies will be found more- or less-suitable in different climates.

3.1 Heating Electrification

For much of the 20th century, customers could heat their homes either using electric resistance systems (which converts one unit of electricity into one unit of heat) or by directly combusting natural gas or some other fossil fuel in a boiler or furnace. Because most electricity was produced by burning fossil fuels in inefficient coal plants, natural gas furnaces generally resulted in both lower costs and lower carbon emissions than electric heating.

Since 1990, the fraction of electricity produced by coal-fired plants has fallen from over 50% to less than 20%. These have been replaced by lower-emissions natural gas plants and zero-carbon renewable resources, which together have grown from representing less than 45% of the electricity supply in 1990 to over 80% today (U.S. Energy Information Administration, 2021c).

At the same time, heat pumps, also known as reverse-cycle air conditioners, have undergone large technical advancements. By leveraging outdoor air or ground temperatures as a heat source, these systems are able to deliver five or more units of heat to a conditioned space for every unit of electricity consumed. A number of major studies have identified electrification of heating, coordinated with an expansion of renewable electricity generation, as a key tool for deep economy-wide decarbonization. EPRI's U.S. National Electrification assessment (Electric Power Research Institute, 2018a) predicts that efficient electrification of heating and transportation could reduce emissions by 20–70% below 2015 levels by 2050. NREL's 2017 Electrification and Decarbonization report (Steinberg et al., 2017, p. vi) concludes that electrification of end-use services could reduce emissions to 41% below 2005 levels by 2050, or by up to 74% below 2005 levels if combined with power sector decarbonization.

The efficiency of a heat pump is described by its coefficient of performance (COP), which is the ratio of heat added to a space relative to the electric energy consumed. The COP varies with ambient conditions: when the ambient temperature is 60°F (15.5°C) and the desired space temperature is 68°F (20°C), the COP of an air source heat pump may be around 4.5 (Goodman, n.d.). This means that for every unit of electricity consumed by the heat pump, 4.5 units of heat

are added to the conditioned space.

A drawback to heat pumps is that both their efficiency and capacity degrade as ambient temperatures drop. Air source heat pumps are particularly susceptible, as they must extract thermal energy from the ambient air (whereas ground source heat pumps extract energy from the soil, which tends to be warmer than the air during the heating season). To accommodate for the degradation in capacity, most residential heat pumps are equipped with supplementary electric resistance heaters that provide additional heat when the building's heating demands exceed the compressor's capabilities. These resistance heaters can provide additional capacity for low capital cost, but only produce one unit of heat for every unit of electricity consumed.

3.1.1 Electric Load Impacts from Heating and Cooling

Despite electrification's promise for reducing emissions, there are persistent concerns that some of the benefits of reduced emissions may be offset by increases in infrastructure requirements needed to meet peak load. Navarro-Espinosa and Mancarella (2014) conclude that the highly-correlated, inflexible electric demand required by heat pumps representing as little as 30–40% of a region's space heating requirements can cause overheating of transformers and feeders in the electric distribution system. Heinen, Burke, and O'Malley (2016) find that installing heat pump-only systems or heat pump systems with auxiliary resistance heaters in as few as 25% of buildings could cause substantial increases in system-wide electricity peaks. Electric Power Research Institute (2018a) estimates that peak loads across the U.S. could increase by 24–52%, which would precipitate the need for costly system reinforcements. Baruah et al. (2014) find that electrification of heating and transportation could increase peak loads by as much as 93% in Great Britain.

The load impacts from broad electrification of heating are likely to vary significantly between regions. Approximately 35% of homes in the United States already use electricity as their main source of heating, predominantly in the hot-humid and mixed-humid climates. About 70% of these homes use some form of electric resistance heating (U.S. Energy Information Administration (EIA), 2015, HC6.6). For these homes, adoption of heat pumps would result

in an overall reduction in electricity demand. Of the remaining homes that use space heating equipment, 80% use natural gas as their primary source of heating energy. For these homes, a move toward heating electrification would increase electric loads.

Waite and Modi (2020) finds that an all-electric heating approach using current technologies would increase peak loads by 70%, but that system peaks in colder climates could increase by more than 300%. Navarro-Espinosa and Ochoa (2016) model random adoption and unmanaged operation of heat pumps, electric vehicles, photovoltaic systems, and micro-CHP (combined heat and power) units on 128 low-voltage feeders in the United Kingdom. The authors find that only about half of the feeders they studied could accommodate broad adoption of any of the above technologies without exhibiting electrical problems.

Steinberg et al. (2017) note that peak load increases from electrification could be mitigated by exploiting the inherent flexibility of these new loads. This can be achieved through managed charging of electric vehicles that avoids consumption during peak hours or using thermal storage to shift heating loads to off-peak times. The benefits of this "smart grid" approach to demand management has been demonstrated in a broad literature, including Callaway and Hiskens (2011), García-Villalobos et al. (2014), Henze, Felsmann, and Knabe (2004), Pieltain Fernández et al. (2011), Pudjianto et al. (2013), Richardson, Flynn, and Keane (2012), Risbeck et al. (2017), Siano and Sarno (2016), Stinner, Huchtemann, and Müller (2016), and Zakariazadeh, Jadid, and Siano (2014).

In our analysis, the minimum temperature observed in the typical meteorological year for the cold climate is -2°F, so we would expect a maximum heating load of $10.0kBTU/F * (65°F - (-2°F)) = 670$ kBTUh. At this temperature, the COP of a 9 HSPF air-source heat pump is only 1.3 $kW_{thermal}/kW_{electric}$ (4.4 kBTUh/kW), so the electric load from heating would be approximately $\frac{670kBTUh}{4.4kBTU/kW} = 152kW$. This is more than double the feeder's existing capacity, even when we include the assumed 50% headroom over the existing peak.

Because the efficiency of a heat pump falls as the temperature decreases, the relationship between the outdoor temperature and the electricity required to heat a home is non-linear. The (convex) relationship between annual HDDs and the electricity required to heat a home can be

seen in Figure 3.1, which compares the HDDs for 1020 locations in the continental United States to the estimated electricity required to heat a single-family home with an ASHP coupled with a backup resistance heater. In colder climates, the electricity required to heat a home with an ASHP increases *superlinearly*. A home in a region with 10,000 HDDs would be expected to use about four times as much electricity to heat as a home in a region with 5,000 HDDs.

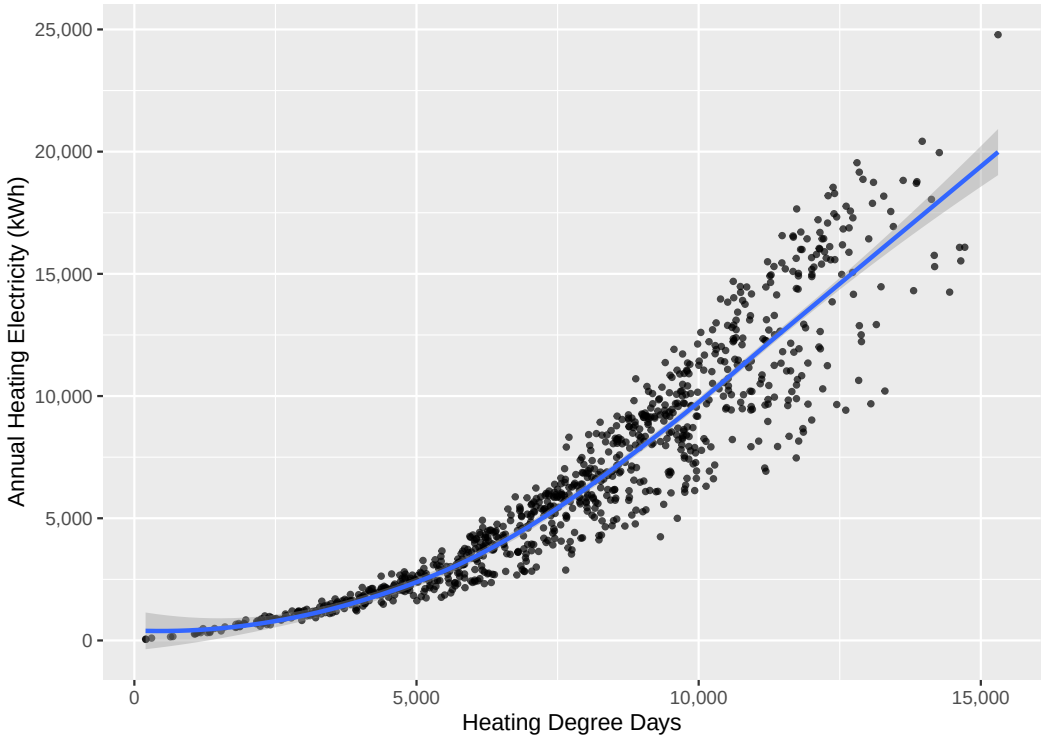

Figure 3.1: Estimated heating electricity vs. heating degree days (HDDs) for 1020 locations in the continental United States. We assume that an ASHP with a heating seasonal performance factor (HSPF) of 9 is backed up by an electric resistance heater, which fulfills all demands at temperatures below 20°F.

3.2 Rooftop Solar PV

Rooftop solar PV generates electricity directly from radiant solar energy collected in the middle of the day. Customers with rooftop PV use the electricity they generate to offset their own consumption, often selling excess generation back to the utility.

Figure 3.2 describes load impacts on an example feeder in Upstate New York in a situation in which 10% of the customers have installed 10 kilowatt PV arrays. The upper plot shows the

unmodified load, where the gray ribbon shows the daily maximum and minimum load and the solid line represents the average load for each day. The lower plot shows the same figure, but with the yellow band, describing the load on the feeder net of solar PV generation, superimposed on top.

We observe that the average daily load decreases slightly with solar PV (from the dark solid line to the dashed white line) and the minimum net load decreases significantly (the lower bound of the yellow ribbon). However, the peak daily loads (judged by the upper bound of the two ribbons) do not significantly change with the introduction of solar PV. This indicates that solar generation is not well-correlated with the feeder's peak demand, and thus does little to reduce distribution capacity needs.

3.3 Distributed Storage

Distributed battery storage serves two main purposes. First, battery storage enables customers exposed to wholesale electricity prices to arbitrage variations in the hourly cost of electricity. This revenue stream is expected to be quite small, because distributed storage is generally more expensive than utility-scale storage, so many of the arbitrage opportunities are likely to be absorbed by market participants upstream who can install battery storage for a lower capital expense.

Second, storage enables customers with rooftop PV to power their loads with stored energy even when the sun is not shining. This effectively smooths the solar generation over a greater number of hours, allowing for greater self-consumption of PV electricity and potentially deferring some distribution capacity upgrades.

Expanding on the example from the previous section, if every residence with a solar array also had battery storage capable of shifting the solar generation to later in the afternoon, the combination of technologies could provide significantly more benefit to the grid. Figure 3.3 illustrates the case where all solar generation is shifted back 6 hours through the use of battery storage. The result is a flatter load curve throughout the day in all seasons (as detailed by the

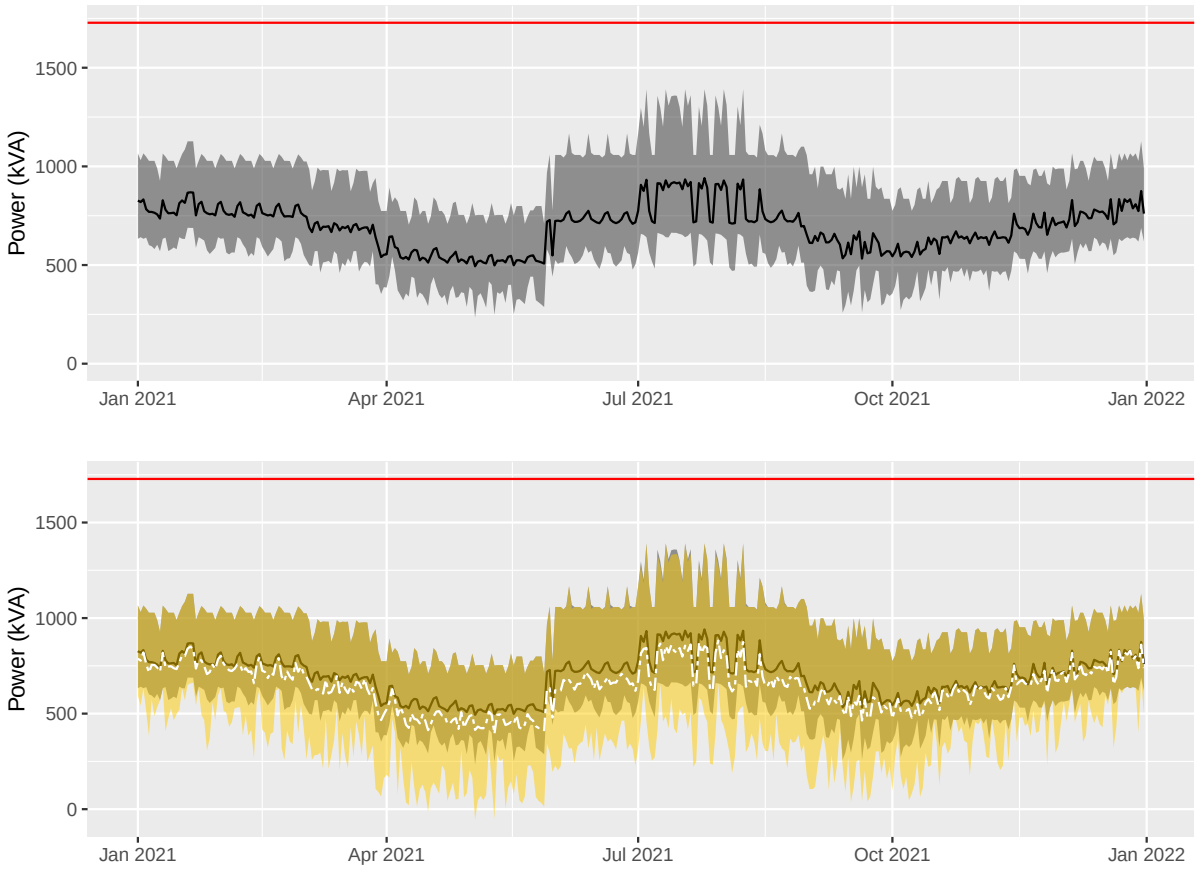

Figure 3.2: Top: Daily electric loads on an example feeder in Upstate New York, where the dark ribbon shows the daily maximum and minimum load and the solid line represents the average load for each day. Bottom: Daily net load after 10% of residences have installed 10kW PV arrays, overlaid on the original profile. The white dashed line maps the average load for each day of the year and the yellow band describes the daily range.

dashed white line) and a modestly reduced summer peak.

In Vibrant Clean Energy, LLC et al. (2020), the authors estimate that co-optimizing distributed PV and storage with other grid investments could result in over $115 billion in savings between 2018 and 2035, relative to a case where choices are not optimized for the distribution system.

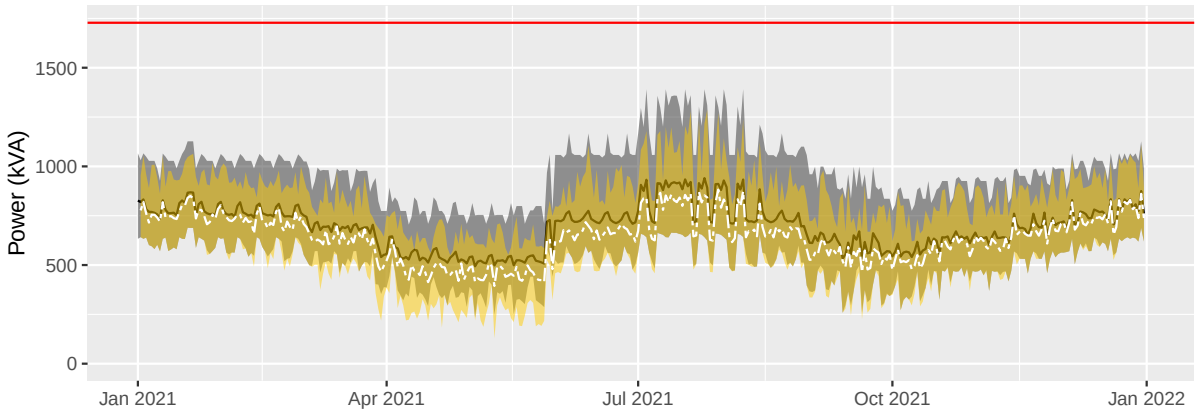

Figure 3.3: Daily net load on feeder from Figure 3.2, assuming 10% of residences have installed 10kW PV arrays and that this generation is shifted 6 hours later in the day by battery storage. The white dashed line maps the average load for each day of the year and the yellow band describes the daily range. In all four seasons, the inclusion of battery storage with PV produces flatter average daily loads (the yellow band is narrower). Summer peaks are also modestly reduced.

3.4 Energy Efficiency

Energy efficiency has historically been characterized as a "low-hanging fruit" for achieving carbon emissions reductions, with many believing that energy efficiency retrofits will pay for themselves.[1] This raises the question: if energy efficiency is such a bargain, why are individuals not taking it upon themselves to make these investments? In the 1980s and 1990s, a number of popular explanations emerged for the slow adoption of efficient technologies. These include: split-incentives (the party that adopts the technology is not always the party that pays the energy bill); high implicit discount rates for energy efficiency investments (customers do not value savings that are observed years in the future); and uncertainty about future energy prices (Jaffe & Stavins, 1994).

More recent empirical work has proposed that the magnitude of profitable unexploited investment opportunities in energy efficiency is much smaller than most engineering-accounting

[1]This was illustrated perhaps most famously by McKinsey and Company in 2009, with their publication of the McKinsey Global GHG abatement cost curve (McKinsey & Company, 2009). The so-called "McKinsey Curve" illustrates various approaches to reducing carbon emissions at different abatement costs. For energy efficiency retrofits, these costs are negative: the intervention is proposed to result in both emissions reductions and (private) cost savings.

studies suggest, because these studies rely on biased engineering analyses and ignore unobserved costs and benefits (Allcott & Greenstone, 2012). In perhaps the most comprehensive empirical analysis to date, (Fowlie, Greenstone, & Wolfram, 2018) find that across 30,000 households in Michigan that participated in the Weatherization Assistance Program (WAP), the upfront costs for weatherization were about twice the cost of the actual energy savings.

3.5 Electric Vehicles

Electric vehicle (EVs) have existed in some form for over 100 years but have gained popularity for very few use cases. Due to recent improvements in battery technology and mounting concerns about the climate impacts of fossil fuel emissions, EVs have gained attention as an option for replacing passenger and fleet vehicles.

EVs store electricity from the grid in on-board batteries, giving them inherent flexibility that allows them to be charged at different times of day. "Smart charging" of EVs can be used to mitigate and smooth peak loads, as well as respond to volatility in upstream renewable generation. Depending on how and when EVs are charged, they can either be an asset to the grid or pose a significant burden.

If a single customer on the example feeder chooses to adopt an EV, the marginal cost incurred by the utility for charging the vehicle is the cost of energy plus losses (assuming the load caused by the vehicle does not trigger infrastructure reinforcements). However, a customer who adopts an EV under the current system of average cost volumetric tariffs will be forced to pay a volumetric delivery charge in addition to the cost of energy. In Figure 3.4, we compare the annual cost of charging a vehicle under volumetric delivery prices to the marginal cost incurred by the utility for on- and off-peak charging. The inclusion of a volumetric delivery charge nearly triples the cost of vehicle charging.

Notably, the annual cost of fueling a vehicle with gas is more than twice the cost of electricity for charging, even if volumetric delivery charges are included. This indicates that the principal barrier to EV adoption is not the cost of energy, but a combination of other factors, including

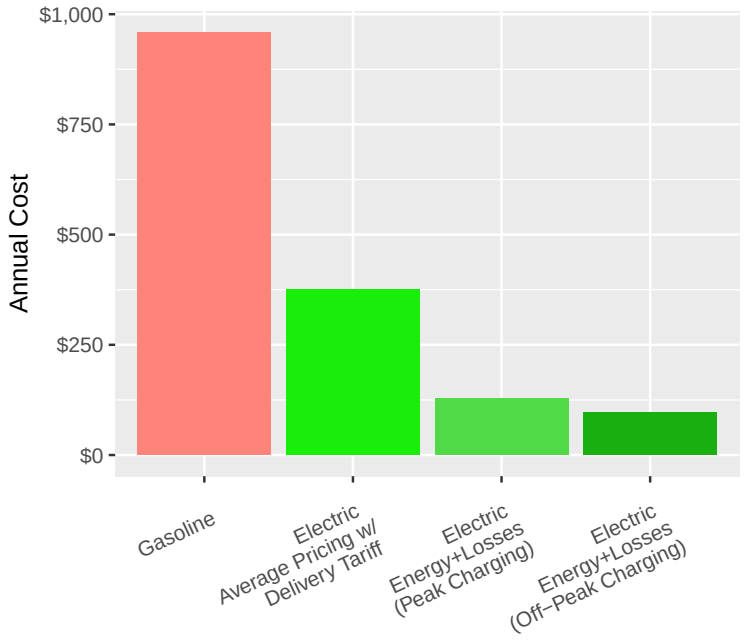

Figure 3.4: Annual cost of fueling a vehicle driven 27.4 miles/day (10,000 miles/year). We assume that gasoline costs $2.50/gallon and an internal combustion vehicle has a fuel economy of 30 mpg. The EV has a fuel economy of 3 miles/kWh. The "Electric Volumetric" bar represents the cost of charging the vehicle at an average cost of 9.8c/kWh, which includes both supply and delivery. The two "Electric Marginal" bars represents the costs of on- and off-peak charging, assuming that customers only pay for the variable cost of energy plus 10% system losses.

upfront cost and range concerns.

To demonstrate the significance of peak vs. off-peak charging to distribution conditions, Figure 3.5 models a scenario in which every home on the feeder has adopted one EV that is driven 31.5 miles/day (11,500 miles/year, which is typical of the annual mileage for a U.S. passenger vehicle (U.S. Department of Transportation Federal Highway Administration, 2020)). At an efficiency of 3 miles/kWh, this adds 1.3 GWh of energy sales to the feeder annually, increasing throughput by 22%.

In both plots of Figure 3.5, the black line represents the average daily load without the addition of EVs and the gray band (which is covered in the lower plot) represents the daily range. The white line and green band describe these same statistics after the EV loads have been added. In the top plot, all of the vehicles are charged at a constant power during the 16 hours of the day with the lowest load under base case conditions (Off-Peak). We observe that the average power

curve shifts up, the diurnal range significantly decreases, and the peak power remains mostly unperturbed. By contrast, in the bottom plot, all of the vehicles are charged during the 8 hours with the highest load (Peak). Under this scenario, capacity constraints are regularly violated throughout the summer and the diurnal range in load exceeds 1000 kVA.

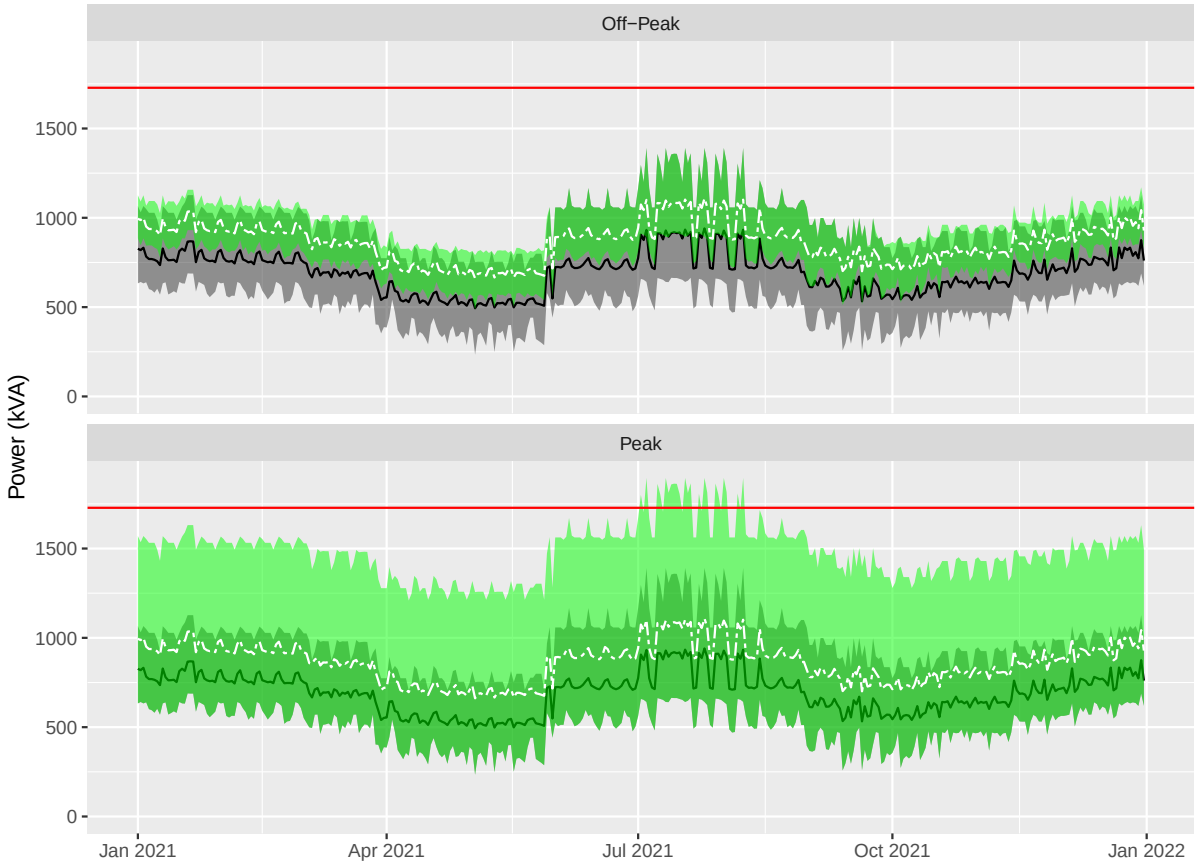

Figure 3.5: Load from example feeder with peak and off-peak EV charging. For both plots the white dashed line maps the average load for each day of the year with EV charging and the green band describes the daily range. The black line and accompanying gray band describe baseline conditions without additional EV charging. This scenario assumes that all 384 homes have adopted a single EV that is driven 27.4 miles/day (10,000 miles/year) at an efficiency of 3 miles/kWh. When vehicles are charged at off-peak times, the volume of sales increases without increasing peaks, and the diurnal range decreases.

For this feeder, charging EVs at off-peak times results in additional volumetric sales without the need for additional distribution capacity. This would lower the average cost of a service ($/kWh), which could ultimately lower rates for customers. If utilities needed to plan for a large

number of vehicles charging during peak periods, that would precipitate the need for costly reinforcements, raising rates. This dichotomy underscores the importance of managed charging.

One of the reasons that this feeder can accommodate so many EVs charging off-peak is because of its wide diurnal range: load is significantly lower at night and in the middle of the day than during peaks, so there is ample capacity that can be filled in by EV charging (this is sometimes referred to as "valley filling" in the literature). Commercial buildings tend to have less peaky loads because they are used more consistently throughout the day, so one would expect that commercial-dominated feeders have fewer opportunities for valley-filling. In the thesis, we will explore DER impacts on predominantly residential feeders, predominantly commercial feeders, and mixed-use feeders.

Chapter 4

Potential For Reducing Costs Using Customer-Side Energy Technologies

In Chapter 1, we broke down the expenses that contribute to residential customer electricity costs and presented a novel data-driven model of distribution capacity costs. In Chapter 2, we used EnergyPlus and ResStock to simulate hourly energy demands for 75 residences in five climate regions throughout the continental United States. In Chapter 3, we provided background on several important emerging customer-side technologies that are poised to disrupt the relationship between electricity producer and consumer. In this chapter, we combine our analyses from the previous chapters to better understand how efficient deployment of emerging technologies may enable reductions in energy expenses and carbon emissions throughout the United States.

There is no one-size-fits-all solution to the problem of optimal customer-side technology choice. While the research into methodologies for optimizing customer-side technologies is quite expansive (Beck et al., 2017; Evins, 2015; Karmellos & Mavrotas, 2019; Mavromatidis, Orehounig, & Carmeliet, 2018; Mehleri et al., 2013; Omu, Choudhary, & Boies, 2013; Risbeck et al., 2017; Sani Hassan, Cipcigan, & Jenkins, 2017), few studies have unpacked how energy resources and needs vary between locations that have different climate profiles and demands for energy services.

Moreover, few papers include thermal loads in their analysis, though these represent 70% of

energy use in U.S. homes (Energy Information Administration, 2021). Today, heating energy in single-family homes is overwhelmingly provided by natural gas, though heat pumps are emerging as an opportunity to efficiently electrify some part of heating demand. Heating and cooling loads vary tremendously between climates: space heating alone represents nearly 60% of residential energy use in New England, falling to less than 30% in the Pacific and Mountain South regions. Space cooling demand represents nearly 20% of residential energy use in the West South Central region, but less than 5% in the Northeast and Midwest (U.S. Energy Information Administration (EIA), 2015, Table CE3.1).

Lastly, the literature overwhelmingly isolates the customer and attempts to minimize their individual expenses, treating the utility and its costs as exogenous. In these studies, the utility is modeled as a "producer of last resort" that can provide electricity as needed at some predetermined rate. By neglecting to describe the utility's costs and capacity constraints explicitly, these models do not minimize energy costs so much as they minimize a given customer's bills. Several authors have pointed out that because retail rates rarely reflect the true cost of energy services, customers making decisions to minimize their own bills often results in a cost shift to other customers rather than a true reduction in the cost of energy services (Schittekatte, Momber, & Meeus, 2018; Wolak, 2018).

In this chapter we construct a mixed-integer linear programming (MILP) model capable of determining the least-cost configuration of distributed resources and traditional grid infrastructure required to satisfy space heating demand, water heating demand, space cooling demand, and electric plug loads for an arbitrary collection of customers. The model can choose from a wide range of traditional and emerging technologies in order to satisfy these demands, including furnaces, air conditioners, heat pumps, resistance heating, solar panels, distributed storage, and energy efficiency. This model is then deployed to minimize the cost of energy services for representative collections of single-family residential customers in five different climate regions throughout the United States.

Additionally we conduct a number of sensitivity analyses, including scenarios that restrict the use of certain technologies and those that change important cost coefficients and constraints.

Using this approach, we are able to better understand how the optimal portfolio and operation of customer-side technologies varies based on features of the customer, climate, and local energy system.

This chapter expands on the existing literature by minimizing the total cost of energy services, rather than simply minimizing a customer's bill; by modeling energy demands in multiple representative climates throughout the United States; by including thermal loads in addition to electric plug loads (allowing for electrification of space and water heating, where economical); and by conducting multiple sensitivity analyses to understand the driving factors behind our results.

4.1 Background and Literature Review

The total cost of serving the energy demands for a collection of customers can be divided into four components:

1. The private cost of energy.
2. The cost of externalities related to energy production.[1]
3. The cost of infrastructure required to transport electricity from the producer to the consumer, including both large-scale transmission equipment as well as smaller distribution infrastructure required to reach a customer's premises. This was the focus of Chapter 1.
4. The cost of equipment installed at the residence, including heating and cooling equipment, distributed PV, and battery storage. We are assuming that all of the existing equipment is at the end of its life and in need of replacement.

The first and second components describe the full cost of energy. At any given time and location, the private marginal cost and external marginal cost of an energy input can be summed to describe its social marginal cost (SMC). If an input is priced below the SMC, customers are incentivized to consume it wastefully because they are not paying the full cost of the input. If an input is priced above the SMC, then customers may decline to use it even if it would be efficient for them to do so.

In practice, the prices that retail customers pay for electricity are based not on the first and

[1] In this analysis we model greenhouse gas (GHG) emissions from electricity combustion and fossil fuel combustion, but do not consider damages from particulate emissions, noise pollution, etc.

second components of the cost of energy, but on the first and third components. These expenses are paid by the utility and allocated to customers through a schedule of rates. The inclusion of fixed infrastructure costs in retail rates and exclusion (or underpricing) of externalities produce opposite, but not necessarily equal, effects on the retail rate. This causes the retail rate to deviate from the SMC in different ways throughout the United States.

In California, which has a relatively clean and affordable wholesale electricity supply but some of the highest retail rates in the country, the price that residential customers pay for a marginal unit of energy can exceed the average wholesale price by nearly a factor of ten (Borenstein & Bushnell, Forthcoming). Conversely, in much of the United States damages from GHG emissions (component 2) are unpriced, depressing the price of energy relative to its social cost.[2]

Borenstein and Bushnell (2021) demonstrates that this mispricing of electricity significantly distorts the cost of operating heat pumps and charging electric vehicles in California, discouraging customers from adopting these emissions-reducing technologies. Wolak (2018) demonstrates that overpricing of electricity in California also over-incentivizes investments in distributed rooftop solar, causing a cost-shift to other customers.

Rather than minimizing aggregate system costs, most of the literature on optimal DER adoption focuses on minimizing a single customer's expenses based on pre-determined retail rates, treating the utility and its expenses as exogenous. For example, Evins (2015), Mehleri et al. (2013), and Omu, Choudhary, and Boies (2013) assume constant volumetric rates for electricity purchased from the grid. Karmellos and Mavrotas (2019) assumes that electricity can be purchased from the grid at a time-of-use rate that varies between 0.0647 and 0.0946 €/kWh. Beck et al. (2017) analyze several scenarios with different volumetric delivery tariffs, but keeps the tariff constant within any scenario-year combination. Mavromatidis, Orehounig, and Carmeliet (2018) assume that electricity prices vary stochastically between years but are constant in any given year.

[2]The electricity sector produced 1.55 billion metric tonnes of CO2 in 2020 (U.S. Energy Information Administration (EIA), 2021b), between 35-40% of which was consumed in homes (U.S. Energy Information Administration (EIA), 2021a). At $51/tonne, this cost about $30 billion in damages. Homes in the United States also used 3,965 trillion BTUs of natural gas (U.S. Energy Information Administration (EIA), 2015), producing 210 million tonnes of CO2 emissions and costing another $10.7 billion in damages.

While the problem definition addressed in most of the literature (a minimization of customer payments) is certainly useful for assessing the potential savings available to a single customer or small group of customers, it does not tell us what configurations of technologies minimize the total cost of energy services. If the goal of these studies is to identify an efficient combination of traditional grid resources and DERs, then they should be evaluating the cost of energy inputs directly, rather than relying on regulated retail rates.

A number of papers acknowledge the mismatch between retail rates and energy costs, focusing specifically on the problem of efficient tariff design. Abdelmotteleb et al. (2018) propose a novel methodology for efficient utility cost recovery, based on SMC pricing, a fixed monthly charge, and a peak-coincident network charge. Relative to the case of simple volumetric tariffs, this approach results in cost savings on the order of 9–10%, achieved through customers curtailing their peak-hour consumption and thus deferring substation upgrades.[3] Schittekatte, Momber, and Meeus (2018) demonstrate that inefficient tariff design creates opportunities for so-called "reactive customers" to reduce their bills by strategically shifting sunk costs in the distribution system to "passive customers." Hoarau and Perez (2019) formulate a non-cooperative game between a grid operator and several groups of customers who have adopted EVs and DERs. The authors find that the choice of network tariff design can create conflicting incentives for the various groups.

In this chapter we sidestep the problem of efficient tariff design, instead constructing a MILP optimization model that minimizes the total cost of serving a collection of customers' energy demands when the costs of all inputs are evaluated on the margin. These costs include the private cost of energy, damages from GHG emissions, the cost of infrastructure, and the cost of equipment. This model is then used to conduct a rigorous analysis of how the optimal portfolio of

[3]This approach of reducing system costs through load curtailment is only possible because the local distribution network is assumed to be in need of an imminent capacity upgrade. Several authors note that that the optimal tariff design (and optimal configuration of DERs) is highly dependent on the condition of the existing network. Schittekatte and Meeus (2018) compare optimal tariff design between theoretical networks that have 100% sunk costs, 100% prospective costs, or a mix of both. The authors demonstrate that distributed generation is effective at reducing network costs if and only if some portion of those costs are prospective. When distribution system capacity exceeds a network's peak demand, distributed generation does not offer any benefit in the form of deferred capital costs. M. A. Cohen, Kauzmann, and Callaway (2016) analyzed 2987 distribution feeders in PG&E's service territory, finding that only 10% of them were in need of distribution upgrades in the coming ten years, and that distributed PV only offered deferral benefits in excess of $60/kW-year to about 1% of them.

DERs and traditional grid resources varies between climates and based on different assumptions about costs and constraints.

4.2 Methodology

We employ a mixed integer linear programming approach to simulate a hypothetical "energy services utility" serving a single electrical feeder with a group of single-family residences. This hypothetical utility is responsible for minimizing the total cost of energy, GHG emissions, infrastructure, and equipment installed in residences while satisfying all customers' energy services demands (including space heating, space cooling, water heating, and electric plug load demands). This utility may select the kinds of equipment installed in each residence, the capacity of each piece of equipment, and its hourly operation. Options include heating and cooling equipment (including gas furnaces, heat pumps, air conditioners, electric baseboards, and water heaters), distributed solar PV panels, and battery storage. Additionally, the utility may provide energy efficiency retrofits to reduce the year-round thermal demands for each residence and expand electric distribution capacity where needed to accommodate increased peak loads from electrification. By modeling a single entity that is responsible for minimizing the total cost of energy services – rather than individual customers responding to prices that are set a priori – we are able to set a lower bound on the total cost of energy services when all decisions are perfectly coordinated.

Another distinguishing feature of this approach is the inclusion of heating electrification. Electrification of heating is poised to dramatically increase the rate of load growth on distribution feeders, producing very steep, highly-correlated peaks on cold days (Mai et al., 2018; Waite & Modi, 2020). A model that does not explicitly include the utility's distribution capacity may prescribe electric heating options that trigger costly upstream reinforcements.

We are minimizing the total cost of energy services subject to a set of constraints governed by energy demands and engineering constraints. The objective function that we are minimizing is: $PrivateEnergyCost + ExternalitiesCost + InfrastructureCost + EquipmentCost$

PrivateEnergyCost is the cost paid by a utility for the energy commodity. For an electric utility in a competitive electricity market, the private cost of energy can be computed based on the hourly location-based marginal price (LBMP or LMP). For an electric utility that generates its own electricity, the private cost of energy is equal to the sum of all capital and O&M expenses associated with operating its generation facilities. For states with cap-and-trade markets, some fraction of the social cost of carbon is privatized into the cost of energy.[4] The private cost of natural gas is based on the wholesale (city gate) price.

ExternalitiesCost describes all costs associated with the utility's operation but not borne by the utility. We exclusively focus on greenhouse gas emissions, though this approach can easily be extended to consider other externalities.

$InfrastructureCost$ describes all utility investments needed to serve load, including upstream transmission, distribution, and administration expenses that do not vary with consumption; the cost of additional distribution capacity required to meet peak load; and generation capacity cost.[5]

EquipmentCost describes the cost of equipment installed at residences, including all heating and cooling equipment, distributed solar, and storage.

The first two terms can be combined into a single expression representing the total (social) cost of energy. This is expressed in Equation 4.1. The first bracketed expression is the total social cost (private plus external) of natural gas in dollars, where γ^{Gas} is the social marginal cost (SMC) of natural gas in \$/kBTU, $E_{\eta,r,t}^{Furnace}$ is the gas consumed by a furnace of efficiency η in residence r at time t, and $E_{UEF,r,t}^{WaterHeater}$ is the gas consumed by a natural gas water heater of efficiency UEF in residence r at time t.

The second bracketed expression in Equation 4.1 is the total social cost of electricity in dollars over the course of a year, where $\gamma_t^{Electric}$ is the social marginal cost (SMC) of electricity in \$/kWh,

[4]We do not factor existing cap-and-trade prices into our analysis. As of 2019 (the price data we are using), the RGGI auction price for carbon emissions was less than \$6 per-ton, barely 10% of the estimated social cost of carbon.

[5]Generation capacity costs could instead be included in *PrivateEnergyCost*. Our decision to categorize them as infrastructure simply allows us to better understand how peaks drive utility expenses.

$E^{HP}_{SEER,r,t}$ is the electricity consumed for space heating by a heat pump of nominal efficiency $SEER$ in residence r at time t, $E^{AC}_{SEER,r,t}$ is the electricity consumed for space cooling by an air conditioner or heat pump of nominal efficiency $SEER$ in residence r at time t, $E^{SupplementalRes.}_{r,t}$ is the electricity consumed by a supplemental resistance heater in residence r at time t, $E^{WaterHeater}_{UEF,r,t}$ is the electricity consumed by an electric (resistance or heat pump) water heater of efficiency UEF in residence r at time t, $E^{Baseboard}_{r,t}$ is the electricity consumed by baseboard resistance heaters in residence r at time t, $E^{PlugLoads}_{r,t}$ is the electricity consumed by miscellaneous plug loads in residence r at time t, $E^{PV}_{r,t}$ is the electricity produced by distributed solar installed at residence r at time t, $E^{Battery^+}_{t}$ is the electricity stored in a battery at time t (installed at the feeder level), and $E^{Battery^-}_{t}$ is the electricity discharged from the battery at time t. The constraints governing the operation of these technologies are described later in this section.

$$
\begin{aligned}
&PrivateEnergyCost + ExternalitiesCost = \\
&\qquad \sum_t \left[\gamma^{Gas} * \sum_{\eta,UEF} \sum_r \left[E^{Furnace}_{\eta,r,t} + E^{WaterHeater}_{UEF,r,t} \right] \right] + \\
&\sum_t \left[\gamma^{Electric}_t * \sum_{\eta,SEER,UEF} \sum_r \left[E^{HP}_{SEER,r,t} + E^{AC}_{SEER,r,t} + E^{SupplementalRes.}_{r,t} + \right. \right. \\
&\qquad \left. \left. E^{WaterHeater}_{UEF,r,t} + E^{Baseboard}_{r,t} + E^{PlugLoads}_{r,t} - E^{PV}_{r,t} + E^{Battery^+}_{t} - E^{Battery^-}_{t} \right] \right] \qquad (4.1)
\end{aligned}
$$

The r subscript is an index for the residence. In our example, r ranges from 1 to 15. The t subscript indexes the hours of the year, from 1 to 8760. η, UEF, and $SEER$ are measures of efficiency for various types of heating equipment.[6] The summation over the efficiency indices simply states that for whatever equipment is selected at each residence, its energy consumption is included in the objective function.

$InfrastructureCost$ is described by Equation 4.2. $Upstream^{Gas}$ and $Upstream^{Electric}$ are

[6] η is the efficiency of a furnace, typically ranging from 80% to 96%. UEF is the Uniform Energy Factor for water heaters, which ranges from less than one for conventional water heaters to greater than 3 for heat pump water heaters. $SEER$ is the Seasonal Energy Efficiency Ratio for air conditioners and heat pumps. The SEER describes the typical ratio of thermal energy produced (in KBTU) to electricity consumed (in kWh). SEERs typically range from 13 to 18.

the upstream gas and electricity expenses that are not a function of consumption on the feeder. Because electrification of space and water heating is poised to increase electric system peaks, we also include a term that describes additional distribution/feeder capacity required to meet peak loads, $C^{FeederCap}$ and a term that describes any negative capacity required to accommodate injections from customers, $C^{FeederMin}$. The last term, $C^{Generation}$, describes the total generation capacity allocated to this feeder, which is assumed to be proportional to the coincident feeder-wide electricity peak.[7] $C^{Generation}$ is always positive as long as there is some electricity demand from the grid, whereas $C^{FeederCap}$ is positive only if the peak demand increases from the pre-optimized loads (e.g. due to heating electrification). $C^{FeederMin}$ is positive only if the net load on the feeder drops below zero due to injections exceeding consumption. We do not include capacity terms for the natural gas system because we assume that it is already sized to meet the residences' full space heating and DHW loads.

$$InfrastructureCost = Upstream^{Gas} + Upstream^{Electric} + \beta^{FeederCap} * C^{FeederCap} + \beta^{FeederMin} * C^{FeederMin} + \beta^{Generation} * C^{Generation} \quad (4.2)$$

EquipmentCost is described by Equation 4.3. A key feature of customer-scale energy optimization is that a significant fraction of investments are lumpy (e.g., installing a furnace incurs a significant upfront cost that does not scale linearly with increasing capacity). These non-linear cost structures are captured by using a binary variable for whether or not a piece of equipment is installed and a separate continuous variable for the capacity of that piece of equipment. The α terms are cost-coefficients associated with the installation of a piece of equipment with a non-linear cost structure.[8] These include annualized installation costs and the annualized cost of a "zero-capacity" piece of equipment (i.e. the intercept term when the

[7]The cost coefficient for generation capacity, $\beta^{Generation}$, is non-zero only in the climate regions that have separate capacity markets.

[8]The use of binary variables also allow us to enforce semi-continuous value constraints on equipment capacities (e.g. a residence can forgo a furnace or install one with a capacity above 40 kBTUh, but cannot install one with a capacity smaller than 40 kBTUh).

non-linear costs are fitted with an OLS regression). The y terms are binary variables indicating whether or not a given category of equipment is installed in a residence. The β terms are capital cost-coefficients ($/kW or $/kBTUh) and the C terms are capacities installed. A_r^{PV} is the area of PV panel installed on the roof of residence r. For a piece of equipment with a non-linear cost structure, such as a natural gas furnace, the annualized cost of a capacity-C unit is equal to $\alpha_{\eta,r}^{Furnace} * y_{\eta,r}^{Furnace} + \beta_{\eta,r}^{Furnace} * C_{\eta,r}^{Furnace}$. As in Equation 4.1, the summation over the efficiency indices simply states that for whatever equipment is selected at each residence, its cost is included in the objective function.

$$
\begin{aligned}
EquipmentCost = \\
\sum_{\eta,SEER,UEF} \sum_{r} \Big[& \alpha_{\eta,r}^{Furnace} * y_{\eta,r}^{Furnace} + \beta_{\eta,r}^{Furnace} * C_{\eta,r}^{Furnace} + \alpha_{SEER,r}^{HP} * y_{SEER,r}^{HP} + \\
& \alpha_{SEER,r}^{AC} * y_{SEER,r}^{AC} + \beta_{SEER,r}^{HP} * C_{SEER,r}^{HP} + \alpha^{SupplementalRes.} * y^{SupplementalRes.} + \\
& \beta_r^{Baseboard} * C_r^{Baseboard} + \alpha_{UEF,r}^{WaterHeater} * y_{UEF,r}^{WaterHeater} + \\
& \beta_r^{PV} * A_r^{PV} + \beta^{Battery} * C^{Battery} + \beta_r^{EE} * C_r^{EE} \Big] \qquad (4.3)
\end{aligned}
$$

Table 4.1: Table of variables.

Variable	Description
η	Furnace efficiency
UEF	Uniform Energy Factor for water heaters
$SEER$	Seasonal Energy Efficiency Ratio for air conditioners and heat pumps
$\alpha_{\eta,r}^{Furnace}$	Cost of a zero-capacity furnace of efficiency η in residence r
$\alpha_{SEER,r}^{HP}$	Cost of a zero-capacity heat pump of efficiency SEER in residence r
$y_{\eta,r}^{Furnace}$	Binary variable indicating whether or not a furnace with efficiency η is installed in residence r
$y_{SEER,r}^{HP}$	Binary variable indicating whether or not a heat pump of efficiency SEER is installed in residence r

Continued on next page

Variable	Description
$y_r^{Baseboard}$	Binary variable indicating whether or not an electric baseboard is installed in residence r
$\beta_{\eta,r}^{Furnace}$	Furnace cost per-unit capacity ($/kBTUh)
$\beta_{SEER,r}^{HP}$	Heat pump cost per-unit capacity ($/kW)
$\beta_r^{Baseboard}$	Baseboard cost per-unit capacity ($/kBTUh)
β_r^{PV}	Photovoltaic panel cost per-unit capacity ($/kW)
$\beta^{Battery}$	Battery cost per-unit capacity ($/kWh)
$\beta^{FeederCap}$	New feeder capacity cost per-unit capacity ($/kW)
β_r^{EE}	Energy efficiency cost ($/sf)
$C_{\eta,r}^{Furnace}$	Furnace capacity (kBTU)
$C_{SEER,r}^{HP}$	Heat Pump capacity (kW)
$C_r^{Baseboard}$	Baseboard heater capacity (kW)
C_r^{PV}	Solar photovoltaic panel capacity (kW)
$C^{Battery}$	Battery capacity (kWh)
$C^{FeederCap}$	New feeder capacity (kW)
$C^{FeederMin}$	Negative feeder capacity to accommodate injections (kW)
C_r^{EE}	Energy efficiency reduction (%)
$C_\eta^{Furnace,Min}$	Minimum possible furnace capacity (kBTUh)
$C_\eta^{Furnace,Max}$	Maximum possible furnace capacity (kBTUh)
$C^{Generation}$	Generation capacity allocated to feeder
$C_{SEER}^{HP,Min}$	Minimum possible heat pump capacity (kWh)
$C_{SEER}^{HP,Max}$	Maximum possible heat pump capacity (kWh)
γ^{Gas}	Social marginal cost (SMC) of natural gas ($/kBTU)
$\gamma_t^{Electric}$	Social marginal cost (SMC) of electricity ($/kWh)
$E_{\eta,r,t}^{Furnace}$	Gas demanded by furnace (kBTUh)
$E_{\eta,r,t}^{HP}$	Electricity demanded by heat pump (kW)
$E_{r,t}^{Baseboard}$	Electricity demanded by baseboard heater (kW)

Continued on next page

Variable	Description
$E_{r,t}^{PlugLoads}$	Electricity demanded by miscellaneous plug loads (kW)
$E_{r,t}^{PV}$	Electricity produced by solar photovoltaic panels (kW)
$E_{t}^{Battery^{+}}$	Electricity added to battery storage (kW)
$E_{t}^{Battery^{-}}$	Electricity removed from battery storage (kW)
$E_{r,t}^{EV}$	EV charging at residence r at time t (kW)
$I_{r,t}^{PV}$	Total irradiance on a roof-mounted solar panel at residence r at time t (kW/m^2)
$\eta_{Storage}$	Battery round-trip efficiency
$\eta^{Baseboard}$	Baseboard heating efficiency (kBTU/kWh)
$COP_{SEER,t}^{HP}$	Coefficient of heating performance of a heat pump of efficiency SEER at time t (kBTU/kWh)
$COP_{SEER,t}^{AC}$	Coefficient of cooling performance of a heat pump or air conditioner of efficiency SEER at time t (kBTU/kWh)
$D_{r,t}^{Heat}$	Demand for heating energy in residence r at time t (kBTUh)
$D_{r,t}^{Cool}$	Demand for cooling energy in residence r at time t (kBTUh)
$D_{r,t}^{DHW}$	Demand for hot water energy in residence r at time t (kBTUh)
$D_{r,d}^{EV}$	Demand for electric vehicle charging on day d
EE_r	Fractional reduction in hourly heating and cooling demands due to envelope retrofits in residence r

The MILP formulation also includes a number of constraints governed by the physical limitations of the installed technologies. The operation of each furnace is constrained by Equations 4.4-4.6. Equation 4.4 ensures that the fuel consumed in a furnace at time t does not exceed the furnace's capacity.[9] Equations 4.5 and 4.6 constrain the domain of possible capacities to those that can reasonably be procured for residential use, while also ensuring that a non-zero capacity is only possible for a piece of equipment if the respective y-term is unity (incurring the installation and zero-capacity costs). The operation of heat pumps are similarly constrained by

[9]Note that the nominal installed capacity for furnaces, heat pumps, and air conditioners is based on the maximum amount of energy (kW or kBTUh) that can be consumed over a given interval, not the maximum amount of heat delivered to the space. The heat delivered to the space is mediated by the system's efficiency, described in Equation 4.15.

Equations 4.7-4.9, and baseboard electric heaters by 4.10.

$$E^{Furnace}_{\eta,r,t} \leq C^{Furnace}_{\eta,r} \tag{4.4}$$

$$C^{Furnace}_{\eta,r} \geq C^{Furnace,Min}_{\eta} y^{Furnace}_{\eta,r} \tag{4.5}$$

$$C^{Furnace}_{\eta,r} \leq C^{Furnace,Max}_{\eta} y^{Furnace}_{\eta,r} \tag{4.6}$$

$$E^{HP}_{SEER,r,t} \leq C^{HP}_{SEER,r} \tag{4.7}$$

$$C^{HP}_{SEER,r} \geq C^{HP,Min}_{SEER} * y^{HP}_{SEER,r} \tag{4.8}$$

$$C^{HP}_{SEER,r} \leq C^{HP,Max}_{SEER} * y^{HP}_{SEER,r} \tag{4.9}$$

$$E^{Baseboard}_{r,t} \leq C^{Baseboard}_{r} \tag{4.10}$$

An important quality of the heat pumps typically used in North American homes is that they are reversible, meaning that they can serve both the heating and cooling needs of a building. While not all single-family residences have ducting that can accommodate this, over 60% do.[10] In Equation 4.14, the electricity used for air conditioning, $E^{AC}_{SEER,r,t}$, is constrained as being no more than the sum of the cooling and heating capacities, C^{AC} and C^{HP}. Furthermore, Equation 4.12 guarantees that at most one central HP or AC is installed in any residence.[11] This allows for the model to use a heat pump to fulfill a building's heating and cooling needs, or an AC paired with a furnace or electric resistance coil. Equations 4.11-4.14 constrain the domain of possible capacities for air conditioners to those that can reasonably be procured for residential use, while also ensuring that a non-zero capacity is only possible if the respective y-term is unity.

[10] According to U.S. Energy Information Administration (EIA) (2015), 61.5% of surveyed single-family homes (attached or detached) have a central air conditioner for cooling and either a furnace or heat pump for heating.

[11] Even without this constraint, it is unlikely that the model would select multiple HPs/ACs for a single residence because it would more expensive than reasonable alternatives.

$$E^{AC}_{SEER,r,t} \leq C^{AC}_{SEER,r} + C^{HP}_{SEER,r} \tag{4.11}$$

$$\sum_{SEER} y^{AC}_{SEER,r} + y^{HP}_{SEER,r} \leq 1 \tag{4.12}$$

$$C^{AC}_{SEER,r} \geq C^{AC,Min}_{SEER} * y^{AC}_{SEER,r} \tag{4.13}$$

$$C^{AC}_{SEER,r} \leq C^{AC,Max}_{SEER} * y^{AC}_{SEER,r} \tag{4.14}$$

Equations 4.15 and 4.16 guarantee that all heating and cooling demand is satisfied at each hour in a given residence. $COP^{HP}_{SEER,t}$ is the coefficient of performance of a heat pump of rated efficiency SEER at time t while operating in heating mode. $COP^{AC}_{SEER,t}$ is the coefficient of performance of an air conditioner or heat pump of rated efficiency SEER at time t operating in cooling mode. C^{EE}_{r} is the percent reduction in hourly thermal demands due to energy efficiency improvements.

$$\sum_{\eta} \eta^{Furnace} * E^{Furnace}_{\eta,r,t} + \sum_{SEER} COP^{HP}_{SEER,t} * E^{HP}_{SEER,r,t} + \eta^{Baseboard} * E^{Baseboard}_{r,t} = D^{Heat}_{r,t} * (1 - C^{EE}_{r}) \tag{4.15}$$

$$\sum_{SEER} COP^{AC}_{SEER,t} * E^{AC}_{SEER,r,t} = D^{Cool}_{r,t} * (1 - C^{EE}_{r}) \tag{4.16}$$

Heat pump and air conditioner efficiencies vary with temperature, so the COP vectors are computed exogenously using dry bulb temperature from the same typical meteorological year (TMY) weather data used to model heating and cooling loads. Note that while an AC or HP's coefficient of performance (COP) is typically non-dimensional, the COP values we use here are computed in kBTU/kWh. This allows us to use a single set of variables to address thermal loads in kBTU while aggregating electrical loads in kWh.

Equation 4.17 ensures that the model can select a supplementary electric resistance coil in a residence only if it also selects an AC or HP. Without an AC or HP, the resistance coil would need an auxiliary blower fan to operate as an electric resistance furnace.

$$y^{SupplementalRes.} \leq \sum_{SEER,\eta,r} y_{\eta,r}^{Furnace} + y_{SEER,r}^{HP} \tag{4.17}$$

Equation 4.18 describes the hourly production from solar panels, where $I_{r,t}^{PV}$ is the total irradiance on a south-facing roof-mounted solar panel at residence r at time t in kW/m^2; η_{PV} is the PV system efficiency; ϵ_r^{PV} is a variable between 0 and 1 for each residence that accounts for losses due to shading and sub-optimal panel orientation; and A_r^{PV} is a decision variable describing the roof area that each customer covers with solar panels.

$$E_{r,t}^{PV} = I_{r,t}^{PV} * \eta_{PV} * \epsilon_r^{PV} * A_r^{PV} \tag{4.18}$$

The model is also able to invest in distributed battery storage to satisfy loads, manage excess solar production, and arbitrage wholesale electricity prices. The continuity constraint for battery charge is described by Equation 4.19. At time t, the stored energy on the battery, $S_t^{Battery}$, is equal to the energy stored from the previous time interval, $S_{t-1}^{Battery}$, plus the energy added to the battery, minus the energy withdrawn. The efficiency term, $\eta_{Storage}$, enforces each battery's round-trip efficiency.

$$S_t^{Battery} = S_{t-1}^{Battery} + E_t^{Battery^+} - \frac{1}{\eta_{Storage}} E_t^{Battery^-} \tag{4.19}$$

Equations 4.20 and 4.21 constrain the maximum charging/discharging rate to 25% of the battery's capacity (Cole & Frazier, 2020).

$$E_t^{Battery^+} \leq 1/4 * C^{Battery} \tag{4.20}$$

$$E_t^{Battery^-} \leq 1/4 * C^{Battery} \tag{4.21}$$

Equation 4.22 sets the upper bound of the storage state as the battery's installed capacity. Equations 4.23 and 4.24 enforce that the battery must start and end the simulation at 50%

charge.

$$S_t^{Battery} \leq C^{Battery} \tag{4.22}$$

$$S_{t=0}^{Battery} = 0.5 * C^{Battery} \tag{4.23}$$

$$S_{t=t_{max}}^{Battery} = .5 * C^{Battery} \tag{4.24}$$

Note that while most technologies are specified for each residence, the model only specifies one battery for the entire feeder. Because loads are aggregated across the entire feeder at a single node, there is no reason that it would be more favorable to install storage at one residence versus another. If separate battery capacities were designated for each residence, the distribution of that capacity between residences would be arbitrary.

Equation 4.25 ensures that the hot water produced from water heaters must satisfy the hourly demand for hot water in each residence. Note that for electric resistance and heat pump water heaters, because $D_{r,t}^{DHW}$ is in units of kBTU and $E^{WaterHeater}$ is in units of kWh, the nominal UEF (a dimensionless unit) is adjusted to kBTU/kWh using a constant conversion factor of 3.412 kBTU/kWh.

$$\sum_{UEF} UEF * E_{UEF,r,t}^{WaterHeater} = D_{r,t}^{DHW} \tag{4.25}$$

The feeder capacity constraint is modeled by Equations 4.26 and 4.27. Equation 4.26 guarantees that the sum of all electric loads (net of PV generation and battery withdrawals) cannot exceed the feeder capacity. Equation 4.27 prevents the net load from dipping below zero, which would necessitate specific reinforcements to allow for a reverse power flow.[12] $C_0^{FeederCap}$ is the assumed feeder capacity before the optimization and $C^{FeederCap}$ is additional feeder capacity added to accommodate increased loads.

[12]We do not provide an option for the feeder to be upgraded to accommodate two-way power flows. This would only be optimal if rooftop solar were significantly less expensive on average than utility-scale power.

$$\sum_{r} E^{HP}_{\eta,r,t} + E^{Baseboard}_{r,t} + E^{PlugLoads}_{r,t} - E^{PV}_{r,t} + (E^{Battery^+}_{t} - E^{Battery^-}_{t}) + E^{EV}_{r,n,t} + E^{WaterHeater}_{UEF,r,t} \leq C^{FeederCap}_{0} + C^{FeederCap} \quad (4.26)$$

$$\sum_{r} E^{HP}_{\eta,r,t} + E^{Baseboard}_{r,t} + E^{PlugLoads}_{r,t} - E^{PV}_{r,t} + (E^{Battery^+}_{t} - E^{Battery^-}_{t}) + E^{EV}_{r,n,t} + E^{WaterHeater}_{UEF,r,t} \geq 0 \quad (4.27)$$

For the climate regions that have generation capacity markets, a constraint is used to compute the allocated generation capacity needed to serve a feeder. The cost of this capacity is included in the objective function.

$$\sum_{r,t} E^{HP}_{\eta,r,t} + E^{Baseboard}_{r,t} + E^{PlugLoads}_{r,t} - E^{PV}_{r,t} + (E^{Battery^+}_{t} - E^{Battery^-}_{t}) + E^{EV}_{r,n,t} + E^{WaterHeater}_{UEF,r,t} \leq C^{Generation} \quad (4.28)$$

While electric vehicle charging is not modeled in the bulk of this analysis, a specialized scenario includes EVs in each residence that must be charged overnight. For this scenario, Equation 4.29 is used to ensure that for each day, d, the requisite amount of energy is added to the car battery during the associated hours, $t \in d$, of the previous night. Equation 4.30 guarantees that charging can only occur overnight (when $ChargeOK_t$ is unity) and constrains the maximum rate of charging to 1.4 kW, which is typical of a Level 1 charger.

$$\sum_{t \in d} E^{EV}_{r,t} = D^{EV}_{r,d} \quad (4.29)$$

$$E^{EV}_{r,t} \leq 1.4 * ChargeOK_{r,t} \quad (4.30)$$

4.3 Data and Assumptions

We use the hourly demands simulated in Chapter 2 as inputs to the optimization. These include hourly space heating energy, water heating energy, space cooling energy, and electric plug loads.

The hourly SMC for electricity (in $/kWh) and constant SMC for gas (in $/kBTU) are computed in Equations 4.31 and 4.32, where the LBMP (location-based marginal price) represents the private costs of electricity and gas in each climate region, SCC_{lb}, is the social cost of carbon in $/lb, $Emissions_{kWh}^{Electric}$ is the local emissions coefficient of the grid in lb/kWh, and $Emissions_{kBTU}^{Gas}$ is the emissions produced from stoichiometric combustion of natural gas in lb/kBTU.[13][14]

$$SMC_t^{Electric} = LBMP_{kWh}^{Electric} + SCC_{lb} * Emissions_{kWh}^{Electric} \tag{4.31}$$

$$SMC^{Gas} = LBMP_{kBTU}^{Gas} + SCC_{lb} * Emissions_{kBTU}^{Gas} \tag{4.32}$$

For both equations, the second term represents the cost of externalities. For the base models, we estimate the social cost of carbon (SCC) as $51/tonne (Environmental Protection Agency, 2020; Interagency Working Group on Social Cost of Greenhouse Gases, United States Government, 2021). Because estimates of the SCC vary widely between analyses, we also include separate optimizations that assume SCCs of $0/tonne and $200/tonne. We do not evaluate the social cost of other chemical emissions, which are known to have localized health impacts. The costs of energy inputs are provided in Table 4.2.

[13] We do not model any additional emissions due to methane leaks throughout the natural gas system. While these leaks may be significant to the natural gas industry's overall global warming impact, there is little reason to believe that the quantity of methane leaked scales with the marginal consumption of an additional unit of consumption. Additionally, we do not measure damages from local particulate emissions.

[14] The hourly value for the SMC of electricity and gas are taken as exogenous parameters. While modeling the SMC as a function of load might be more accurate, it would create a large number of quadratic constraints, dramatically increasing the computational complexity of the model

Table 4.2: Average energy costs and emissions for each of the five locations considered. Average LBMPs, SMCs, and standard deviations for electricity are based on 2019 hourly data and computed using the modeled feeder load as a weighting factor. Natural gas costs are taken as annual averages, while the LBMP for electricity varies hourly. Emissions factors for electricity are based on Environmental Protection Agency (2020) whereas emissions from natural gas assumes stoichiometric combustion.

	Erie County, NY	San Diego, CA	Harris County, TX	Alexandria, VA	Marin County, CA
Building America Climate Region	Cold	Hot-Dry	Hot-Humid	Mixed-Humid	Marine
IECC Climate Region	5A	3B	2A	4A	3C
			Electricity		
Carbon Emissions[15], lb/kWh	0.2539	0.4987	0.9361	0.7475	0.4987
Average Private Cost, $/kWh (SD)	$0.028[16] ($0.015)	$0.040[17] ($0.026)	$0.058[18] ($0.240)	$0.029[19] ($0.011)	$0.041[20] ($0.028)
Average SMC[21], $/kWh (SD)	$0.035 ($0.015)	$0.052 ($0.026)	$0.082 ($0.240)	$0.048 ($0.011)	$0.053 ($0.028)
Generation Capacity Cost, $/kW-year	$27.64[22]	-	-	$38.64[23]	-
Add'l Feeder Capacity Cost, $/kW-year	$50	$50	$50	$50	$50
Negative Feeder Capacity Cost, $/kW-year	$50	$50	$50	$50	$50
			Natural Gas		
Private Cost[24], $/MMBTU	$4.25	$3.10	$3.02	$4.52	$3.10
SMC[25], $/MMBTU	$7.23	$6.08	$6.00	$7.50	$6.08

We provide the model with multiple options for space heating, space cooling, and water heating (DHW) equipment. These include both traditional and condensing furnaces (80% and 96% efficiencies, respectively), low- and high-efficiency heat pumps (14 and 18 SEER), low- and high-efficiency air conditioners (14 and 18 SEER), electric resistance baseboard heaters (which cannot easily be combined with other heating options), and electric resistance supplementary coils (which must be used with a HP, AC, or furnace). Likewise, the model can choose from multiple options for natural gas water heaters, electric resistance water heaters, and heat pump water heaters. Each of these is assumed to have a constant efficiency consistent with its rated UEF (universal energy factor). Data on equipment and installation costs were collected from HVACDirect (2020) and Navigant Consulting (2018). The equipment cost assumptions are summarized in Table 4.3.[26]

[15]Environmental Protection Agency (2020)

[16]NYISO (2021)

[17]California ISO (2021)

[18]ERCOT (2021)

[19]PJM (2021)

[20]California ISO (2021)

[21]Computed by combining private cost with damages from emissions, estimated at $51/tonne (Interagency Working Group on Social Cost of Greenhouse Gases, United States Government, 2021).

[22]NYSERDA (2019, p. 40)

[23]PJM (2019)

[24]Private cost of gas based on citygate price.

[25]Computed by combining private cost with damages from emissions, estimated at $51/tonne (Interagency Working Group on Social Cost of Greenhouse Gases, United States Government, 2021).

[26]Linear regression is used to determine separate fixed and variable costs for each piece of household equipment. The fixed cost includes the annualized zero-intercept cost of the equipment, the annualized cost of installation, and the recurring operations and maintenance cost. The variable cost (which scales with capacity) and the zero-intercept cost are determined through regression using data on multiple units of comparable equipment from HVACDirect (2020). For ACs and HPs, a single regression model is fit to 24 points using the equation: $Cost = \alpha_{AC} + \alpha_{HP-AC} * HP_i + \alpha_{SEER18} * SEER18_i + \beta_C * C_i + \beta_{SEER18,C} * (SEER18_i * C_i) + \omega_i$. α_{AC} represents the cost of zero-capacity AC system, α_{HP-AC} is the cost difference between a HP and an AC of the same capacity and SEER, HP_i is a dummy variable that indicates whether the piece of equipment is a HP, α_{SEER18} is the cost difference between an 18 SEER unit and a 14 SEER unit, $SEER18_i$ is a dummy variable indicating whether the equipment is 18 SEER, β_C is the variable cost per-kW for a 14 SEER unit, C_i is the equipment capacity, and $\beta_{SEER18,C}$ is the additional per-kW cost for an 18 SEER unit (this allows the model to fit different slopes for the 14 and 18 SEER units). The resulting model has 19 degrees of freedom and a multiple R-squared of 0.97. A similar models is constructed for furnaces, but without the additional fixed-effect terms for ACs vs. HPs. Several items, including water heaters and electric supplementary heating coils, have very few sizing options and are thus represented as only having a fixed cost. Conversely, electric baseboards, which are standalone units that do not require any central system, are presumed to only have a variable cost ($/kW).

Table 4.3: Annualized cost coefficients for equipment installed in residences. Upfront costs are annualized over the equipment's lifetime using a discount rate of 10%.

	Fixed Cost (α)	Variable Cost (β)
Gas Furnace (80%)	$ 243.87	$0.51 /kBTUh
Gas Furnace (96%)	$ 277.84	$0.78 /kBTUh
Low-Eff. HP (14 SEER)	$ 423.86	$58.70 /kW
High-Eff. HP (18 SEER)	$ 588.04	$106.25 /kW
Low-Eff. AC (14 SEER)	$ 359.52	$55.23 /kW
High-Eff. AC (18 SEER)	$ 486.57	$99.98 /kW
Electric Resistance (Baseboard)	$ -	$22.08 /kW
Electric Resistance Supplementary Coil (20kW)	$ 20.84	$ -
Gas Water Heater (UEF 0.63)	$ 271.00	$ -
Gas Water Heater (UEF 0.81)	$ 432.89	$ -
Electric Water Heater (UEF 0.93)	$ 119.66	$ -
Electric Water Heater (UEF 0.95)	$ 172.45	$ -
HP Water Heater (UEF 3.28)	$ 292.12	$ -
HP Water Heater (UEF 3.55)	$ 348.43	$ -
Solar PV		300 $/kW
Battery Storage		50 $/kWh

Most types of heating and cooling equipment need to be replaced every 10–20 years (Seiders et al., 2007). In the optimization, we assume that all residences are in need of new heating and cooling equipment.

While the existing heating and cooling equipment does not factor into the optimization, it is nonetheless informative to consider the types of fuels currently used for heating in each county as a point of comparison. Figure 4.1 shows the distribution of heating equipment used in single-family detached homes in each of the five counties studied, as estimated in the RESstock probability mass functions. In all five counties, natural gas (burned in either boilers or furnaces) represents the largest share of fuels. In Harris County, TX, electricity is the primary heating fuel in about one-third of single-family homes. By contrast, in Erie County, NY (which has the largest heating loads), electricity is used as the primary heating fuel in just 2% of homes. Up to 8% of homes in each of the counties studied use propane, fuel oil, or some other fuel (including solar thermal and biomass).

In the base scenario, we assume that all feeders have a headroom of 50% above the existing electric peak, inclusive of plug loads and any thermal loads already served by electricity in the simulations (a 10 kW load is served by a 15 kW-capacity feeder). This estimate is based on an analysis of the distribution feeders in National Grid's New York State Service Territory. (National Grid, 2020). The full set of National Grid feeders range in capacity from 260 kVA (kilovolt-amps) to nearly 6.7 MVA (megavolt-amps). The National Grid dataset includes the rated capacity at the base of each feeder as a well as historical time series of consumption. A large number of feeders have considerable headroom at their base: the summer peak on the median feeder only reaches 53% of its rated capacity and fewer than 25% of feeders reach summer peaks exceeding 70% of rated capacity.[27] These data are provided in Table 4.4.

The solar irradiance on the roof of each residence, $I_{r,t}^{PV}$, is estimated using procedure outlined in Sandia National Laboratories (2018). The weather data was pulled from the same typical meteorological year file we used to model each building's hourly energy demands. All rooftops are

[27]Pillai et al. (2012) find that the overhead capacity for electrification on a low-voltage Danish distribution system varies from 0-40%.

Figure 4.1: Distribution of heating equipment used in single-family detached homes in each of the five counties studied, as estimated by (National Renewable Energy Lab (NREL), 2021). In all five counties, natural gas is the dominant heating fuel.

Table 4.4: Summary statistics of National Grid feeder data. The median ratio of summer peak to feeder capacity is 53%, indicating that a large number of feeders have ample headroom for accommodating additional load.

	N	1%	25%	Median	Mean	75%	99%
Voltage(kV)	1920	4.16	4.16	4.80	8.58	13.20	13.20
Rated Current (A)	1904	142	300	360	360	425	515
Peak Current 2018 (A)	1907	14	120	183	186	246.00	388
Peak Current 2019 (A)	1906	11	116	172	175	229	356
Peak/Capacity Ratio	1901	0.06	0.37	0.53	0.54	0.70	0.97

modeled as pointing South and have the same tilt of 26.57 degrees (per the ResStock assumptions). All scenarios assume a solar panel efficiency of 16%. ϵ_r^{PV}, which accounts for sub-optimal panel orientation and losses due to shading, is sampled for each residence from a uniform distribution between 0.7 and 1 (Gagnon et al., 2016).

The battery, where installed, is assumed to have a round-trip efficiency of 80% (U.S. Energy Information Administration, 2021d).

The annualized cost of a fractional reduction in hourly space heating/cooling demands due to energy efficiency improvements, β_r^{EE}, is estimated as 15¢ per-sf-percentage-point. In other words, reducing space heating and cooling demands by 10% for a 2,000 square-foot residence would be expected to cost $\$0.15 * 10 * 2,000 = \$3,000$-per-year. The fractional reduction in space heating and cooling demands is capped at 40% (Urban Green Council, 2019).

We estimate that additional electric distribution capacity can be built at a long-run cost of $50 per-kW-year. This is based on estimates produced in Rauschkolb et al. (2021), which uses regression analysis to describe the relationship between distribution capital costs and the growth of distribution system peaks. Additionally, if the net load on the feeder drops below zero due to solar injections, "negative feeder capacity" can be built at the same $50 per-kW-year.

Additionally, we assume that there are certain upstream transmission, distribution, and administrative costs that are independent of the level of consumption on the feeder. These include

$727-per-customer for upstream electric infrastructure costs and $478-per-customer for upstream gas infrastructure costs (R. L. Fares & King, 2017; U.S. Energy Information Administration, 2020). These costs are treated as unavoidable, except in the microgrid case wherein the collection of customers must produce all of their own energy.

4.4 Scenarios Analyzed

We study how the least-cost configuration of distributed technologies and traditional grid resources varies between regions and under a range of different assumptions about costs and constraints. In the "base" scenario, we use the best available estimates for emissions factors and the current costs of energy inputs and existing technologies. The results from this scenario provide an estimate of the cost of serving customers' energy demands using a least-cost configuration of technologies, without any additional constraints. A "No HP/Solar/Storage" scenario is also constructed that restricts the use of rooftop solar PV, distributed storage, and heat pumps. In this scenario, the model can only choose from gas furnaces or electric resistance as heating options, and cannot use distributed solar and/or storage to defer feeder upgrades. To complement the "No HP/Solar/Storage" scenario, we include an "all-electric" scenario that restricts the use of natural gas for space and water heating. This scenario simulates an "electrify everything" policy that prohibits natural gas use.

To understand how technology development and a greener grid may impact results, the above three scenarios are also run using a set of progress assumptions. Relative to the base scenario, the progress scenarios assume that economies of scale result in a 30% reduction in the installed cost of heat pumps, air conditioners, rooftop solar PV, battery storage, energy efficiency, and feeder capacity. Additionally, we assume a 70% reduction in emissions from the electric grid relative to 2018 coefficients. This scenario is expected to strongly favor electrification of space and water heating.

Lastly, a number of additional scenarios are run that isolate specific variables of interest. These include scenarios the vary the social cost of carbon and the feeder headroom; a "microgrid" scenario that prohibits all electricity and gas imports; a scenario that includes loads from electric

vehicle charging; and a scenario that assumes a 50% higher cost for AC/HP installation.

4.5 Results

4.5.1 Base Scenario

Figure 4.2 shows the technologies adopted in each climate in the base scenario. Electric resistance DHW heaters are nearly ubiquitous in the least-cost portfolio in all five climates, while gas DHW heaters – which are common today – are absent. HP DHW heaters are also uncommon in the optimized scenarios, most likely because the capital cost cannot be justified by operational cost savings. This explanation is borne out by a hand calculation: if a typical residence requires 10 MMBTU of hot water energy each year, then an electric resistance water heater with a UEF of 0.93, would require 3,151 kWh of electricity. At 5¢/kWh, this would cost $156. A HP water heater with a UEF of 3.28 would only require 894 kWh of electricity, costing $45 ($112 less). However, because the HP water heater has an annualized cost that is $172 higher than the resistance heater, the savings do not justify the increased fixed costs. In order for the HP DHW to be cost-effective, the customer would need to consume at least 15 MMBTU of heat for hot water.

Of note is the absence of distributed solar or battery storage. Rooftop solar PV panels are available to the model at a cost of $300/kW-year. A 1 kW solar system in the hot-dry climate (which has the greatest potential for solar generation) can be expected to produce about 1,600 kWh of electricity each year. For this to be a cost-effective investment on its own, the full social value of the avoided electricity must average at least $\$300/1,600kWh = 19¢/kWh$. However, the electricity in this climate only has an average SMC of about 5.2¢/kWh.

Distributed battery storage is generally cost-effective if at least one of three conditions apply: (1) solar is cost-effective and the batteries are needed to store excess generation during the day, (2) the variability in the hourly value of electricity from the grid is great enough that the arbitrage opportunities for storage (charging when electricity is inexpensive and discharging when the electricity price goes up) justify its fixed costs, or (3) storage can be strategically discharged to

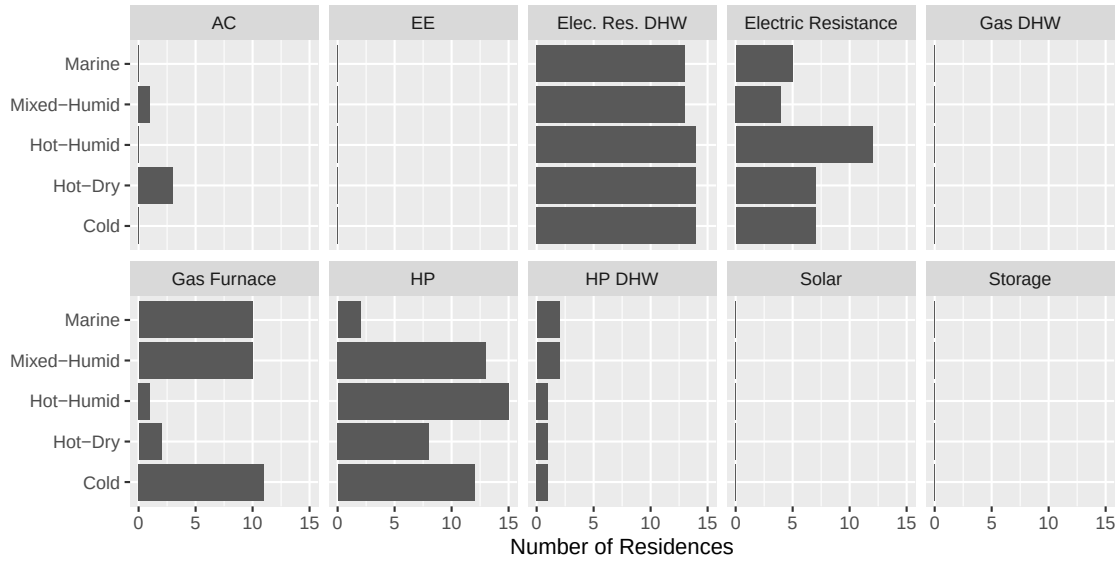

Figure 4.2: Number of residences adopting a given technology in each climate in the optimized models. "AC" and "HP" denote space cooling and heating energy. "EE" denotes energy efficiency. Heat pumps and electric resistance water heaters are nearly ubiquitous in the optimized portfolios.

curtail peak loads on the feeder, deferring the need for costly distribution system reinforcements. None of these conditions appear to apply in any of the five example regions.

Though neither distributed solar nor rooftop PV are found to be part of a least-cost portfolio in any of the climates we analyzed, another emerging technology – air source electric heat pumps – are found to be a major part of a least-cost portfolio in the mixed-humid, hot-humid, and cold climates. In the hot-humid climate in particular, heat pumps are used to satisfy nearly the entirety of the annual heating load. The cost-effectiveness of this choice can be borne out by a simple calculation: if the average COP of a low-efficiency heat pump is 3.6, then the electricity required to provide 1 MMBTU of heating energy is:

$$1MMBTU * \frac{293kWh}{1MMBTU} * \frac{1}{3.6} = 81.4kWh$$

The cost of providing this electricity at an SMC of 5¢/kWh[28] is:

[28]While the load-weighted SMC of electricity in the hot-humid climate is 8.2¢/kWh (per Table 4.2), this estimate is skewed by very high prices and demands during the summer months. The unweighted average SMC is 6.2¢, and the unweighted average during the winter months - when heating energy is required - is approximately 5¢/kWh.

$$81.4kWh * \$0.05 = \$4.07$$

To provide the same heating energy using an 80% efficiency furnace with natural gas at a natural gas SMC of \$6/MMBTU is:

$$1MMBTU * \frac{\$6}{MMBTU} * \frac{1}{80\%} = \$7.50$$

Moreover, because these homes all require air conditioning, the additional investment for a heat pump of the same size as the requisite air conditioner is simply the difference in fixed-costs plus the difference in capacity costs. For a 3 kW, 14 SEER heat pump, this amounts to \$423.86-\$359.52=\$64.34/year in additional fixed costs plus 3*(\$58.70-\$55.23)=\$10.41/year in capacity costs. This is significantly less than the approximately \$300/year investment required to install and maintain a gas furnace. Thus, electrifying heating with HPs reduces both capital and operating costs for residences in the hot-humid climate.

One potential caveat is that if the new load from heating electrification significantly raises the feeder peak above the existing feeder capacity, the cost of upgraded capacity could offset the operational and equipment savings realized at the household level. Additionally, for climate regions with non-zero generation capacity prices (in our example, the cold and mixed-humid climates), any increase to the feeder peak raises costs, even if there is already existing distribution capacity.

Figure 4.3 plots the daily peak electric loads for each of the five climates in the least-cost optimization. The solid red line represents the pre-existing feeder capacity (assuming 50% headroom above the pre-optimized loads) and the dashed line represents the peak after optimization. For the hot-humid climate, there is ample headroom in the winter months for heating electrification without increasing distribution or generation costs.

In the cold climate, the model is balancing two priorities: minimizing equipment and operational expenses while also managing the feeder peak, which can increase generation capacity

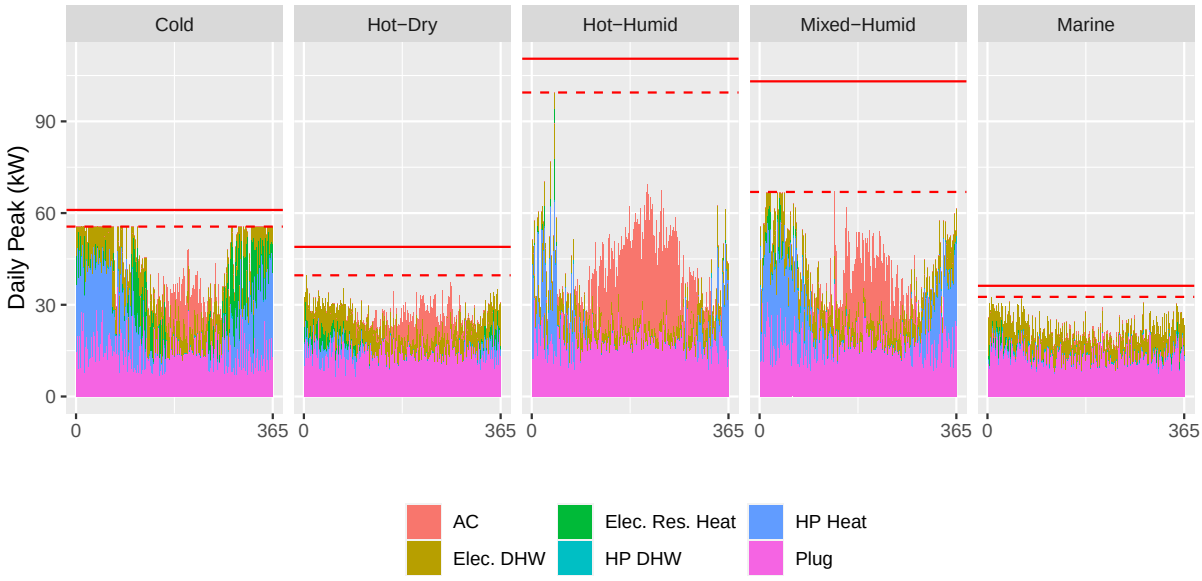

Figure 4.3: Annual profile of daily peak electric loads in the optimized models. The solid red line is the existing feeder capacity before the optimization, assuming 50% headroom relative to the incumbent peak. The dashed line is the optimized peak.

and distribution costs. This results in a "cropped" electric load in the winter months, where heat pumps are operated such that the feeder peak is kept below 60 kW. These heat pumps provide at most 5–6 MMBTU/day of space heating demand, with the remaining energy coming from furnaces (Figure 4.4).

In the hot-humid climate, nearly all heating demand is provided by heat pumps. In the mixed-humid and hot-dry climates, about 80% of heating energy is provided by electricity. In the cold climate, about two-thirds of heating demand is satisfied by either heat pumps or electric resistance, with the remaining load met by gas furnaces.

Heat pumps are not found to be part of the least-cost portfolio in most residences in the marine climate. This is most likely because most of these residences do not have air conditioning loads. Because the heat pump is only used during the heating season, the operational cost savings do not justify the increased capital cost of transitioning from a furnace (without an AC) to a heat pump.

We note that the distribution of heating technologies in these optimized scenarios looks

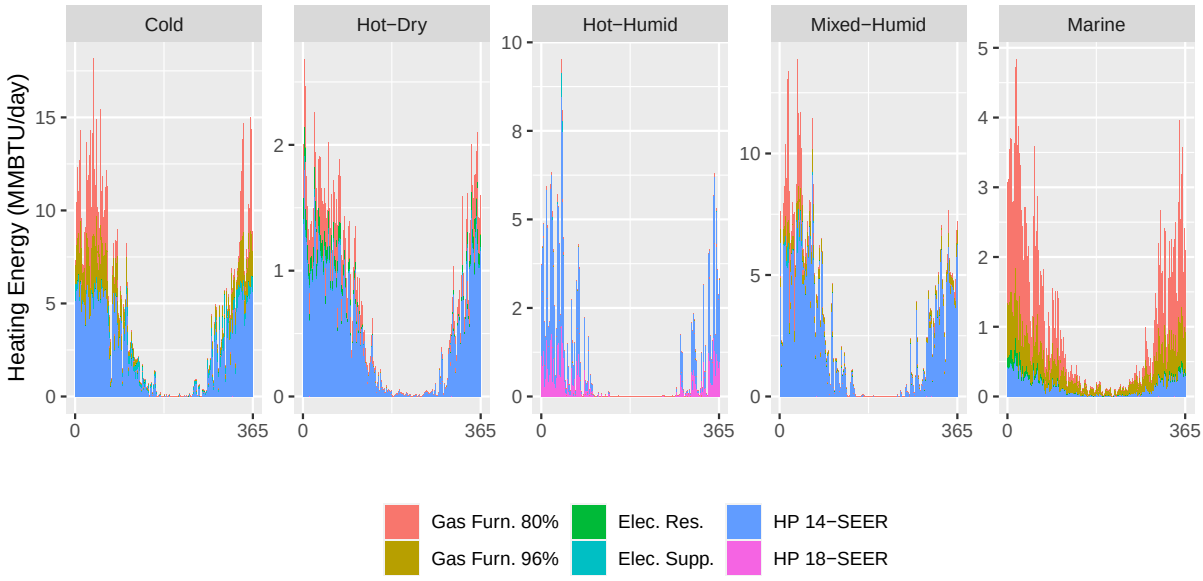

Figure 4.4: Annual profile of daily heating energy coming from various heating technologies, aggregated across all 15 residences for each feeder. In the cold and mixed-humid climates, which represent an outsize share of heating energy, low-efficiency (14-SEER) heat pumps are used to satisfy most of the residences' heating demands on all but the coldest days.

quite different than the actual distribution of technologies used in the example counties (see Figure 4.1). While natural gas is the dominant heating fuel used in the U.S. today, these results indicate that an approach that includes a greater share of electric heat pump heating could ultimately lower the cost of energy services. We note here that customers act as individuals, so this lower-cost reality will only be achieved if customers are individually incentivized to invest in the technologies that lower the total cost of energy services.

4.5.2 Conventional and All-Electric Scenarios

In order to understand how results from the least-cost portfolio compare to other approaches, we also run the same set of models in two specialized scenarios. A "No HP/Solar/Storage" scenario restricts the use of heat pumps (DHW and space heating), solar, and battery storage. By comparing the results from this model to the unconstrained base model, we are able to better understand the degree to which emerging technologies enable cost reductions. We also include an "all-electric" scenario that restricts the use of natural gas for space and water heating, allowing us

to explore how such a policy would affect the overall cost of serving residential energy demands.

Table 4.5 summarizes the major results from these scenario. Relative to the "No HP/Solar/Storage" approach, the least-cost case results in cost reductions in all climates, ranging from 1.7–7.0%. This is achieved predominantly by using heat pumps either in lieu of, or in addition to, traditional gas furnaces (this is known as "hybrid" or "dual-fuel" heating). For every climate except marine, at least 65% of heating energy is satisfied by electricity in the base case.

Notably, the hybrid heating approach strategy results in reductions in both private costs and emissions damages. Private costs (which include the private energy costs, utility infrastructure, and equipment costs) fall between 1–5% in the least-cost case relative to the "No HP/Solar/Storage" approach, while emissions damages fall by 9–35%. While the model formulation guarantees that the total cost in the least-cost case must not exceed the total cost in the "No HP/Solar/Storage" approach, it is not guaranteed that private costs will independently fall; the model could reduce total costs by lowering emissions and at the same time increase private costs. Nonetheless, in all five climates, HP space and water heaters enable reductions in private costs. The role that emissions damages play in driving the model is explored in Section 4.5.4.

While the use of electric heat pumps can enable significant cost and emissions reductions, they can also cause cost increases. For the cold climate, where full electrification of space and water heating would require significant system reinforcements, an all-electric policy increases the total cost of energy services by over 27% relative to the least-cost case. This is driven predominantly by the need for additional feeder capacity, additional heat pump capacity, and increased generation capacity to accommodate increased winter peaks (see Figure 4.5). A similar phenomenon occurs in the mixed-humid climate, though the increased feeder peak is less severe. Both of these scenarios also result in steep drops in the feeder load factor, from 41–57% to 17–31%.[29]

The marine climate sees cost increases on the order of 10% in its all-electric scenario. This

[29]We assume that maintaining natural gas infrastructure costs $478-per-customer ($7,170 for a 15-residence feeder), regardless of its level of use (U.S. Energy Information Administration, 2020). If a regional strategy of "pruning" the natural gas system reduces some of these expenses, that could significantly close the cost gap between an all-electric heating strategy and a hybrid/dual-fuel strategy in colder climates.

Table 4.5: Summary statistics for the optimized loads in the least-cost, "No HP/Solar/Storage", and all-electric scenarios. Energy costs include both the private cost of energy sold in wholesale electricity markets as well as any generation capacity costs required to serve the feeder. The average cost of electricity (¢-per-kWh) is computed as the sum of utility infrastructure costs, imported electricity costs, and distributed generation costs divided by the total electricity consumption from all sources.

		Cold	Hot-Dry	Hot-Humid	Mixed-Humid	Marine
Feeder Peak (kW)	Least-Cost	56	40	99	67	33
	No HP/Sol./Stor.	54	40	97	66	33
	All-Electric	213	40	98	138	48
Gas Consumption (MMBTU)	Least-Cost	607	57	3	186	348
	No HP/Sol./Stor.	1,327	216	273	991	424
	All-Electric	-	-	-	-	-
Electricity Cons. Total | Imports (MWh)	Least-Cost	277 | 277	149 | 149	228 | 228	249 | 249	117 | 117
	No HP/Sol./Stor.	243 | 243	156 | 156	228 | 228	193 | 193	119 | 119
	All-Electric	322 | 322	152 | 152	232 | 232	253 | 253	142 | 142
Carbon Emissions (tonnes)	Least-Cost	71	40	107	104	49
	No HP/Sol./Stor.	109	52	123	130	54
	All-Electric	41	38	108	95	35
Private Energy Cost	Least-Cost	$ 10,886	$ 5,982	$ 10,915	$ 10,071	$ 5,573
	No HP/Sol./Stor.	$ 12,529	$ 6,717	$ 11,299	$ 11,988	$ 5,895
	All-Electric	$ 14,336	$ 6,007	$ 11,179	$ 12,205	$ 5,707
Emissions Cost	Least-Cost	$ 3,606	$ 2,061	$ 5,448	$ 5,306	$ 2,522
	No HP/Sol./Stor.	$ 5,535	$ 2,627	$ 6,268	$ 6,645	$ 2,779
	All-Electric	$ 2,087	$ 1,938	$ 5,531	$ 4,820	$ 1,804
Utility Infrastructure Cost	Least-Cost	$ 18,106	$ 18,069	$ 18,069	$ 18,069	$ 18,069
	No HP/Sol./Stor.	$ 18,069	$ 18,069	$ 18,069	$ 18,069	$ 18,090
	All-Electric	$ 26,858	$ 18,069	$ 18,069	$ 20,608	$ 18,944
Equipment Cost	Least-Cost	$ 11,897	$ 8,239	$ 12,813	$ 12,430	$ 5,707
	No HP/Sol./Stor.	$ 11,342	$ 8,284	$ 13,042	$ 12,358	$ 5,608
	All-Electric	$ 13,434	$ 8,642	$ 12,828	$ 15,565	$ 8,591
Total Cost	Least-Cost	$ 44,495	$ 34,351	$ 47,246	$ 45,877	$ 31,871
	No HP/Sol./Stor.	$ 47,475	$ 35,697	$ 48,678	$ 49,060	$ 32,372
	All-Electric	$ 56,715	$ 34,657	$ 47,608	$ 53,197	$ 35,045
Feeder Load Factor	Least-Cost	57%	43%	26%	43%	41%
	No HP/Sol./Stor.	51%	45%	27%	34%	41%
	All-Electric	17%	43%	27%	21%	34%
Space Heating Energy from Electricity (%)	Least-Cost	64%	81%	99%	83%	17%
	No HP/Sol./Stor.	17%	28%	32%	6%	7%
	All-Electric	100%	100%	100%	100%	100%
Average Electricity Cost (per-kWh)	Least-Cost	7.65 ¢	12.52 ¢	11.96 ¢	10.01 ¢	14.55 ¢
	No HP/Sol./Stor.	8.11 ¢	12.18 ¢	11.78 ¢	11.57 ¢	14.39 ¢
	All-Electric	11.20 ¢	12.37 ¢	11.92 ¢	12.05 ¢	13.60 ¢

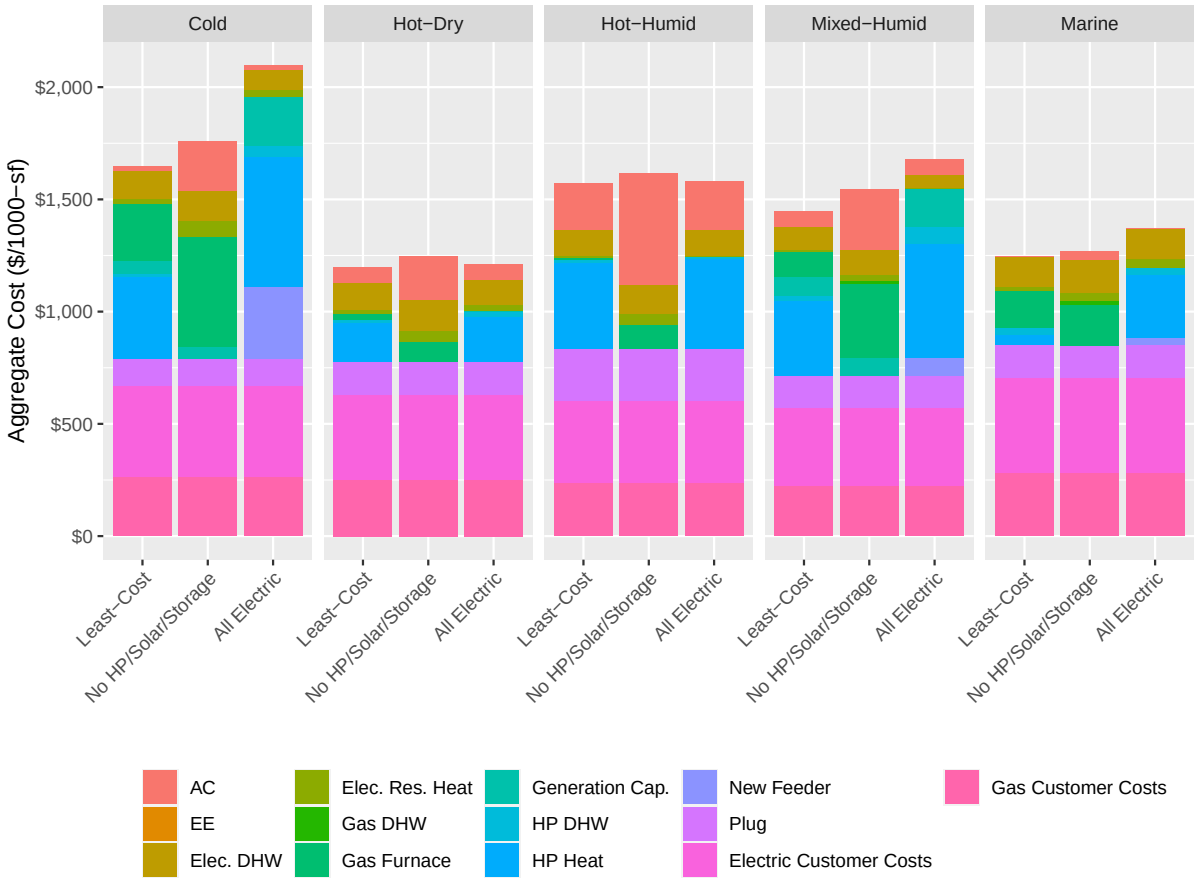

Figure 4.5: Categorization of costs in each scenario. "Electric Customer Costs" are estimated as $727-per-customer, while "Gas Customer Costs" are estimated as $478-per-customer (R. L. Fares & King, 2017; U.S. Energy Information Administration, 2020). These costs pay for upstream transmission, distribution, and administrative expenses, and are treated as unavoidable. "New Feeder" represents the cost of additional distribution capacity required to serve load that exceeds the existing feeder capacity (including headroom). "Generation Capacity" describes the cost of capacity payments in markets that have a separate capacity auction; this is proportional to the feeder-wide peak, independent of the feeder capacity. All of the other cost categories ("AC", "HP Heat", "Plug", etc.) combine equipment costs, private costs, and externalities.

can be explained in part because this climate has very little demand for cooling, so the heat pump is only used in the heating season and the fixed equipment cost outweighs the operational savings. For the marine climate, the private cost of energy is comparable across the base, "No HP/Solar/Storage," and all-electric scenarios, and the emissions (and associated damages) fall significantly in the all-electric scenario. However, these savings are outweighed by an additional $2,884 in equipment costs.

The average cost of electricity, reported in Table 4.5, is computed by summing the social cost of electric energy consumed from the grid, the cost of generation capacity allocated to the feeder, common electric utility costs associated with the feeder (including allocated upstream costs and the cost of additional distribution capacity) and the cost of distributed generation, then dividing by the amount of electricity consumed. In the least-cost case, this figure ranges from less than $0.08 per-kWh in the cold climate to over $0.14 per-kWh in the marine climate. The range in these numbers is driven by a number of factors, including differences in the wholesale price of electricity (per Table 4.2) and in the amount of electricity consumed by residences in different regions.

The annual profile of daily electric peaks are plotted for the all-electric and "No HP/Solar/Storage" scenarios in Figure 4.6. We note that for the cold climate (and to a lesser extent the mixed-humid climate), the all-electric heating strategy produces steep winter peaks that require additional feeder capacity. For the cold climate with all-electric heating, the feeder peak reaches 213 kW, per Table 4.5. For the hot-dry and hot-humid climates, full heating electrification can be facilitated without exceeding existing feeder capacity.

For the "No HP/Solar/Storage" technologies scenario, a significant amount of load from electric resistance heating appears on the feeder profiles in the cold, hot-dry, and hot-humid climates. However, this demand only represents 18–32% of heating energy, per Table 4.5.

Across all five climates, both the least-cost and all-electric scenarios realize significant emissions reductions relative to the "No HP/Solar/Storage" approach. For the cold climate, the all-electric scenario results in a 62% drop in emissions, while the least-cost case results in a 35% reduction. For the hot-humid and mixed-humid environments, emissions reductions due to

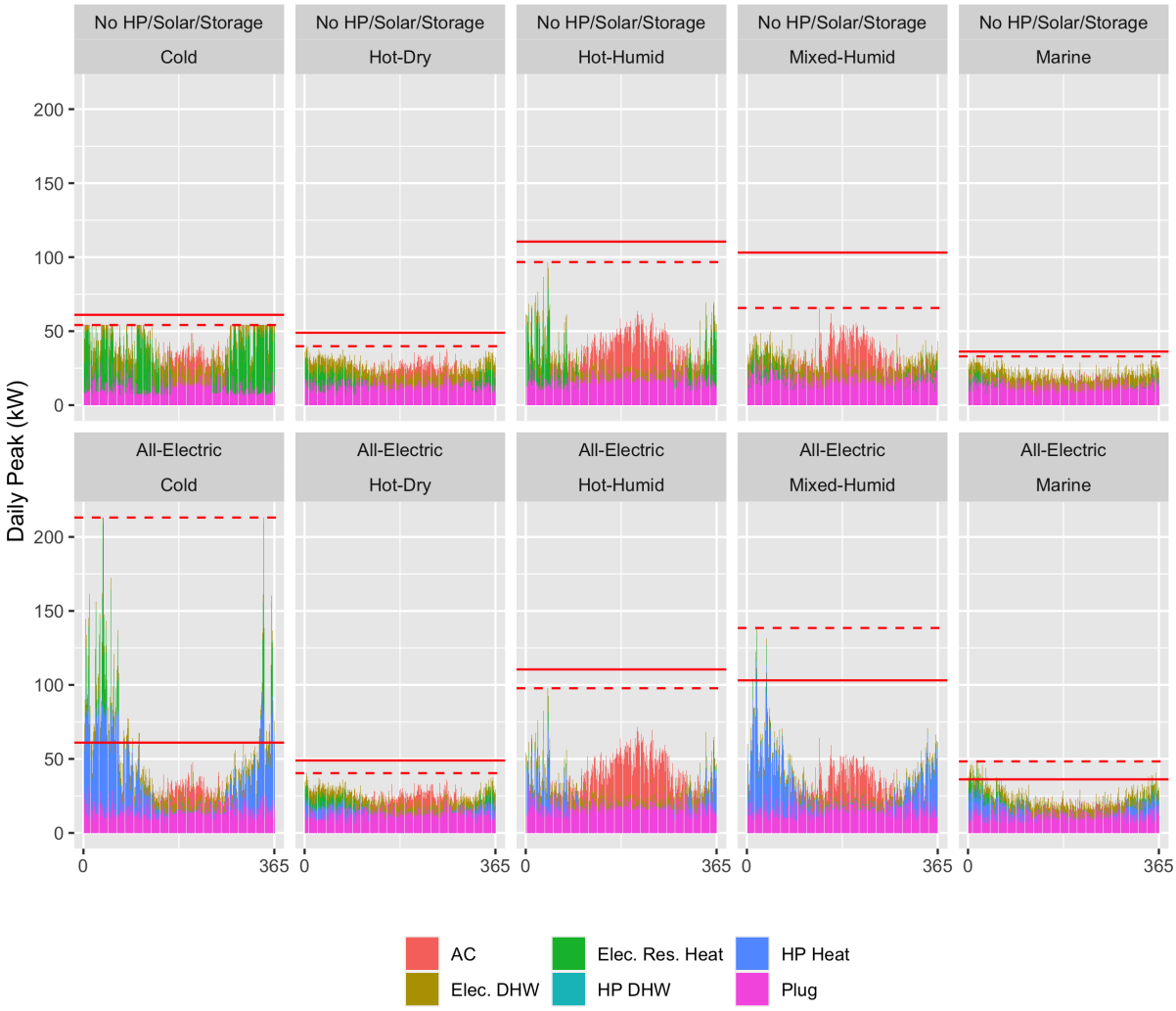

Figure 4.6: Annual profile of daily electric peak loads in the optimized models for the all-electric case (top) and the "No HP/Solar/Storage" case (bottom). The solid red line is the existing feeder capacity before the optimization (assuming 50% headroom relative to the incumbent peak). The dashed line is the optimized peak. The all-electric strategy produces significant increases in the required feeder capacity in the cold and mixed-humid climates.

electrification range from 11–27%.

For the cold and marine climates, emissions in the all-electric scenario are 42% and 29% lower than in the least-cost scenario, but the total costs of serving customers (including emissions damages) are higher. This indicates that the cost of minimizing emissions by fully electrifying space and water heating exceeds its benefit. To understand how the assumed social cost of carbon (SCC) influences the results, two specialized scenarios are presented in section 4.5.4 that assume SCCs of $0 and $200.

We note that the emissions results are particularly sensitive to the assumptions about emissions coefficients. For this analysis, we assumed a constant emissions factor for each climate region based on the 2018 average, as reported by Environmental Protection Agency (2020). For the representative cold climate (located in Upstate New York), this amounts to 0.2539 lb/kWh (see Table 4.2), which reflects the region's low-carbon electricity supply, backed by an abundance of nuclear and hydropower. By contrast, the average emissions factor in the hot-humid climate (Texas) is nearly four times higher.

When modeling new loads, most authors will use the non-baseload emissions factor (sometimes called "marginal emissions factor"). This coefficient, also reported in Environmental Protection Agency (2020), estimates the average emissions of all plants with variable output that follow variation in demand. For most regions, this coefficient is significantly higher than the average emissions coefficient because the load-following plants are predominantly powered by natural gas. To better understand how the grid emissions factor influences the emissions impact of heating electrification, we construct a simple example:

Let us say that we would like to produce 1 kWh (thermal) of heating energy. If we produce this with an electric heat pump, the electricity required is $q_{elec} = \frac{1kWh}{COP}$, where COP is the heat pump's coefficient of performance. If we produce this heat with natural gas, the natural gas required must have a caloric value of $q_{gas} = \frac{1kWh}{\eta}$, where η is the efficiency of the furnace. The ratio of the emissions produced from providing this heat with a heat pump to the emissions produced from providing this heat with a gas furnace can then be expressed:

$$r = \frac{Emissions_{elec}}{Emissions_{gas}} = \frac{e_{elec} * q_{elec}}{e_{gas} * q_{gas}} = \frac{e_{elec} * \frac{1kWh}{COP}}{e_{gas} * \frac{1kWh}{\eta}} = \frac{e_{elec}}{e_{gas}} * \frac{\eta}{COP}$$

Rearranging this equation to isolate e_{elec} and setting r equal to 1 tells us the value for e_{elec} at which the grid emissions for heat pump heating would equal the emissions produced by directly combusting natural gas in a furnace. For a low-efficiency heat pump in the cold climate with an average COP of 3, a low-efficiency furnace with an efficiency of 80%, and assuming stoichiometric combustion of natural gas ($e_{gas} = 0.117lb/kBTU = 0.4lb/kWh$), this figure simplifies to:

$$r = \frac{e_{elec}}{0.4lb/kWh} * \frac{80\%}{3} = 0.67 * e_{elec}$$

$$e_{elec} = 1.50lb/kWh$$

In other words, for there to be no emissions benefit to heat pump heating in the cold climate, the grid emissions would have to exceed 1.5 lb/kWh. This is 57% higher than the national average grid emissions of 0.952 lb/kWh, but only slightly above the national average non-baseload (load following) emissions of 1.423 lb/kWh (Environmental Protection Agency, 2020). If one employs the non-baseload emissions factor – assuming that all of the electricity required to power newly-electrified loads comes from existing load-following plants – then the emissions benefits of heating electrification all but disappear.

Most advocates of heating and transportation electrification will argue that an electrification strategy must go hand-in-hand with a major expansion of renewable electricity production. While it is unsound to imagine that 100% of the electricity required to electrify heating and transportation will come from zero-emissions renewables, it is equally unlikely that this new load will be met entirely by existing thermal plants. While the historical eGrid numbers are very precise estimates of historical emissions factors, they are merely a snapshot; they do not offer meaningful insight into how the grid is changing.

Increased demand from electrification will spur new investments in generation, much of which is poised to come from wind and solar. Insofar as these new demands are flexible (thanks

to managed EV charging schedules, dual-fuel heat pump configurations, and perhaps thermal and/or battery storage), their loads can be shaped to match the output of variable renewable resources. This suggests that there is room for a symbiotic relationship between growth in renewables and electrification.[30]

4.5.3 Progress Scenarios

As renewables are added to the grid and there is greater adoption of emerging technologies, the emissions and cost implications of adopting various customer-side technologies can be expected to change. To gain a better understanding of what a least-cost portfolio of technologies would be in a lower-carbon future, we include a set of "progress" scenarios that assume a 30% reduction in the installed cost of heat pumps, air conditioners, rooftop solar PV, battery storage, energy efficiency, and feeder capacity, and a 70% reduction in emissions from the electric grid.

Table 4.6 summarizes the major results from these scenarios. As expected, the progress scenarios result in significantly lower costs and emissions than the base scenarios. The largest cost reductions in both relative and absolute terms for the least-cost cases are found in the hot-humid and mixed-humid environments, where the total cost of serving customer loads decreases by \$6,087–\$7,617 (13–16%). This appears to be driven by lower equipment costs and the reduced (social) cost of electricity purchased from the grid. These climates also see the greatest absolute emissions reductions, of 69–76 tonnes (66–71%).

The percentage of heating energy provided by electricity increases in all five climates. Notably, the marine climate, which only sees 17% of heating energy satisfied by electricity in the base case, has 50% of its heating energy satisfied by electricity in the progress case. In the cold climate, the percentage of heating energy provided by electricity increases from 65% to 75%. Gas consumption falls from 599 MMBTU to 445 MMBTU and emissions drop by 34 tonnes (48%).

In the progress scenario, the model selects 94 kWh of battery storage in the hot-humid

[30]The most-thorough approach to understanding how these technologies could spread in tandem would involve building a generation model that is endogenous to the customer-level optimization. Rather than including emissions and energy/generation costs as input parameters, this model would simultaneously optimize generation investments and customer-side technology adoption.

Table 4.6: Summary statistics for the optimized loads in the progress scenarios. Energy costs include both the private cost of energy sold in wholesale electricity markets as well as any generation capacity costs required to serve the feeder. The average cost of electricity (¢-per-kWh) is computed as the sum of utility infrastructure costs, imported electricity costs, and distributed generation costs divided by the total electricity consumption from all sources.

		Cold	Hot-Dry	Hot-Humid	Mixed-Humid	Marine
Feeder Peak (kW)	Least-Cost	55	35	99	63	31
	No HP/Sol./Stor.	54	40	102	73	33
	All-Electric	212	36	99	137	45
Gas Consumption (MMBTU)	Least-Cost	450	19	-	156	233
	No HP/Sol./Stor.	1,209	216	240	769	424
	All-Electric	-	-	-	-	-
Electricity Cons. Total | Purchases (MWh)	Least-Cost	266 | 266	140 | 140	220 | 226	233 | 233	106 | 106
	No HP/Sol./Stor.	278 | 278	156 | 156	230 | 230	249 | 249	119 | 119
	All-Electric	306 | 306	141 | 141	217 | 224	243 | 243	124 | 124
Carbon Emissions (tonnes)	Least-Cost	36	12	32	35	22
	No HP/Sol./Stor.	81	24	46	73	34
	All-Electric	12	11	31	27	9
Private Energy Cost	Least-Cost	$ 10,129	$ 5,651	$ 7,197	$ 9,665	$ 4,970
	No HP/Sol./Stor.	$ 12,898	$ 6,846	$ 11,190	$ 13,096	$ 5,994
	All-Electric	$ 14,010	$ 5,651	$ 7,059	$ 12,198	$ 5,107
Emissions Cost	Least-Cost	$ 1,857	$ 592	$ 1,619	$ 1,798	$ 1,101
	No HP/Sol./Stor.	$ 4,145	$ 1,239	$ 2,361	$ 3,715	$ 1,719
	All-Electric	$ 594	$ 538	$ 1,601	$ 1,392	$ 471
Utility Infrastructure Cost	Least-Cost	$ 18,069	$ 18,069	$ 18,069	$ 18,069	$ 18,069
	No HP/Sol./Stor.	$ 18,069	$ 18,069	$ 18,162	$ 18,069	$ 18,084
	All-Electric	$ 24,193	$ 18,069	$ 18,069	$ 19,789	$ 18,563
Equipment Cost	Least-Cost	$ 10,709	$ 6,988	$ 13,128	$ 10,482	$ 6,063
	No HP/Sol./Stor.	$ 9,689	$ 6,811	$ 10,542	$ 9,468	$ 5,327
	All-Electric	$ 10,252	$ 7,125	$ 13,391	$ 11,526	$ 7,292
Total Cost	Least-Cost	$ 40,765	$ 31,299	$ 40,014	$ 40,014	$ 30,204
	No HP/Sol./Stor.	$ 44,802	$ 32,965	$ 42,255	$ 44,349	$ 31,123
	All-Electric	$ 49,049	$ 31,384	$ 40,121	$ 44,906	$ 31,433
Feeder Load Factor	Least-Cost	55%	46%	26%	42%	39%
	No HP/Sol./Stor.	59%	45%	26%	39%	41%
	All-Electric	16%	45%	26%	20%	31%
Space Heating Energy from Electricity (%)	Least-Cost	75%	94%	100%	86%	48%
	No HP/Sol./Stor.	25%	28%	40%	24%	7%
	All-Electric	100%	100%	100%	100%	100%
Average Electricity Cost (per-kWh)	Least-Cost	7.44 ¢	12.18 ¢	10.51 ¢	9.12 ¢	14.68 ¢
	No HP/Sol./Stor.	7.04 ¢	11.37 ¢	10.09 ¢	8.91 ¢	13.58 ¢
	All-Electric	10.35 ¢	12.11 ¢	10.55 ¢	10.77 ¢	13.74 ¢

climate. This storage is used to arbitrage wholesale electricity prices. The battery is charged at a weighted-average SMC of 2.3¢ and discharged at a weighted-average SMC of 12.0¢.

4.5.4 Social Cost of Carbon

One important source of uncertainty is the estimated social cost of carbon (SCC). The social cost of carbon measures the damage that one unit of carbon dioxide emissions does to the economy through its contribution to anthropogenic climate change. At \$51/tonne,[31] these damages account for 25–30% of the social cost of electricity and nearly half of the social cost of natural gas. Other estimates of the SCC range from nearly \$0/tonne to over \$200/tonne, and ongoing work is required to revise the SCC used in federal calculations (Carleton & Greenstone, 2021; Interagency Working Group on Social Cost of Greenhouse Gases, United States Government, 2021). While a broad range of policies are advisable in both low-SCC and high-SCC scenarios (Kaufman, 2018), the precise estimate used in an optimization exercise can determine which fuels are best utilized for various purposes. Figure 4.7 illustrates the private and emissions costs of consuming electricity and natural gas under a range of SCC estimates. At \$200/tonne, the emissions cost becomes dominant for both electricity and gas.

For higher estimates of the SCC, the balance of technologies used for heating shifts in favor of higher efficiency equipment and electrification. In Figure 4.8, each column describes the equipment used to provide space heating energy in a different scenario. In the cold climate, raising the estimated SCC from \$51/tonne to \$200/tonne raises the fraction of space heating energy satisfied by electricity from 65% to 85%. Using a SCC of \$0/tonne lowers the fraction of space heating energy satisfied by electricity to 54%.

The precise value of the SCC has a modest effect on space heating equipment selection in the cold climate: at \$51/tonne, three residences use only a furnace for heating, four use only a HP, and eight use a combination of a HP and a furnace. At \$200/tonne, one residence uses only a furnace, four use only a heat pump, and the remaining ten use both. These results indicate that while the precise value of the SCC can determine the optimal balance of heating fuels, hybrid

[31] This is the central value estimated for 2020 in (Interagency Working Group on Social Cost of Greenhouse Gases, United States Government, 2021)

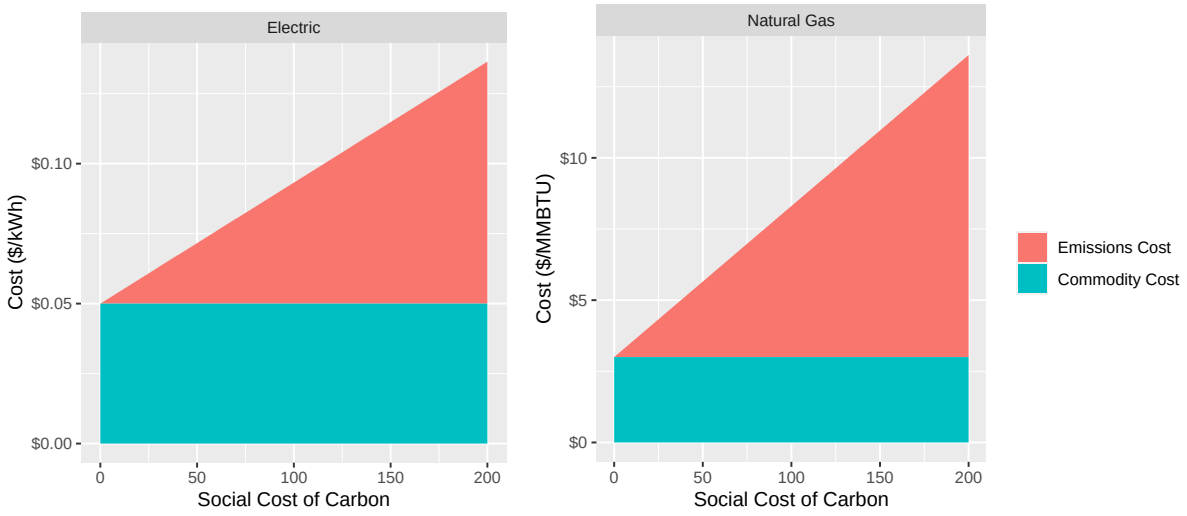

Figure 4.7: Commodity and emissions costs for electricity and gas, over a range of values for the social cost of carbon (SCC). The commodity cost of electricity is taken as 5¢/kWh and the emissions factor is assumed to be 0.9529 lb-CO2-equivalent/kWh. The commodity cost of gas is taken as $3/MMBTU and we assume stoichiometric combustion (117lb/MMBTU).

HP/furnace systems appear to be a robust least-cost solution for cold climate space heating over a range of estimates of the SCC.

In the hot-humid climate, higher estimates for the SCC incentivize adoption of higher-efficiency HPs. If the SCC is assumed to be $51/tonne, the majority of heat is delivered by a 14-SEER HP and only about 10% is delivered by an 18-SEER HP. At $200/tonne, more than 90% of space heating energy is delivered by an 18-SEER HP. In the marine climate, higher estimates for the SCC shift the balance of heating energy from being predominantly provided by low-efficiency furnaces to being predominantly provided by HPs and high-efficiency furnaces.

In addition to varying the SCC using the base assumptions, we also vary the SCC in scenarios that use the progress assumptions. For all values of the SCC in all climates, the progress scenario has s greater fraction of space heating energy supplied by electricity. In the hot-dry and hot-humid climates, combining the progress assumptions with a SCC of $200/tonne results in 100% electrification of space heating as a least-cost solution. In the other three climates, electricity is used to provide between 86–94% of space heating energy.

Table 4.7 summarizes the results from several additional optimization scenarios, including

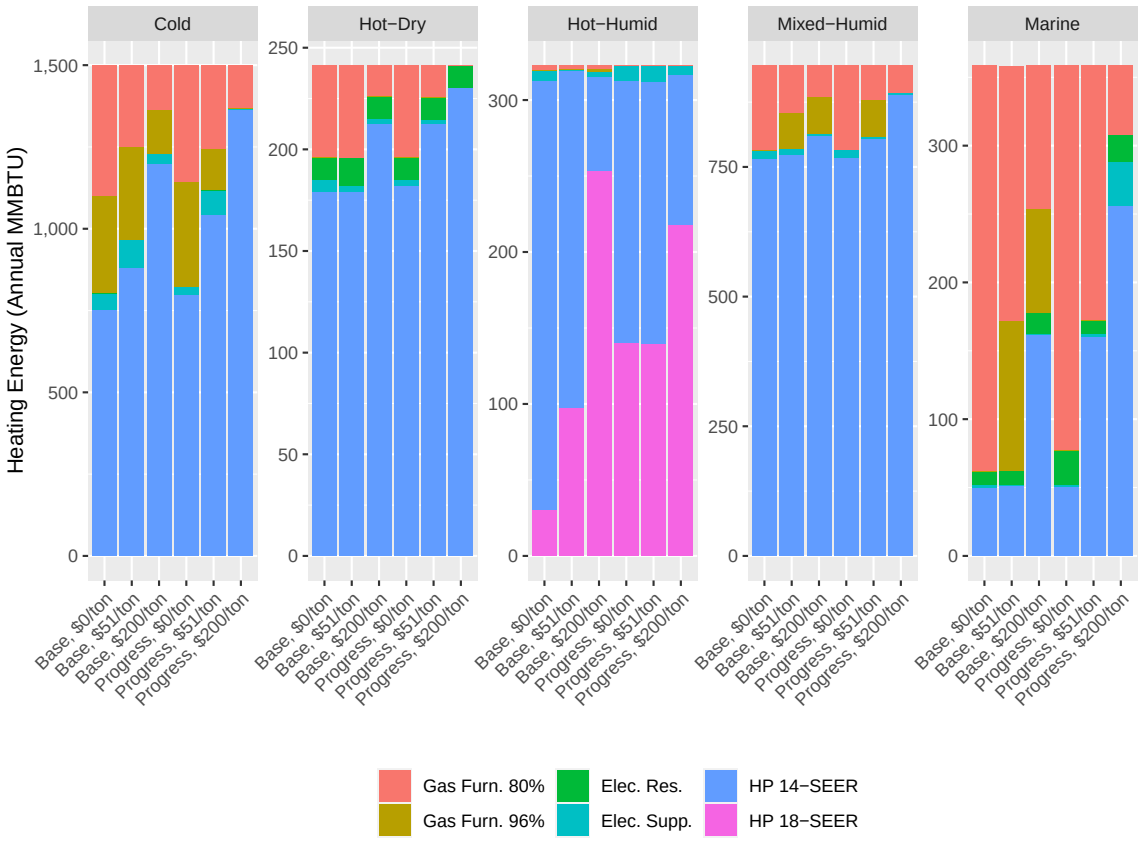

Figure 4.8: Breakdown of delivered heating energy in each climate in optimized models, using different estimates for the social cost of carbon (SCC). In both the base and progress scenarios, higher estimates for the SCC promote greater use of HPs. In the hot-humid climate, this includes adoption of high-efficiency HPs.

those that vary the SCC. Notably, the optimized feeder peaks in most of these scenarios rarely exceed the existing feeder capacities, so there is no need to reinforce the distribution system. Consequently, utility infrastructure cost is relatively constant, reflecting only upstream fixed costs.

Table 4.7: Summary statistics for the optimized loads in the additional scenarios. Energy costs include both the private cost of energy sold in wholesale electricity markets as well as any generation capacity costs required to serve the feeder. The average cost of electricity (¢-per-kWh) is computed as the sum of utility infrastructure costs, purchased electricity costs, and distributed generation costs divided by the total electricity consumption from all sources.

		Cold	Hot-Dry	Hot-Humid	Mixed-Humid	Marine
Feeder Peak (kW)	Low HR	47	36	66	62	31
	High HR	59	38	115	67	37
	No SCC	56	39	99	66	33
	$200/ton SCC	58	35	99	63	33
	Progress, No SCC	46	35	99	64	33
	Progress, $200/ton SCC	72	34	99	63	36
	Microgrid	-	-	-	-	-
	Base + EV	56	44	99	67	33
	High AC/HP Costs	55	43	101	66	33
	Constant $0.05 SMC	44	36	76	66	33
	Solar+Storage Favored	37	29	66	62	22
Gas Consumption (MMBTU)	Low HR	697	57	46	218	348
	High HR	596	56	-	186	325
	No SCC	808	56	4	224	401
	$200/ton SCC	308	19	4	149	210
	Progress, No SCC	777	56	-	203	352
	Progress, $200/ton SCC	162	-	-	66	63
	Microgrid	-	-	-	-	-
	Base + EV	708	56	3	190	348
	High AC/HP Costs	685	47	42	203	378
	Constant $0.05 SMC	971	57	2	173	336
	Solar+Storage Favored	872	57	4	218	372

Continued on next page

		Cold	Hot-Dry	Hot-Humid	Mixed-Humid	Marine
Electricity Cons. Total | Purchases (MWh)	Low HR	255 | 255	145 | 145	220 | 220	237 | 237	111 | 111
	High HR	285 | 285	148 | 148	230 | 230	249 | 249	122 | 122
	No SCC	253 | 253	153 | 153	239 | 239	253 | 253	119 | 119
	$200/ton SCC	271 | 271	140 | 140	196 | 196	231 | 231	110 | 110
	Progress, No SCC	225 | 225	138 | 138	223 | 230	238 | 238	109 | 109
	Progress, $200/ton SCC	276 | 276	133 | 133	198 | 203	238 | 238	122 | 122
	Microgrid	225 | 0	120 | 0	190 | 0	185 | 0	98 | 0
	Base + EV	315 | 315	203 | 203	280 | 280	303 | 303	171 | 171
	High AC/HP Costs	276 | 276	156 | 156	240 | 240	253 | 253	119 | 119
	Constant $0.05 SMC	209 | 209	145 | 145	238 | 238	248 | 248	119 | 119
	Solar+Storage Favored	224 | 226	145 | 147	228 | 237	236 | 236	115 | 118
Carbon Emissions (tons)	Low HR	66	36	96	92	44
	High HR	64	36	98	94	45
	No SCC	72	38	102	98	48
	$200/ton SCC	48	33	84	86	36
	Progress, No SCC	49	12	29	35	26
	Progress, $200/ton SCC	18	9	26	28	12
	Microgrid	-	-	-	-	-
	Base + EV	74	49	119	113	57
	High AC/HP Costs	68	38	104	97	47
	Constant $0.05 SMC	142	66	103	116	69
	Solar+Storage Favored	72	36	101	92	46
Private Energy Cost	Low HR	$ 10,815	$ 6,014	$ 11,062	$ 10,145	$ 5,586
	High HR	$ 11,454	$ 6,125	$ 11,461	$ 10,564	$ 5,991
	No SCC	$ 11,467	$ 6,336	$ 12,037	$ 10,784	$ 6,051
	$200/ton SCC	$ 10,135	$ 5,708	$ 9,740	$ 9,767	$ 5,144
	Progress, No SCC	$ 10,419	$ 5,731	$ 7,410	$ 10,212	$ 5,528
	Progress, $200/ton SCC	$ 10,096	$ 5,399	$ 7,108	$ 9,616	$ 5,207
	Microgrid	$ -	$ -	$ -	$ -	$ -
	Base + EV	$ 12,240	$ 8,042	$ 12,113	$ 11,713	$ 7,637
	High AC/HP Costs	$ 11,513	$ 6,438	$ 12,324	$ 10,721	$ 5,980
	Constant $0.05 SMC	$ 10,675	$ 5,349	$ 8,948	$ 9,537	$ 5,552
	Solar+Storage Favored	$ 10,341	$ 5,545	$ 5,943	$ 10,120	$ 5,251

Continued on next page

		Cold	Hot-Dry	Hot-Humid	Mixed-Humid	Marine
Emissions Cost	Low HR	$ 3,386	$ 1,826	$ 4,884	$ 4,686	$ 2,224
	High HR	$ 3,286	$ 1,860	$ 4,978	$ 4,814	$ 2,290
	No SCC	$ -	$ -	$ -	$ -	$ -
	$200/ton SCC	$ 9,507	$ 6,539	$ 16,709	$ 17,240	$ 7,189
	Progress, No SCC	$ -	$ -	$ -	$ -	$ -
	Progress, $200/ton SCC	$ 3,631	$ 1,812	$ 5,170	$ 5,552	$ 2,333
	Microgrid	$ -	$ -	$ -	$ -	$ -
	Base + EV	$ 3,770	$ 2,498	$ 6,074	$ 5,756	$ 2,916
	High AC/HP Costs	$ 3,478	$ 1,923	$ 5,307	$ 4,934	$ 2,392
	Constant $0.05 SMC	$ 7,232	$ 3,346	$ 5,244	$ 5,928	$ 3,541
	Solar+Storage Favored	$ 3,688	$ 1,854	$ 5,140	$ 4,671	$ 2,369
Utility Infrastructure Cost	Low HR	$ 18,639	$ 18,455	$ 18,069	$ 18,069	$ 18,580
	High HR	$ 18,069	$ 18,069	$ 18,069	$ 18,069	$ 18,069
	No SCC	$ 18,106	$ 18,069	$ 18,069	$ 18,069	$ 18,089
	$200/ton SCC	$ 18,236	$ 18,069	$ 18,069	$ 18,069	$ 18,069
	Progress, No SCC	$ 18,069	$ 18,069	$ 18,069	$ 18,069	$ 18,091
	Progress, $200/ton SCC	$ 18,728	$ 18,069	$ 18,069	$ 18,069	$ 18,216
	Microgrid	$ -	$ -	$ -	$ -	$ -
	Base + EV	$ 18,106	$ 18,069	$ 18,069	$ 18,069	$ 18,069
	High AC/HP Costs	$ 18,096	$ 18,069	$ 18,152	$ 18,069	$ 18,089
	Constant $0.05 SMC	$ 18,069	$ 18,069	$ 18,069	$ 18,069	$ 18,111
	Solar+Storage Favored	$ 18,069	$ 18,069	$ 18,069	$ 18,069	$ 18,069
Equipment Cost	Low HR	$ 12,440	$ 8,466	$ 13,969	$ 13,091	$ 6,099
	High HR	$ 11,682	$ 8,314	$ 12,507	$ 12,430	$ 5,542
	No SCC	$ 11,513	$ 8,093	$ 12,011	$ 11,980	$ 5,415
	$200/ton SCC	$ 14,924	$ 9,309	$ 16,452	$ 13,956	$ 7,394
	Progress, No SCC	$ 10,201	$ 6,834	$ 13,149	$ 9,969	$ 5,397
	Progress, $200/ton SCC	$ 12,026	$ 7,494	$ 13,925	$ 11,090	$ 6,801
	Microgrid	$ 368,556	$ 79,315	$ 152,918	$ 256,421	$ 172,008
	Base + EV	$ 11,736	$ 8,244	$ 13,161	$ 12,540	$ 5,686
	High AC/HP Costs	$ 14,766	$ 10,777	$ 16,453	$ 16,026	$ 6,011
	Constant $0.05 SMC	$ 12,375	$ 8,466	$ 12,433	$ 12,444	$ 5,606
	Solar+Storage Favored	$ 13,510	$ 9,161	$ 16,904	$ 13,443	$ 6,846

Continued on next page

		Cold	Hot-Dry	Hot-Humid	Mixed-Humid	Marine
Total Cost	Low HR	$ 45,281	$ 34,760	$ 47,985	$ 45,991	$ 32,488
	High HR	$ 44,491	$ 34,368	$ 47,016	$ 45,877	$ 31,892
	No SCC	$ 41,086	$ 32,498	$ 42,117	$ 40,833	$ 29,555
	$200/ton SCC	$ 52,802	$ 39,625	$ 60,970	$ 59,032	$ 37,797
	Progress, No SCC	$ 38,689	$ 30,634	$ 38,628	$ 38,250	$ 29,015
	Progress, $200/ton SCC	$ 44,481	$ 32,774	$ 44,272	$ 44,327	$ 32,557
	Microgrid	$ 368,556	$ 79,315	$ 152,918	$ 256,421	$ 172,008
	Base + EV	$ 45,852	$ 36,853	$ 49,417	$ 48,079	$ 34,308
	High AC/HP Costs	$ 47,854	$ 37,207	$ 52,237	$ 49,750	$ 32,471
	Constant $0.05 SMC	$ 48,352	$ 35,230	$ 44,694	$ 45,978	$ 32,810
	Solar+Storage Favored	$ 45,608	$ 34,629	$ 46,055	$ 46,303	$ 32,536
Feeder Load Factor	Low HR	62%	46%	38%	44%	41%
	High HR	55%	45%	23%	43%	38%
	No SCC	52%	45%	27%	44%	41%
	$200/ton SCC	53%	46%	23%	42%	38%
	Progress, No SCC	55%	45%	26%	42%	37%
	Progress, $200/ton SCC	44%	44%	23%	43%	38%
	Microgrid	-	-	-	-	-
	Base + EV	65%	53%	32%	52%	60%
	High AC/HP Costs	57%	41%	27%	44%	41%
	Constant $0.05 SMC	54%	46%	36%	43%	41%
	Solar+Storage Favored	70%	57%	41%	44%	62%
Space Heating Energy from Electricity (%)	Low HR	60%	81%	89%	83%	17%
	High HR	65%	81%	100%	83%	22%
	No SCC	54%	81%	99%	83%	17%
	$200/ton SCC	82%	94%	99%	86%	50%
	Progress, No SCC	55%	81%	100%	83%	22%
	Progress, $200/ton SCC	91%	100%	100%	94%	86%
	Microgrid	100%	100%	100%	100%	100%
	Base + EV	59%	81%	99%	83%	17%
	High AC/HP Costs	60%	84%	90%	83%	17%
	Constant $0.05 SMC	43%	81%	99%	84%	20%
	Solar+Storage Favored	49%	81%	99%	83%	15%

Continued on next page

		Cold	Hot-Dry	Hot-Humid	Mixed-Humid	Marine
Average Electricity Cost (per-kWh)	Low HR	8.16 ¢	12.97 ¢	12.10 ¢	10.20 ¢	15.48 ¢
	High HR	7.55 ¢	12.54 ¢	11.89 ¢	10.01 ¢	14.14 ¢
	No SCC	7.51 ¢	11.16 ¢	9.61 ¢	8.17 ¢	13.24 ¢
	$200/ton SCC	9.65 ¢	16.34 ¢	19.01 ¢	15.44 ¢	18.57 ¢
	Progress, No SCC	8.02 ¢	11.92 ¢	9.75 ¢	8.47 ¢	14.15 ¢
	Progress, $200/ton SCC	8.29 ¢	13.57 ¢	13.02 ¢	10.52 ¢	14.49 ¢
	Microgrid	141.49 ¢	54.92 ¢	64.79 ¢	112.85 ¢	142.91 ¢
	Base + EV	6.98 ¢	10.39 ¢	10.38 ¢	8.91 ¢	11.36 ¢
	High AC/HP Costs	7.65 ¢	12.20 ¢	11.83 ¢	9.90 ¢	14.41 ¢
	Constant $0.05 SMC	10.85 ¢	13.27 ¢	10.55 ¢	10.20 ¢	15.00 ¢
	Solar+Storage Favored	8.77 ¢	12.88 ¢	11.36 ¢	10.22 ¢	15.17 ¢

It is worth noting that the majority of heating is provided by heat pumps in four out of the five climates studied even if the SCC is assumed to be \$0/tonne. This indicates that heat pumps are an essential part of a least-cost technology portfolio, independent of any considerations about emissions damages.

4.5.5 High/Low Headroom

In the base scenarios, we assume that all feeders have a headroom of 50% over the pre-optimized peak. Because there is considerable variability in the available headroom for electrification between different feeders (National Grid, 2020), we include the results from two specialized scenarios for each feeder: one with zero headroom (the feeder is fully-congested during peak hours) and one with 100% headroom (the pre-optimization peak is half of the feeder's capacity).

Figure 4.9 shows the daily peaks in the cold and hot-humid climates for the zero headroom, base, and 100% headroom scenarios. Relative to the base case, the zero headroom scenario has a lower peak in the cold climate, with less heating energy provided by heat pumps and electric resistance heating. For the hot-humid climate, the higher headroom in the latter scenarios appears to only affect the equipment operation a few days per-year.

Even in the zero headroom scenario – wherein the feeder's capacity is highly-constrained – the model does not select distributed solar PV and/or storage to supplement electricity from the grid. For PV to be part of a least-cost portfolio of technologies, it would need to enable cost reductions from avoided energy and capacity in excess of its cost. In the hot-dry region, the average SMC of electricity is $\gamma_t^{Electric} = 5.2¢$, and a 1 kW PV array can be expected to produce 1,500–2,000 kWh/year, worth no more than $5.2¢ * 2,000 = \$104$ in avoided energy costs. This means that the value of avoided feeder capacity would have to be nearly \$200/year, approximately four times our estimate of the cost of additional distribution capacity.[32]

Notably, the change in total cost between the zero headroom, 50% (base), and 100% headroom

[32]Some authors will estimate a locational marginal capacity cost based on the present value of deferring a planned upgrade by a certain number of years, per the approach outlined in Woo et al. (1994). Using this approach, an author may produce much larger estimates for the value of avoided feeder capacity value if a DER project allows the utility to defer an expensive upgrade.

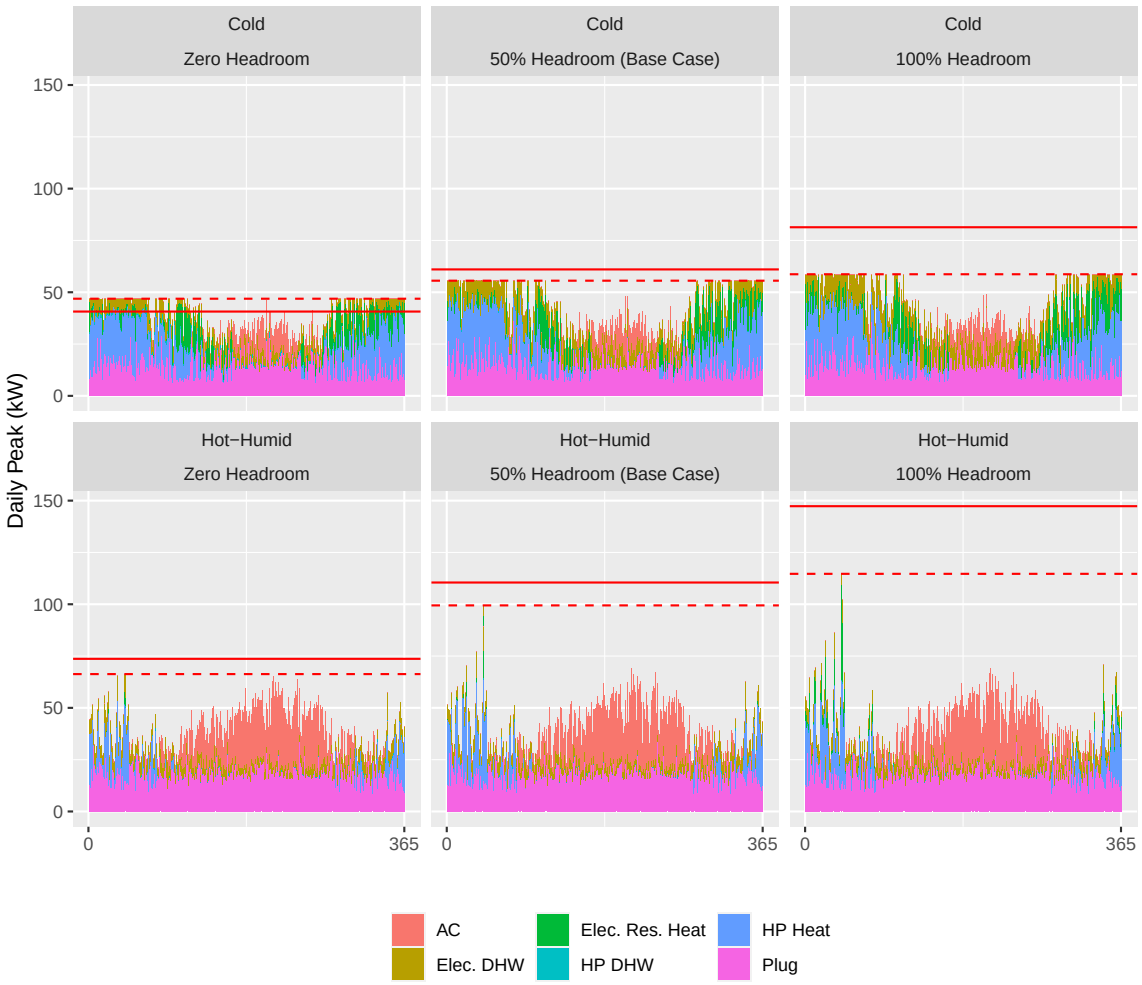

Figure 4.9: Top: daily peaks in the cold climate for the zero headroom, 50%, and 100% headroom scenarios. Bottom: daily peaks in the hot-humid climate for the zero headroom, 50%, and 100% headroom scenarios.

scenarios is relatively small in all climates. This makes sense in an optimized scenario, because the model is able to simultaneously adjust decisions at the household and utility levels to minimize costs. This further implies that modifying the estimate for the annualized cost of additional distribution capacity (say, from $50 per-kW to $300 per-kW) would only have a modest impact on cost as the model could simply refrain from increasing distribution capacity altogether.

In a model where customers are operating independently in response to pricing signals from the utility (especially rather blunt ones like volumetric tariffs), this delicate balance would be far more difficult to achieve. This is explored in Chapter 5.

4.5.6 Microgrid

The growing availability of inexpensive solar PV panels and battery storage raises the possibility that it will become economical for customers to abandon their utility services altogether and generate their own electricity. While skeptics of this decentralized approach will cite the higher cost of residential-scale rooftop solar relative to utility-scale installations, advocates have argued that the savings in upstream utility expenses justify the additional customer-side expenses.

To simulate a situation in which customers abandon their utilities and instead produce all of their energy locally using solar and storage, we construct a "microgrid" scenario. To create this scenario in our model, we simply set the upper bound of all purchases (electric and gas) to zero. Consequently, any consumption from equipment must be concurrently produced by solar panels or discharged from batteries.

Table 4.8 summarizes the equipment capacities chosen by the model for each region. The cold and mixed-humid climates have the greatest generation and storage requirements, reflecting their large heating and cooling requirements. The hot-dry climate has the smallest generation and storage requirements, due to its high solar potential and minimal thermal loads. The average load is computed over the course of the entire year and the storage duration is computed by dividing the storage capacity by the average load. In the shoulder seasons, the storage duration is significantly greater than the reported figure; in the heating and cooling seasons, it is significantly less.

Table 4.8: Summary of distributed energy resources in microgrid scenarios.

	Cold	Hot-Dry	Hot-Humid	Mixed-Humid	Marine
Solar Cap (kW)	120	19	39	67	36
Storage Cap (kWh)	2,980	573	1,251	2,914	1,862
Average Load (kW)	32	14	24	25	12
Storage Duration (Hours)	92	42	52	114	153

To put the storage figures in perspective, we can estimate the storage duration by dividing the storage capacity by the average feeder-wide load (including plug loads and thermal loads). The storage duration ranges from 42 hours for the hot-dry climate to 153 hours for the marine climate. The hot-dry climate is optimal for a solar-plus-storage arrangement because it has strong solar potential with low inter-day variation and very consistent year-round energy requirements.

Of note is the inefficient use of energy produced by the solar PV in the microgrid scenarios. Figure 4.10 shows the breakdown of energy potential from the solar panels. In all climates, more than half of the energy that can be produced by the PV array is either curtailed at the panel or dissipated by the battery. For the cold and marine climates, less than 25% of energy is utilized.

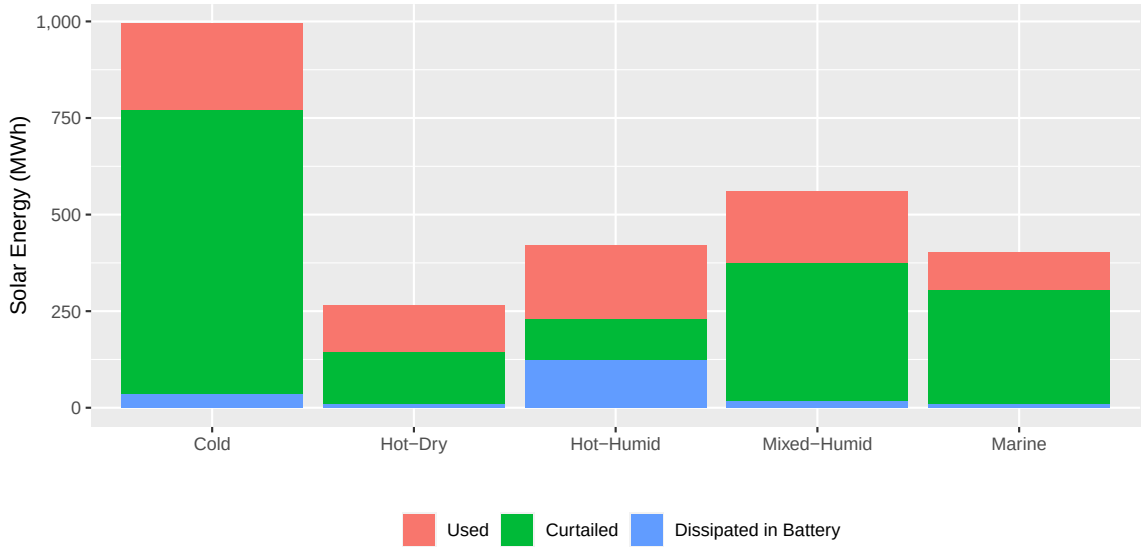

Figure 4.10: Breakdown of energy potential at solar panel.

Due to the high cost of distributed generation and its inefficient use, the cost of operating a microgrid system is significantly higher than the least-cost scenario in all climates, even when accounting for the sizable reduction in fixed costs. In the hot-dry climate, which has the

greatest solar potential and the smallest annual space-heating demand, the annual cost of serving a collection of customers with solar and storage is $2,768 per-1000-sf (including annualized equipment costs). This is more than twice as large as the least-cost configuration, which includes over $630 per-1000-sf ($18,000 total) in unavoidable utility costs. In other climates, the cost is even higher. The results of this analysis are presented in Figure 4.11.

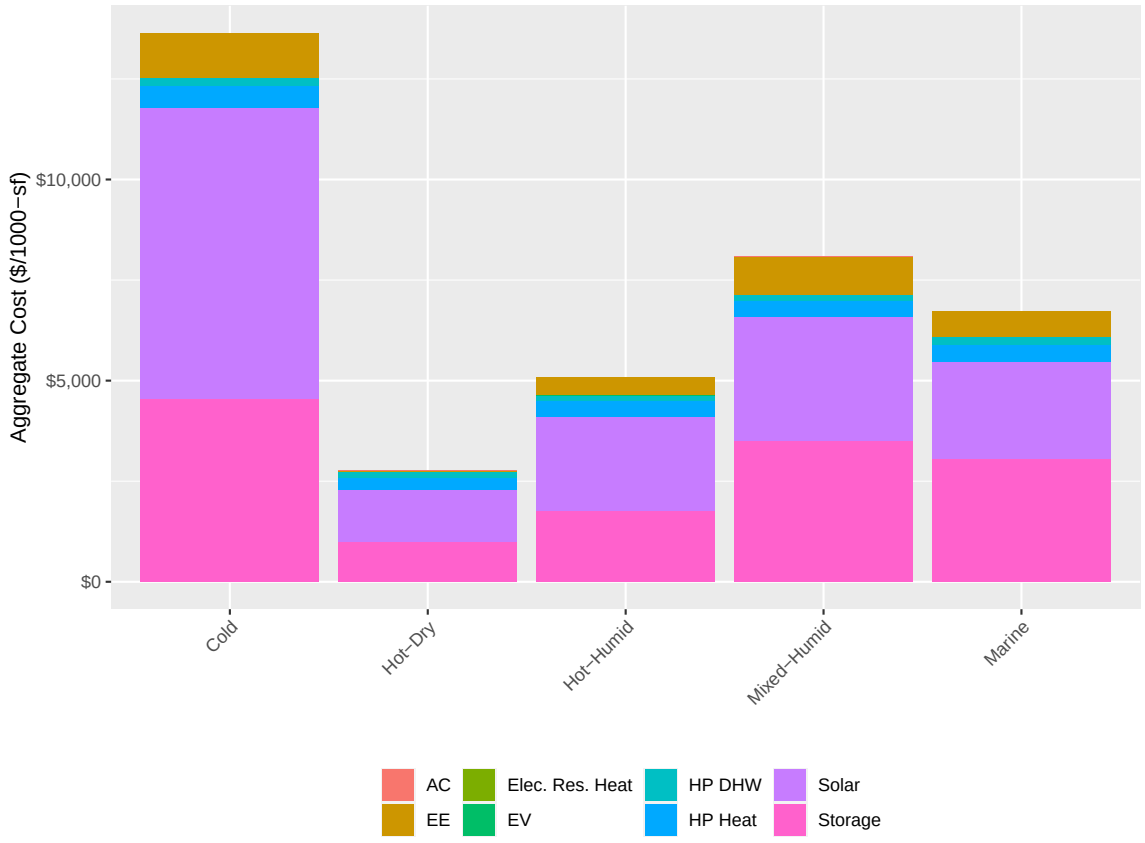

Figure 4.11: Breakdown of costs for microgrid scenarios. Solar and storage costs are dominant in all five regions.

For the cold climate, which has large heating and cooling loads, the annual cost of a solar-and-storage microgrid is approximately $17,400 per-1000-sf, more than ten times larger than $1,656 required to provide energy services in the base scenario.

For the microgrid scenario, we assume that there is no grid connection, so the average cost of electricity in each climate is computed by simply dividing the total expenditure on solar and

storage by the quantity of electricity consumed by equipment onsite.[33] This figure ranges from $0.55 per-kWh for the hot-dry climate to $1.43 per-kWh for the marine climate. By comparison, in the base case, the average cost of grid-provided electricity (including infrastructure costs) is $0.07 to $0.15 per-kWh. Furthermore, the costs associated with the microgrid scenario are likely underestimated, as there would be some cost to maintaining poles and conductors between residences.

4.5.7 EV Charging

In the United States, 36% of CO2 emissions from energy consumption is associated with the transportation sector U.S. Energy Information Administration (2021e). Historically, most of the reduction in vehicle emissions have come from incremental improvements in fuel efficiency. However, because most vehicles in the United States directly combust petroleum, it is impossible to eliminate emissions from vehicles altogether without switching to non-petroleum fuels.

Electric vehicles, coupled with an expansion of zero-carbon electricity generation, have emerged as an opportunity to reduce emissions from automobiles. Steinberg et al. (2017) demonstrate that electrification of end uses (including transportation, buildings, and industry) and simultaneous power sector decarbonization can achieve reductions of economy-wide fossil fuel emissions by 74% by 2050 (relative to 2005 levels). Even without power sector decarbonization, electrification could reduce fossil fuel emissions by 41%. Mai et al. (2018) estimate that electric vehicles could make up between 11–81% of the light-duty fleet by 2050, depending on technology advancement and consumer preference.

To understand how loads from electric vehicle charging affect the feeder, we include a specialized scenario wherein each residence has one electric vehicle that must receive 10 kWh of charging each night[34].

The results of this optimization are described in Table 4.7. We find that including EV charging in the model only increases the feeder peak in the hot-dry region, though this new peak

[33]This does not include electricity dissipated by the battery through the charging cycle.

[34]This would allow a customer to drive approximately 30 miles-per-day or 10,890 miles-per-year. Charging must occur from 8 PM - 6 AM and assumed to be satisfied with a Level 1 Charger that has a maximum power of 1.4 kW.

is still well below the feeder's assumed capacity and results in no additional infrastructure costs. EV charging results in an additional 54,450 kWh of consumption[35] and increases the total energy cost by between $1,551—$2,507. By comparison, driving the same distance in gasoline-powered vehicles that get 40 miles-per-gallon would require $\frac{15*10{,}890 miles}{40 MPG} = 4{,}084$ gallons of gas, costing approximately $\$4,084 * \$3.50 = \$14,294$ in private costs plus several thousand more dollars in emissions damages.

Figure 4.12 shows the EV charging, space heating, and various other loads in the mixed-humid climate on an example day in January. The left-hand plot shows the least-cost model without any EV charging, while the righthand plot shows the same model with EV demands. The inclusion of EV charging loads predominantly fills in excess capacity on the feeder and slightly depresses the amount of space heating energy produced by the heat pump, but does not raise the feeder's peak.[36]

The competition for limited feeder capacity between EVs and heat pumps results in modest reductions in the output from heat pumps, with the remaining space heating demand satisfied by natural gas furnaces. In the cold climate, the fraction of space heating energy produced by electricity falls from 65% to 60% when EVs are included. In the other climates, the difference does not exceed 2% of annual heating demand.

4.5.8 High AC/HP Costs

In an additional scenario we assume a 50% premium on the installed cost of a new air conditioner or heat pump. This extra allowance captures conditions where, for example, a residence does not have all the proper ducting in place for a new central unit and needs to install higher-cost ductless units instead. As expected, total equipment costs are higher in most climates. The exception is the marine climate, where equipment costs are about 1.5% lower (this is most likely due to residual error in the optimization algorithm, which, for performance, only converges

[35] 15 residences * 10 kWh * 363 days = 54,450 kWh. No charging occurs on the first or last day because there is not a full night over which to charge.

[36] Even though the feeder's capacity, denoted by the solid red line, is well above the observed load, the model still attempts to minimize the peak (the dashed line) in order to reduce generation capacity requirements and associated costs

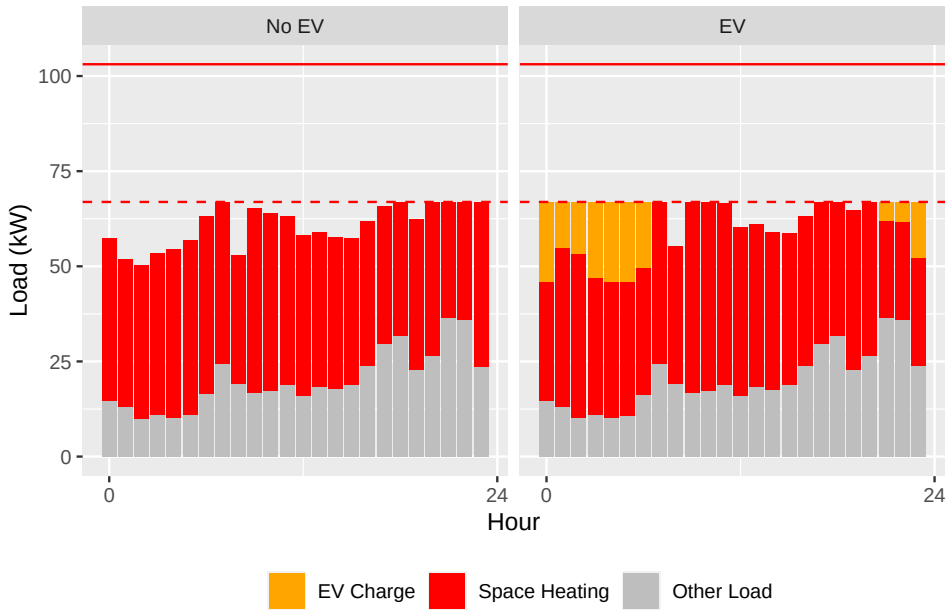

Figure 4.12: EV charging, space heating, and various other loads in the mixed-humid climate on an example day in January. Left: least-cost model without any EV charging. Right: the same model with EV charging demands.

to an MIP gap of 2%).

There are modest reductions in the fraction of space heating energy coming from electricity relative to the base case in two climates, from 64% to 60% in the cold climate and from 99% to 90% in the hot-humid climate. Notably, the fraction of space heating energy coming from electricity increases slightly in the hot-dry climate when we assume the higher equipment cost, from 81% to 84%. This cannot be explained by the inputs and is most likely the result of error in the reported solution.

4.5.9 Constant SMC

We also include a scenario in which the SMC of electricity is set to a constant \$0.05 per-kWh in all five climate regions and the cost of generation capacity is set at a constant \$30 per-kW. This allows us to isolate the effect of climate variability.

The results from this scenario are summarized in the "Constant \$0.05 SMC" row of Table 4.7. While there a few notable differences between the outcomes from this scenario and the base

case (e.g. only 43% of space heating energy is electrified in the cold climate, compared to 64% in the base case, leading to higher gas consumption and lower electricity consumption), the results are generally consistent. This suggests that the modeling results shown throughout this chapter are robust to changes in the specific sample of historical electricity prices used as inputs to the optimization.

4.5.10 Solar + Storage Favored

We have seen very limited adoption of solar and storage in most of the scenarios so far. As a stress test, we produce a final scenario wherein the feeder is highly capacity-constrained (with only enough capacity to satisfy the pre-optimization loads), additional feeder capacity costs $200 per-kW-year (four times larger than the estimate used elsewhere), and solar and storage are both priced at 50% of their estimated cost in the base case ($150 per-kW-year for solar and $25 per-kWh-year for storage).

The results from this scenario are listed in row "Solar+Storage Favored" of Table 4.7. None of the regions adopt any solar, but battery storage is used in the cold, hot-humid, hot-dry, and marine climates, with capacities ranging from 28 kWh in the hot-dry climate to 156 kWh in the hot-humid climate.

The battery is used for two purposes. The first is energy arbitrage: charging when power is inexpensive and discharging when the price goes up. In Figure 4.13, we plot the battery state of charge and SMC for a 7-day period in the hot-humid climate in the summer, which has the greatest hour-to-hour electric price volatility. We observe that the battery is charged each day in the early morning when the SMC is low, then discharged when the SMC is high in the afternoon and early evening.

The battery is also used to shave peak loads. Figure 4.14 decomposes the electric loads in the hot-humid climate for a 7-day period in the winter, when the distribution feeder is under significant stress due to electric heating loads. Here we observe that the battery charges in anticipation of heating peaks on the third and fourth days, then discharges during the peak event so that the net load on the feeder (the solid black line) never exceeds 66 kW, as this would incur

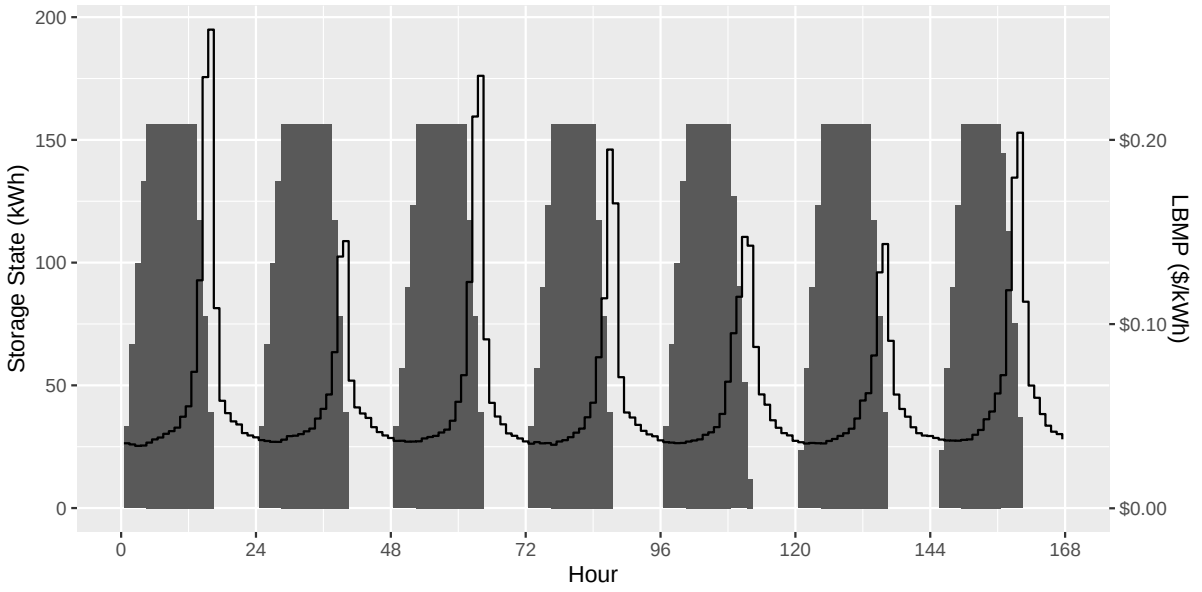

Figure 4.13: The battery state of charge and SMC for a 7-day period in the hot-humid climate in the summer. The battery is charged each day in the early morning when the SMC is low, then discharged when the SMC is high in the afternoon and early evening.

additional distribution costs.

We note that the use of historical hourly price data most likely creates a false sense of precision. In a world where batteries are available at $25 per-kWh, it is likely that most of the opportunities for energy arbitrage will be captured at the bulk power system scale (thus smoothing the electricity prices seen by utilities). Nonetheless, it seems entirely plausible that batteries could be advantageously deployed on certain capacity-constrained feeders to manage peak loads and defer system reinforcements.

4.6 Generalization to Other Climate Regions

In this section, we describe the key climate variables that govern the optimal configuration of heating and cooling systems in each of the five regions studied. This allows us to generalize our results to other climates not directly analyzed.

In general, cooling loads increase as the ambient temperature rises above the desired indoor

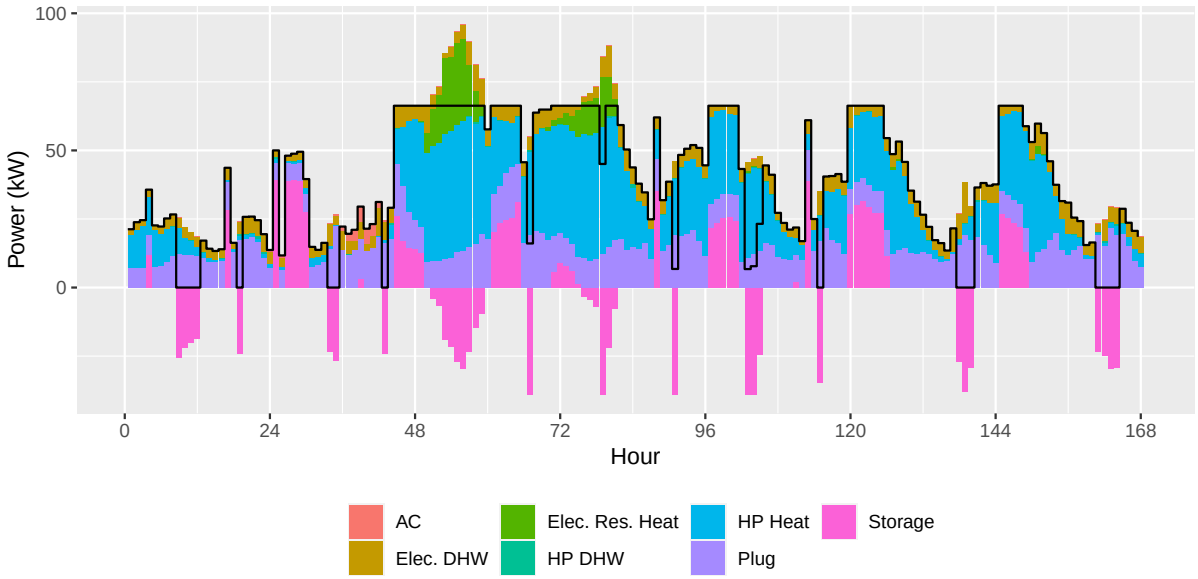

Figure 4.14: Decomposition of electric loads in the hot-humid climate for a 7-day period in the winter. The battery is charged and discharged strategically so that the net load on the feeder (the solid black line) never exceeds 66 kW.

temperature and heating loads increase as the ambient temperature drops. This can be seen in Figure 4.15, which plots the space heating and cooling loads for a sample residence in each climate against the ambient outdoor temperature. The distribution of points around the central trend is due to other factors that impact the residence's heating and cooling loads, including humidity, solar radiation, and internal generation of heat within the building.

The lines on Figure 4.15 describe the maximum heating and cooling capacities of a 14-SEER AC/HP. Due to thermodynamic constraints on the vapor-compression cycle used by these units, the capacity decreases as the difference between the ambient temperature and the desired room temperature (approximately 65–70°F) grows.

The model is constrained such that heating and cooling equipment in a residence must be able to satisfy the residence's full respective demands at all hours of the year. Consequently, for a heat pump to function as a standalone unit, its capacity line must exceed all of the heating and cooling points on the plot. In the hot-dry climate, both the heating and cooling loads can be satisfied by a 1.5 kW heat pump. In the cold climate, a 2 kW unit is capable of satisfying

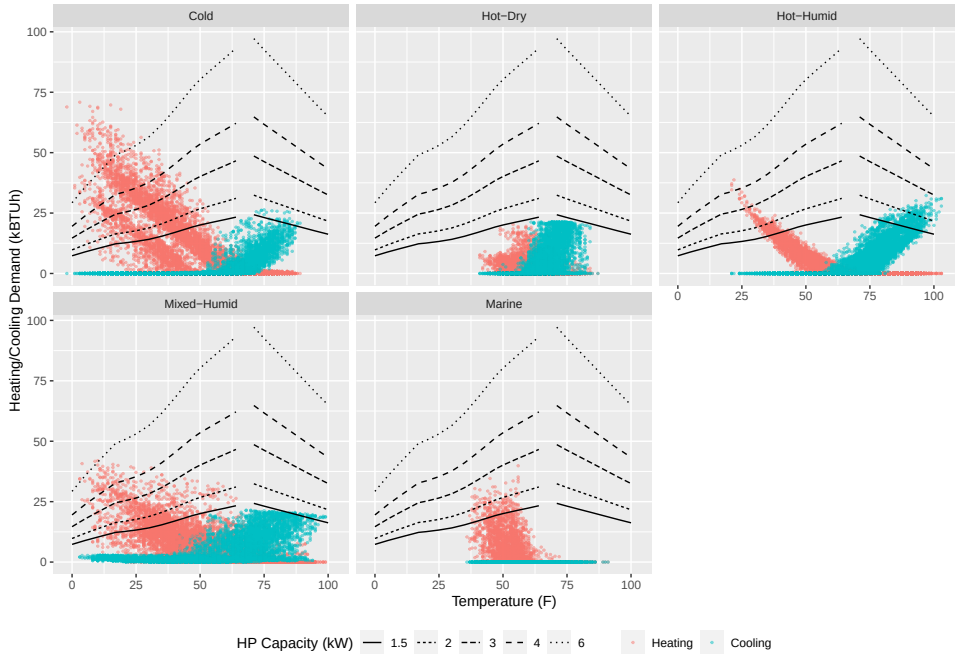

Figure 4.15: Heating and cooling loads vs. ambient outdoor temperature for representative residences in each of the five climates. The black lines describe the heating and cooling capacities of a 14-SEER heat pump. In order for a given heat pump to satisfy the full heating/cooling loads in a given region, the capacity line must exceed all the points in the scatterplot.

the residence's full cooling load but even a 6 kW unit cannot satisfy the residence's full heating load. This figure helps explain why the model selects supplementary furnaces in the cold and mixed-humid climates, as these can be used to satisfy heating load that exceeds the capacity of a heat pump sized based on the residence's cooling loads.

The marine climate represents an outlier: even though temperatures in this climate can exceed 80°F, only two of the fifteen residences use air conditioning (per the housing stock distributions found in ResStock). The absence of demand for space cooling helps explain why heat pumps are less-utilized in this climate: they do not serve the dual purpose of heating in the winter and cooling in the summer. However, if increasing summer temperatures prompts more customers in this climate to adopt air conditioning, this would significantly shift the economics of heating to favor heat pumps.

Because the required capacity of a heat pump scales with the maximum and minimum observed temperatures in a given climate region, it is informative to look at the relationship between these extremes in different climates. In Figure 4.16, we plot the maximum observed temperature in a typical meteorological year against the minimum observed temperatures for 990 locations throughout the United States, including the five analyzed in detail in the preceding sections. We also include the maximum heating degrees (approximated as 65°F minus the minimum temperature) and the maximum cooling degrees (approximated as the maximum temperature minus 65°F).

The black line has a slope of unity, passing through locations that have symmetric heating and cooling extremes (e.g., the coldest day of the year is 30 degrees below 65°F and the hottest day of the year is 30 degrees above 65°F).[37] To a first-order approximation, a heat pump sized to fulfill a building's full cooling load in one of these climates should also satisfy its full heating load. Climates further to the right have heating extremes in excess of their cooling extremes.

The maximum heating degrees, maximum cooling degrees, and difference between them

[37]Notably, there is much more range in the distribution of maximum heating degrees than in the distribution of maximum cooling degrees: 80% of the surveyed stations have maximum cooling degrees between 24.1F and 40.8F (maximum temperatures between 89.1F and 106F). The heating degrees over the same interval range from 38.4F to 88.8F (minimum temperatures of -23.8F to 26.6F).

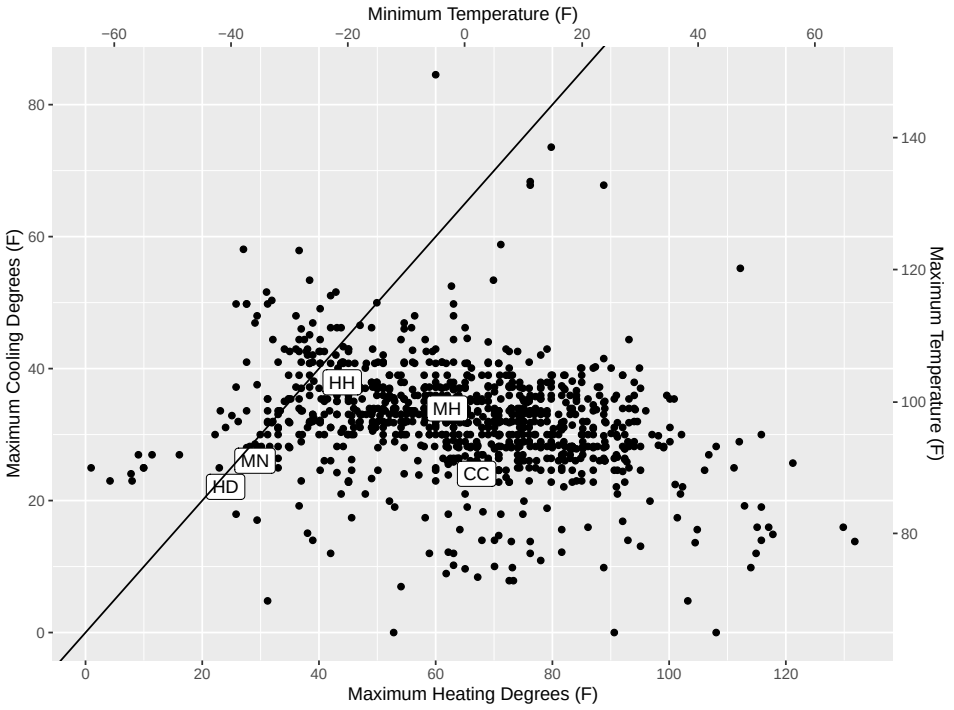

Figure 4.16: Maximum heating degrees vs maximum cooling degrees for 990 climate regions throughout the United States, including the five analyzed in this study. Climates closer to the black line have heating extremes close to their cooling extremes. Climates further to the right have heating extremes in excess of their cooling extremes.

is mapped for the continental United States in Figure 4.17. As we observed in Figure 4.16, the range in maximum cooling degrees observed in a typical meteorological year is relatively modest compared to the range in maximum heating degrees. The difference between maximum heating degrees and maximum cooling degrees (max heating minus max cooling) shows significant continental variation: in much of the South and Western United States, the maximum heating degrees do not significantly exceed the maximum cooling degrees, meaning that a heat pump sized based on cooling needs should be able to satisfy much of a residence's heating needs. In New England and the Upper Midwest, the maximum number of heating degrees can exceed the maximum number of cooling degrees by 50 degrees or more. In these climate regions, supplementary heating equipment would be required to fulfill a residence's full heating needs. The load implications of different heating electrification strategies for the continental United States are detailed in Waite and Modi (2020).

4.7 Discussion and Conclusion

The results of this chapter point toward several important findings. First, heat pump space heaters and electric water heaters are found to be an essential part of a least-cost portfolio of technologies in four of the five climates studied. In the cold and mixed-humid climates, which have significantly higher space heating loads than the other climates, electric heat pumps are used in conjunction with gas furnaces, serving between 65–83% of the residences' heating demands. In the hot-dry and hot-humid climates, full electrification of space and water heating can be achieved without increasing feeder capacity or significantly raising costs relative to the base scenario. In the marine climate, low demand causes the model to favor natural gas for heating because of the low cost of gas furnaces.

In the progress scenarios, where we assume a 70% reduction in emissions from the electric grid and a 30% reduction in the installed cost of heat pumps, air conditioners, rooftop solar PV, battery storage, and feeder capacity, the mix of technologies shifts to further favor heating electrification. The model also adopts a small amount of battery storage in the hot-humid climate, which it uses to arbitrage wholesale electricity prices.

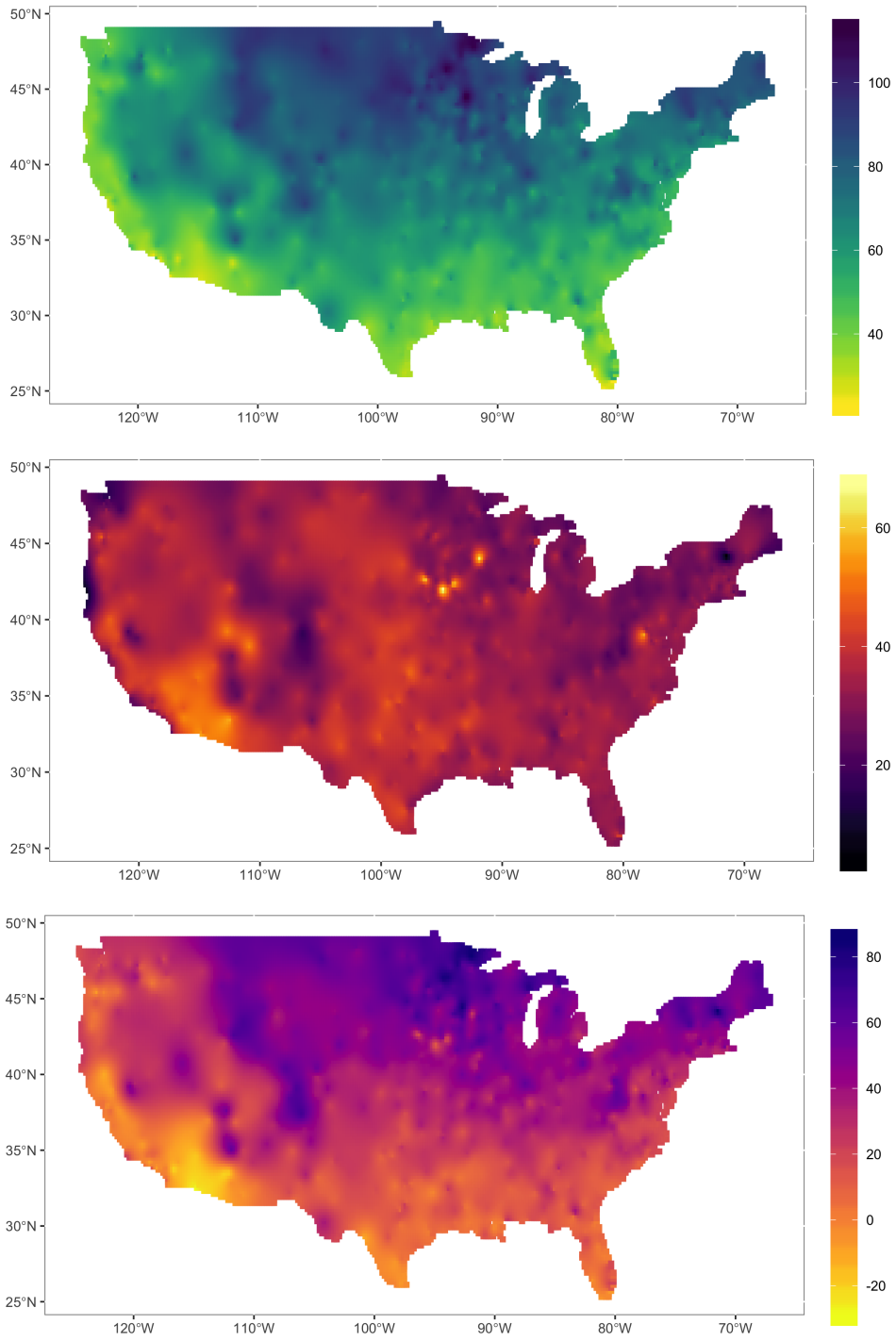

Figure 4.17: Top: Maximum heating degrees. Middle: Maximum cooling degrees. Bottom: Difference between maximum heating degrees and maximum cooling degrees. In the bottom plot, the regions that are darker than orange have maximum heating degrees exceeding their maximum cooling degrees. Residences in these regions will generally need some form of supplementary heating to augment the output of a heat pump. Ordinary kriging is used to interpolate points between the 990 observed weather stations.

Neither solar PV nor battery storage are found to significantly reduce costs in any of the scenarios studied. This is generally consistent with Fu, Feldman, and Margolis (2018), which finds that distributed solar PV is more than twice as expensive as utility-scale solar as a source of generation, and M. A. Cohen, Kauzmann, and Callaway (2016), which finds that distributed PV can only be used to defer capacity upgrades on about 1% of feeders.

These results appear to be robust to a range of different assumptions about costs and constraints. Even when the social cost of carbon is set to zero, effectively ignoring the cost of externalities, the mix of technologies does not change drastically. The model shifts slightly to favor technologies with lower capital costs, but otherwise selects similar portfolios in all five climates. Likewise, the scenarios that modify the headroom on the feeder over the existing peak also produce similar results to the base models.

In the microgrid scenario, which eliminates all imports of electricity and natural gas, costs rise dramatically in all five climates. The hot-dry climate sees the smallest increase, with the feeder-wide cost of serving customers only doubling. In the cold climate, which has large winter heating loads, a microgrid approach would increase the cost of serving customers by a factor of 10. The inclusion of electric vehicles does not have a major effect on the optimal portfolio of technologies, as EV charging can generally be scheduled around other loads. There appears to be a small amount of competition for space on the feeder between EVs and heat pumps during the winter season, resulting in modest reductions in the output from heat pumps during peak weather events when EV charging is also required. The residual heating load is satisfied by increased production from gas furnaces.

Lastly, we find that the presence of both heating and cooling demands is essential to the economic viability of heat pumps. The hot-humid region, which has the largest cooling demand, also sees the greatest level of heating electrification in the base scenario. Conversely, the marine climate, which has almost no cooling demand, sees surprisingly little heating electrification. If regions that have historically had very little demand for summer cooling see greater demand in the future due to climate change, this new cooling demand may improve the economics of heating electrification with heat pumps.

There are a number of important sources of uncertainty in this analysis. First, we do not treat upstream electricity or natural gas infrastructure costs as avoidable, except in the microgrid scenarios. These upstream costs include $727-per-customer for electricity and $478-per customer for natural gas (R. L. Fares & King, 2017; U.S. Energy Information Administration, 2020). It is likely that if some portion of these upstream cost were avoidable, the optimization may eliminate one of these utility connections. For example, in the hot-humid climate, the least-cost optimization prescribes 1 MMBTU of natural gas consumption. This costs the objective function $6. However, if eliminating natural gas entirely enabled even a modest reduction in upstream utility costs (which amount to $\$478 * 15 = \$7,170$ per-year for the entire feeder), it is likely that the model would abandon the natural gas connection altogether. Future work should consider the cost reductions that could be realized if full electrification of buildings allowed for strategic pruning of the gas distribution system in some areas. While much of the investment in the gas system is sunk costs, the savings generated from avoiding ongoing operations and maintenance expenses may be non-trivial.

Furthermore, we do not consider the supply side of the electricity generation system. In order to manage the computational complexity of the model, hourly electricity prices were taken as exogenous inputs based on historical data. However, a large increase in demand (such as from broad electrification of space and water heating) would likely increase wholesale electricity prices during hours of peak consumption. This is a matter of particular concern in the all-electric scenario, where a large amount of inflexible demand for heating during cold weather events could cause electricity prices to spike. Conversely, if electrification leads to a flatter electricity demand profile (or more flexible demand), this is likely to put downward pressure on wholesale electricity prices because it would reduce the need for peaker plants that only operate a few dozen hours each year. To better understand this, future work should include simultaneous modeling of the bulk power system and demand-side technologies.

Lastly, we do not enforce any constraints on the simultaneous operation of heat pumps and furnaces in the hybrid arrangements, which is recommended by engineering standards to prevent damage to the heat pump. While it would be preferable to restrict the model so that at most

one heating system could be operated at a time, doing so with either SOS (special ordered set) constraints or hourly binary variables was found to increase the computational complexity of the model by several orders of magnitude. Avoiding simultaneous operation of a heat pump and furnace would most likely necessitate modest upsizing of the furnace in hybrid arrangements. This larger furnace would be used to fulfill the building's full heating load in hours that are currently met by both technologies operating concurrently.

This analysis indicates that heat pumps are a central part of a least-cost technologies portfolio in most climates in the United States. This result is robust to various assumptions about the local feeder capacity and different estimates of the social cost of carbon. This analysis concerns itself only with the least-cost portfolio across a group of customers, not the individual incentives faced by customers. Further work should investigate how to ensure that electric retail rates incentivize customers to adopt emerging technologies – like heat pumps – that reduce both energy costs and emissions.

Chapter 5

Incentivizing Efficient Adoption of Customer-Side Technologies

In the previous chapter, we constructed a mixed-integer linear optimization model to determine what combinations of technologies would result in the least-cost provision of energy services for collections of customers in different climate regions. In this chapter, we adapt that model from the previous chapter to simulate how cost-minimizing customers would rationally respond when faced with different electric tariffs set by a utility. Customers are able to invest in solar panels, battery storage, and various options for heating and cooling equipment, and operate these equipment strategically to minimize their costs. By examining how customer-side investments change as the tariff is varied, we are able to observe how different strategies for cost allocation can influence customer behavior.

This work adds to the literature in three significant ways. First, whereas most of the literature presumes a single existing tariff structure and examines just one or two regions, we analyze how customer choices vary over a wide range of tariff options, under different technology assumptions and in five different climate regions. Second, we evaluate the actual cost of energy services (described in the previous chapter) implied by a set of customer actions, rather than just the individual customer's expenses. Lastly, we include multiple gas and electric options for satisfying

heating demands, which are often excluded from studies that only focus on energy demands that are already electrified. By looking at the variability in outcomes across multiple climates, we are able to better understand how the design of retail tariffs can influence customers decisions about how to satisfy their energy needs and what impact these decisions have on the total cost of energy services and associated emissions.

5.1 Background and Literature Review

The average utility spends approximately $700–800 per-customer each year ($58–67/month) on transmission, distribution, and administrative (TD&A) expenses (R. L. Fares & King, 2017). The overwhelming majority of these costs do not scale with increased consumption. In Rauschkolb et al. (2021), we used linear regression to estimate the fraction of distribution costs that scale with load growth, finding that less than 10% of distribution capital expenses could be explained by growth in system capacity. In Borenstein, Fowlie, and Sallee (2021), the authors estimate that for the three major California utilities, 80–88% of distribution costs and 58–94% of transmission costs are fixed.

Even though a large portion of their costs do not scale with energy consumption, most utilities in the United States allocate their fixed costs to residential customers as part of a volumetric delivery charge that is proportional to each customer's total energy consumption. The level of this tariff is typically based on the average cost of energy sold by the utility and is used to recover the bulk of the utility's revenue requirement. If a utility sells 8 billion kilowatt-hours to residential customers and needs to collect $1 billion through the volumetric tariff to recover their fixed and variable costs, then the tariff would be set equal to 12.5 cents per-kWh. This is called "average cost" pricing.

By allocating a large portion of their fixed costs to customers using average cost pricing, many utilities raise the effective per-kWh rate the customers pay to well above the cost of an additional unit of energy, discouraging consumption (Borenstein & Bushnell, Forthcoming). While this has historically been politically acceptable because it promoted energy efficiency and was economically progressive (wealthier customers paid more), it has also been observed

to encourage uneconomic adoption of rooftop solar panels that enable some customers to shift fixed costs to other customers (Biggar & Hesamzadeh, 2014; Borenstein, 2017; S. Burger et al., 2019; Wolak, 2018). More recently, a handful of economists, including Borenstein and Bushnell (2021), have posited that average cost pricing could also discourage customers from adopting heat pumps and electric vehicles by raising the price of electricity.

While there are a number of competing proposals about how to improve the efficiency of residential tariffs, most seem to agree that the price that a customer pays for an additional unit of electricity should be set closer to the social marginal cost of producing that energy.[1] Borenstein (2016) argues that a better strategy on both efficiency and equity grounds is to combine a time-variant electricity price with a higher fixed customer charge. Perez-Arriaga, Jenkins, and Batlle (2017) develops a framework in which customers are charged their location-specific SMC at all hours, future capital costs are levied on consumption during peak hours, and residual costs are allocated in a manner that does not produce any distortion in behavior, such as increased fixed charges or broader taxes. Rodríguez Ortega et al. (2008) proposes allocating costs through a fixed charge, a locational demand charge, and a locational energy charge.

5.1.1 Quantifying Inefficiencies

The most common approach for estimating the inefficiency caused by average cost pricing is to assume a fixed price elasticity for demand and then quantify the deadweight loss resulting from under- or over-consumption of electricity services.

Most authors agree that consumers are more likely to respond to long-run changes in price than short-run volatility.[2] In a review of other literature, Gillingham, Newell, and Palmer (2009) provide estimates of residential electricity price elasticity ranging of -0.14 to -0.44 in the short-run, and from -0.32 to -1.89 in the long-run. Deryugina, MacKay, and Reif (2020) recently exploited a natural experiment in Illinois to quantify customers' short- and long-run price elasticities to price

[1]The social marginal cost (SMC) is the sum of private and external costs, including damages from emissions.

[2]Here, we use "short-run" broadly to refer to both intra-day volatility and sustained price changes over longer periods (e.g. several months) that are still too short for customers to reasonably make changes to the technologies installed in their homes.

shocks. The authors produce the much more modest estimates for price elasticity of demand ranging from -0.09 in the first 6 months after the price change to -0.27 in the period 25–30 months after the price change.

A handful of authors have questioned how technology choices impact customer elasticities. Borenstein and Bushnell (Forthcoming) posit that emerging technologies that enable hourly load shifting of demand may eventually increase the magnitude of short-run elasticity, so that customers will become more responsive to short-run perturbations in price signals. Faruqui and Wood (2008) use data from the California Statewide Pricing Pilot to develop customer-specific elasticities. The authors observe that customers with central air conditioners are much more willing to shift their loads to off-peak times in response to price signals (elasticity = -0.13) than customers without these systems (elasticity = -0.05).

Among the papers focusing on short-run price volatility, Borenstein (2005) estimates that a move toward real-time pricing for energy (while retaining a flat delivery tariff) for a theoretical utility would result in a reduction of energy expenses by 4.2%-12% for elasticities ranging from -0.05 to -0.50. Borenstein and Bushnell (Forthcoming) expands on this work by estimating the deadweight loss resulting from the residential electricity price deviating from the SMC for 2,104 real utilities. In the updated model, the authors consider the social cost of emissions and do not assume that customers face a flat delivery tariff. For a constant demand elasticity of -0.2, the authors estimate that the average deadweight loss resulting from volumetric prices deviating from the SMC is 0.31 cents-per-kWh.

In a quasi-experimental study of short-run price volatility, Fabra et al. (2021) analyze the consumer response to a large-scale real-time pricing (RTP) program in Spain, – wherein customers' electricity rates vary hourly based on the wholesale electricity market – and find no statistically significant difference in behavior between those customers on RTP and those in the control group. They suggest that enabling RTP to act as an effective tool for managing load would require greater opportunities for cost reductions[3] and a suite of enabling technologies. They further

[3]The average maximum possible savings for perfectly-elastic customers in this program was less than 2 Euros-per-month.

suggest that time-of-use pricing (ToU), wherein different predefined rates are used during peak and off-peak times during the day, could be a more effective alternative to RTP because of its certainty and salience.

Pérez-Arriaga and Knittel (2016, Ch. 4) model how smart air conditioning systems installed in homes with some innate thermal storage capacity could be used to arbitrage a dynamic tariff. The authors find that under a cost-reflective tariff, changes in the customer's consumption patterns would reduce marginal system costs (including energy, generation capacity, and network capacity) by 17–33% compared to flat rate tariffs. This would result in savings for a typical household of as much as $400 per year.

Among those studies focusing on long-run changes in electricity prices, S. P. Burger et al. (2020) compare the efficiency of the existing volumetric tariff for a midwestern utility to several alternative designs. The authors study three cases: one where price elasticity for demand is zero (alternative tariffs allocate costs differently among customers but do not result in changes to overall consumer surplus), as well as "low" and "high" elasticity cases. Under the preferred tariff structure, customers are billed a volumetric rate equal to the SMC and common costs are recovered through a substantially increased monthly customer charge. In the high elasticity case (-0.3), this structure is estimated to increase average consumer surplus for residential customers by 29–48% of annual expenditures.

Abdelmotteleb et al. (2018) model the customer response to four different tariff structures on a 2.5 MW distribution network, assuming that the cost of load curtailment during peak hours is $300/MWh. The authors find that the implementation of a tariff that includes a peak-coincident network charge decreases existing system costs (including energy, DER investments, and network cost recovery) by 10% and future network costs by 23%, relative to the volumetric charge base case.

Schittekatte and Meeus (2018) employ a game-theoretical approach to model how active consumers respond to different tariff designs by investing in solar PV panels and/or batteries. The authors illustrate that the extent to which reformed tariffs improve economic efficiency is dependent on the constraints of the network: where network costs are entirely prospective

(driven by peak demand rather than sunk), the move from volumetric charges to capacity charges incentivizes customers to adopt solar PV and batteries to reduce their peak demand, decreasing system costs by 6–7%. Where network costs are entirely sunk, the move from volumetric charges to higher fixed charges (which are considered optimal in this case) does not reduce system costs but significantly increases the share of network costs borne by customers with smaller demand. The authors also note that volumetric tariffs set above the cost of energy incentivize active customers to adopt solar PV panels to reduce their share of network costs, even if doing so does not decrease system costs in aggregate. Though space and water heating account for 62% of residential energy use in the United States (U.S. Energy Information Administration, 2018), there has been very little scholarship studying how tariff design influences customers' heating choices. A key contribution of this work is the inclusion of thermal demands across multiple climates.

5.2 Methodology and Assumptions

We adapt the optimization algorithm described in Chapter 4 to simulate how individual customers respond to different electric tariff designs. Rather than simultaneously optimizing decisions across the utility and the 15 customers, the utility sets an electric tariff and each customer responds by making decisions to minimize their individual expenses.

After performing the separate optimizations for each customer, we evaluate the actual costs borne by the utility to serve load, the revenue from the volumetric tariff, any residual costs that need to be recovered through other means, and the total cost of energy services including energy, emissions, equipment, and infrastructure. For simplicity, these analyses assume a constant SMC of $0.05 per-kWh for electricity (borne entirely by the utility) and a constant SMC of 0.006307 per-kBTU ($6.307 per-MMBTU) for natural gas. We also assume a constant emissions factor of 0.953 lb per-kWh in all five climates in the base and "No HP/Solar/Storage" scenarios and 0.2859 lb per-kWh in the progress scenario. As before, we assume that the feeder has 50% headroom over the existing (pre-optimization) peak. Cost assumptions are summarized in Table 5.1.

[4]Environmental Protection Agency (2020)

Table 5.1: Average energy costs and emissions for each of the five locations considered. Average LBMPs, SMCs, and standard deviations for electricity are computed using the modeled feeder load as a weighting factor. Natural gas costs are taken as annual averages, while the LBMP for electricity varies hourly. Emissions factors for electricity are based on Environmental Protection Agency (2020) whereas emissions from natural gas assumes stoichiometric combustion.

	Erie County, NY	San Diego, CA	Harris County, TX	Alexandria, VA	Marin County, CA
Building America Climate Region	Cold	Hot-Dry	Hot-Humid	Mixed-Humid	Marine
IECC Climate Region	5A	3B	2A	4A	3C
			Electricity		
Carbon Emissions[4], lb/kWh	0.953	0.953	0.953	0.953	0.953
Volumetric Tariff (Status Quo)	$0.11	$0.32	$0.12	$0.11	$0.28
Volumetric Tariff (Experimental)			Varies from $0.01 to $0.40 per-kWh		
SMC, $/kWh	$0.05	$0.05	$0.05	$0.05	$0.05
Generation Capacity Cost, $/kW-year	$30	$30	$30	$30	$30
Add'l Feeder Capacity Cost, $/kW-year	$50	$50	$50	$50	$50
			Natural Gas		
Private Cost, $/MMBTU	$10	$10	$10	$10	$10
SMC, $/MMBTU	$6.307	$6.307	$6.307	$6.307	$6.307

This accounting analysis allows us to understand the conditions under which utilities are able to recover their full revenue requirement from customers and what kinds of tariffs lead to more or less efficient customer decisions about technology adoption and use.

5.3 Scenarios Analyzed

We perform optimizations for sets of 15 customers residing on the five example feeders in different climate regions throughout the United States. In order to minimize their expenses, these customers can respond by investing in and strategically operating different heating technologies, cooling technologies, and distributed energy resources. For each scenario, the volumetric electricity tariff is modified in discrete values between \$0.01/kWh and \$0.40/kWh.[5] We assume that any residual utility costs not recovered through the volumetric tariff are recovered through a monthly fixed charge.

In the "No HP/Solar/Storage" scenario, customers do not have access to heat pumps, solar panels, or battery storage. For heating, customers may choose from high- and low-efficiency furnaces, supplementary electric resistance heating, and electric resistance baseboards. For cooling, customers can choose from high- or low-efficiency air conditioners.

In the "base" scenario, we introduce heat pumps, solar panels, and battery storage, observing how the availability of these technologies influence customers' responses to changing volumetric tariffs.

In the "progress" scenario, the cost of heat pumps, air conditioners, solar panels, battery storage, and distribution capacity are all assumed to have decreased by 30%, and the emissions from the grid are assumed to have decreased by 70% (from 0.953 lb/kWh to 0.286 lb/kWh). This provides insight into how the cost and emissions implications of emerging technologies might change as the costs of these technologies decrease and the grid becomes cleaner.

Except where noted, all scenarios allow for full net-metering of solar injections.

[5]The precise values of the volumetric tariff in \$ per-kWh are: \$0.01, \$0.02, \$0.03, \$0.04, \$0.05, \$0.06, \$0.07, \$0.08, \$0.09, \$0.10, \$0.11, \$0.12, \$0.13, \$0.14, \$0.16, \$0.18, \$0.20, \$0.24, \$0.28, \$0.32, \$0.40.

5.4 Results and Discussion

5.4.1 Customer Response to Tariffs

In Figure 5.1, we plot the daily profiles of electricity demand in the five climate regions in response to the existing volumetric tariff. The top plot shows an example day in the winter. We see that residences in all five regions adopt some amount of electric heat pump heating, though this new load is most prominent in the hot-humid and mixed-humid climates.

While we do not have comprehensive survey data of the fraction of heating load satisfied by a given technology in each region, U.S. Energy Information Administration (EIA) (2015) reports the fraction of customers in a given climate region use a specific fuel as their primary heating source. In the cold climate, which has the greatest demand for space heating, electricity provides 12.4% of annual space heating energy in the simulation (per Table 5.2); according to U.S. Energy Information Administration (EIA) (2015, HC6.6), 18% of homes in the cold climate use electricity as their primary source for space heating.

Table 5.2: Summary statistics for customer behaviors given the current volumetric tariffs. Notably, there is significant electrification of space and water heating in four out of the five climates.

	Cold	Hot-Dry	Hot-Humid	Mixed-Humid	Marine
Volumetric Tariff	$ 0.11	$ 0.32	$ 0.12	$ 0.11	$ 0.28
Total Electric Consumption (kWh)	151,678	67,144	203,212	227,023	47,357
Total Electric Injections (kWh)	-	67,144	-	-	47,357
Space Heating Energy from Electricity (%)	12%	77%	100%	80%	14%
Water Heating Energy from Electricity (%)	100%	20%	100%	100%	1%

By contrast, in the hot-humid climate, 100% of space heating demand is fulfilled by electricity in the simulation; according to U.S. Energy Information Administration (EIA) (2015, HC6.6), 61% of homes in the hot-humid climate use electricity as their primary source for space heating.

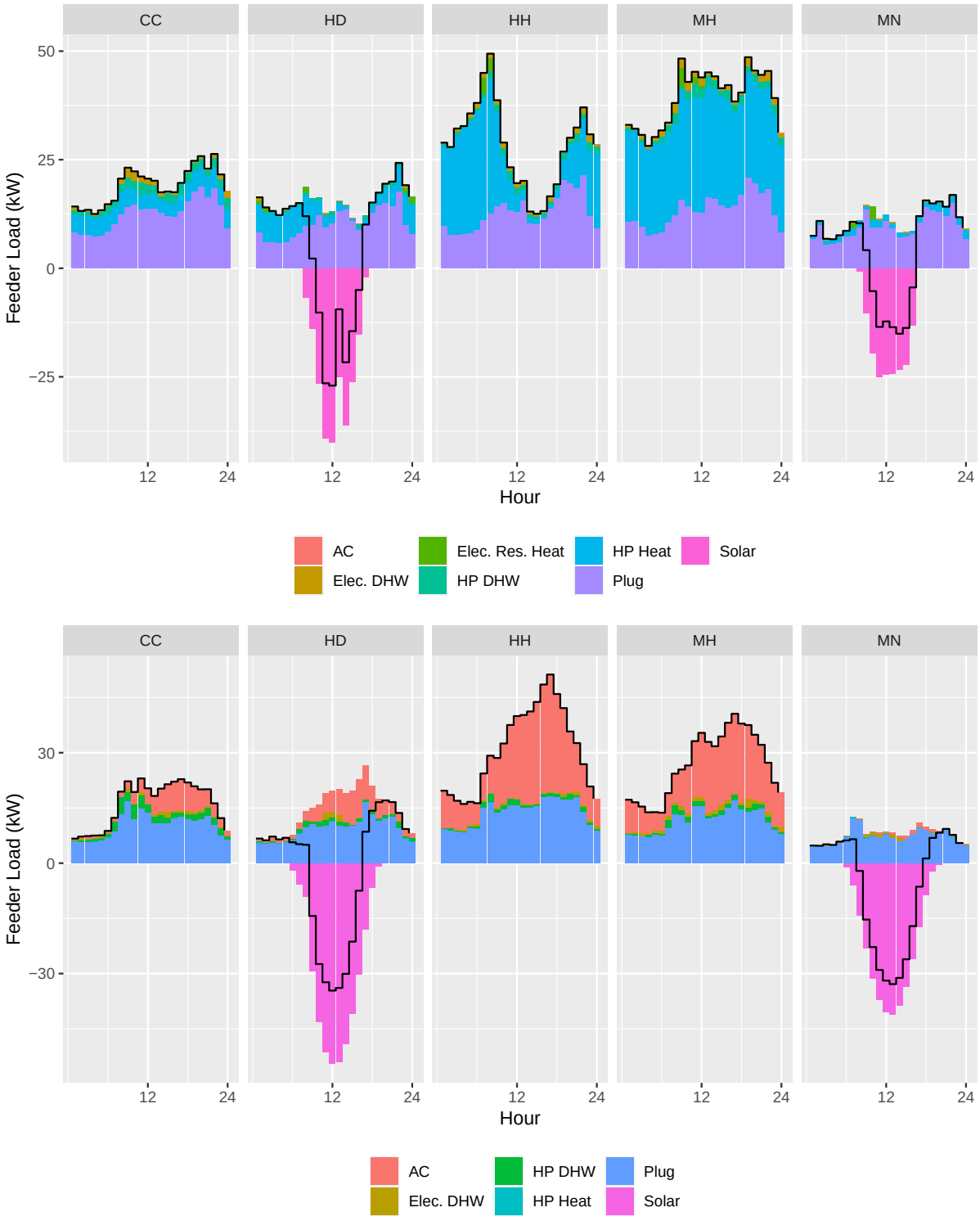

Figure 5.1: Simulated electric load profiles under the status quo tariffs for 24-hour periods in the winter and summer. The top plot shows the winter profiles for all five climates; the bottom plot shows the summer profiles. The black line describes the electric load net of solar generation.

The strong correlation observed between simulated and real heating choices serve as an important source of validation to the modeling.

Because these regions have nearly identical volumetric tariffs ($0.11 per-kWh in the cold climate and $0.12 per-kWh in the hot-humid climate), this difference in heating electrification is best explained by differences in the climate. In the hot-humid climate, customers need to adopt large air conditioners to fulfill their conditioning loads. Thus it is prudent to pay the additional cost of purchasing a heat pump and use it year-round for heating and cooling (this also obviates the need to invest in a new furnace).

By contrast, the heating peak is the cold climate is significantly greater than the cooling peak. In order for customers to full-electrify their heating, they would either need to invest in a very high-capacity heat pump or supplement a smaller heat pump with electric resistance heating. Both of these options are significantly more expensive than using a furnace to back up a heat pump that is sized based on peak cooling demand.

Despite the high volumetric tariff in the hot-dry climate ($0.32 per-kWh), customers still satisfy 77% of their space heating demand with electric sources in the simulation. At this tariff, the cost of electric heating far exceeds the cost of gas heating on a per-BTU basis.[6] However, because the annual space heating demand is low, customers can still benefit from electrification because they realize significant savings from not having to install a furnace.

Additionally, we see significant adoption of solar PV in the hot-dry and marine climates. This is predominantly driven by high volumetric electricity prices and net-metering policies, which incentivize customers to reduce their aggregate (year-round) electricity consumption by producing electricity with solar and using it to offset their consumption at other hours. This observation is consistent with reality: in the United States, California (which contains both the example hot-dry climate and the example marine climate) is responsible for 40% of generation from distributed solar (Energy Information Administration, 2022), despite having just 12% of the population.

[6] At $0.32 per-kWh, 1 MMBTU of heat would cost $\frac{\$0.32}{kWh} * \frac{293kWh}{MMBTU} * \frac{1}{COP}$. For an average COP of 4.2, this amounts to $22.32 per-MMBTU, more than twice the fuel cost of natural gas.

In Figure 5.1, we see that midday electricity generation from solar panels in the hot-dry and marine climates far exceed demand, leading to steep negative loads. In both regions, customers optimize their adoption of solar panels to fully offset their aggregate consumption of grid-supplied power over the course of a year. This is made possible by the assumed "annual net-metering" policy, wherein customers are only billed based on their net consumption (total consumption minus total injections). An alternative policy that reduces the compensation that customers receive for solar injections would likely lead to a different outcome.

5.4.1.1 Varying the Volumetric Tariff

As we have already seen, volumetric tariffs vary widely between utilities throughout the United States. In this section, we ask: how could changing the level of a volumetric tariff influence customers' decisions about what technologies to adopt and how to use them?

In the simulations, customers respond to different volumetric tariffs by choosing the equipment with which they satisfy their thermal demands and electing whether or not to install rooftop solar panels. Figure 5.2 plots simulated electric and gas load profiles for a 24-hour period in the cold climate during the winter. Each box describes the customer response to a different volumetric tariff, ranging from \$0.01 per-kWh to \$0.20 per-kWh. We observe that if the volumetric electricity price is set at \$0.01 per-kWh (significantly below the SMC), customers use a large amount of electric resistance heating to satisfy their space heating needs. When the tariff is set at the SMC (\$0.05 per-kWh), this electric resistance load all but disappears and the electricity consumption (and heat generated) by heat pumps roughly doubles. A small amount of natural gas is also used to supplement the heat pumps. As the tariff is increased to \$0.10 per-kWh, much of the heat pump load disappears, with this demand instead fulfilled by natural gas. At \$0.20 per-kWh, the full space heating load is satisfied by natural gas. Additionally, electric water heating load is replaced by gas water heating load and there is a very small amount of solar generation.

The same data are plotted in Figure 5.3, but for an example day in the summer (July 1). As the price varies from \$0.01 per-kWh to \$0.10 per-kWh, the primary customer response is to use heat pump domestic hot water heaters in lieu of electric resistance water heaters, reducing

Figure 5.2: Simulated electric and gas load profiles for a 24-hour period in the cold climate during the winter. Each box describes the customer response to a different volumetric tariff, ranging from \$0.01 per-kWh to \$0.20 per-kWh. The black line on the top plots describes the electric load net of solar generation. As the tariff is raised, customers substitute natural gas heating for electric heat pumps.

their aggregate electricity demand. If the tariff is set at $0.20 per-kWh, customers transition from electric water heating to natural gas water heaters and adopt solar panels to reduce their aggregate consumption. These panels produce significantly more energy in the summer than in the winter months.

Figure 5.3: Simulated electric and gas load profiles for a 24-hour period in the cold climate during the summer. Without heating loads, customers are less responsive to changes in the volumetric tariff for rates ranging from \$0.01 per-kWh to \$0.10 per-kWh.

Figures 5.4 and 5.5 show the same set of plots for the hot-dry climates. The results are quite similar, though the magnitude of space heating demand is much smaller and the electricity produced by solar in the $0.20 per-kWh case is much larger.

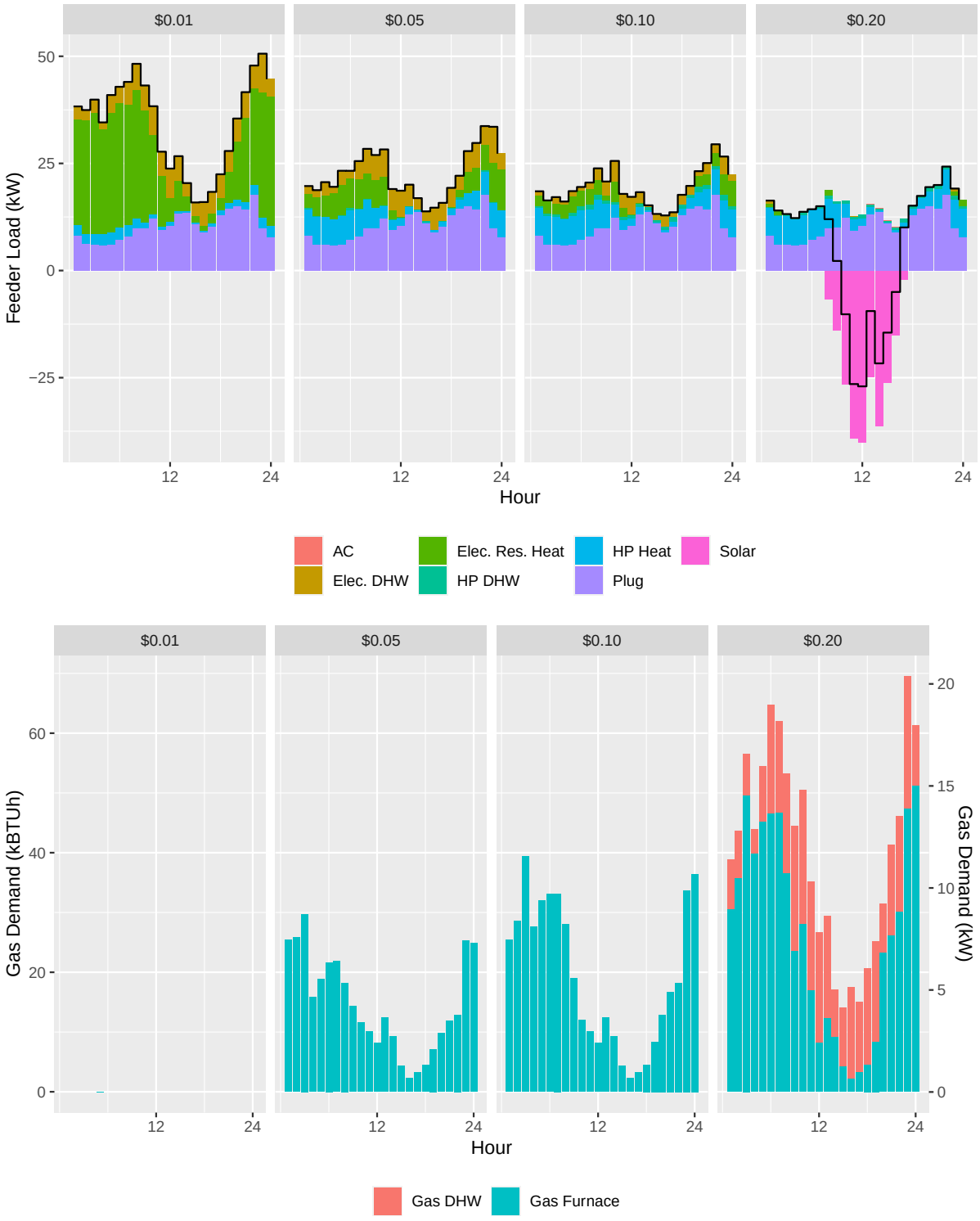

Figure 5.4: Simulated electric and gas load profiles for a 24-hour period in the hot-dry climate during the winter.

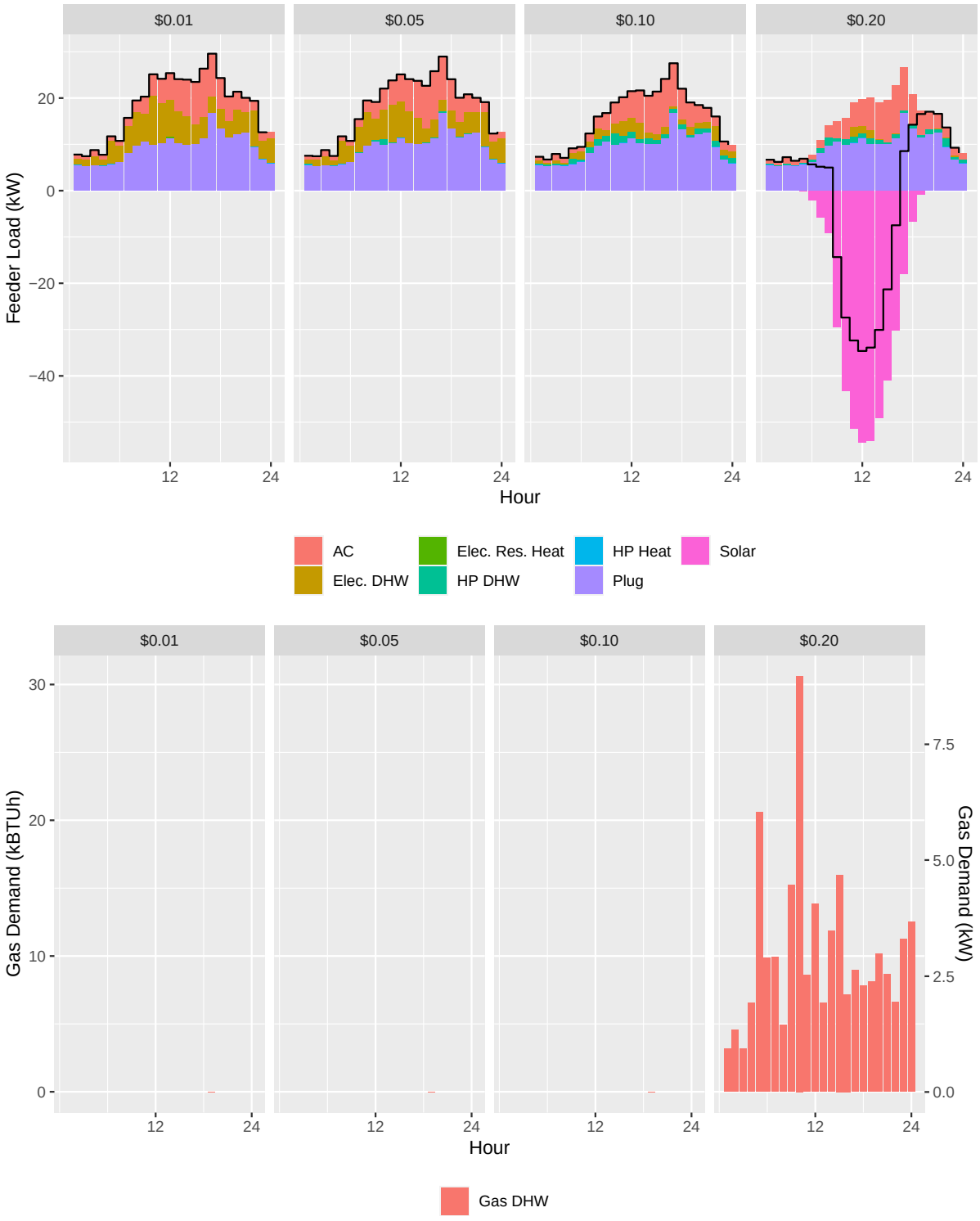

Figure 5.5: Simulated electric and gas load profiles for a 24-hour period in the hot-dry climate during the summer.

5.4.1.2 Space Heating

Space heating is the single largest energy use in U.S. homes, representing 43% of residential energy use (U.S. Energy Information Administration, 2018). The choice of technology used for space heating can have an outsize effect on both the cost of providing energy services for a home and the associated emissions.

In Figure 5.6, we observe how the customer's choice of space heating equipment changes in each climate between the "No HP/Solar/Storage", base, and progress scenarios. In the "No HP/Solar/Storage" scenario, the majority of space heating energy is satisfied by natural gas furnaces in the cold, mixed-humid, and marine climates for all volumetric tariffs above roughly \$0.06/kWh. This means that choosing a tariff between these two values should not motivate a change in customers' preferred choice of heating technologies. For the hot-dry and hot-humid climates (which have relatively modest heating demands), customers presented with the feeder-cost-recovery tariff are incentivized to use a combination of gas furnaces and supplementary electric resistance heat.

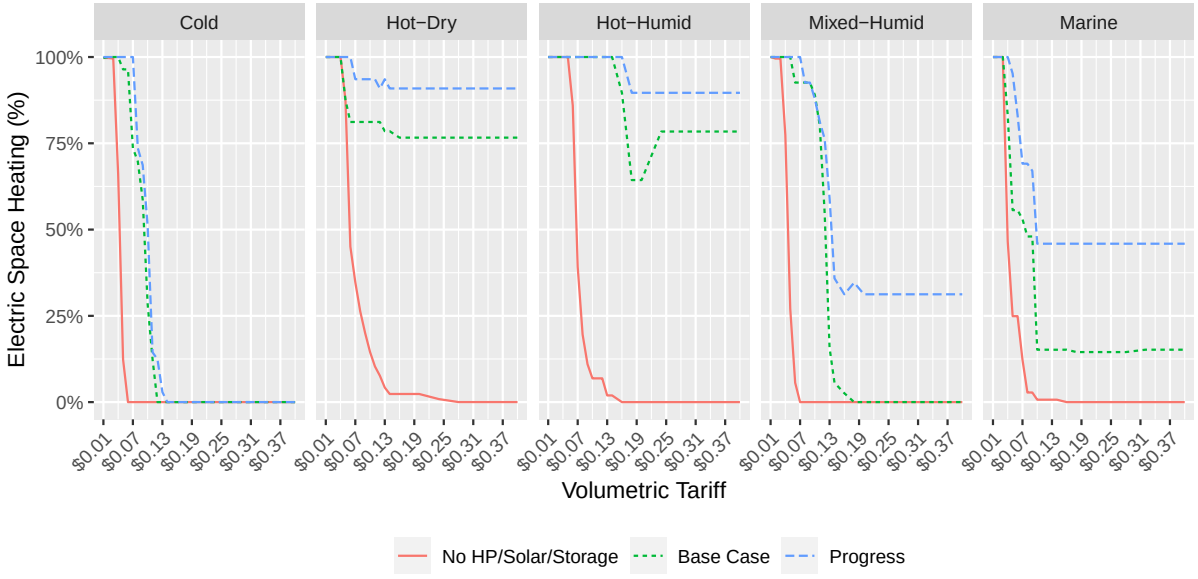

Figure 5.6: Breakdown of space heating energy choices vs. volumetric tariff in each climate region. As the tariff is increased, customers are more likely to opt for natural gas heating instead of electric options.

In the base scenario, which allows customers to use heat pumps, the level of the volumetric tariff has a much more significant effect on heating choices. In the cold climate, customers presented with the feeder-cost-recovery tariff (about \$0.08/kWh) fulfill approximately two-thirds of their space heating demand using heat pumps. At the total-cost-recovery tariff (\$0.15/kWh), customers fulfill their entire heating demand with gas furnaces. In the mixed-humid climate, 93% of space heating demand is fulfilled by electricity at the feeder-cost-recovery tariff (\$0.08/kWh) and just 10% of space heating demand is fulfilled by electricity at the total-cost-recovery tariff (\$0.13/kWh).

As of 2015, the only climate region wherein electric heating options (heat pumps and electric resistance) represented a majority or primary heating equipment was the hot-humid climate (U.S. Energy Information Administration (EIA), 2017). This is consistent with our calculations for the base scenario, which estimates that a majority of customers are likely to opt for electric heating options in the hot-humid region for volumetric tariffs up to \$0.18/kWh. The hot-humid climate has very large cooling demands (necessitating that customers invest in large air conditioners) and mild winter temperatures (resulting in high HSPFs for heat pumps). Consequently, it is economical for customers in this climate to invest in large, high-efficiency heat pumps that serve both their space heating and cooling demands, even when faced with a relatively high electricity price.

This tipping point between electric heat pumps and natural gas furnaces can be rationalized by a simple back-of-the envelope calculation. If a customer pays \$0.01/kBTU (\$10/MMBTU) for natural gas and burns it in a furnace with an efficiency between 80-96%, they pay approximately \$10.42-\$12.50 per-MMBTU of delivered space heating energy. In the five climates studied, the weighted-average HSPF[7] ranges from 10.1-16.8 kBTU/kWh (per Table 4.2). This means that for a heat pump to be competitive with a gas furnace on operating expenses alone, electricity would have to be available at a price point between $\frac{\$10.42}{MMBTU} * \frac{0.0101 MMBTU}{kWh} = \$0.11/kWh$ and $\frac{\$12.50}{MMBTU} * \frac{0.0168 MMBTU}{kWh} = \$0.21/kWh$. By allocating fixed costs to residential customers as a volumetric delivery charge – increasing the total volumetric charge upwards of \$0.15/kWh –

[7]The HSPF (heating seasonal performance factor) describes the ratio of heating energy produced by a heat pump (in kBTU) to electricity consumed (in kWh) over the course of a typical year.

electric utilities are making heat pumps less attractive to consumers.

5.4.1.3 Water Heating

In addition to studying how customers' choices of space heating equipment responds to different volumetric tariffs, we also consider customers' choices of water heating (DHW) equipment. Figure 5.7 is analogous to Figure 5.6, but plots water heating energy instead of space heating energy. The overall trend is similar: faced with very low volumetric electricity tariffs, customers opt for inexpensive (but inefficient) electric resistance DHW heaters. As the tariff is increased, customers transition to using heat pumps, which carry higher upfront costs but are far more efficient. If the tariff is raised too high, customers forgo electric water heating, instead opting to use natural gas water heaters.

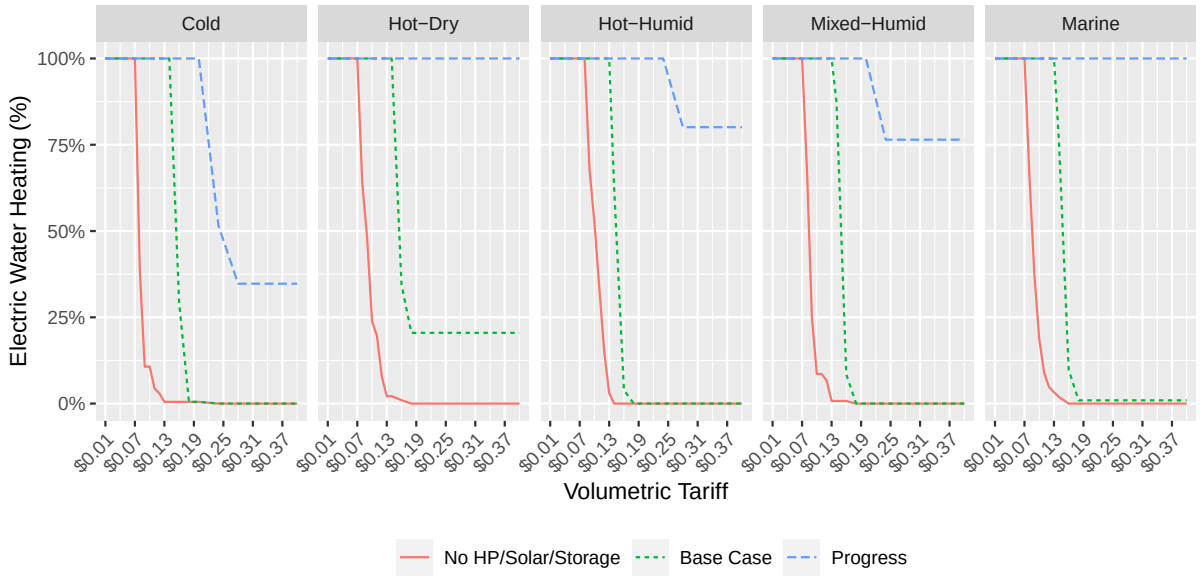

Figure 5.7: Breakdown of water heating energy choices vs. volumetric tariff in each climate region. As the tariff is increased, customers are more likely to opt for natural gas water heating instead of electric options.

5.4.1.4 Space Cooling

Figure 5.8 plots the source of space cooling energy vs. the volumetric tariff for each climate and scenario. In all three scenarios, across all five climates, customers faced with higher volumetric

tariffs are incentivized to adopt higher-efficiency air conditioners or heat pumps to meet their space cooling needs. The tipping point at which customers begin to shift from low-efficiency units to high-efficiency units is not the same in each climate region. In the hot-humid region, which has the largest space cooling demands, customers begin to shift from low-efficiency units to high-efficiency units as the tariff rises above about \$0.05/kWh. In the cold climate, it is only cost-effective for customers to adopt high-efficiency units as the volumetric tariff rises above \$0.18-\$0.20/kWh, and only in the base and progress cases where heat pumps are used for both heating and cooling demands.[8] For the marine climate, the minuscule cooling demand is fulfilled by low-efficiency units for nearly all scenarios and values of the tariff.

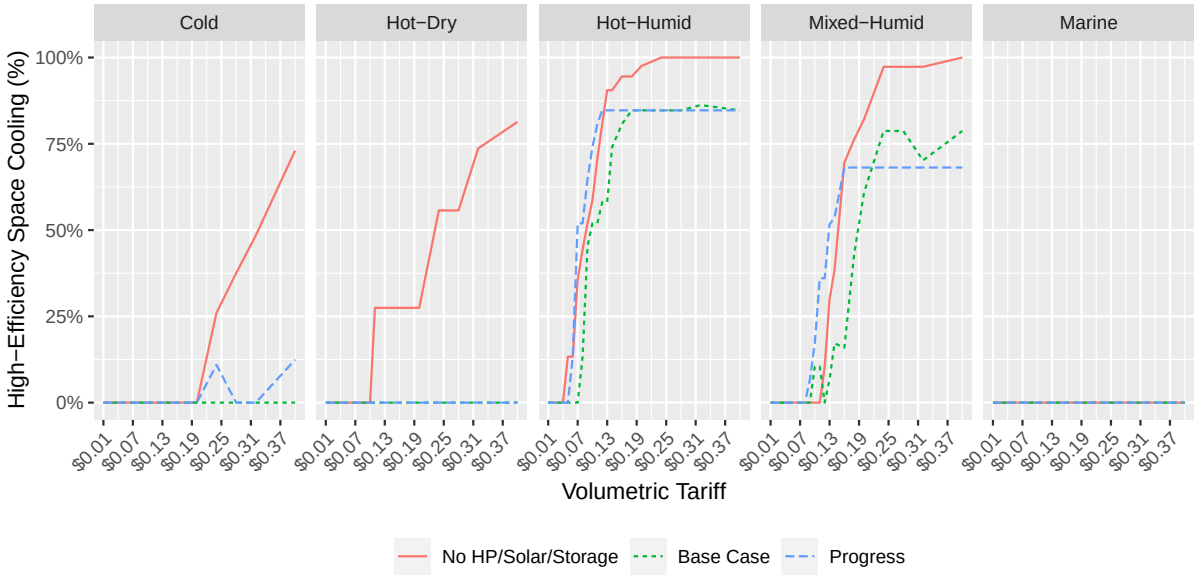

Figure 5.8: Breakdown of space cooling energy choices vs. volumetric tariff in each climate region. As the tariff is increased, customers are incentivized to choose higher-efficiency units.

We do not assume that there is any elasticity in the quantity of cooling energy demanded. A customer facing a lower electricity price will not respond by cooling their home to a colder temperature. This is an important source of error that should be interrogated in future work.

[8]In "the No HP/Solar/Storage" scenario, customers continue to use low-efficiency air conditioners for all tested values of the tariff.

5.4.1.5 Solar and Storage Adoption

In addition to changing their choice of heating and cooling technologies, customers can respond to increased electricity tariffs by adopting rooftop solar panels and battery storage. The patterns of load defection resulting from solar and storage adoption can be observed in Figure 5.9. In the hot-dry climate, customers begin adopting solar and storage to decrease the electricity consumption from the grid as prices rise above \$0.09/kWh for the progress case and \$0.13/kWh for the base case. In the cold climate, which is less favorable for rooftop solar due to weaker sunlight and more cloud cover, prices must rise above \$0.13/kWh and \$0.17/kWh respectively to incentivize load defection through solar/storage adoption. These estimates are consistent with a back-of-the-envelope calculation: a roof-mounted solar panel can produce approximately 200–350 kWh of electricity per-meter-squared, depending on the climate. This translates to 1300–2300 kWh per-kW of solar capacity. At an annualized cost of \$300-per-kW-capacity (the base assumption), the levelized cost of solar is \$0.13-\$0.23/kWh. In the progress scenario, the cost of solar panels drops to \$210 per-kW-capacity (30% decrease) and the levelized cost of solar power falls to \$0.09-\$0.16/kWh.

In Figure 5.10, we plot for each feeder the gross consumption of utility-supplied electricity (purchases), the amount of electricity sold back to the utility (injections), and the net consumption of utility-supplied power. In the presence of a net-metering policy, injections begin to rise at roughly the same tariff that motivates adoption of rooftop solar. In other words, there is no significant band of tariffs that promotes self-consumption of electricity generated from rooftop PV. In the hot-dry, mixed-humid, and marine climates, customers achieve a "net zero" status for tariffs above \$0.19 - \$0.27 per-kWh. In the cold and hot-humid climates, customers adopt the maximum amount of solar PV that can be accommodated on their rooftop, resulting in modest net consumption of utility-supplied power.

We note that even though the customers on these feeders achieve net-zero or near-net-zero status, their gross consumption of grid-produced power levels out around 2,500 kWh-per-1000-sf for all feeders.

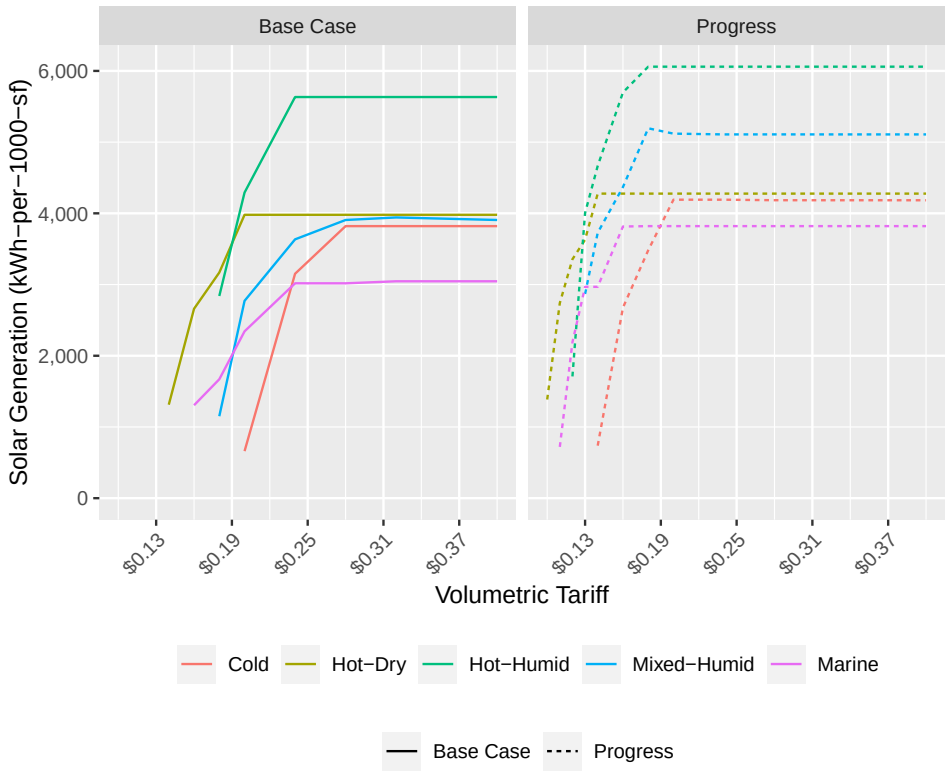

Figure 5.9: Fraction of electricity consumption generated by rooftop solar. As the tariff is increased, customers adopt solar panels and battery storage in order to reduce their payments to the utility.

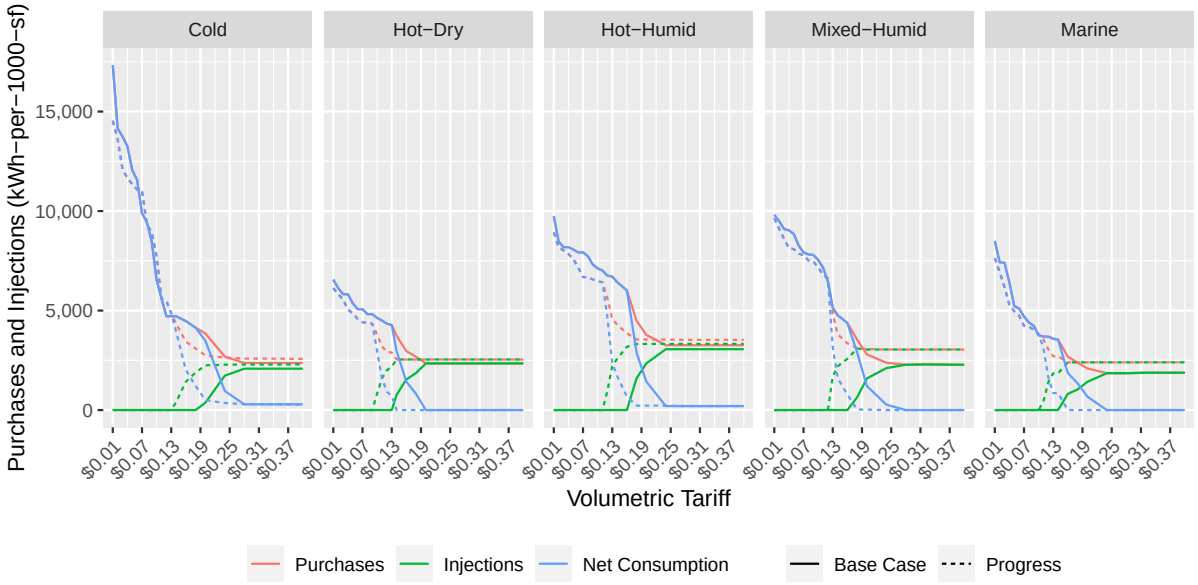

Figure 5.10: Purchases, injections, and net consumption vs. the volumetric tariff. In the hot-dry, mixed-humid, and marine climates, customers achieve a "net zero" status for tariffs above $0.19 - $0.27 per-kWh. In the cold and hot-humid climates, customers adopt the maximum amount of solar PV that can be accommodated on their rooftop, resulting in modest net consumption of grid-produced power.

5.4.1.6 Feeder Peaks

The adoption of rooftop solar does little to mitigate the feeder's peak demand. This is observed in Figure 5.11: as the tariff increases from \$0.05 per-kWh to about \$0.13 per-kWh, the feeder peak drops due to decreased use of electric heating. In the \$0.13-\$0.25 per-kWh regime, where we see large uptake of rooftop solar, the peaks plateau.

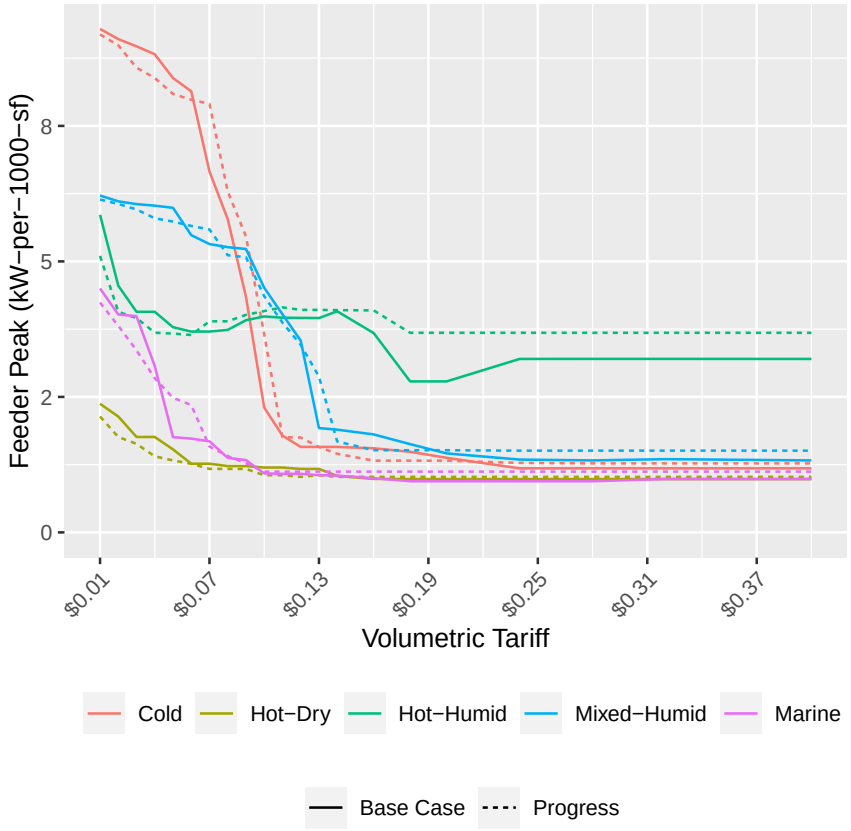

Figure 5.11: Peak load vs. the volumetric tariff. Peaks plateau as the tariff increases above \$0.13 per-kWh, even as customers adopt large amounts of rooftop PV.

In practice, the largest adoption of rooftop solar panels is found in California (U.S. Energy Information Administration, 2021b), where volumetric electricity prices can exceed \$0.40/kWh for residential customers with the highest levels of consumption (Pacific Gas & Electric, 2022; Southern California Edison, 2022). Under these conditions, customers are strongly incentivized to adopt solar panels to reduce their net consumption from the grid.

Depending on the level of the volumetric tariff, customers adopt different portfolios of

technologies that can significantly impact their feeder's peak load. In Figure 5.12, we plot the ratio of the simulated feeder peak to the incumbent peak (before optimization) for each of the five climates across three scenarios. For very low tariffs, customers use electric resistance heating to satisfy their space and water heating needs, driving very large peak loads. This is seen most prominently in the cold climate where the electricity peak increases by a factor of six relative to the pre-optimized loads when the tariff is decreased to \$0.01 per-kWh. Surprisingly, the marine region also sees a nearly five-fold increase in peak demand due to adoption of electric resistance heating, despite having a relatively mild climate.

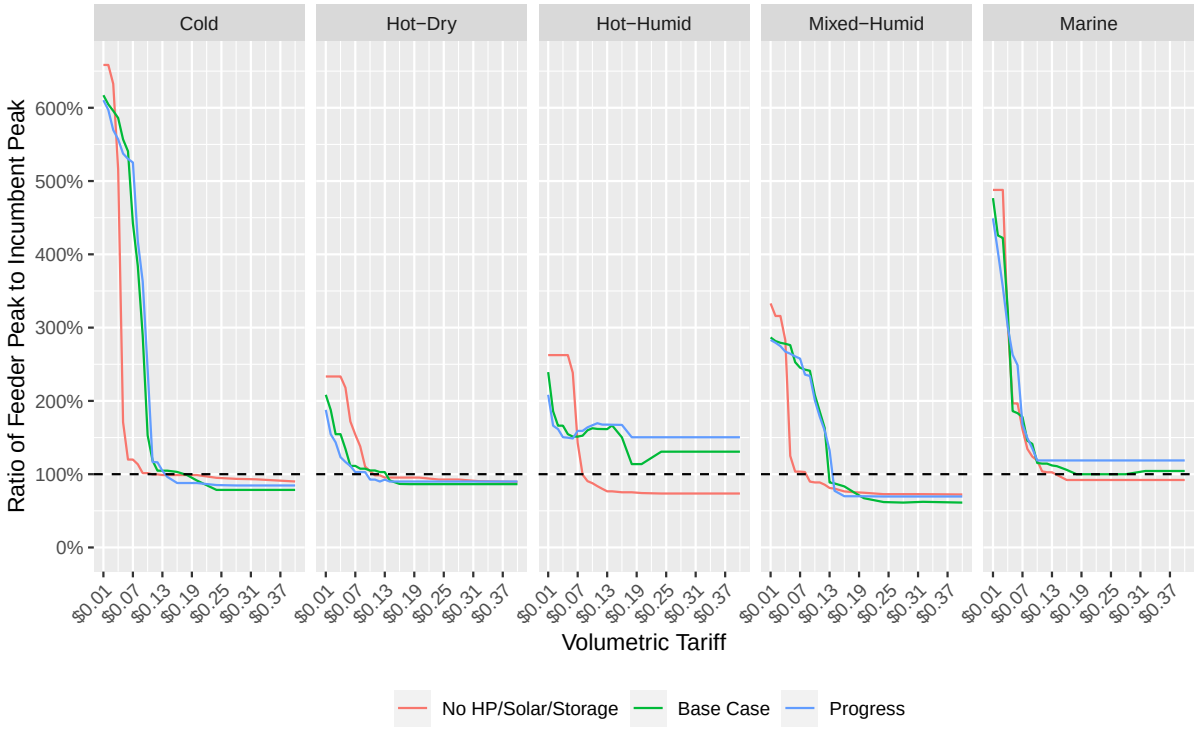

Figure 5.12: Feeder peak vs. the volumetric tariff. For very low tariffs, customers use electric resistance heating to satisfy their space and water heating needs, driving very large peak loads. As the tariff is increased, the peak load drops as customers switch from electric resistance to heat pumps and natural gas heating.

As the tariff is increased, the peak load ratio drops precipitously in all five climates and all three scenarios as customers switch from electric resistance to heat pumps and natural gas heating. In the cold, hot-dry, and marine climates, the peak load ratio plateaus at approximately 100%

(that is, the simulated peak is roughly equal to the pre-optimized peak). In the mixed-humid climate, the peak load plateaus at about 70% of the original peak in all three scenarios. In the hot-humid climate, where electric heat pumps are used as the primary source of space heating energy in the base and progress cases even as the tariff rises to $0.40 per-kWh, the simulated peaks plateau at about 125% and 150% of the incumbent peak, respectively.

5.4.1.7 Emissions

Even though raising the volumetric tariff for electricity to recover fixed costs may increase the total cost of service, this practice may be considered acceptable if it also decreases emissions. In Figure 5.13, we plot the emissions vs. the tariff for each region and scenario. Each tile describe a different scenario-region combination. The red area represents emissions from electricity production, while the blue area represents emissions from gas combustion. The black function describes total emissions net of any solar generation.[9]

In the "No HP/Solar/Storage" scenarios, emissions generally fall as the tariff is increased because customers are incentivized to adopt higher-efficiency air conditioners and switch from electric resistance heating to furnaces.

[9]Solar generation is assumed to reduce aggregate emissions by avoiding centralized generation. The same emissions rate is used whether the generated electricity is consumed behind-the-meter or injected to the grid.

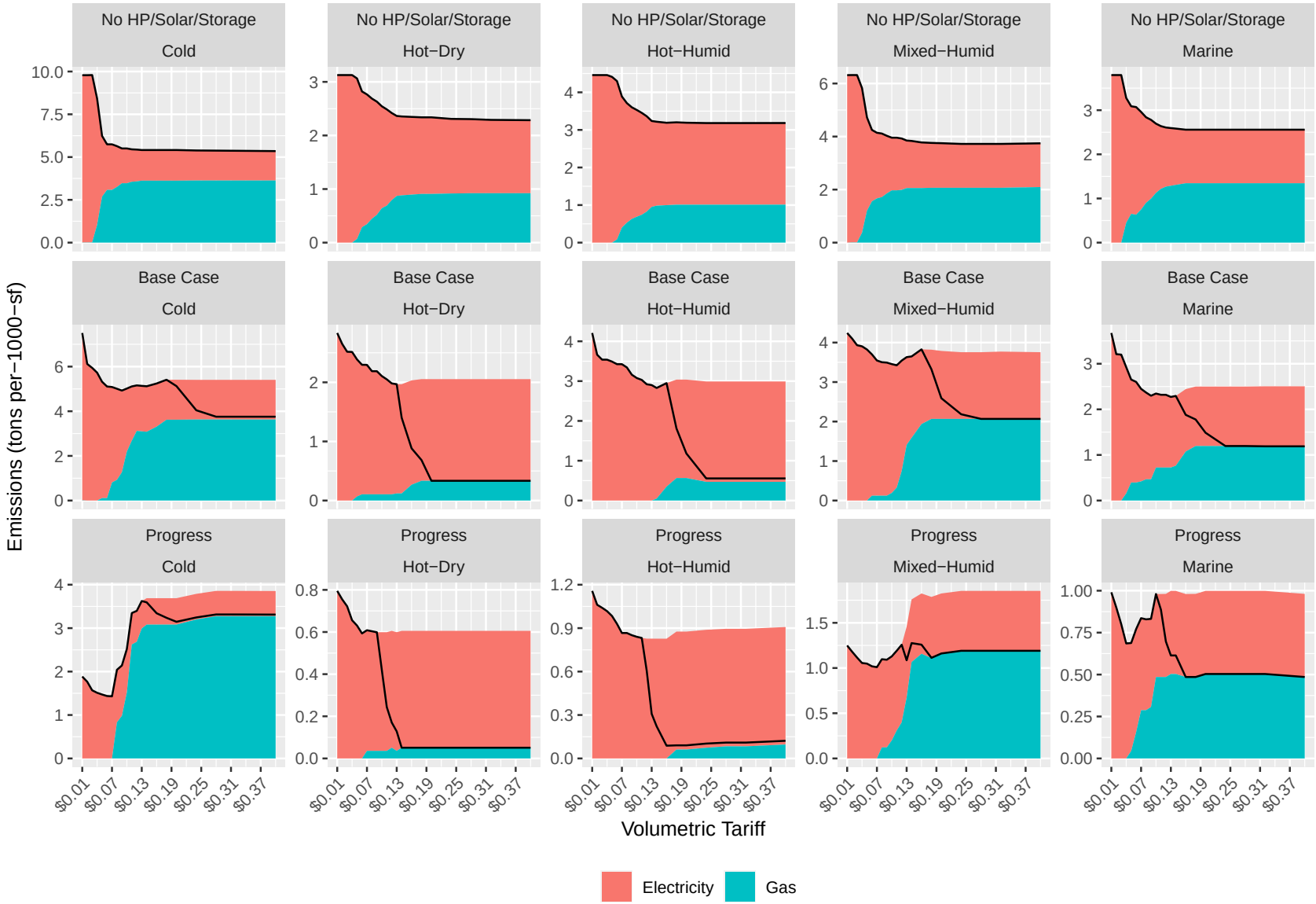

Figure 5.13: Total emissions vs. the volumetric tariff. The black function describes total emissions net of any solar generation.

In the base scenario, emissions fall sharply as the tariff is increased above \$0.15-\$0.20 per-kWh, as customers adopt rooftop solar photovoltaic panels to reduce their net consumption of grid-supplied power.

In the progress scenario, we observe a notable departure from the trend of increasing tariffs resulting in decreasing emissions for the cold climate. At lower tariffs, customers are incentivized to use heat pumps as their primary source of heating, resulting in significantly lower emissions than a gas furnace. As the electricity tariff is raised, customers are encouraged to use natural gas furnaces instead of heat pumps, increasing both emissions and the total cost of energy services. In the mixed-humid climate, emissions are relatively constant. As the tariff is increased, the additional emissions from gas heating are roughly canceled out by emissions reductions from solar generation.

This is a notable exception to the dialogue that frames residential retail rate reform as a conflict between improving economic efficiency and reducing carbon emissions. In models where customers mainly respond to high volumetric tariffs by adopting solar panels, high volumetric rates lead to increased aggregate energy costs but decreased emissions. As we observe here, there are also cases where lowering retail rates could decrease both energy costs and emissions by incentivizing economical electrification of heating.

Despite this result appearing in the "progress" case, there are already conditions in the United States today that look quite similar to the modeled scenario. In Upstate New York, the average carbon emissions from the grid is 0.254 lb/kWh, slightly below the assumed emissions in the progress case. In New England, the average emissions from electricity generation is 0.528 lb/kWh (Environmental Protection Agency, 2020). In both of these regions, incentivizing even a small fraction of customers to electrify their space and/or water heating loads through more attractive electricity rates could result in steep emissions reductions.

5.4.2 Cost Recovery and Efficiency

Two principal functions of rate design are (1) guaranteeing that a utility is able to recover its full costs plus a fair rate of return on capital expenses and (2) promoting efficient use of energy

services. In this section, we analyze how changing the level of the volumetric tariff impacts the utility's ability to recover its costs; discuss residual costs not recovered through a given tariff, and describe how tariff design can impact the total cost of providing energy services to a collection of customers. Additionally, we consider how net-metering reform influences customers' decisions about rooftop solar adoption, the utility's ability to recover its costs, and the total cost of energy services.

5.4.2.1 Utility Costs and Revenues

In Figure 5.14, we report the utility's costs and revenue for each feeder vs. the tariff. The solid black line describes the annual revenue collected from the customers through the volumetric tariff in \$/1000-sf (each feeder has 25,000–30,000 square-feet of conditioned residential space). The dashed black line describes the annual revenue collected from customers through the volumetric tariff *plus* the financial value of the electricity injections that the utility receives.[10]

[10]Here we make the strong assumption that excess distributed generation injected into the feeder by customers displaces wholesale generation that would otherwise cost the utility \$0.05 per-kWh. In reality, energy costs are typically lower in the middle of the day when excess solar is available and higher in the afternoon and evening, especially in warmer climates.

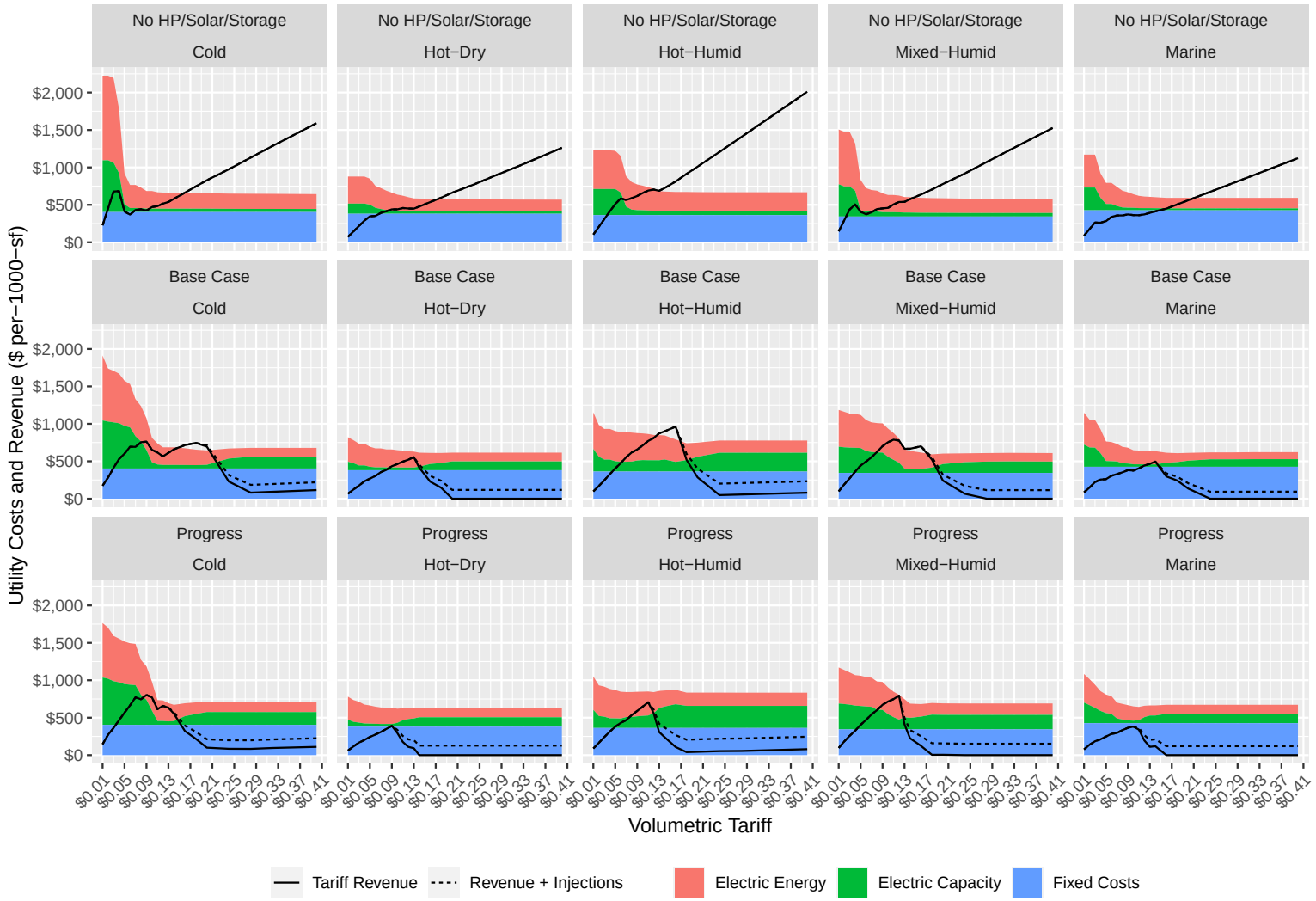

Figure 5.14: Total revenue collected from customers through the volumetric tariff (black line) and total cost of serving customers (colored areas). In the base and progress cases, the tariff revenue converges to near-zero for sufficiently high volumetric tariffs as customers adopt large amount of rooftop solar panels. Capacity costs first decrease as the tariff is raised because customers shift from electric resistance heating to heat pumps and furnaces. As the tariff continues to increase in the base and progress cases, capacity costs increase again as the utility invests in additional distribution capacity to accommodate the injections from rooftop solar. The financial value of the energy received from solar injections (assuming it displaces generation elsewhere) is represented by the difference between the dashed line and the solid line.

For the "No HP/Solar/Storage" case, the solid black line is monotonically increasing on the right side of the graph. This tells us that as the utility continues to increase the tariff, revenue increases. When the black line exceeds the colored region, the tariff is high enough to recover the utility's revenue requirement. Under these circumstances, the challenge of tariff design is simply to set a tariff that is high enough to recover the utility's revenue requirement without creating an undue burden for customers.

For the base and progress cases, this trend no longer holds: when the tariff is increased above \$0.20-\$0.25/kWh, the utility's revenue plateaus and begins to decrease as customers adopt solar panels in order to decrease their volumetric charges. The revenue from the volumetric tariff converges to near-zero for sufficiently high volumetric tariffs. In the presence of distributed solar and net-metering, it is no longer guaranteed that raising the volumetric tariff will increase revenue.

The colored areas describe the utility's costs. The blue area describes fixed electric transmission, distribution, and administrative expenses that occur upstream of the feeder and are not impacted by customer behavior, but are allocated to these residential customers. We estimate these expenses as \$727/customer (\$10,905 for the feeder) (R. L. Fares & King, 2017).

The green area is the cost of capacity, including both generation capacity charges (which are proportional to the coincident peak of loads on the feeder) and the annualized cost of any additional feeder capacity required to meet peak loads.[11] Capacity costs first decrease as the tariff is raised because customers shift from electric resistance heating to heat pumps and furnaces. As the tariff continues to increase in the base and progress cases, capacity costs increase again as the utility invests in additional distribution capacity to accommodate the injections from rooftop solar.

The red region is the cost of electricity, which is set at an average price of \$0.05 per-kWh. We assume that this represents the full social cost of electricity, which is borne in entirety by the utility. Energy costs converge to some non-zero value, equal to the gross energy that customers

[11] Annualization is based on an assumed weighted-average cost of capital of 10%, which includes the cost of debt and regulated profits on equity.

consume from the grid to serve loads at hours when electricity from distributed solar is not available.

The most important observation is that in the base and progress cases, the revenue that the utility collects through the volumetric tariff does not always exceed the utility's cost of serving customers. In the scenarios where customers achieve net zero consumption, the difference between the utility's cost of serving load and the revenue collected from the volumetric tariff is equal to the sum of: the customers' share of the utility's fixed costs, capacity-related costs for the feeder, and the cost of electricity consumed by customers on the feeder when solar isn't available. While the utility does receive some injected electricity that may be used to displace generation expenses elsewhere, the value of this electricity is only a fraction of the total cost of serving these customers.

5.4.2.2 Residual Fixed Costs

In the presence of emerging technologies, it is not guaranteed that utilities can recover their full costs from residential customers through a volumetric tariff alone. In Figure 5.15, we plot the fraction of the utility's revenue requirement recovered through the volumetric tariff vs. the value of the tariff. In the "No HP/Solar/Storage" scenario, the revenue collected from customers increases monotonically with the level of the tariff, so there is guaranteed to be a tariff such that the utility recovers its full costs. When we introduce rooftop solar in the base and progress cases, this trend no longer holds: as the utility raises the tariff above \$0.09 to \$0.17 per-kWh, customers begin to curtail their net consumption by adopting rooftop solar. In the base case, this load defection makes it impossible for utilities to recover their full revenue requirement using volumetric tariffs in the marine and hot-dry climates. In the progress scenarios, full cost recovery is impossible in all five climates using volumetric tariffs alone.

Residual costs not recovered from the volumetric tariff can be recovered through some other means, such as through a monthly fixed charge. In Figure 5.16, we compute the fixed charge required to allow full cost recovery given an arbitrary choice of the volumetric tariff. As the volumetric tariff is increased to about \$0.17/kWh, the required fixed charge falls in all three

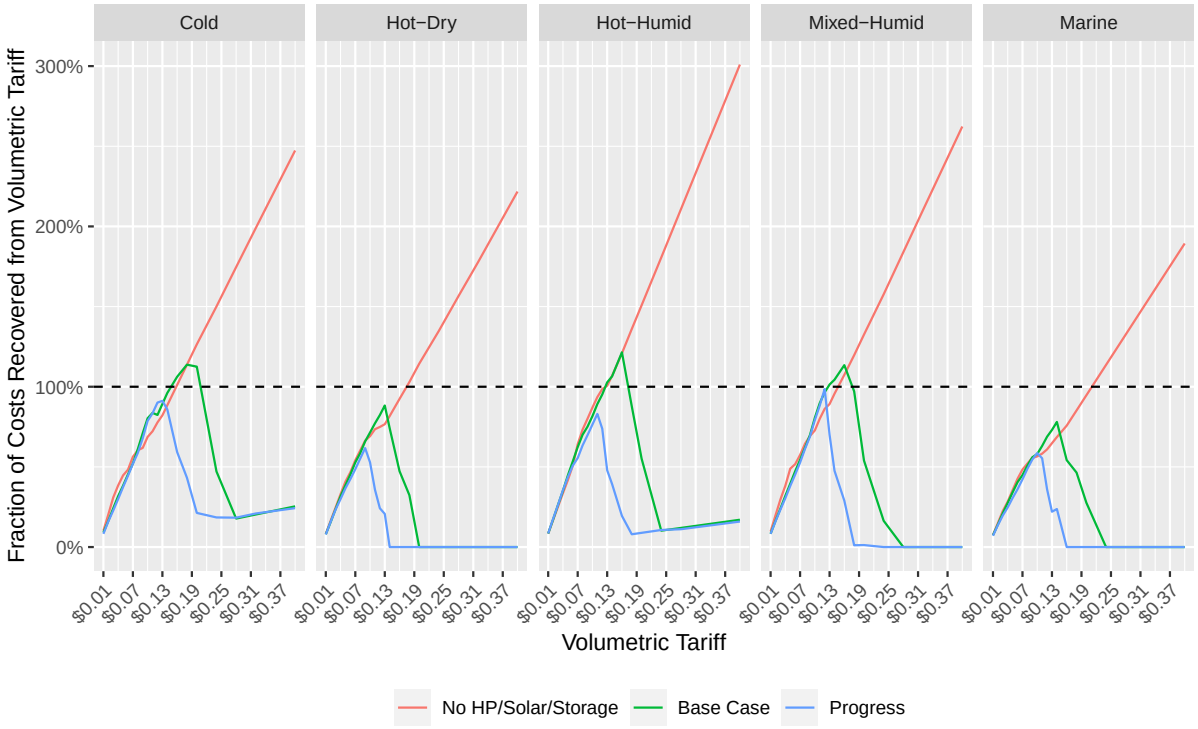

Figure 5.15: Fraction of revenue requirement recovered through the volumetric tariff.

scenarios. Under the "No HP/Solar/Storage" assumption, this trend continues until the required monthly fixed charge has fallen below zero. Under the base and progress assumptions, higher tariffs incentivize customers to decrease their consumption from the grid by adopting solar and storage. This effect ultimately causes the residual cost vs. tariff curve to slope back up. In other words, not only would raising the volumetric tariff above roughly \$0.20/kWh fail to eliminate the need for a monthly fixed charge, it would actually increase the residual costs that need to be recovered through such a charge.

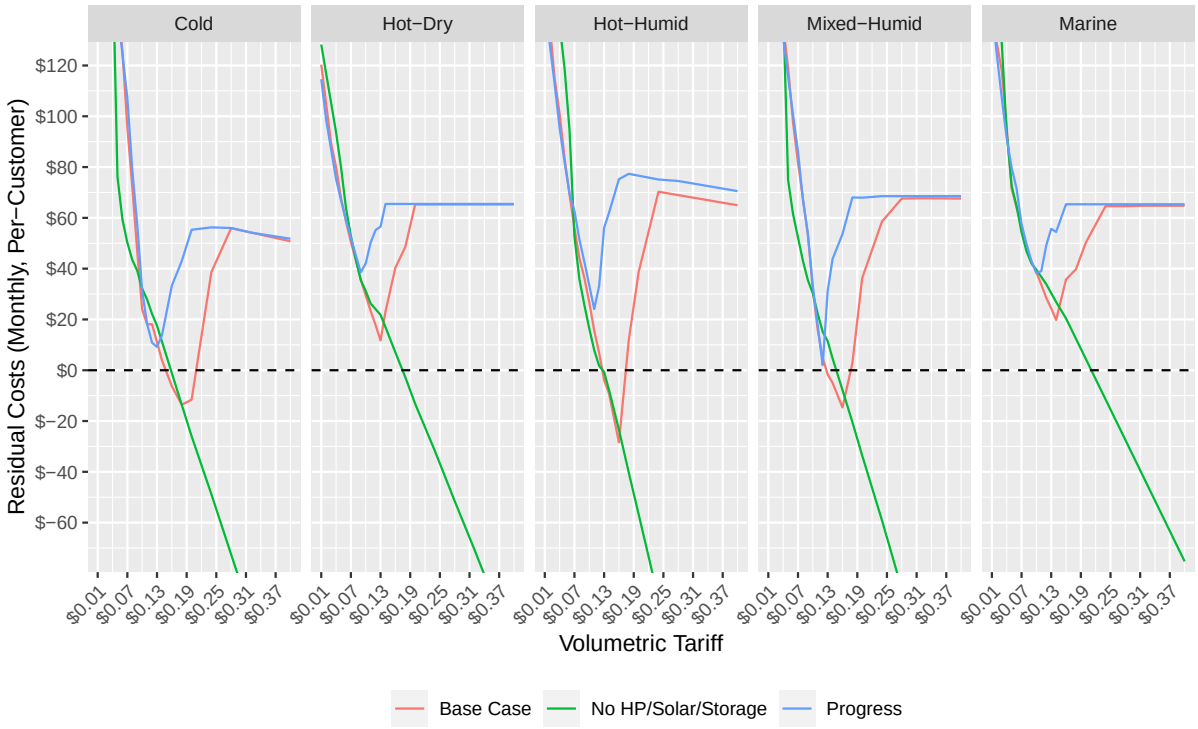

Figure 5.16: Required monthly fixed charge needed to recover a utility's full revenue requirement vs. the volumetric tariff. As the volumetric tariff is increased to about \$0.17/kWh, the required fixed charge falls in all three scenarios. Under the "No HP/Solar/Storage" assumption, this trend continues until the required monthly fixed charge has fallen below zero. Under the base and progress assumptions, higher tariffs incentivize customers to decrease their consumption from the grid by adopting solar and storage, causing the residual cost vs. tariff curve to slope back up.

If all electric energy and capacity costs are recovered through a volumetric tariff (these tariffs would range from \$0.06 per-kWh to \$0.09 per-kWh), the residual fixed costs would be approximately \$727 per-customer each year (R. L. Fares & King, 2017). This could be recovered

through a monthly customer charge of approximately $61. While it is worth stressing that such a policy would most likely reduce the total cost of energy services, it is all but guaranteed that such a policy would create winners and losers. Several authors, including (S. P. Burger et al., 2020).

In the progress case, the minimum monthly fixed charge that would still allow the utility to recover its remaining costs through a volumetric tariff ranges from $2 in the mixed-humid climate to $38 in the hot-dry and marine climates. These latter values are significantly higher than the monthly fixed charges typically used for residential customers today (Faruqui & Leyshon, 2017).

5.4.2.3 Total Energy Services Costs

One of the principal functions of rate design is to promote efficient production and consumption of energy services. In order to evaluate the extent to which different tariff design strategies achieve this goal, we evaluate the total cost of energy services, including annualized equipment costs, gas and electric energy costs, and capacity costs.

In Figure 5.17, we plot the total cost of providing energy services to the 15 customers (per-1000-sf) vs. the volumetric tariff.[12] The colored area plot describes the separate cost components.

[12]We assume that the natural gas distribution system has adequate capacity to serve the space and water heating loads on each feeder, so there are no marginal gas capacity costs to minimize.

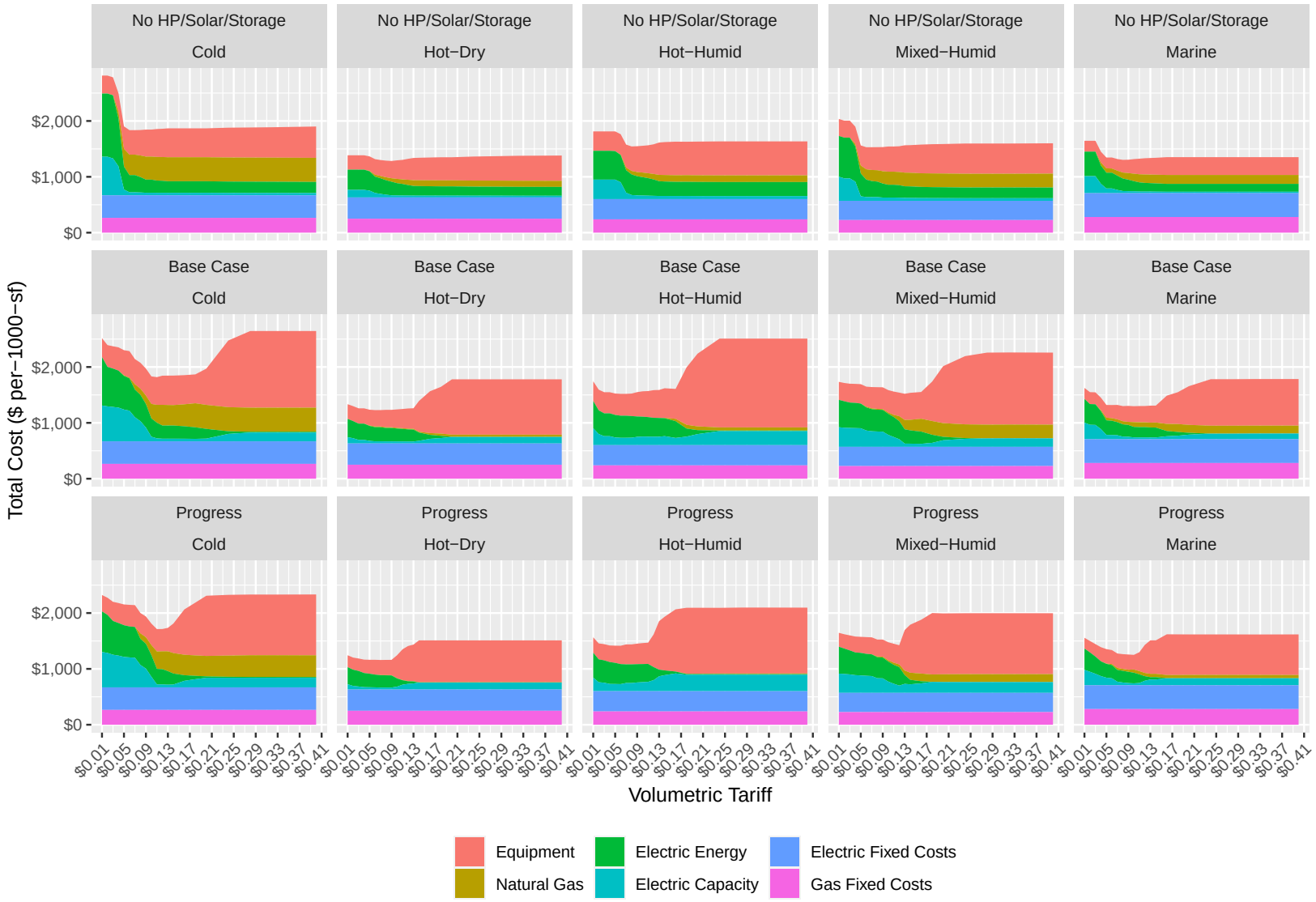

Figure 5.17: Total cost of energy services. As the tariff is increased in the base and progress cases, the total cost of energy services increases significantly. In the "No HP/Solar/Storage" scenario, the total cost of energy services plateaus for tariffs above approximately $0.07 per-kWh, as customers are given relatively few means to reduce their energy consumption without sacrificing energy services. In the base and progress scenarios (i.e., in the presence of emerging technologies), there is a much more precipitous increase in costs as customers shift from heat pumps to furnaces and adopt rooftop solar to reduce their net consumption of electricity.

In the "No HP/Solar/Storage" scenario, we observe that the total cost of energy services decreases in the cold and mixed-humid climates (and to a lesser extent the hot-humid and marine climates) as the volumetric tariff is increased from \$0.01 per-kWh to approximately \$0.05 per-kWh. These cost-savings are achieved because customers shift their space heating equipment from electric resistance to gas furnaces.

As the tariff continues to increase, the total cost of energy services quickly plateaus. While customers shift from low-efficiency furnaces and air conditioners to higher-efficiency units, this has a modest effect on the total cost of energy services. Consequently, the choice of a \$0.10 per-kWh tariff vs. a \$0.20 per-kWh tariff has a minimal impact on cost.

In the base and progress cases, we see much more precipitous increases in costs as the tariff is raised. This is predominantly driven by customers adopting rooftop solar to reduce their net consumption of utility-provided power. We note that while this does result in the total cost of energy converging to zero as net consumption goes to zero,[13] these savings are substantially outweighed by increased equipment costs (which include solar PV). Because we have assumed an annual net metering policy, the behavior only persists until customers have decreased their net annual consumption of grid power to zero, after which point continuing to increase the tariff does not have any effect on customer decisions.

The cost-minimizing tariffs are achieved at prices between \$0.06-\$0.13 per-kWh for the base case and \$0.06-\$0.12 per-kWh for the progress case. These tariffs strike a balance between discouraging inefficient use of electricity (load that is valued at less than the cost of energy and/or necessitates inefficient capacity expansion) while not being so high as to encourage inefficient solar adoption. These results are generally consistent with the recommendations produced by Borenstein (2016) and Perez-Arriaga, Jenkins, and Batlle (2017), which advise that the price of electricity should be set close to its social marginal cost (here assumed to be \$0.05 per-kWh). The volumetric tariffs on the higher end of these ranges discourage over-consumption of electricity that could drive up capacity costs. This signaling could most-likely be done more efficiently by

[13] In evaluating total costs, we simply sum the net energy consumption over the course of a year and multiply by the cost of energy. This is a different procedure than we used to compute the energy portion of utility costs, as the utility still needed to purchase energy at off-peak hours to re-sell to customers.

combining a lower energy price with a separate tariff that discourages consumption at hours when the feeder is near its capacity.

We note that the computed electric capacity costs in Figure 5.17 are governed by our estimate of the annualized cost of additional electric distribution capacity ($50 per-kW each year). This estimate was informed by the econometric analysis in Chapter 1. Many analyses, such as Elmallah, Brockway, and Callaway (2022) and Larson et al. (2020), use significantly higher estimates for the cost of additional distribution capacity. If we estimate the annualized cost of additional distribution capacity as $300 per-kW-year, we are given Figure 5.18.[14] Here we see that the total cost of energy services increases much more sharply for both low and high volumetric tariffs. This makes it even more important that the tariff be set in the "goldilocks zone" that encourages efficient electrification of heating with heat pumps, doesn't encourage wide-scale adoption of electric resistance heating in colder climates (which can drive up peaks), and doesn't incentivize load attrition through inefficient adoption of distributed rooftop solar.

[14]This $300 per-kW-year figure applies to both additional distribution capacity for electrified loads and "negative distribution capacity" needed to receive excess solar injections during hours when the net feeder load is negative.

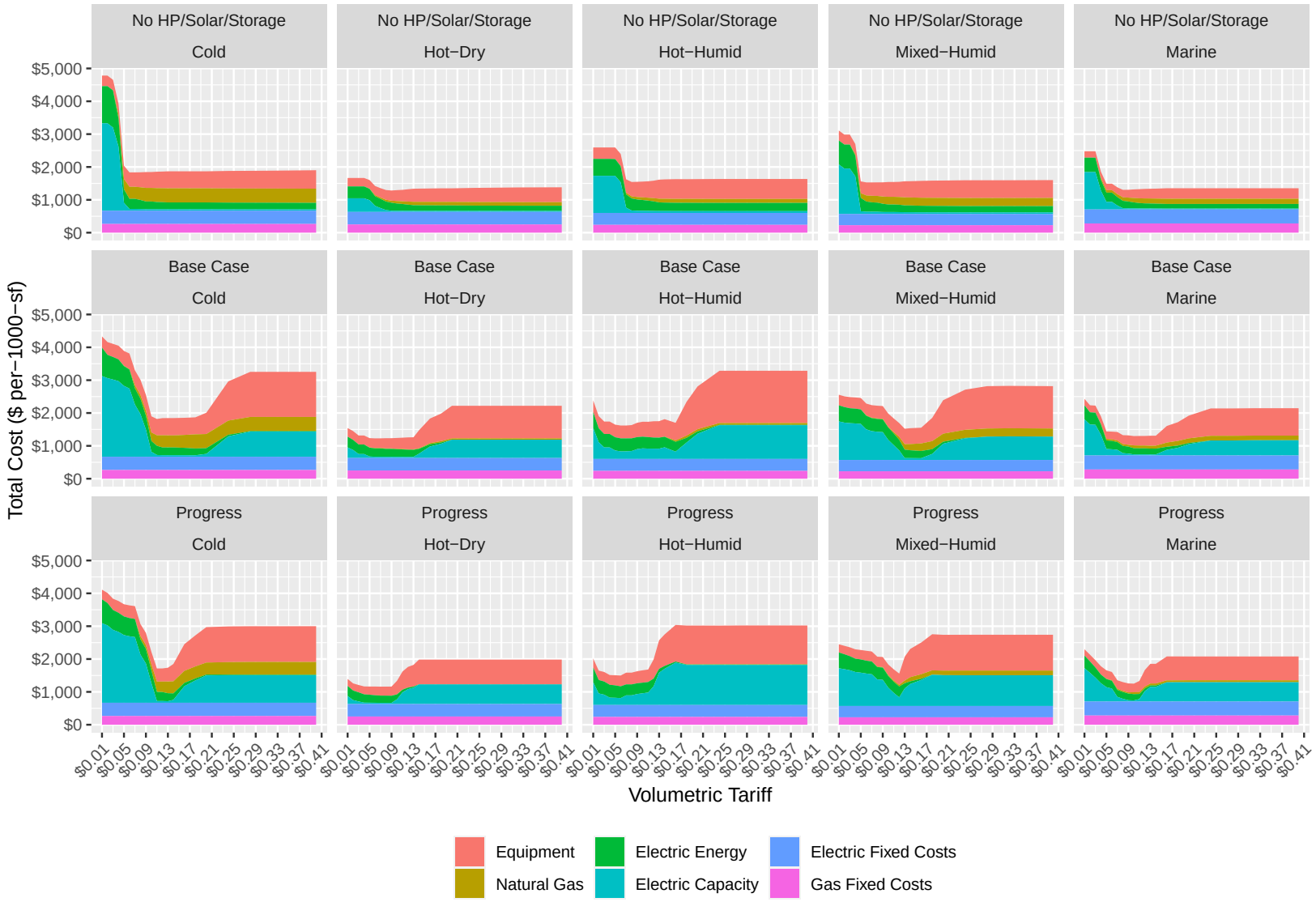

Figure 5.18: Total cost of energy services, assuming additional distribution capacity costs $300 per-kW-year. Compared to Figure 5.17, the total cost of energy services increases much more sharply for both low and high volumetric tariffs.

There are a number of cost-recovery mechanisms other than volumetric tariffs that may send more accurate price signals to customers, thus further reducing the cost of energy services. These include time-of-use (ToU) pricing, wherein the price of electricity changes based on fixed daily/seasonal schedule; real-time pricing (RTP), wherein the price of electricity changes at hourly intervals in response to the wholesale market; and demand charges, wherein customers are billed in part based on their individual peak load during a monthly period. One notable strategy, detailed in Pérez-Arriaga and Knittel (2016, Ch. 4), separately recovers energy costs based on the SMC of electricity, marginal capacity costs based on a forward-looking peak-coincident charge, and the residual through a fixed customer charge. Further work should investigate how the relative efficiency of these different strategies varies between climates and in the presence of emerging technologies.

5.4.3 Additional Scenarios

5.4.3.1 Net-Metering

"Net energy metering" (NEM) is a policy employed by a number of states that compensates retail customers for injected to the grid at the same rate that they pay for purchasing it. In other words, if a residential retail tariff is $0.20 per-kWh, then $0.20 is subtracted from the bill for every kilowatt-hour that a customer injects to the grid.

This policy has drawn sharp criticism because the retail rate often significantly exceeds the value of a marginal unit of electricity injected to the grid. This case is particularly strong in California, where a retail rates can exceed in $0.30 per-kWh but midday wholesale prices can fall below zero during the middle of the day, when there is excess solar generation on the grid California ISO (2021).

A number of states, including California, have begun implementing reforms to NEM that reduce the level of compensation for electricity to injected to the grid. Some of these programs also charge customers higher fixed charges and direct customers to switch to time-of-use (ToU) billing.

Our model of volumetric retail pricing assumes NEM is used in the default case. To test

how this policy affects customer behaviors, we also run a separate set of models that substitutes the NEM policy with a "net billing" policy that compensates customers for injected electricity at the assumed social marginal cost of electricity ($0.05 per-kWh), rather than the volumetric tariff. These models are optimized across the same range of volumetric tariffs used in base models, allowing us to understand how the presence of a NEM policy can impact customers differently depending on the level of their tariff.

Figure 5.19 shows the 24-hour load profile for a day with high solar production in the hot-dry climate. The black line represents the net load on the feeder, including the net effects of any solar generation and storage injections. The colored bar plots describe the solar generation and storage operation. The plots on the top row show the load and solar/storage operation for four different levels of the volumetric tariff ($0.12 per-kWh, $0.16 per-kWh, $0.20 per-kWh, $0.24 per-kWh, $0.32 per-kWh) assuming net-metering. The plots on the bottom row show the same profiles without net metering (injections to the grid are compensated at $0.05 per-kWh instead of at the tariff).

Without net-metering, customers are far less incentivized to build out excess solar generation because the electricity they inject to the grid is only compensated at a $0.05 per-kWh feed-in tariff rather than the much higher retail rate. Consequently, the "No NEM" case sees less adoption of solar at a given tariff than the base case.

In the bottom-right plot, we see adoption of distributed storage in addition to solar. This allows customers to "bank" excess solar power generated during the middle of the day and use it to reduce their net consumption during the nighttime and early morning. These banked kilowatt-hours are effectively compensated at the retail rate (rather than the much lower feed-in tariff) because they allow customers to reduce their consumption of expensive grid-supplied power.

Because solar power generated and consumed behind the meter is effectively compensated at the volumetric tariff, high retail tariffs over-incentivize the adoption of distributed generation even if net-metering has been eliminated.[15] This is a point frequently left out of policy debates

[15]See Biggar and Hesamzadeh (2014), Chapter 20 for a detailed discussion of this phenomenon.

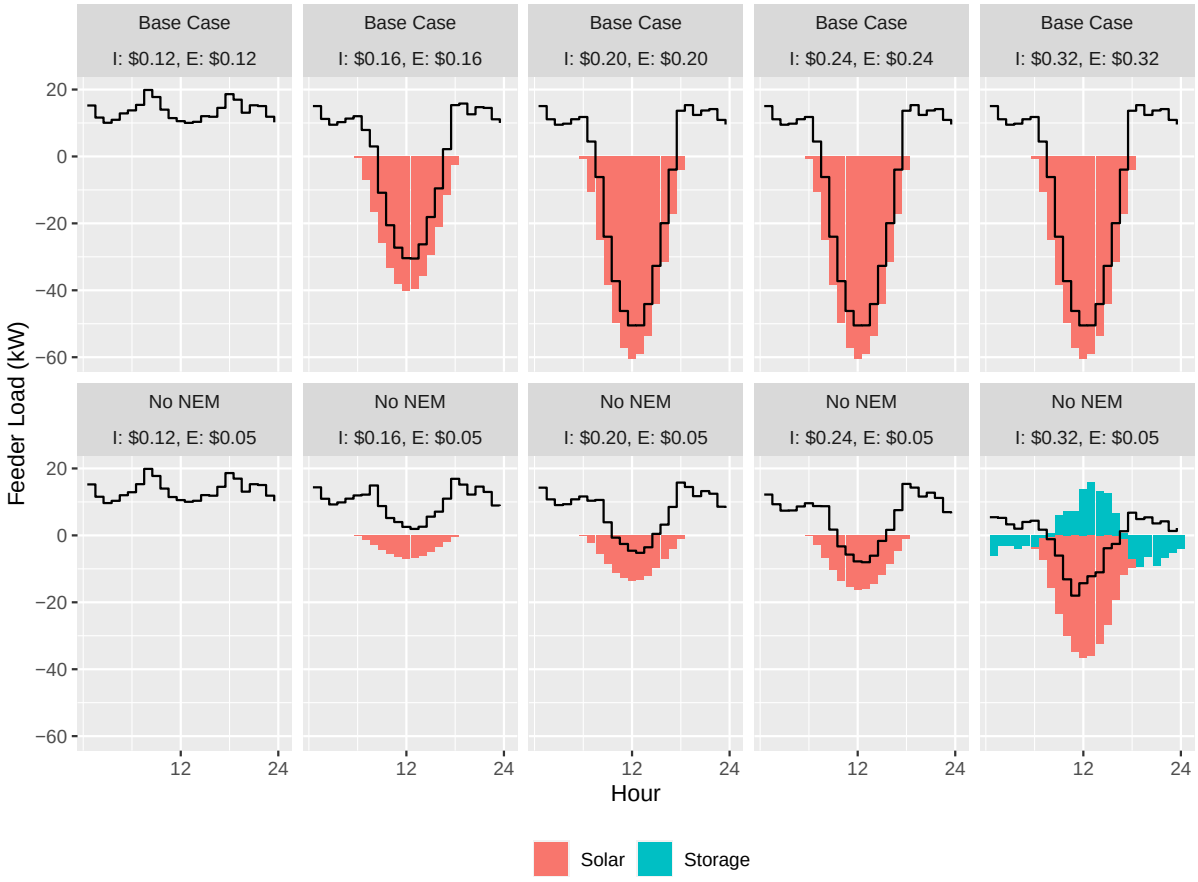

Figure 5.19: 24-hour load profile for a day with high solar production in the hot-dry climate. The black line represents the net load on the feeder, including the net effects of any solar generation and storage injections. The colored bar plots describe the solar generation and storage operation. Without net-metering, customers are less incentivized to invest in solar generation at any given tariff. At higher tariffs, customers are incentivized to augment their solar investments with distributed battery storage so that they can use stored solar energy to reduce their net load in the evening and morning hours.

about retail rate design.

Figure 5.20 compares the amount of solar PV generation in the hot-dry climate with and without net-metering. Without net metering, customers are far less incentivized to adopt rooftop solar PV, producing far less electricity from solar at any given tariff than in the case with net metering.

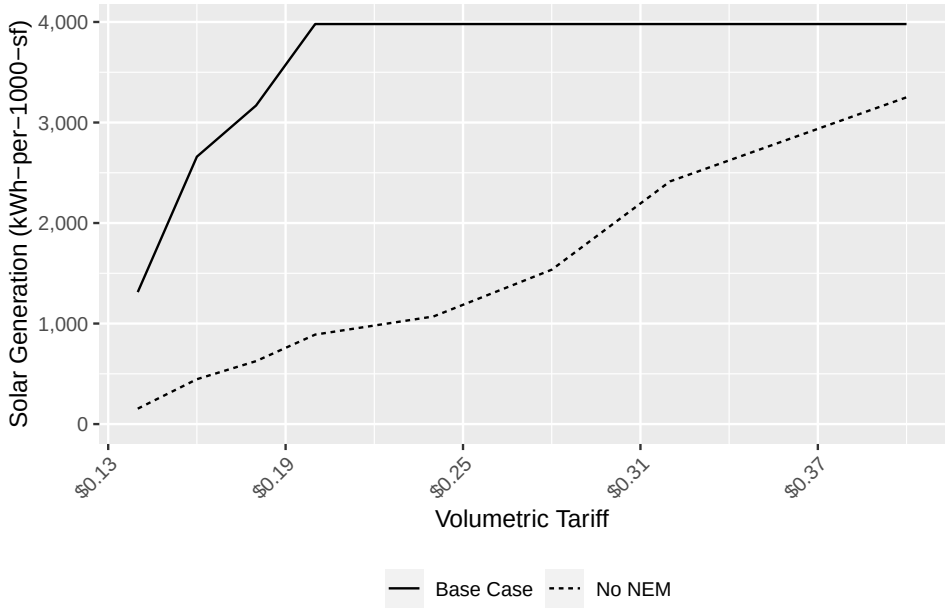

Figure 5.20: Total solar generation in the hot-dry climate, with and without net metering. Without net metering, the amount of solar generation increases much more gradually as the tariff is increased than in a scenario with net metering. This is because customers are not as strongly incentivized to inject excess generation to the grid.

In Figure 5.21, we see that the removal of a net metering policy discourages customers from selling electricity back to the utility at any given tariff, decreasing total injections. However, a corollary is that customers are much more inclined to find ways to consume their own generation behind-the-meter, such as by adopting battery storage. Consequently, at the highest tariffs, injections and purchases are both significantly lower in the "No NEM" case than in the base case.

Removing the net metering policy results in a modest reduction in the feeder peak for higher tariffs relative to the base case, as seen in Figure 5.22. This is likely due to the adoption of distributed storage in addition to solar PV, which is used to shift excess solar generation to other

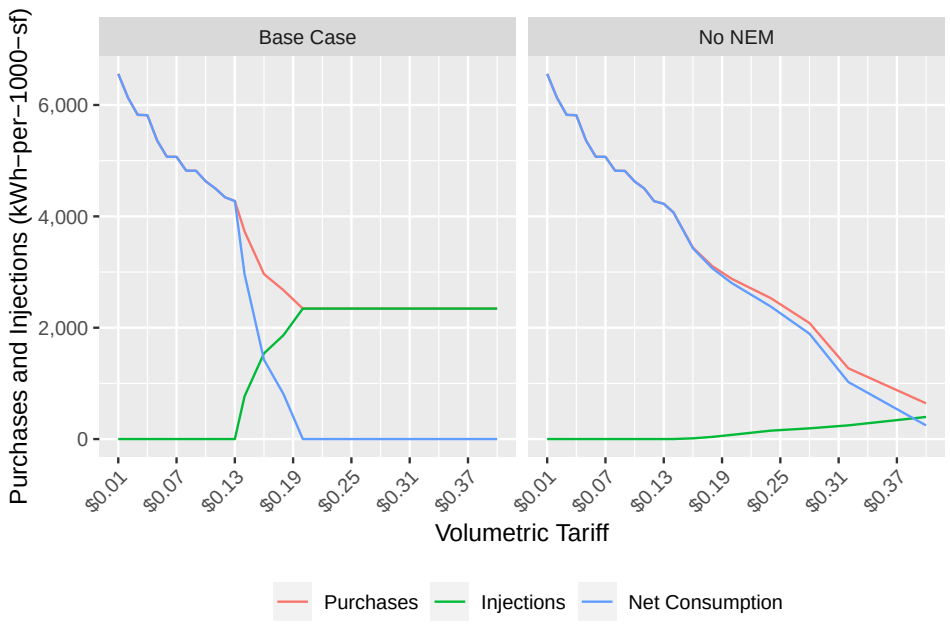

Figure 5.21: Purchases, injections, and net consumption vs. the volumetric tariff for the hot-dry climate, with and without net metering. Removing the net-metering policy discourages customers from injecting electricity to the grid and encourages them to consume it behind-the-meter. This results in decreases in both injections and purchases.

hours of the day. We note that there is no direct incentive for customers to reduce their peak load under volumetric pricing (with or without net metering). Some other tariff design that directly incentives load reductions during peak hours, such as a peak-coincident demand charge or time-of-use pricing, would be more effective at encouraging customers to shave their peaks than net metering reform alone.

The utility's costs and revenues are plotted in Figure 5.23. We observe that in the "No NEM" case, the black line rises above the colored region. This indicates that there exists a range of volumetric tariffs under which the utility is able to recover its full expenses. This does not hold in the base case, where the net-metering policy makes it impossible for the utility to recover its full costs through a volumetric tariff alone.

The total cost of energy services vs. the tariff is plotted in Figure 5.24. The left plot is identical to the hot-dry base case plot in Figure 5.17. As the tariff increases from approximately \$0.13 per-kWh to \$0.20 per-kWh, the total cost of energy services increases sharply as customers

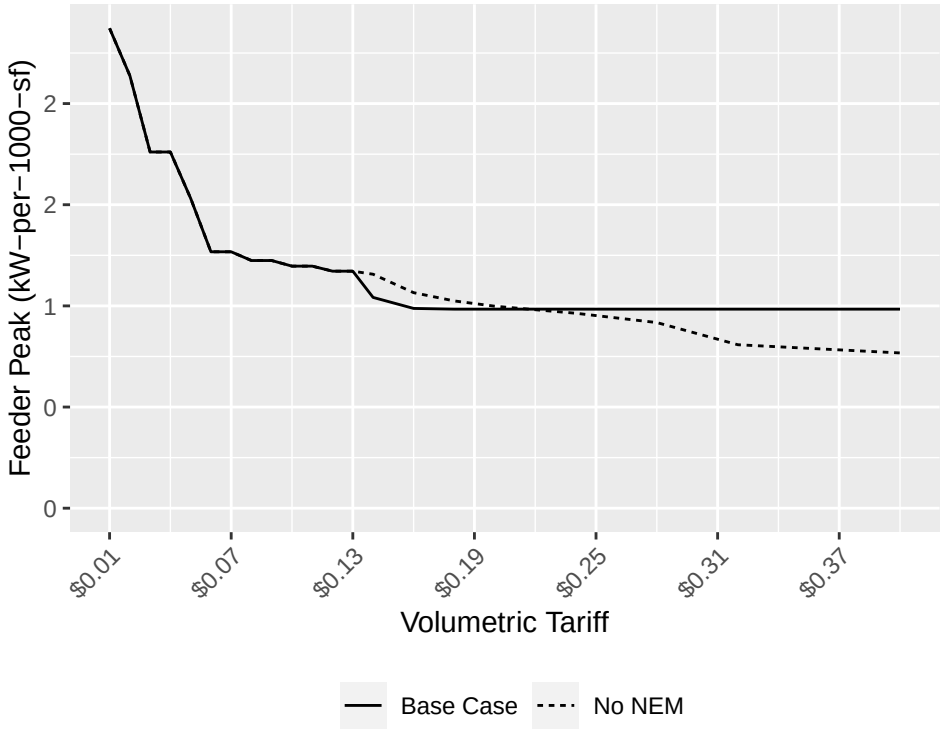

Figure 5.22: Peak load vs. the volumetric tariff in the hot-dry climate, with and without net metering. Removing the net metering policy results in a modest reduction in the feeder peak for higher tariffs relative to the base case.

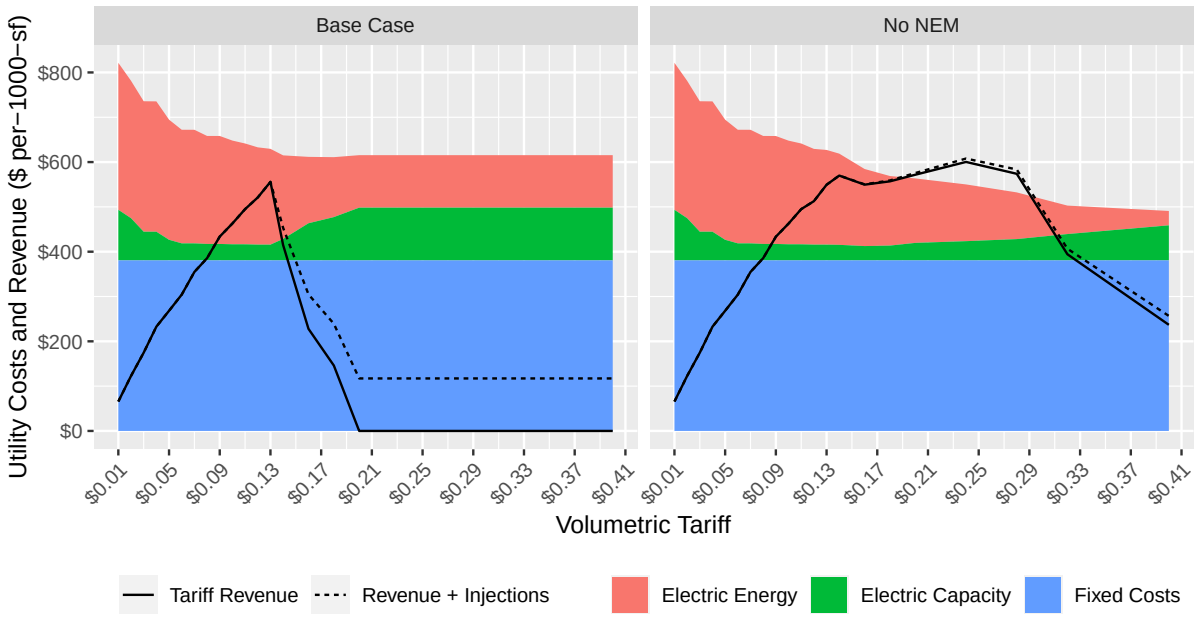

Figure 5.23: Total revenue collected from customers through the volumetric tariff (black line) and total cost of serving customers (colored areas) for the hot-dry climate in the base case and "No NEM" scenario. In the "No NEM" case, the black line rises above the colored region, indicating that there is a range of volumetric tariffs under which the utility is able to recover its full expenses. This does not hold in the base case. The financial value of the energy received from solar injections (assuming it displaces generation elsewhere) is represented by the difference between the dashed line and the solid line.

adopt solar panels. This adoption is a form of "inefficient bypass": it reduces an individual customer's expenses but increases the total cost of energy services on the feeder. As the tariff continues to increase above $0.20 per-kWh, there is no additional behavioral change because every customer has adopted enough solar capacity to reduce their net consumption of grid-supplied power to zero. At this point, all expenses associating with maintaining the utility's infrastructure (which is still necessary for serving load during most hours of the day) would need to be recovered by means other than a volumetric tariff, such as through a monthly customer charge.

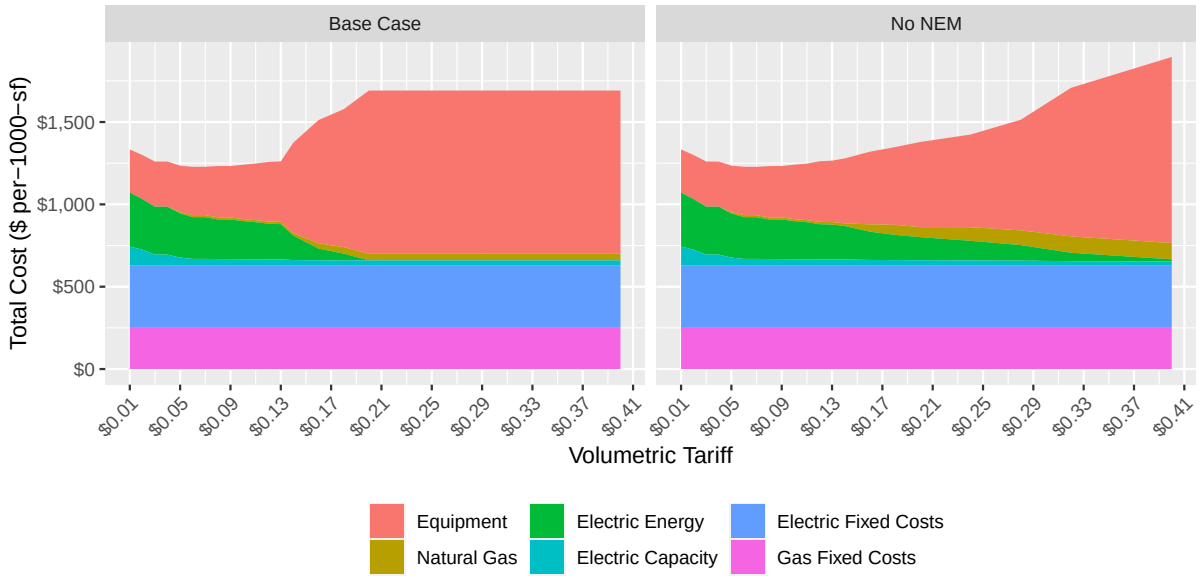

Figure 5.24: Total cost of energy services vs. the volumetric tariff for the base case and "No NEM" scenarios. For the base case (which has full net-metering) the cost of energy services increases with the volumetric tariff until the tariff reaches $0.20 per-kWh, at which point every customer has a net generation of zero. For the "No NEM" scenario, wherein customers are only compensated at a rate of $0.05 per-kWh for electricity injected to the grid, the total cost of energy services is lower for tariffs less than $0.30 per-kWh but higher for tariffs greater than $0.30 per-kWh, as customers are incentivized to store excess solar generation using batteries.

The right plot shows the total cost of energy services for the scenarios that eliminate net-metering. For volumetric tariffs less than $0.30 per-kWh, eliminating net-metering reduces the total cost of energy services by discouraging customers from adopting solar panels as a form of inefficient bypass. Nonetheless, as the volumetric tariff increases in either scenario, customers continue to adopt more and more solar capacity, increasing the total cost of energy services.

Notably, for tariffs above roughly $0.30 per-kWh, the total cost of energy services is actually higher in the "No NEM" scenario than in the base case. This result is not immediately intuitive: if the inefficiency in the system is caused by mispricing of energy services, then correcting this pricing (even if only for injections) should reduce costs.

This surprising result can be better understood when we disaggregate the equipment costs into separate categories. In Figure 5.25, we plot the equipment cost vs. the tariff for the base and "No NEM" scenarios. Here we see that the as the volumetric tariff rises above $0.23 per-kWh, customers begin adopting distributed storage in order to bank the excess electricity they generate behind the meter. As the volumetric tariff rises above $0.30 per-kWh the aggregate cost of equipment, including solar panels and storage, exceeds the equipment cost in the base case.

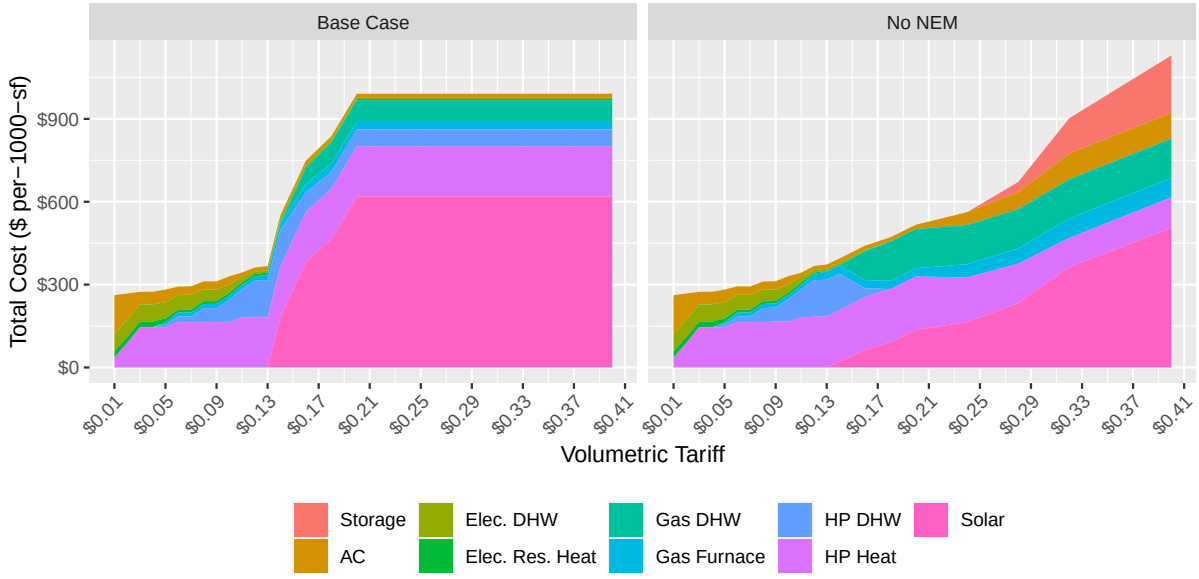

Figure 5.25: Equipment cost vs. volumetric tariff for the "Base Case" and "No NEM" scenarios. As the volumetric tariff rises above $0.23 per-kWh for the "No NEM" case, customers begin adopting distributed battery storage in order to store excess electricity generated by solar panels. This leads to a higher total cost of energy services as the tariff increases past $0.30 per-kWh.

In this example, NEM reform can be said to close a door while opening a window. Even though it is effective in discouraging customers from inefficiently adopting rooftop solar and can help utilities recover their expenses through a simple volumetric tariff, it also creates an arbitrage opportunity for customers that is not grounded in substantive variations in the cost of energy.

This leads customers to inefficiently adopt large amounts of solar and storage that ultimately increase costs.

5.4.3.2 Demand Charges

"Demand charges" are a cost-recovery mechanism used by utilities wherein a portion of a customer's bill is computed based on their peak power demand (in kW) over a billing period. While there are several different ways to implement demand charges, they generally encourage customers to keep their consumption as flat as possible. Demand charges are typically reserved for commercial and industrial customers, but there has been movement to implement them for certain classes of residential customers (Hledik, 2014).

To study the impact that demand charges are likely to have on the behavior of residential customers, we implement a separate version of the model wherein customers are faced with a monthly demand charge ranging from \$1 per-kW to \$20 per-kW. This demand charge is assessed based on each individual customer's peak hourly consumption during the month (some other designs for demand charges bill customers based on their peak consumption during a specific time interval). Additionally, customers pay a volumetric energy charge of \$0.05 per-kWh on every unit of electricity consumed, which is reflective of the assumed SMC.

In Figure 5.26, we plot the coincident feeder peak for each climate regions vs. the demand charge in two months: February and August. As the demand charge is increased, customers are incentivized to decrease their peak consumption. Insofar as these peaks are correlated (as heating and cooling peaks in a given location often are), this behavior reduces the total coincident peak reported on the y-axis. The functional relationship between the feeder peak and the demand charge is seen most prominently in the cold climate in February. As the demand charge is increased, customers shift their heating loads from heat pumps to gas furnaces in order to reduce their individual expenses.

In Figure 5.27 we plot the electric utility's costs and revenues vs. the demand charge. In general, the utility's costs decrease as the demand charge is increased because customers are discouraged from operating peaky loads that drive capacity costs. As the demand charge is

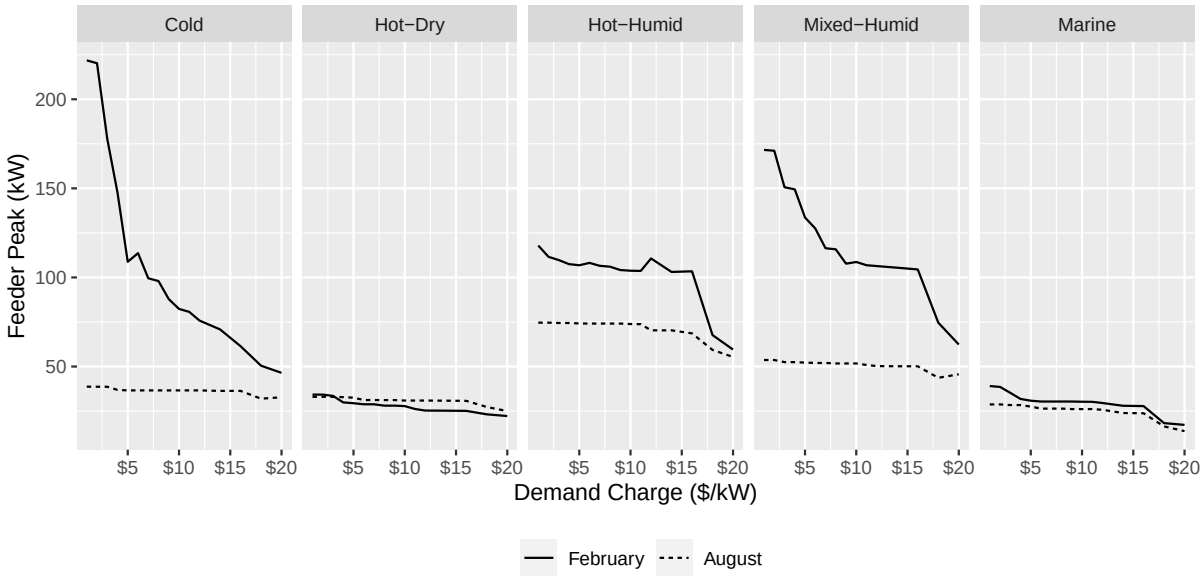

Figure 5.26: Peak February and August loads vs. the demand charge in all five climate regions. As the demand charge is increased, customers are incentivized to decrease their peak consumption, reducing the feeder peak. This is seen most prominently in the cold climate in February.

increased from \$1 to \$16 per-kW, utility revenue increases. For tariffs above \$16 per-kW, the utility's revenue drops off precipitously. Notably, in three out of the five climates, the utility's revenue from demand charges (plus the \$0.05 per-kWh energy charge) never exceeds the utility's costs. In these circumstances, the utility would need to increase either the volumetric tariff or add some other cost recovery mechanism in order to fulfill its revenue requirement.

Figures 5.28 and 5.29 plot the total cost of energy services and the equipment cost vs. the demand charge, respectively. For the cold and mixed-humid climates, increasing the demand charge from \$1 to \$16 reduces the total cost of energy services. For the other three climates, the total cost of energy services either remains constant or slightly increases as the demand charge is increased. In all five climates, as the demand charge is increased above \$16 per-kW, customers adopt large amounts of storage in order to reduce their peaks. While this behavior does indeed result in modest reductions in electric capacity costs (light blue in Figure 5.28), these savings are far outweighed by additional equipment costs.

These results indicate that while demand charges may be effective at sending an economic

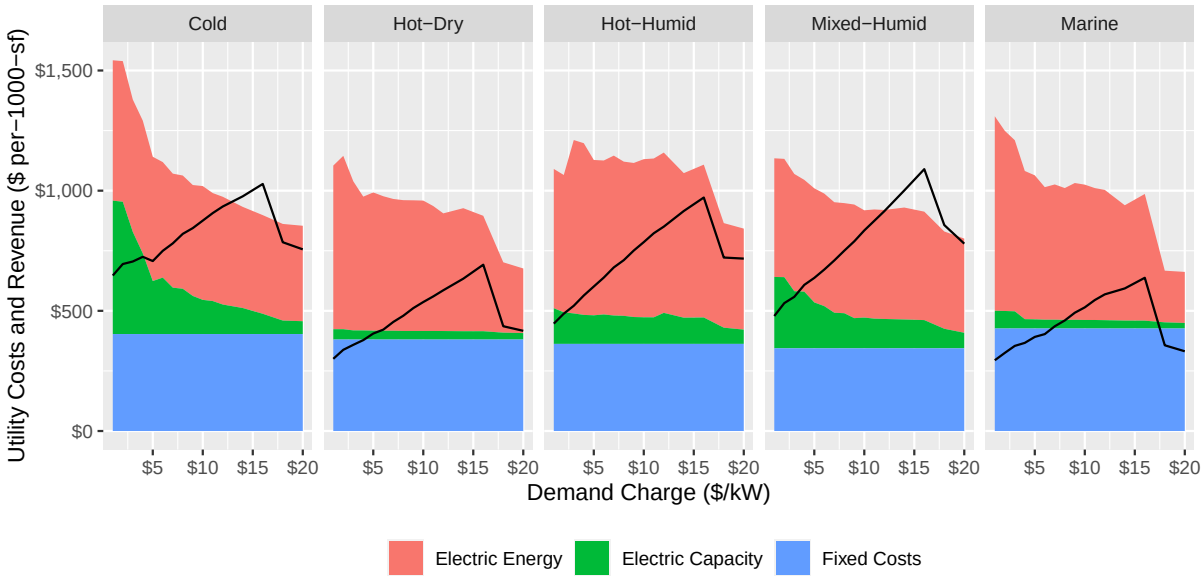

Figure 5.27: Electric utility's costs and revenues vs. the demand charge. The utility's costs decrease as the demand charge is increased because customers are discouraged from operating peaky loads that drive capacity costs. As the demand charge is increased from $1 to $16 per-kW, utility revenue increases; for tariffs above $16 per-kW, the utility's revenue drops off precipitously due to adoption of battery storage.

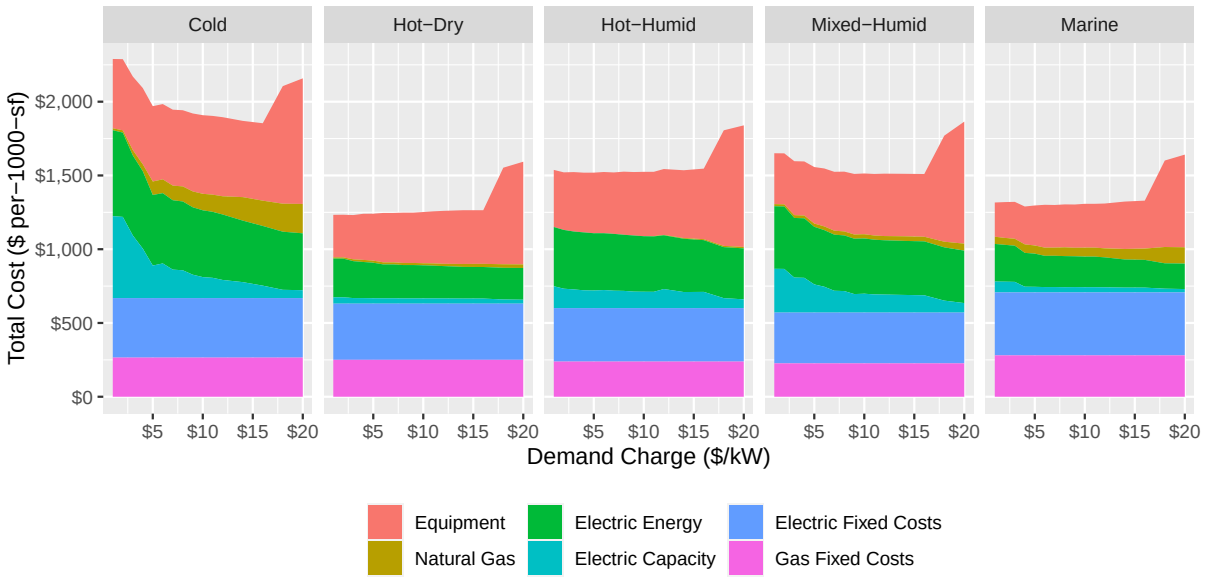

Figure 5.28: Total cost of energy services vs. the demand charge. For the cold and mixed-humid climates, increasing the demand charge from $1 to $16 reduces the total cost of energy services. For the other three climates, the total cost of energy services either remains constant or slightly increases as the demand charge is increased.

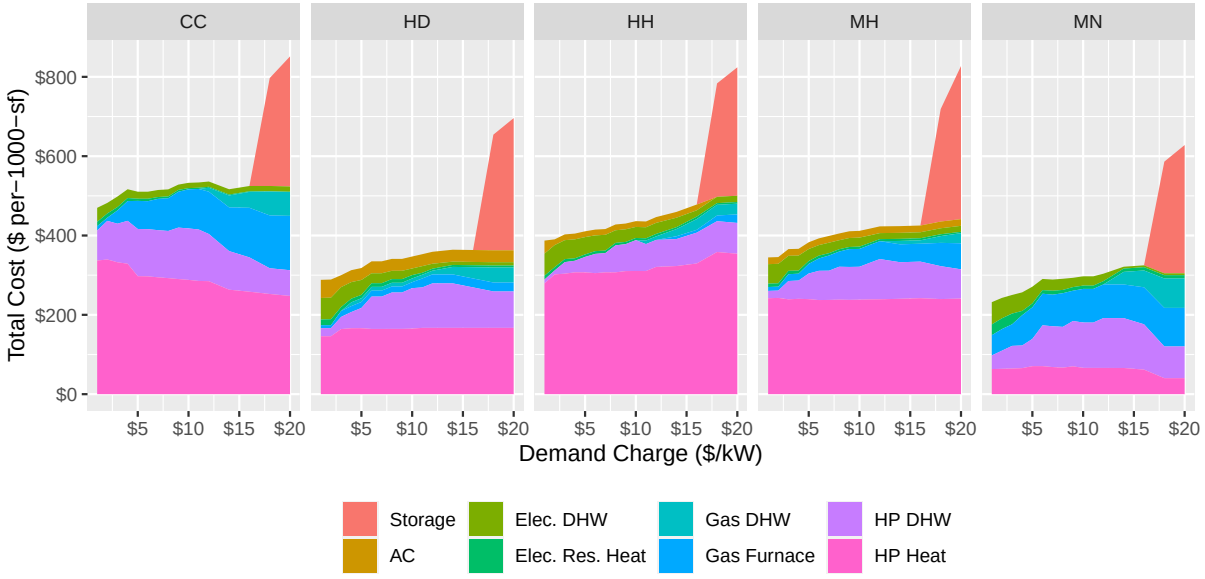

Figure 5.29: Equipment cost vs. the demand charge. Equipment costs increase gradually as the demand charge is increased from $1 to $16 because customers adopt higher-efficiency equipment and gas furnaces to reduce their peaks. As the demand charge is increased above $16, they also adopt large amounts of battery storage in order to reduce their payments.

signal that volumetric tariffs alone do not send (that is, that electricity peaks are a substantial cost-driver and ought to be mitigated), they need to be properly-tuned to be effective. If demand charges are set too low or too high, they could promote inefficient adoption and operation of heat pumps or battery storage.

Figure 5.30 plots the total emissions from electricity and natural gas against the demand charge for all five climate regions. While increasing the demand charge incentivizes customers to shift their loads from electricity to gas (thus shifting the relative contribution of emissions from each), the total emissions are relatively static. We note that these results are particular to the specific assumptions about emissions coefficients built in to our modeling (that is, that the electric grid has a constant emissions factor of 0.953lb per-kWh). If we assumed lower grid emissions due to renewables adoption or greater volatility of grid emissions, the results may look different.

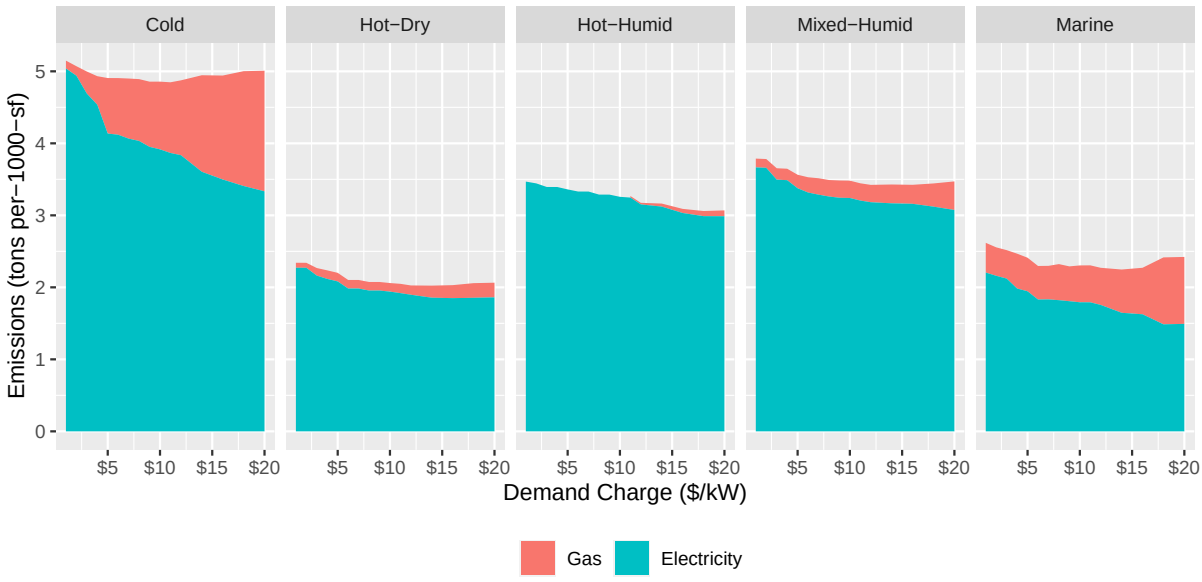

Figure 5.30: Total emissions from electricity and natural gas vs. the demand charge for all five climate regions. While increasing the demand charge incentivizes customers to shift their loads from electricity to gas, the total emissions are relatively static.

Another notable issue with demand charges is that because they are assessed every month, they encourage customers to curtail their consumption even in off-peak seasons. This is illustrated

in Figure 5.31. As the demand charge is increased, customers reduce their loads year-round, not just during the peak season. Load reduction in the off-peak season does little to reduce generation or distribution capacity costs.

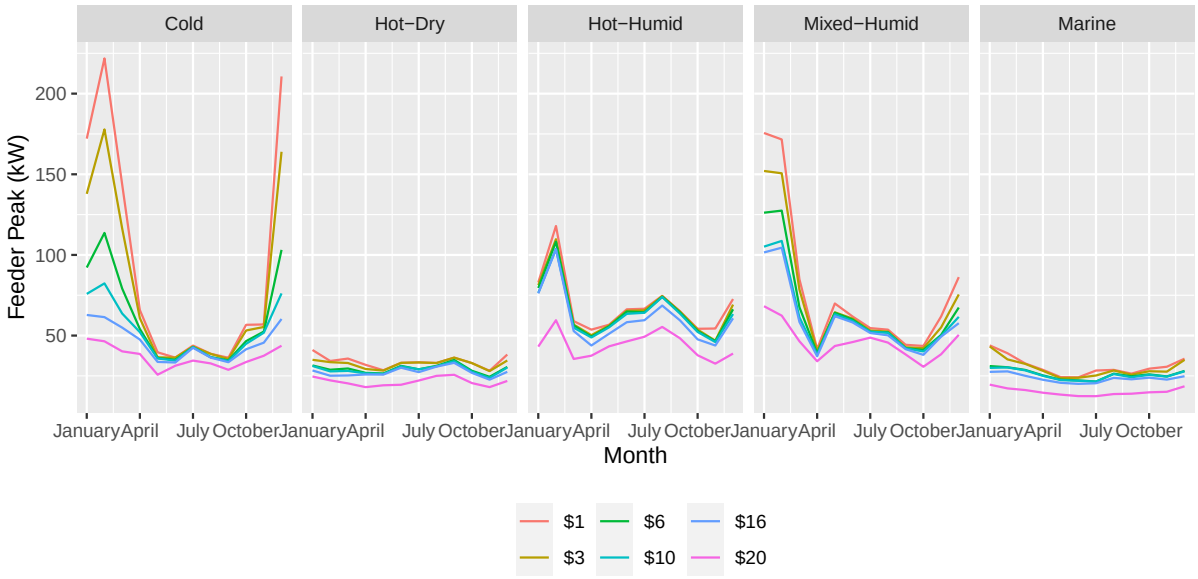

Figure 5.31: Feeder peaks throughout each month of the year in all five regions for the demand charge scenarios. The color of the line represents the demand charge. As the demand charge is increased, customers reduce their loads year-round, not just during the peak season. Load reduction in the off-peak season does little to reduce generation or distribution capacity costs.

5.4.3.3 Historical Prices

In this chapter we evaluated the utility's costs by assuming constant SMCs for electricity and gas ($0.05 per-kWh and $6.307 per-MMBTU, respectively), and the same cost coefficient for generation capacity in all five climate regions ($30 per-kW). This allowed us to focus on how the variability in energy demands between climate regions affected the efficiency of different tariff designs, while holding the parameters of the energy market constant.

To better understand how this choice has affected our results, we augment the "utility cost" and "total cost of energy services" functions plotted in Figures 5.14 and 5.17 with estimates using the region-specific historical electricity and generation capacity price data presented in Section 4.3. Additionally, we modify the hourly electricity pricing data by keeping the mean

constant and increasing the standard deviation by a factor of two. This allows us to evaluate the extent to which the results hold in a more volatile electricity market with a higher dispersion of hourly prices (as might be expected in a future with greater penetration of renewables). The distribution of hourly prices for these two scenarios is plotted in Figure 5.32. We note that in all cases, the median electricity price is somewhat lower than the $0.05 per-kWh used throughout this chapter, but that the distributions have long tails.

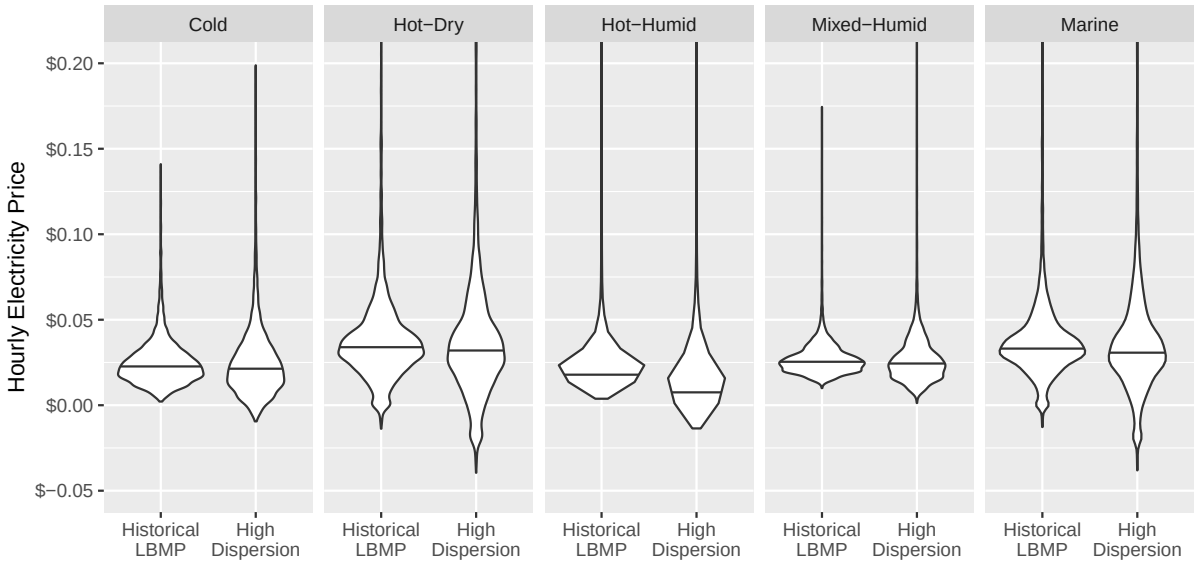

Figure 5.32: Distribution of electricity prices in the historical data and the "High Dispersion" scenario. The black line in each violin plot is the median price. Note that the area of the plot is cropped to exclude outliers.

In Figure 5.33, we report the utility's costs for each feeder vs. the tariff. As in Figure 5.14, the blue area describes fixed electric transmission, distribution, and administrative expenses that occur upstream of the feeder and are not impacted by customer behavior, but are allocated to these residential customers; the green area is the cost of capacity, including both generation capacity costs and the annualized cost of any additional feeder capacity required to meet peak loads; and the red region is the cost of electricity. The solid and dashed black lines (which predominantly overlap) describe the utility's total cost evaluated using the historical price data from Section 4.3 and the modified "High Dispersion" data described above.

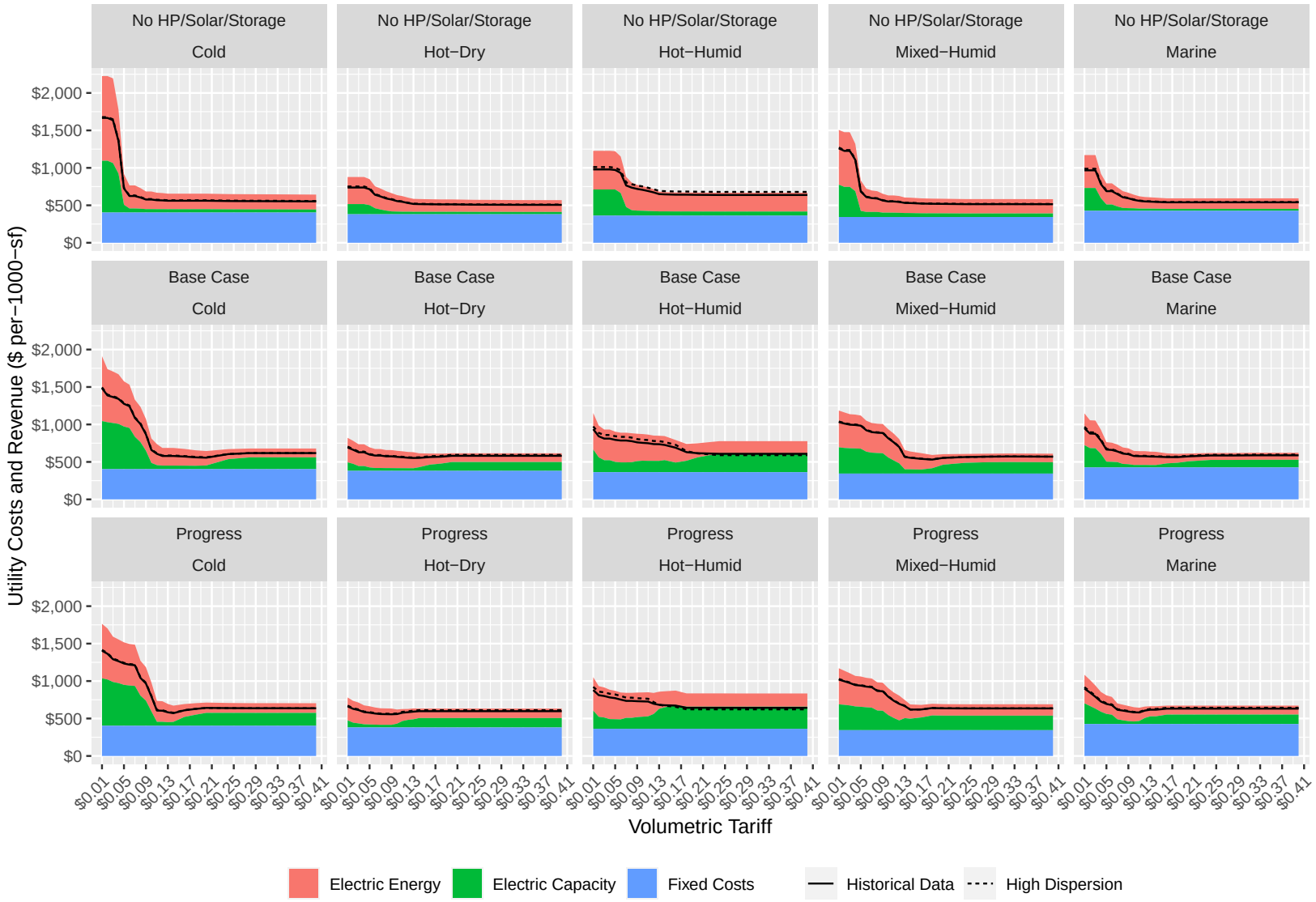

Figure 5.33: Total cost of serving customers (colored areas). The solid and dashed black lines describe the utility's total cost evaluated using the historical price data from Section 4.3 and the modified "High Dispersion" data described above.

We see that the use of region-specific historical energy cost data rather than constant energy and capacity cost assumptions modestly decreases the evaluated utility's costs in all five regions, but does not change the overall shape of the utility cost plots. Additionally, the same costs evaluated using the "High Dispersion" data nearly perfectly overlap the historical data costs, indicating that the demand for electricity on the feeder is not correlated with the wholesale market price. Together, these results indicate that our choice to hold the SMC and generation capacity costs constant most likely did not bias the results of the analysis presented earlier in this chapter.

Likewise, in Figure 5.34, we produce a modified version of Figure 5.17. As before, the stacked colored region plots the total cost of providing energy services to the 15 customers (per-1000-sf) vs. the volumetric tariff using the data from 5.2. The solid and dashed lines plot is the total cost evaluated using the historical energy and capacity cost assumptions from Section 4.3 and the "High-Dispersion" data described above.

As one would expect, the particular assumptions about energy and capacity costs do effect the total evaluated costs, but only have a modest impact on the overall shape of these curves. The general observation that costs can be minimized by setting the volumetric tariff in a "goldilocks zone" (high enough to encourage efficient use of electricity for space and water heating but not so high that it encourages load attrition through solar) still holds.

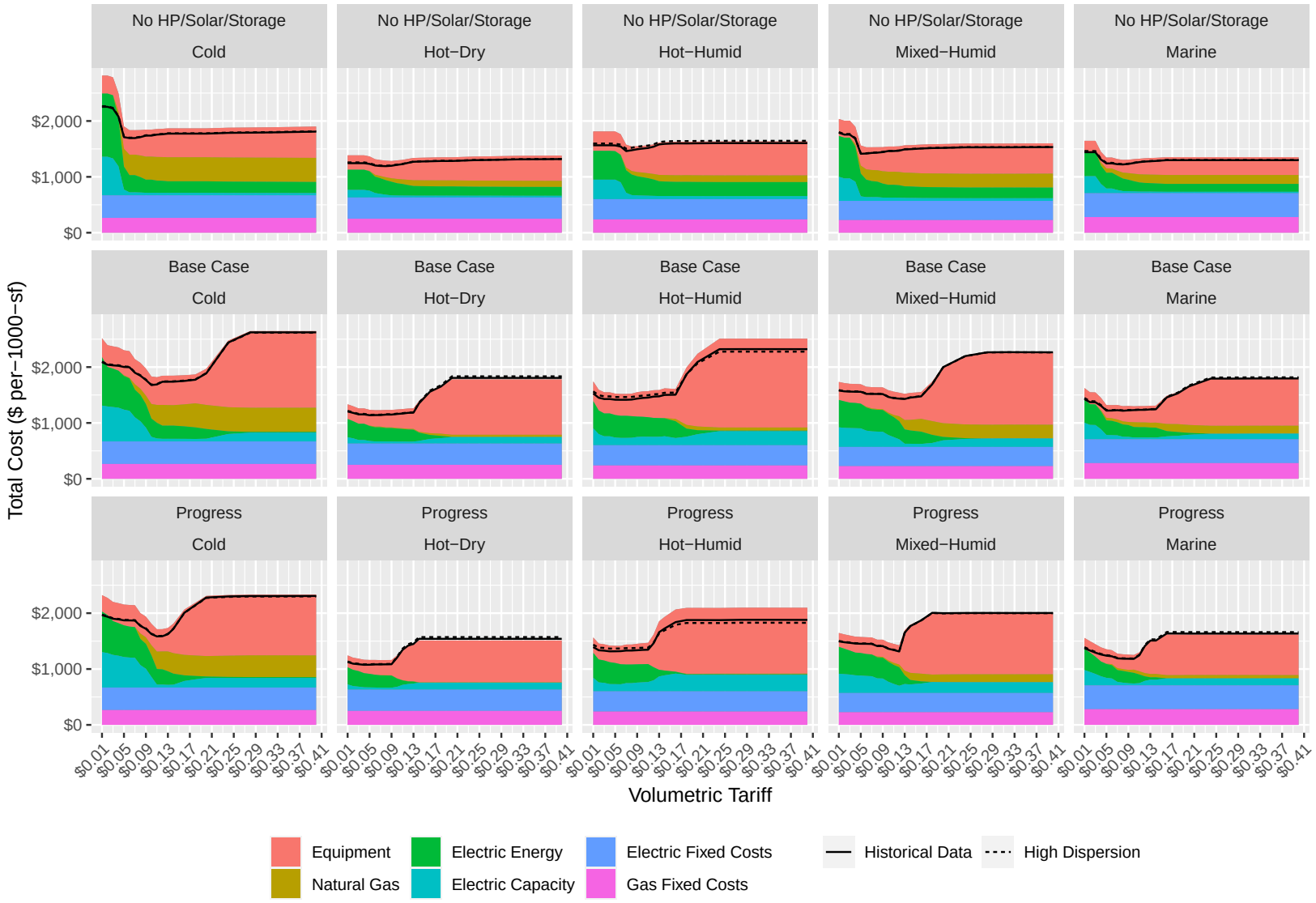

Figure 5.34: Total cost of energy services, using historical SMC and generation capacity cost data. The pale gray "shadow" behind the colored area plot is the total utility cost evaluated using the assumptions in Section B5.2. The use of historical energy and capacity cost data, rather than assuming constant prices, has only a modest effect on the estimated cost of energy services.

5.5 Role of Subsidies

In Section 5.4.2, we found that keeping volumetric retail electricity tariffs close to the cost of energy could reduce the total cost of energy services, particularly in the presence of emerging technologies such as heat pumps, distributed rooftop solar, and battery storage. We also noted that doing so would result in significant residual costs that would have to be recovered by some other means, such as a monthly customer charge that could have a regressive impact on some low-income customers.

As early as the 1930s, economists such as Hotelling (1938) proposed using public subsidies to recover the fixed costs of businesses such as utilities so that prices for services could be set efficiently. This proposed strategy fell out of favor with economists by the 1950s (Frischmann & Hogendorn, 2015).

According to (R. Fares, 2021), the 191 major utilities included in their analysis spent a combined $84.5 billion in 2019 on transmission and distribution expenses and another $50.7 billion on administration. These utilities sold 2.6 billion megawatt hours of electricity that year, approximately 68% of total electricity sales that year.

Extrapolating from these data (and assuming that the small utilities not included in the dataset have similar per-MWh expenses to the large regulated utilities), we can estimate that recovering transmission, distribution, and administrative expenses for all utilities through a public subsidy would cost approximately $(\$84.5 + \$50.7) * \frac{1}{0.68} = \$200$ billion each year. This estimate serves as an upper bound of the residual fixed costs, as some amount of these costs could be recovered from customers through forward-looking capacity charges and externality pricing.

While using tax revenue to recover fixed transmission, distribution, and administrative costs may be politically untenable for a wide variety of reasons, there is still substantial room for policy interventions to lift some of the cost recovery burden from electric utilities. Many state governments fund an array of public programs through excise taxes on electricity sales. (Borenstein, Fowlie, & Sallee, 2021) estimated that for non-subsidized customers served by

California's three major utilities, these taxes raised the volumetric price of electricity by 1.26 cents-per-kWh to 1.77 cents-per-kWh. Shifting these programs to the state budget[16] – and thus lowering volumetric tariffs – could be a meaningful step toward incentivizing more efficient use of the electricity system.

5.6 Conclusion

In this chapter, we modeled residential customers' responses to different volumetric electricity tariffs. We found that in the presence of emerging technologies (including heat pumps, solar panels, and battery storage) volumetric tariffs that are set significantly above the social marginal cost of energy can cause customers to make inefficient investments that increase the total cost of grid services. Relative to an optimized feeder, the use of a volumetric tariff that is calibrated to recover a utility's full revenue requirement increases the total cost of energy services by 5–25%.

In the progress scenario – which assumes a 70% cleaner grid and a 30% reduction in the cost of heat pumps, air conditioners, solar panels, and battery storage – raising tariffs high enough to recover a utility's full revenue requirement causes a near-doubling of emissions in the cold climate as customers are discouraged from adopting heat pumps, instead relying on natural gas furnaces. In the hot-dry and marine climates, the availability of rooftop solar panels and battery storage make it impossible for utilities to recover their full revenue requirement through volumetric tariffs because customers' load defection exceeds additional revenue from the increased tariff.

We found that a policy that replaces net-metering with a $0.05 per-kWh feed-in tariff can effectively discourage uneconomic adoption of rooftop solar photovoltaic panels when the volumetric tariff is set at prices in the range of $0.13 to $0.30 per-kWh. This reduces the total cost of energy services relative to a full-net metering policy. However, for tariffs set above $0.30 per-kWh, the asymmetry between the volumetric consumption tariff and the feed-in tariff actually leads to higher system costs, as customers augment their uneconomic photovoltaic investments with uneconomic battery storage investments.

[16]The government of Ontario recently shifted its renewables subsidies from the "Global Adjustment Charge," which is recovered from utility bills, to the general tax base.

Chapter 6

Conclusion and Future Work

In this thesis, we described the potential for emerging customer-side technologies to reduce the cost of residential energy services and analyzed how to adapt residential electric tariffs to incentivize more efficient technology adoption. In these final paragraphs, we discuss a number of outstanding questions that should be addressed in future work.

Most urgently, we need to develop a better understanding of the efficiency implications of using cost recovery mechanisms other than volumetric pricing and demand charges, such as time-of-use rates and real-time pricing. These tariff structures can provide more accurate price signals, but may be too complicated for many customers to accept. One potentially valuable lane of research would be to determine how internet-of-things (IoT) enabled devices could respond to price signals from a utility without the need for direct customer involvement.

A major constraint of the model used in Chapters 4 and 5 (and a limitation to using it to study hyper-accurate tariffs like real-time pricing) is that it presumes that there is a predetermined electricity price that is independent of the activities taking place on the feeder. We know that the electricity price is a function of both supply and demand, so a more accurate model would determine the price endogenously. One approach would be to include a generation module that allows for wholesale electricity prices to respond to load. A dynamic wholesale generation model would also allow us to interrogate what kinds of generation are promoted (or discouraged) by

the adoption of various demand-side technologies

Additionally, further work should test the efficacy of other policies, such as rebates for certain equipment and equipment mandates (such as requiring all new air conditioners to be sold with heat pump functionality). The approach outlined in Chapter 5 could readily be adapted to forecast how cost-minimizing customers would respond to such incentives and policies.

In our analysis of tariffs, we hold retail natural gas prices constant while modifying electricity rates. However, there is also reasonable uncertainty in the future retail price of natural gas. If consumption of natural gas falls as customers adopt electric space and water heating options, gas utilities will need to increase their rates to recover their considerable fixed costs. This will no doubt further discourage customers form consuming natural gas, which could cause a utility death spiral. Further work should analyze these dynamics between electricity tariffs, gas tariffs, and customer incentives for equipment adoption and use.

Our results indicate that there may be some benefit in "pruning" the natural gas distribution system in regions where fully-electrified heating is cost-competitive with natural gas heating. Further work is needed to understand how retiring portions of the natural gas distribution system would impact costs. Additionally, in colder climates that benefit from some form of hybrid or dual-fuel heating, it would be worth exploring heating topologies that pair a heat pump with a liquid fuel such as fuel oil or kerosene (or a green alternative to one of these). This would obviate the need to maintain the natural gas distribution system, which may become redundant in the future if heat pumps become significantly more popular.

Bibliography

Abdelmotteleb, I., Gómez, T., Chaves Ávila, J. P., & Reneses, J. (2018). Designing efficient distribution network charges in the context of active customers. *Applied Energy*, *210*, 815–826. Retrieved August 29, 2019, from Link
existing network (2.5 MW) costs 657,000 per year lumpy network reinforcement costs 20% of existing costs for load growth up to 20%

Administration, U. E. I. (2022). Use of energy in homes - U.S. Energy Information Administration (EIA). Retrieved July 22, 2022, from Link

Allcott, H., & Greenstone, M. (2012). Is There an Energy Efficiency Gap, 39.

Baruah, P. J., Eyre, N., Qadrdan, M., Chaudry, M., Blainey, S., Hall, J. W., Jenkins, N., & Tran, M. (2014). Energy system impacts from heat and transport electrification. *Proceedings of the Institution of Civil Engineers-Energy*, *167*(3). Retrieved December 10, 2019, from Link

Baughman, M., & Bottaro, D. (1976). Electric power transmission and distribution systems: Costs and their allocation. *IEEE Transactions on Power Apparatus and Systems*, *95*(3), 782–790. Retrieved November 26, 2019, from Link

Beck, T., Kondziella, H., Huard, G., & Bruckner, T. (2017). Optimal operation, configuration and sizing of generation and storage technologies for residential heat pump systems in the spotlight of self-consumption of photovoltaic electricity. *Applied Energy*, *188*, 604–619. Retrieved May 19, 2021, from Link

Biggar, D. R., & Hesamzadeh, M. (2014). *The Economics of Electricity Markets*. Wiley.

Borenstein, S. (2005). The Long-Run Efficiency of Real-Time Electricity Pricing. *The Energy Journal*, 24. Link

Borenstein, S. (2016). The economics of fixed cost recovery by utilities. *The Electricity Journal*, *29*(7), 5–12. Retrieved August 29, 2019, from Link

Borenstein, S. (2017). Private Net Benefits of Residential Solar PV: The Role of Electricity Tariffs, Tax Incentives, and Rebates. *Journal of the Association of Environmental and Resource Economists*, *4*(S1), S85–S122. Retrieved May 20, 2021, from Link

Borenstein, S., & Bushnell, J. B. (2021). *Headwinds and Tailwinds: Implications of Inefficient Retail Energy Pricing for Energy Substitution* (tech. rep.). National Bureau of Economic Research. Link

Borenstein, S., & Bushnell, J. B. (Forthcoming). Do Two Electricity Pricing Wrongs Make a Right? Cost Recovery, Externalities, and Efficiency. *American Economic Journal: Economic Policy*. Retrieved August 30, 2022, from Link

Borenstein, S., Fowlie, M., & Sallee, J. (2021). *Designing Electricity Rates for an Equitable Energy Transition* (tech. rep.). Energy Institute at Haas. Link

Burger, S., Schneider, I., Botterud, A., & Pérez-Arriaga, I. (2019). Fair, Equitable, and Efficient Tariffs in the Presence of Distributed Energy Resources. *Consumer, Prosumer, Prosumager* (pp. 155–188). Elsevier. Retrieved December 2, 2019, from Link

Burger, S. P., Knittel, C. R., Perez-Arriaga, I. J., Schneider, I., & Scheidt, F. v. (2020). The Efficiency and Distributional Effects of Alternative Residential Electricity Rate Designs. *The Energy Journal*, *Volume 41*(1). Link

California ISO. (2021). OASIS. Retrieved July 1, 2021, from Link

Callaway, D. S., & Hiskens, I. A. (2011). Achieving Controllability of Electric Loads. *Proceedings of the IEEE*, *99*(1), 184–199. Retrieved August 29, 2019, from Link

Carleton, T., & Greenstone, M. (2021). Updating the United States Government's Social Cost of Carbon. *SSRN Electronic Journal*. Retrieved February 25, 2022, from Link

Central Hudson Gas & Electric Corporation. (2017). Electric Infrastructure and Operations Panel Exhibits. Retrieved June 17, 2019, from Link

Cohen, M. A., Kauzmann, P. A., & Callaway, D. S. (2016). Effects of distributed PV generation on California's distribution system, part 2: Economic analysis. *Solar Energy*, *128*, 139–152. Retrieved December 1, 2019, from Link

Cohen, S., Becker, J., Bielen, D., Brown, M., Cole, W., Eurek, K., Frazier, W., Frew, B., Gagnon, P., Ho, J., Jadun, P., Mai, T., Mowers, M., Murphy, C., Reimers, A., Richards, J., Ryan, N., Spyrou, E., Steinberg, D., … Zwerling, M. (2019). Regional Energy Deployment System (ReEDS) Model Documentation: Version 2018. *Renewable Energy*, 135. Link

Cole, W., & Frazier, A. (2020). *Cost Projections for Utility-Scale Battery Storage: 2020 Update* (tech. rep. NREL/TP-6A20-75385, 1665769, MainId:6883). Retrieved December 15, 2020, from Link

Davis, L. W. (2017). Evidence of a Decline in Electricity Use by U.S. Households, 17. Link

Demand Side Analytics. (2018). 2018 Central Hudson Location Specific Transmission and Distribution Avoided Costs Using Probabilistic Forecasting and Planning Methods. Link

Department of Homeland Security. (2019). Electric Retail Service Territories. Retrieved December 2, 2019, from Link

Deryugina, T., MacKay, A., & Reif, J. (2020). The Long-Run Dynamics of Electricity Demand: Evidence from Municipal Aggregation. *American Economic Journal: Applied Economics*, *12*(1), 86–114. Retrieved August 31, 2022, from Link

Electric Power Research Institute. (2018a). U.S. National Electrification Assessment, 64. Link

Electric Power Research Institute. (2018b). US-REGEN Model Documentation. Link

Elmallah, S., Brockway, A. M., & Callaway, D. (2022). Can distribution grid infrastructure accommodate residential electrification and electric vehicle adoption in Northern California?, 65.

Energy Information Administration. (2017). Per capita residential electricity sales in the U.S. have fallen since 2010. Retrieved January 16, 2020, from Link

Energy Information Administration. (2019a). Annual Electric Power Industry Report, Form EIA-861 detailed data files. Retrieved June 7, 2021, from Link

Energy Information Administration. (2019b). *Assumptions to the Annual Energy Outlook 2019: Electricity Market Module* (tech. rep.). Link

Energy Information Administration. (2019c). Availability of the National Energy Modeling System (NEMS) Archive. Retrieved December 30, 2019, from Link

Energy Information Administration. (2019d). Electricity Data. Retrieved December 13, 2019, from Link

Energy Information Administration. (2020). EIA expects U.S. electricity generation from renewables to soon surpass nuclear and coal - Today in Energy. Retrieved May 12, 2020, from Link

Energy Information Administration. (2021). Use of energy in homes. Retrieved March 2, 2022, from Link

Energy Information Administration. (2022). Electric Power Monthly with data for June 2022, 286. Link

Environmental Protection Agency. (2020). *eGRID2018 Summary Tables* (tech. rep.). Link

ERCOT. (2021). Market Information. Retrieved November 24, 2021, from Link

Evins, R. (2015). Multi-level optimization of building design, energy system sizing and operation. *Energy*, *90*, 1775–1789. Retrieved May 19, 2021, from Link

Fabra, N., Rapson, D., Reguant, M., & Wang, J. (2021). Estimating the Elasticity to Real-Time Pricing: Evidence from the Spanish Electricity Market. *AEA Papers and Proceedings*, *111*, 425–429. Retrieved August 29, 2022, from Link

Fares, R. (2021). FERC Form 1 Electric Utility Cost, Energy Sales, Peak Demand, and Customer Count Data 1994-2019 (C. King, Ed.). Link

Fares, R. L., & King, C. W. (2017). Trends in transmission, distribution, and administration costs for U.S. investor-owned electric utilities. *Energy Policy*, *105*, 354–362. Retrieved October 17, 2019, from Link

Faruqui, A., & Leyshon, K. (2017). Fixed charges in electric rate design: A survey. *The Electricity Journal*, *30*(10), 32–43. Retrieved August 29, 2019, from Link

Faruqui, A., & Wood, L. (2008). *Quantifying the Benefits of Dynamic Pricing in the Mass Market* (tech. rep.). Edison Electric Institute.

Federal Energy Regulatory Commission. (2009). Form 1 - Electric Utility Annual Report. Retrieved December 2, 2019, from Link

Fenrick, S. A., & Getachew, L. (2012). Cost and reliability comparisons of underground and overhead power lines. *Utilities Policy*, *20*(1), 31–37. Retrieved February 17, 2020, from Link

Filippini, M., Hrovatin, N., & Zorič, J. (2004). Efficiency and regulation of the Slovenian electricity distribution companies. *Energy Policy*, *32*(3), 335–344. Retrieved April 17, 2020, from Link

Filippini, M., & Wild, J. (2001). Regional differences in electricity distribution costs and their consequences for yardstick regulation of access prices. *Energy Economics*, *23*(4), 477–488. Retrieved April 17, 2020, from Link

Fowlie, M., & Callaway, D. (2021). Distribution Costs and Distributed Generation. Retrieved August 3, 2021, from Link

Fowlie, M., Greenstone, M., & Wolfram, C. (2018). Do Energy Efficiency Investments Deliver? Evidence from the Weatherization Assistance Program*. *The Quarterly Journal of Economics*, *133*(3), 1597–1644. Retrieved March 8, 2022, from Link

Frischmann, B. M., & Hogendorn, C. (2015). Retrospectives: The Marginal Cost Controversy. *The Journal of Economic Perspectives*, *29*(1), 193–205. Retrieved July 22, 2021, from Link

Fu, R., Feldman, D., & Margolis, R. (2018). U.S. Solar Photovoltaic System Cost Benchmark: Q1 2018. *Renewable Energy*, 63.

Gagnon, P., Margolis, R., Melius, J., Phillips, C., & Elmore, R. (2016). *Rooftop Solar Photovoltaic Technical Potential in the United States. A Detailed Assessment* (tech. rep. NREL/TP–6A20-65298, 1236153). Retrieved May 18, 2022, from Link

García-Villalobos, J., Zamora, I., San Martín, J. I., Asensio, F. J., & Aperribay, V. (2014). Plug-in electric vehicles in electric distribution networks: A review of smart charging approaches. *Renewable and Sustainable Energy Reviews*, *38*, 717–731. Retrieved June 22, 2020, from Link

Gelman, A. (2018). You need 16 times the sample size to estimate an interaction than to estimate a main effect. Retrieved January 17, 2020, from Link

Gillingham, K., Newell, R. G., & Palmer, K. (2009). Energy Efficiency Economics and Policy. *Annual Review of Resource Economics*, *1*(1), 597–620. Retrieved May 19, 2020, from Link

Goodman. (n.d.). 2.5 Ton 14 SEER Goodman Heat Pump. Retrieved April 3, 2020, from Link

Hanser, P. Q., Tsuchida, T. B., Donohoo-Vallett, P., Zhang, L., & Schoene, J. (2018). *Marginal Cost of Service Study* (tech. rep.). Consolidated Edison. Link

Heinen, S., Burke, D., & O'Malley, M. (2016). Electricity, gas, heat integration via residential hybrid heating technologies – An investment model assessment. *Energy*, *109*, 906–919. Retrieved August 29, 2019, from Link

Henze, G. P., Felsmann, C., & Knabe, G. (2004). Evaluation of optimal control for active and passive building thermal storage. *International Journal of Thermal Sciences*, *43*(2), 173–183. Retrieved August 29, 2019, from Link

Hledik, R. (2014). Rediscovering Residential Demand Charges. *The Electricity Journal*, *27*(7), 82–96. Retrieved November 11, 2020, from Link

Hoarau, Q., & Perez, Y. (2019). Network tariff design with prosumers and electromobility: Who wins, who loses? *Energy Economics*, *83*, 26–39. Retrieved June 20, 2020, from Link

Hotelling, H. (1938). The General Welfare in Relation to Problems of Taxation and of Railway and Utility Rates. *Econometrica*, *6*(3), 242–269. Retrieved March 30, 2022, from Link

HVACDirect. (2020). Heat Pump Systems. Retrieved August 3, 2020, from Link

ICF Consulting. (2005). *Avoided Energy Supply Costs in New England* (tech. rep.). Link

Interagency Working Group on Social Cost of Greenhouse Gases, United States Government. (2021). *Technical Support Document: Social Cost of Carbon, Methane,* (tech. rep.).

Jaffe, A. B., & Stavins, R. N. (1994). The energy-efficiency gap What does it mean? *Energy Policy*, *22*(10), 804–810. Retrieved May 18, 2020, from Link

Karmellos, M., & Mavrotas, G. (2019). Multi-objective optimization and comparison framework for the design of Distributed Energy Systems. *Energy Conversion and Management*, *180*, 473–495. Retrieved August 27, 2020, from Link

Kaufman, N. (2018). The Social Cost of Carbon in Taxes and Subsidies, 12.

Kopsakangas-Savolainen, M., & Svento, R. (2008). Estimation of cost-effectiveness of the Finnish electricity distribution utilities. *Energy Economics*, *30*(2), 212–229. Retrieved April 17, 2020, from Link

Larson, E., Greig, C., Jenkins, J., Mayfield, E., Pascale, A., Zhang, C., Drossman, J., Williams, R., Pacala, S., Socolow, R., Baik, E., Birdsey, R., Duke, R., Jones, R., Haley, B., Leslie, E., Paustian, K., & Swan, A. (2020). *Net-Zero America: Potential Pathways, Infrastructure, and Impacts, interim report* (tech. rep.). Princeton University. Princeton, NJ. Retrieved August 3, 2021, from Link

Lazar, J. (2016). *Electricity Regulation In the US: A Guide. Second Edition.* The Regulatory Assistance Project. Retrieved May 3, 2020, from Link

MacDonald, A. E., Clack, C. T. M., Alexander, A., Dunbar, A., Wilczak, J., & Xie, Y. (2016a). Future cost-competitive electricity systems and their impact on US CO_2 emissions. *Nature Climate Change*, *6*(5), 526–531. Retrieved September 16, 2019, from Link
68% for generation and transmission, 32% for distribution (so distribution costs scale with generation?)

MacDonald, A. E., Clack, C. T. M., Alexander, A., Dunbar, A., Wilczak, J., & Xie, Y. (2016b). Future cost-competitive electricity systems and their impact on US CO2 emissions - Supplementary Information. *Nature Climate Change*, *6*(5). Retrieved September 16, 2019, from Link
p. 23) local distribution costs not explicitly modeled, accounted for final estimated cost of electricity distribution costs independent of generation mix within power system no attempt to model sociopolitical, grid integration or other costs

Mai, T. T., Jadun, P., Logan, J. S., McMillan, C. A., Muratori, M., Steinberg, D. C., Vimmerstedt, L. J., Haley, B., Jones, R., & Nelson, B. (2018). *Electrification Futures Study: Scenarios of Electric Technology Adoption and Power Consumption for the United States* (tech. rep. NREL/TP–6A20-71500, 1459351). Retrieved March 23, 2020, from Link

Marston, A. D. (1935). Degree Days For Cooling. *Bulletin of the American Meteorological Society*, *16*(10), 242–244. Retrieved July 20, 2022, from Link

Mavromatidis, G., Orehounig, K., & Carmeliet, J. (2018). Uncertainty and global sensitivity analysis for the optimal design of distributed energy systems. *Applied Energy*, *214*, 219–238. Retrieved August 27, 2020, from Link

McKinsey & Company. (2009). *Pathways to a low-carbon economy: Version 2 of the global greenhouse gas abatement cost curve* (tech. rep.). Retrieved March 8, 2022, from Link

Mehleri, E. D., Sarimveis, H., Markatos, N. C., & Papageorgiou, L. G. (2013). Optimal design and operation of distributed energy systems: Application to Greek residential sector. *Renewable Energy*, *51*, 331–342. Retrieved August 27, 2020, from Link

NARUC. (1992). Electric Utility Cost Allocation Manual. Link

National Grid. (2020). System Data Portal. Retrieved December 11, 2020, from Link

National Oceanic and Atmospheric Administration. (2018). When average temperature misses the mark. Retrieved July 21, 2022, from Link

National Renewable Energy Lab (NREL). (2021). ResStock Analysis Tool. Retrieved January 5, 2021, from Link

National Renewable Energy Laboratory (NREL). (2022). EnergyPlus. Retrieved July 18, 2022, from Link

Navarro-Espinosa, A., & Mancarella, P. (2014). Probabilistic modeling and assessment of the impact of electric heat pumps on low voltage distribution networks. *Applied Energy*, *127*, 249–266. Retrieved August 29, 2019, from Link

Navarro-Espinosa, A., & Ochoa, L. F. (2016). Probabilistic Impact Assessment of Low Carbon Technologies in LV Distribution Systems. *IEEE Transactions on Power Systems*, *31*(3), 2192–2203. Retrieved August 29, 2019, from Link

Navigant Consulting. (2018). *Technology Forecast Updates – Residential and Commercial Building Technologies – Reference Case* (tech. rep.). Retrieved March 18, 2021, from Link

NYISO. (2021). Energy Market & Operational Data. Retrieved July 1, 2021, from Link

NYSERDA. (2019). *New Efficiency: New York - Analysis of Residential Heat Pump Potential and Economics* (tech. rep.). Link

Omu, A., Choudhary, R., & Boies, A. (2013). Distributed energy resource system optimisation using mixed integer linear programming. *Energy Policy*, *61*, 249–266. Retrieved August 27, 2020, from Link

Pacific Gas & Electric. (2018). Exhibit 017: PG&E-04: Electric Distribution - Prepared Testimony Chapters 11-19. Link

Pacific Gas & Electric. (2022). Tiered Rate Plan (E-1). Retrieved April 25, 2022, from Link

Pacific Northwest National Laboratory. (2015). Building America Best Practices Series: Volume 7.3, Guide to Determining Climate Regions by County, 50. Link

Parmesano, H. S., & Martin, C. S. (1983). The Evolution in U.S. Electric Utility Rate Design. *Annual Review of Energy*, *8*(1), 45–94. Retrieved July 20, 2021, from Link

Perez-Arriaga, I. J., Jenkins, J. D., & Batlle, C. (2017). A regulatory framework for an evolving electricity sector: Highlights of the MIT utility of the future study. *Economics of Energy & Environmental Policy*, *6*(1). Retrieved August 29, 2019, from Link

Pérez-Arriaga, I., & Knittel, C. (2016). Utility of the Future. Link

Pieltain Fernández, L., Gomez San Roman, T., Cossent, R., Mateo Domingo, C., & Frías, P. (2011). Assessment of the Impact of Plug-in Electric Vehicles on Distribution Networks. *IEEE Transactions on Power Systems*, *26*(1), 206–213. Link

Pillai, J. R., Thøgersen, P., Møller, J., & Bak-Jensen, B. (2012). Integration of Electric Vehicles in low voltage Danish distribution grids. *2012 IEEE Power and Energy Society General Meeting*, 1–8. Link

PJM. (2019). Capacity Market (RPM). Retrieved November 25, 2021, from Link

PJM. (2021). Markets & Operations. Retrieved July 1, 2021, from Link

Pudjianto, D., Djapic, P., Aunedi, M., Gan, C. K., Strbac, G., Huang, S., & Infield, D. (2013). Smart control for minimizing distribution network reinforcement cost due to electrification. *Energy Policy*, *52*, 76–84. Retrieved March 8, 2020, from Link

Rauschkolb, N., Limandibhratha, N., Modi, V., & Mercadal, I. (2021). Estimating electricity distribution costs using historical data. *Utilities Policy*, *73*, 101309. Retrieved November 1, 2021, from Link

Richardson, P., Flynn, D., & Keane, A. (2012). Optimal Charging of Electric Vehicles in Low-Voltage Distribution Systems. *IEEE Transactions on Power Systems*, *27*(1), 268–279.

Risbeck, M. J., Maravelias, C. T., Rawlings, J. B., & Turney, R. D. (2017). A mixed-integer linear programming model for real-time cost optimization of building heating, ventilation, and air conditioning equipment. *Energy and Buildings*, *142*, 220–235. Retrieved August 30, 2019, from Link

Roberts, M. J. (1986). Economies of Density and Size in the Production and Delivery of Electric Power. *Land Economics*, *62*(4), 378–387. Retrieved April 17, 2020, from Link

Rodríguez Ortega, M. P., Pérez-Arriaga, J. I., Abbad, J. R., & González, J. P. (2008). Distribution network tariffs: A closed question? *Energy Policy*, *36*(5), 1712–1725. Retrieved August 29, 2019, from Link

Sandia National Laboratories. (2018). PV Performance Modeling Collaborative | Plane of Array (POA) Irradiance. Retrieved February 3, 2021, from Link

Sani Hassan, A., Cipcigan, L., & Jenkins, N. (2017). Optimal battery storage operation for PV systems with tariff incentives. *Applied Energy*, *203*, 422–441. Retrieved September 9, 2021, from Link

Schittekatte, T., & Meeus, L. (2018). Least-cost Distribution Network Tariff Design in Theory and Practice. *The Energy Journal*, *41*(01). Retrieved June 3, 2020, from Link

Schittekatte, T., Momber, I., & Meeus, L. (2018). Future-proof tariff design: Recovering sunk grid costs in a world where consumers are pushing back. *Energy Economics*, *70*, 484–498. Retrieved August 29, 2019, from Link

Seiders, D. D., Ahluwalia, G., Melman, S., Quint, R., Chaluvadi, A., Liang, M., Silverberg, A., Bechler, C., & Jackson, J. (2007). National Association of Home Builders/ Bank of America Home Equity Study of Life Expectancy of Home Components, 19. Link

Siano, P., & Sarno, D. (2016). Assessing the benefits of residential demand response in a real time distribution energy market. *Applied Energy*, *161*, 533–551. Retrieved August 29, 2019, from Link

Southern California Edison. (2022). Tiered Rate Plan. Retrieved April 25, 2022, from Link

S&P Global. (2021). MI Office Screener | Application. Retrieved July 14, 2021, from Link

State of New York Public Service Commission. (2017). Order on Net Energy Metering Transition, Phase One of Value of Distributed Energy Resources, and Related Matters. Link

Steinberg, D., Bielen, D., Eichman, J., Eurek, K., Logan, J., Mai, T., McMillan, C., Parker, A., Vimmerstedt, L., & Wilson, E. (2017). *Electrification & Decarbonization: Exploring U.S. Energy Use and Greenhouse Gas Emissions in Scenarios with Widespread Electrification and Power Sector Decarbonization* (tech. rep.). Link

Stinner, S., Huchtemann, K., & Müller, D. (2016). Quantifying the operational flexibility of building energy systems with thermal energy storages. *Applied Energy*, *181*, 140–154. Retrieved August 29, 2019, from Link

Synapse Energy Economics. (2018). Avoided Energy Supply Components in New England: 2018 Report. Link

Urban Green Council. (2019). *Retrofit Market Analysis* (tech. rep.). Retrieved March 7, 2022, from Link

U.S. Department of Energy, & Pacific Northwest National Laboratory. (2015). *Building America Best Practices Series: Volume 7.3, Guide to Determining Climate Regions by County* (tech. rep.). Link

U.S. Department of Transportation Federal Highway Administration. (2020). *ANNUAL VEHICLE DISTANCE TRAVELED IN MILES AND RELATED DATA - 2018* (tech. rep.). Retrieved July 6, 2020, from Link

U.S. Energy Information Administration. (2018). Space heating and water heating account for nearly two thirds of U.S. home energy use - Today in Energy. Retrieved December 2, 2019, from Link

U.S. Energy Information Administration. (2020). Natural Gas Annual 2019 (NGA). Retrieved February 15, 2022, from Link

U.S. Energy Information Administration. (2021a). *Electric Power Annual 2020* (tech. rep.). Retrieved June 27, 2022, from Link

U.S. Energy Information Administration. (2021b). Texas and Florida had large small-scale solar capacity increases in 2020. Retrieved April 25, 2022, from Link

U.S. Energy Information Administration. (2021c). U.S. Natural Gas Prices. Retrieved October 5, 2021, from Link

U.S. Energy Information Administration. (2021d). Utility-scale batteries and pumped storage return about 80% of the electricity they store. Retrieved May 24, 2022, from Link

U.S. Energy Information Administration. (2021e). Where greenhouse gases come from. Retrieved March 8, 2022, from Link

U.S. Energy Information Administration. (2022a). In 2020, 27% of U.S. households had difficulty meeting their energy needs. Retrieved June 27, 2022, from Link

U.S. Energy Information Administration. (2022b). *U.S. Natural Gas Summary* (tech. rep.). Retrieved June 27, 2022, from Link

U.S. Energy Information Administration (EIA). (2015). Residential Energy Consumption Survey (RECS) - Data. Retrieved September 26, 2019, from Link

U.S. Energy Information Administration (EIA). (2017). U.S. households' heating equipment choices are diverse and vary by climate region - Today in Energy. Retrieved July 29, 2021, from Link

U.S. Energy Information Administration (EIA). (2021a). Electric Power Annual 2020, 239.

U.S. Energy Information Administration (EIA). (2021b). Frequently Asked Questions (FAQs) - U.S. Energy Information Administration (EIA). Retrieved March 3, 2022, from Link

US EPA, O. (2019). Documentation for IPM Platform v6 November 2018 Reference Case - All Chapters. Retrieved December 1, 2019, from Link

Vibrant Clean Energy, LLC, Clack, C. T. M., Choukulkar, A., Coté, B., & McKee, S. A. (2020). *Why Local Solar For All Costs Less: A New Roadmap for the Lowest Cost Grid* (tech. rep.). Retrieved July 13, 2021, from Link

Waite, M., & Modi, V. (2020). Electricity Load Implications of Space Heating Decarbonization Pathways. *Joule*, *4*(2), 376–394. Retrieved June 23, 2020, from Link

Wilcox, S., & Marion, W. (2008). Users Manual for TMY3 Data Sets. *Technical Report*, 58.

Wolak, F. (2018). *The Evidence from California on the Economic Impact of Inefficient Distribution Network Pricing* (tech. rep. w25087). National Bureau of Economic Research. Cambridge, MA. Retrieved August 29, 2019, from Link

Woo, C. K., Orans, R., Horii, B., Pupp, R., & Heffner, G. (1994). Area- and time-specific marginal capacity costs of electricity distribution. *Energy*, *19*(12), 1213–1218. Retrieved December 23, 2019, from Link

Yatchew, A. (2001). Incentive Regulation of Distributing Utilities Using Yardstick Competition. *The Electricity Journal*, *14*(1), 56–60. Retrieved April 17, 2020, from Link

Zakariazadeh, A., Jadid, S., & Siano, P. (2014). Multi-objective scheduling of electric vehicles in smart distribution system. *Energy Conversion and Management*, *79*, 43–53. Retrieved June 22, 2020, from Link

Zhang, C., Jenkins, J., & Larson, E. D. (2020). *Princeton's Net-Zero America study Annex G: Electricity Distribution System Transition* (tech. rep.). Princeton University. Link

Appendix A

List of Utilities

Utility	State	Region	C_i	$Growth_i$	$Underground_i$	$Density_i$	$Residential_i$
Alabama Power Company	AL	SE	11,511	1.5%	8.3%	21.6	32.6%
Alaska Electric Light and Power Company	AK	WE	64	2.0%	20.4%	1.5	42.0%
ALLETE (Minnesota Power)	MN	MW	1,515	1.4%	18.1%	26.3	11.1%
Appalachian Power Company	OH	MW	6,974	2.7%	9.1%	28.4	38.8%
Arizona Public Service Company	AZ	WE	6,501	4.7%	41.5%	19.1	45.4%
Atlantic City Electric Company	DE	MA	2,726	3.4%	10.8%	114.7	44.5%
Avista Corporation	WA	WE	1,734	0.7%	18.4%	8.7	40.6%
Baltimore Gas and Electric Company	MD	MA	6,808	1.6%	31.5%	309.5	40.0%
Black Hills Power, Inc.	SD	MW	398	1.9%	17.7%	2.1	29.5%
Central Hudson Gas & Electric Corporation	NY	MA	1,154	3.3%	10.0%	65.0	43.2%
Central Maine Power Company	ME	NE	1,633	1.8%	4.6%	24.5	23.0%

(continued)

Utility	State	Region	C_i	$Growth_i$	$Underground_i$	$Density_i$	$Residential_i$
Cleco Power LLC	LA	SW	1,915	2.0%	8.7%	23.5	39.6%
Cleveland Electric Illuminating Company	OH	MW	4,559	0.8%	20.4%	245.1	27.4%
Commonwealth Edison Company	IL	MW	22,251	1.6%	33.6%	155.2	30.6%
Connecticut Light and Power Company	CT	NE	5,272	1.6%	21.5%	131.7	42.2%
Consolidated Water Power Company	WI	MW	231	0.3%	18.8%	0.4	0.6%
Consumers Energy Company	MI	MW	8,277	1.6%	11.0%	30.6	35.6%
Dayton Power and Light Company	OH	MW	3,176	0.6%	14.4%	55.5	35.1%
Delmarva Power & Light Company	DE	MA	3,876	3.3%	19.3%	52.7	37.0%
DTE Electric Company	MI	MW	11,764	0.8%	18.0%	45.1	33.3%
Duke Energy Carolinas, LLC	NC	SE	17,003	0.7%	18.7%	44.8	32.8%
Duke Energy Florida, LLC	FL	SE	9,698	2.8%	19.0%	39.7	50.5%
Duke Energy Indiana, LLC	IN	MW	5,999	1.8%	15.4%	19.4	30.7%
Duke Energy Kentucky, Inc.	OH	MW	828	2.2%	17.3%	265.8	35.9%
Duke Energy Ohio, Inc.	OH	MW	5,250	0.8%	19.6%	197.3	34.3%
Duke Energy Progress, LLC	NC	SE	11,407	1.8%	18.9%	22.2	36.5%
Duquesne Light Company	PA	MA	2,897	1.6%	17.0%	417.2	28.4%
El Paso Electric Company	TX	SW	1,447	0.6%	22.7%	17.1	30.2%
Emera Maine	ME	NE	305	0.4%	2.9%	2.9	36.2%
Empire District Electric Company	MO	MW	1,062	2.3%	11.2%	115.0	40.4%
Entergy Arkansas, LLC	AR	SE	6,889	0.8%	8.7%	10.0	35.8%
Entergy Mississippi, LLC	MS	SE	3,216	1.3%	5.7%	12.1	39.5%
Entergy New Orleans, LLC	LA	SW	1,276	0.1%	29.0%	674.2	33.5%
Fitchburg Gas and Electric Light Company	NH	NE	98	1.6%	10.4%	6.2	33.4%
Florida Power & Light Company	FL	SE	20,461	2.7%	28.9%	130.1	52.9%

(continued)

Utility	State	Region	C_i	$Growth_i$	$Underground_i$	$Density_i$	$Residential_i$
Georgia Power Company	GA	SE	15,865	2.5%	20.8%	24.9	29.4%
Green Mountain Power Corporation	VT	NE	364	2.2%	14.1%	7.4	29.2%
Gulf Power Company	FL	SE	2,459	2.0%	10.4%	40.9	47.2%
Idaho Power Company	ID	WE	2,996	1.3%	18.0%	6.2	34.2%
Indiana Michigan Power Company	OH	MW	4,778	0.0%	15.7%	66.8	30.2%
Indianapolis Power & Light Company	IN	MW	3,025	1.0%	22.8%	466.3	34.2%
Jersey Central Power & Light Company	OH	MW	6,004	3.1%	15.2%	184.6	43.4%
Kansas City Power & Light Company	MO	MW	3,549	1.5%	29.8%	151.6	35.3%
Kansas Gas and Electric Company	KS	MW	2,374	0.4%	16.4%	12.6	31.4%
Kentucky Power Company	KY	MW	1,636	2.5%	1.9%	28.8	34.7%
Kentucky Utilities Company	KY	MW	3,996	2.2%	6.3%	75.0	34.3%
Kingsport Power Company	OH	MW	432	2.4%	9.4%	23.5	35.4%
Lockhart Power Company	SC	SE	80	0.6%	0.7%	5.8	32.9%
Louisville Gas and Electric Company	KY	MW	2,679	1.2%	20.1%	323.7	33.8%
Madison Gas and Electric Company	WI	MW	715	1.6%	38.6%	214.1	25.7%
Metropolitan Edison Company	OH	MW	2,713	2.9%	11.9%	87.3	37.4%
MidAmerican Energy Company	IA	MW	3,964	1.4%	15.3%	14.0	29.4%
Mississippi Power Company	MS	SE	2,593	0.5%	6.9%	9.4	23.9%
Monongahela Power Company	OH	MW	2,062	1.4%	3.8%	19.0	29.4%
Mt. Carmel Public Utility Company	IL	MW	34	0.1%	1.8%	34.6	36.5%
Nevada Power Company	NV	WE	5,021	4.3%	43.0%	93.2	42.1%
New York State Electric & Gas Corporation	NY	MA	2,752	3.1%	7.8%	28.0	41.9%
Northern Indiana Public Service Company	IN	MW	3,089	1.3%	14.8%	39.1	19.8%
Northern States Power Company - MN	MN	MW	8,211	3.1%	33.0%	34.7	28.3%

(continued)

Utility	State	Region	C_i	$Growth_i$	$Underground_i$	$Density_i$	$Residential_i$
Northwestern Wisconsin Electric Company	WI	MW	36	3.0%	20.4%	3.3	45.8%
NSTAR Electric Company	MA	NE	3,575	4.4%	43.2%	115.4	28.1%
Ohio Edison Company	OH	MW	6,616	1.2%	14.9%	75.5	34.5%
Ohio Power Company	OH	MW	6,642	0.0%	8.7%	19.8	26.3%
Oklahoma Gas and Electric Company	OK	SW	5,897	2.1%	22.1%	17.0	34.6%
Orange and Rockland Utilities, Inc.	NY	MA	1,437	3.6%	16.9%	98.8	37.1%
Pacific Gas and Electric Company	CA	WE	18,977	2.0%	29.5%	44.7	35.6%
PacifiCorp	OR	WE	8,923	1.7%	18.5%	6.5	29.0%
Pennsylvania Electric Company	OH	MW	2,812	2.1%	9.4%	18.7	31.1%
Pennsylvania Power Company	OH	MW	1,036	2.0%	13.9%	57.3	34.9%
Pioneer Power and Light Company	WI	MW	7	2.2%	29.6%	12.9	72.3%
Portland General Electric Company	OR	WE	4,073	0.0%	23.0%	92.8	39.8%
Potomac Edison Company	OH	MW	3,050	3.0%	20.1%	49.7	39.3%
Potomac Electric Power Company	DC	MA	6,472	2.0%	41.6%	679.7	29.2%
PPL Electric Utilities Corporation	PA	MA	7,198	1.6%	13.1%	79.1	36.9%
Public Service Company of Colorado	CO	SW	6,383	3.6%	37.7%	45.6	31.3%
Public Service Company of New Hampshire	NH	NE	1,614	2.3%	9.6%	26.1	37.4%
Public Service Company of New Mexico	NM	SW	1,648	4.8%	30.1%	58.9	32.7%
Public Service Company of Oklahoma	OK	SW	3,952	1.3%	13.5%	8.2	34.0%
Public Service Electric and Gas Company	NJ	MA	10,432	1.7%	23.5%	811.3	30.2%
Puget Sound Energy, Inc.	WA	WE	4,847	0.1%	35.8%	43.7	49.5%
Rochester Gas and Electric Corporation	NY	MA	1,596	2.3%	33.8%	96.0	37.2%
Rockland Electric Company	NY	MA	447	2.7%	21.1%	232.3	45.1%
Sierra Pacific Power Company	NV	WE	1,660	1.8%	28.0%	4.4	25.5%

(continued)

Utility	State	Region	C_i	$Growth_i$	$Underground_i$	$Density_i$	$Residential_i$
Southern California Edison Company	CA	WE	20,989	1.8%	31.8%	59.3	32.7%
Southern Indiana Gas and Electric Company	IN	MW	1,249	1.8%	16.7%	54.3	27.6%
Southwestern Electric Power Company	LA	SW	4,711	1.1%	12.7%	13.7	32.0%
Southwestern Public Service Company	TX	SW	4,600	1.9%	9.4%	4.1	20.4%
Superior Water, Light and Power Company	WI	MW	93	2.7%	13.0%	97.2	14.7%
Tampa Electric Company	FL	SE	3,914	2.5%	19.2%	271.9	45.1%
Toledo Edison Company	OH	MW	2,146	1.3%	15.9%	73.0	22.8%
Tucson Electric Power Company	AZ	WE	2,126	4.3%	28.3%	240.7	40.0%
Union Electric Company	MO	MW	8,459	0.4%	18.0%	31.9	36.6%
United Illuminating Company	CT	NE	1,350	1.9%	20.5%	143.6	38.8%
Upper Peninsula Power Company	MI	MW	151	0.6%	13.4%	2.0	35.6%
Virginia Electric and Power Company	VA	SE	16,618	1.1%	28.3%	59.2	37.5%
West Penn Power Company	OH	MW	3,705	1.9%	7.3%	39.7	34.4%
Western Massachusetts Electric Company	MA	NE	797	1.5%	29.4%	39.3	37.4%
Wheeling Power Company	OH	MW	322	3.6%	12.1%	27.9	21.5%
Wisconsin Electric Power Company	WI	MW	6,261	0.9%	35.2%	50.2	28.5%
Wisconsin Power and Light Company	WI	MW	2,775	2.0%	16.8%	21.3	32.8%
Wisconsin Public Service Corporation	WI	MW	2,095	3.6%	12.8%	19.4	27.6%

Note: reported value for C_i, $Growth_i$, $Underground_i$, $Density_i$, and $Residential_i$ is the mean of that value for utility i from 2000-2007.

Appendix B

Uniqueness

In mixed-integer optimization, it is sometimes the case that a well-defined problem does not have a unique solution. This is often the case when incorporating storage, as it is possible for a battery to charge at different rates or at different hours while imposing the same cost on the objective function. This can affect the speed at which the optimization algorithm converges on a unique solution, as the algorithm can vacillate back and forth between multiple near-optimal (but entirely different) solutions without significantly reducing the objective function.

In our optimizations, we do not impose any cost on keeping a battery fully charged (e.g. by forcing the battery to leak charge over time or by having the state of charge impact the battery's lifespan), which creates the possibility that an optimization could have non-unique solutions. To test how the algorithm responds in such a circumstance, we create a reduced scenario for a single residence that only includes a battery with a fixed capacity of 1 kW and a time-variant electricity tariff. In the first 100 hours, the tariff (which applies to both consumption from the grid and injections to the grid from the battery) is set to \$0.01 per-kWh; for all remaining hours, the tariff is set to \$1 per-kWh. The customer can charge the battery to its full capacity at any time in the first 100 hours, then discharge at anytime thereafter, and will enjoy the same total benefit.

We run eight sample simulations using different seeds. The charging and discharging behavior are plotted in Figure B.1. In seven of the eight simulation, the algorithm charges the battery

close to its full capacity in the first hours of the low-price period, completes charging near the end of the low-price period, then discharges near the end of the high-price period. The eighth scenario follows a similar path, except that the battery discharges to 75% at the beginning of the high-price period, then completes discharging at the end. There is no explanation for this behavior that can be ascribed to the problem formulation; it is simply a vestige of heuristics used in the optimizer.

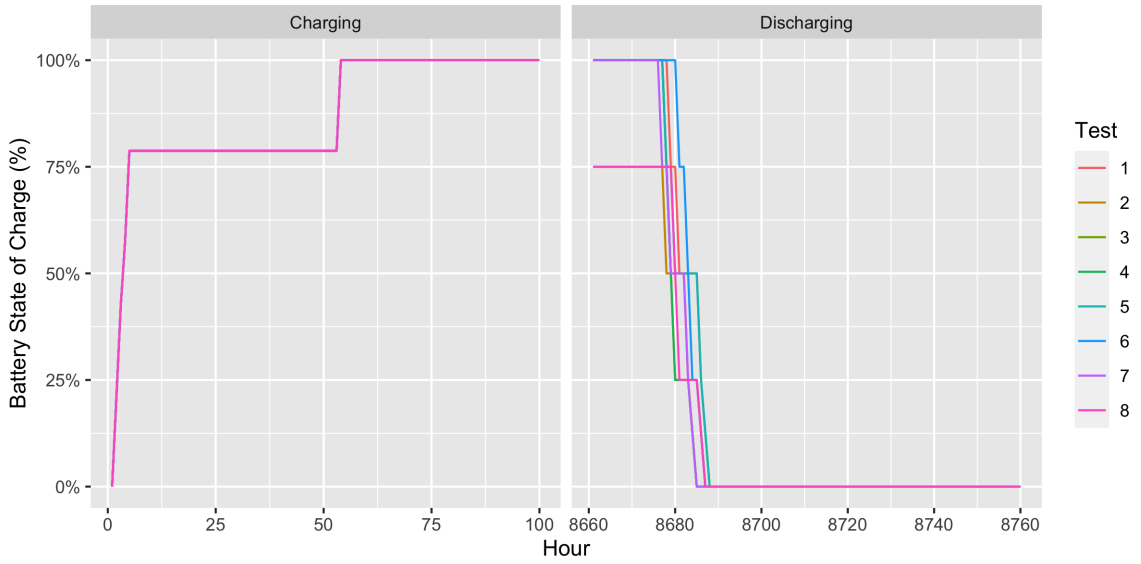

Figure B.1: Charging and discharging of the battery in the eight sample simulations. The plot on the left shows charging during the first 100 hours. The plot on the right shows discharging in the last 100 hours. In all tests except test 8, the algorithm waits to discharge the battery until the last 85 hours.

One way to prevent non-uniqueness from interfering with optimization performance is by imposing a small non-zero cost on storing energy in the battery, such as by causing the state of charge to deteriorate over time. This is achieved by adding a coefficient to the first term on the right-hand side of Equation 4.19. In Equation , below, we set this coefficient to 0.999, meaning that the battery charge deteriorates by one-tenth of one percent every hour.

$$S_t^{Battery} = 0.999 * S_{t-1}^{Battery} + E_t^{Battery^+} - \frac{1}{\eta_{Storage}} E_t^{Battery^-} \tag{B.1}$$

The resulting charging behavior is plotted in Figure B.2. We see that with the degradation

factor, the algorithm is incentivized to postpone charging the battery until the last hours of the low-price period, then sell the electricity back to the grid immediately in the first hours of the high-price period. This minimizes the energy lost in storage, maximizing the profit from arbitraging the rates.

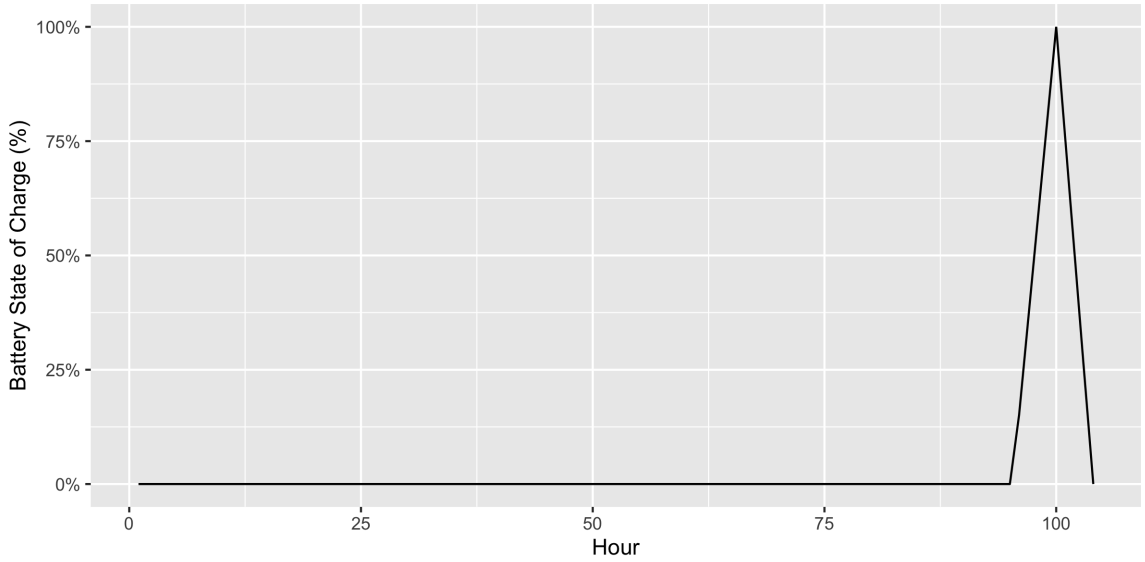

Figure B.2: Charging and discharging of the battery in the updated algorithm that includes a small degradation factor. The algorithm postpones charging the battery until the last hours of the low-price period, then discharges at the beginning of the high-price period.